Accepted Manuscript

Potential of Aryl-urea-Benzofuranylthiazoles hybrids as multitasking agents in Alzheimer's disease

Belma Zengin Kurt, Isil Gazioglu, Livia Basile, Fatih Sonmez, Tiziana Ginex, Mustafa Kucukislamoglu, Salvatore Guccione

PII: S0223-5234(15)30135-5

DOI: 10.1016/j.ejmech.2015.07.005

Reference: EJMECH 7986

To appear in: *European Journal of Medicinal Chemistry*

Received Date: 2 February 2015

Revised Date: 18 May 2015

Accepted Date: 2 July 2015

Please cite this article as: B.Z. Kurt, I. Gazioglu, L. Basile, F. Sonmez, T. Ginex, M. Kucukislamoglu, S. Guccione, Potential of Aryl-urea-Benzofuranylthiazoles hybrids as multitasking agents in Alzheimer's disease, *European Journal of Medicinal Chemistry* (2015), doi: 10.1016/j.ejmech.2015.07.005.

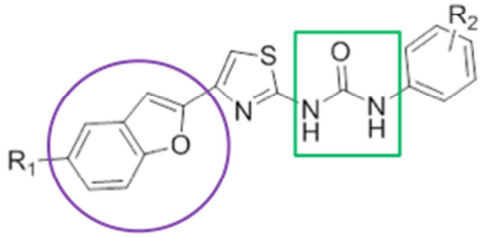

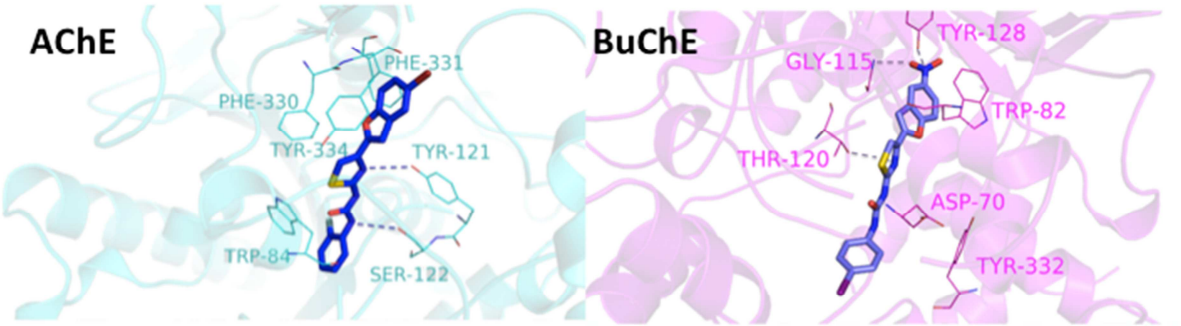

+ Antioxidant Activity

Potential of Aryl-urea-Benzofuranylthiazoles hybrids as multitasking agents in Alzheimer's disease

Belma Zengin Kurt,[a] Isil Gazioglu,[a] Livia Basile,*[b] Fatih Sonmez,*[c] Tiziana Ginex,[d] Mustafa Kucukislamoglu[e] and Salvatore Guccione[b]

[a]*Bezmialem Vakif University, Faculty of Pharmacy, Department of Analytical and Medicinal Chemistry, 34093, Istanbul, TURKEY*

[b]*Department of Drug Sciences, University of Catania, Viale A. Doria 6 Ed. 2, Città Universitaria, I- 95125, Catania, ITALY*

[c]*Sakarya University, Pamukova Vocational High School, 54900, Sakarya, TURKEY*

[d]*Molecular Modelling Laboratory, Department of Food Science, University of Parma, Parco Area delle Scienze 17/A, Parma 43124, ITALY*

[e]*Sakarya University, Faculty of Arts and Science, Department of Chemistry, 54055, Sakarya, TURKEY*

*Corresponding authors: University of Catania, Department of Drug Sciences, Viale A. Doria 6 Ed. 2, Città Universitaria, I- 95125, Catania, ITALY. Tel. +39 095 738-4020; fax +39 095 738-4208; email address: basilelivia@gmail.com (L. Basile); Sakarya University, Pamukova Vocational High School, 54900, Sakarya, TURKEY. Tel.: +90-264-2953378; fax: +90-264-2953679; e-mail address: fsonmez@sakarya.edu.tr (F.Sonmez).

Keywords: Aryl-urea-Benzofuranylthiazoles, Inhibitors, Acetylcholinesterase, Butyrylcholinesterase, Antioxidant, Docking.

Abstract

New benzofuranylthiazole derivatives containing the aryl-urea moiety were synthesized and evaluated *in vitro* as dual acetylcholinesterase (AChE)-butyrylcholinesterase (BuChE) inhibitors. In addition, the cupric reducing antioxidant capacities (CUPRAC) and ABTS cation radical scavenging abilities of the synthesized compounds were assayed. The result showed that all the synthesized compounds exhibited inhibitory activity on both AChE and BuChE with 1-(4-(5-bromobenzofuran-2-yl)thiazol-2-yl)-3-(2-fluorophenyl)urea (**e25**, IC_{50} value of 3.85 µM) and 1-

(4-iodophenyl)-3-(4-(5-nitrobenzofuran-2-yl)thiazol-2-yl)urea (**e38**, IC_{50} value of 2.03 µM) as the strongest inhibitors against AChE and BuChE, respectively. Compound **e38** was 8.5-fold more potent than galanthamine. The selectivity index of **e25** and **e38** was 2.40 and 0.37 against AChE and BuChE, respectively. Compound **e2**, **e4** and **e11** (IC_{50}= 0.2, 0.5 and 1.13 µM, respectively) showed a better ABTS cation radical scavenging ability than the standard quercetin (IC_{50}= 1.18 µM). Best poses of compounds **e38** on BuChE and **e25** on AChE indicate that the thiazole ring and the amidic moiety are important sites of interaction with both ChEs. In addition, the benzofuran ring and phenyl ring are anchored to the side chains of both enzymes by π-π(pi-pi) interactions.

1. Introduction

Alzheimer's disease (AD) is the most common neurodegenerative disease with symptoms of memory loss, cognition defect and behavioural impairment [1-3]. The classical hypothesis of AD, named "cholinergic hypothesis", suggests that acetylcholinesterase inhibitors (AChEI) could increase ACh levels in AD patients through the inhibition of AChE and, therefore, relieve some symptoms experienced by AD patients [4,5]. AD is probably associated with multifaceted etiologies and pathogenic phenomena. In any case, oxidative stress can be considered the causative unifying factor [6].

Cholinergic system is the earliest and most profoundly affected neurotransmitter system in AD, with substantial loss of the forebrain, cortex, and hippocampus. Ach and the above mentioned brain regions are critical in the acquisition, processing, and storage of memories and have supported the use of cholinomimetics in the treatment of AD [7]. It is well known that two forms of cholinesterases coexist ubiquitously throughout the body, i.e., acetylcholinesterase (AChE; EC 3.1.1.7) and butyrylcholinesterase (BuChE; EC 3.1.1.8). Among its functions, AChE regulates the impulse transmission at cholinergic synapses by rapid hydrolysis of the neurotransmitter ACh. BuChE, also known as pseudocholinesterase, is primarily localized in plasma, liver, and muscle tissues.

The pharmacological role of BuChE was not yet completely understood but it is supposed that it may have a compensatory role in the modulation of the hydrolysis of ACh in brains causing degenerative changes. Consequently, BuChE may be a target for increasing the cholinergic tone in AD patients [8,9].

Based on these findings, many efforts have been made in the search for potent AChE inhibitors, and a large number of naturally occurring and synthetic AChE inhibitors such as galantamine,

huperzine A, physostigmine, ambenonium and tacrine have already been reported (Fig. 1) [10-13].

Crystallographic structure of AChE from *Torpedo californica* [14] shows three main binding sites, namely (a) the catalytic triad at the bottom of active site including Ser200, His440 and Glu327; (b) the catalytic anionic site (CAS) at the vicinity of the catalytic triad consisting of Trp84, Tyr130, Gly199, His441 and His444; (c) peripheral anionic site (PAS) at the gorge rim comprising Tyr70, Asp72, Tyr121, Trp279 and Tyr334 [15,16]. Inhibition of AChE can be accomplished by three different ways depending on the nature of the interaction of the inhibitor with the enzyme binding site [17]. Irreversible inhibitors, such as organophosphates, form a strong covalent bond with the serine residue in the catalytic triad. Pseudo-irreversible inhibitors, as carbamates, lead to formation of a carbamylated serine into the catalytic triad that is slowly hydrolysed to regenerate the active enzyme. Reversible inhibitors give a transient non-covalent binding through electrostatic interactions with the active and/or peripheral sites. The reversible inhibitors may be classified as (a) active-site inhibitors directed toward the catalytic anionic sub-site at the bottom of the gorge, (b) peripheral anionic site inhibitors which bind at the entrance to the gorge, or (c) elongated gorge-spanning inhibitors which bridge the two sites [17].

Recently, some works on AChE inhibitors with a benzofuran moiety have been reported [18,19]. Amide or imide-based AChE inhibitors have also been reported [20-21] with both these functionalities acting as hydrogen bond donors towards oxygen or nitrogen lone pairs of Tyr72, Tyr124, Tyr203 and Tyr337 of the enzyme. Amidic or imidic fragments interact with the catalytic triad Ser203-Glu334-His447 of the active binding site. Hydrogen bonds with Tyr70 and His447 were also reported for compounds having urea, carbamate or sulphonamide moieties as spacers [22-25].

Dibenzofuran and tricyclic tacrine-ferrulic acid derivatives as multifunctional anti-Alzheimer agents were also previously reported by Fang and co-workers [26,27]. Tricyclic and heterocyclic rings derivatives, such as tacrine, quinolizidinyl, piperidine and indolinone derivatives give strong parallel π-π (pi-pi) stacking with residues at CAS [28-33]. An additional π-π (pi-pi) stacking interaction was also observed between the furan ring and Phe330 [18,19]. Moreover, it has been reported that thiazolo-triazin derivatives form a hydrogen bond with Tyr124 and π-π interaction with Trp286 [34]. Docking into the BuChE gorge, which is larger than that of AChE, showed that heterocyclic rings give (i) a cation-π interaction with Trp82 and Trp430 and also (i) hydrophobic and/or π-π (pi-pi) stacking interactions with Phe118 and Trp231 [3,24].

Overall, heterocyclic and aromatic rings can have strong parallel π-π stacking with residues at the CAS of the enzyme whereas the urea moiety might contribute to inhibitor activity by additional interactions.

On the basis of the above reported evidences a series of 38 novel urea substituted benzofuran derivatives (**e1-e38**), including the thiazole ring as an additional spacer, was designed and synthesized (Fig. 2). AChE/BuChE inhibition and antioxidant properties were evaluated. Structure-activity relationships are described and rationalized by docking studies.

2. Results and discussion

2.1. Chemistry

The synthetic procedures are depicted in Scheme 1. 2-Acetyl benzofuran derivatives **b1-b3** were prepared as previously reported [35]. 1-(1-benzofuran-2-yl)-2-bromoethanone derivatives (**c1-c3**) were prepared by brominating of 2-acetyl benzofuran using molecular bromine in chloroform. The reaction of **c1-c3** with thiourea in ethanol gave 4-(1-benzofuran-2-yl)-1,3-thiazol-2-amines (**d1-d3**). These compounds were reacted with arylisocyanates in THF to get the final products (**e1-e38**) at high yields.

All the new compounds were characterized through ^{1}H NMR, ^{13}C NMR, IR, MS and elemental analysis. Infrared spectra for **e1-e38** show absorptions between 3500 and 3000 cm^{-1} related to N-H stretching, absorptions at 1650-1700 cm^{-1} from the urea carbonyl moiety stretching and absorptions at 1550 cm^{-1} for the thiazole C=N moiety stretching. Furthermore, absorptions among 3111 cm^{-1} and 2950 cm^{-1} indicated C-H stretching for the thiazole and furan rings, respectively. In case of ^{1}H NMR spectra, the resonance for the hydrogen attached to the amide nitrogen was between 8.20 and 11.50 ppm. Signals for aromatic protons were observed between 6.50 and 8.52 ppm and those for the proton of thiazole and furan ring were detected around 7.10 and 7.50 ppm as a singlet. Regarding ^{13}C NMR spectra, carbon atoms of urea carbonyl, benzofuran ring (C_2 and C_8) and thiazole ring (C_3) were observed between 150.7 and 161.4 ppm.

2.2. Biological activities

2.2.1. Inhibitory activities on AChE and BuChE

The Ellman's method with galanthamine as the reference compound [36] was applied to measure AChE and BuChE inhibitory activity for all synthetized compounds (**e1-e38**). The IC_{50} values for AChE and BuChE inhibition are summarized in Table 1.

The results show that the synthesized compounds exhibit low to moderate AChE inhibition. IC_{50}

values are between 3.85 and 78.85 µM for AChE and between 2.03 and 154.08 µM for BuChE. Among the synthesized compounds, **e25** (IC_{50} = 3.85 µM) shows the highest inhibitory activity on AChE. The value was less than that of galantamine (IC_{50} = 2.41 µM) but close to that of rivastigmine (IC_{50} = 3.01 µM).

e38 exhibited the strongest inhibition against BuChE with an IC_{50} value of 2.03 µM, which was 8.5-fold and 2.3 more than that of galanthamine (IC_{50} = 17.38 µM) and donepezil (IC_{50} = 4.66 µM), respectively. Furthermore, eight of the synthesized compounds (**e8**, **e11**, **e20**, **e22**, **e24**, **e25**, **e33** and **e38**) showed higher inhibition against BuChE than galanthamine.

Moving the fluorine atom in the phenyl ring from the *orto*-position (**e25**, IC_{50} = 3.85 µM for AChE, IC_{50} 9.25 µM for BuChE) to the *meta*-position (**e26**, IC_{50} = 29.38 for AChE, IC_{50} = 40.16 for BuChE) or the *para*-position (**e27**, IC_{50} = 35.62 for AChE, IC_{50} = 64.32 for BuChE) led to a major decline of the inhibitory activity for both ChEs (**Table 1**). An opposite trend was observed for compounds **e9** (IC_{50} = 30.92 µM for AChE, IC_{50} = 41.66 µM for BuChE), **e10** (IC_{50} = 48.99 µM for AChE, IC_{50} = 17.98 µM for BuChE) and **e11** (IC_{50} = 55.03 µM for AChE, IC_{50} = 7.45 µM for BuChE) were the above mentioned replacement led to a decrease of the inhibitory activities against AChE (Table 1), but to an increase in the BuChE inhibition (Table 1). It can be speculated on a more volume allowed in the active site of the latter enzyme to accommodate the alternate *meta* and *para* substitutions (vide *infra* Docking Results). Hydrophobic interactions also combined with the H-bond acceptor character of the fluorine atom might play a role.

Moving the chlorine atom in the phenyl ring from the *meta*-position (**e12,** IC_{50} = 9.67 µM for AChE, IC_{50} = 21.52 µM for BuChE; **e28**, IC_{50} = 7.93 µM for AChE, IC_{50} = 26.32 µM for BuChE) to the *para*-position (**e13**, IC_{50} = 42.55 µM for AChE, IC_{50} = 38.58 µM for BuChE; **e29**, IC_{50} = 22.23 µM for AChE, IC_{50} = 36.93 µM for BuChE**)** led to a decrease of the inhibitory activity for both ChEs (Table 1).

Moving the nitro group in the phenyl ring from the *orto*-position (**e6**, IC_{50} = 41.91 µM for AChE, IC_{50} = 79.93 µM for BuChE) to the *meta*-position (**e7**, IC_{50} = 41.19 µM for AChE, IC_{50} = 26.81 µM for BuChE) and above all the *para*-position (**e8**, IC_{50} = 5.23 µM for AChE, IC_{50} = 3.44 µM for BuChE) led to a major enhancement of the inhibitory activity for both ChEs. This effect was not observed for compounds **e22** (IC_{50} = 8.82 µM for AChE, IC_{50} = 5.12 µM for BuChE), **e23** (IC_{50} = 17.45 µM for AChE, IC_{50} = 78.97 µM for BuChE) and **e24** (IC_{50} = 4.78 µM for AChE, IC_{50} = 3.12 µM for BuChE), with a R_1 was bromine atom as R_1 substituent. The bromine atom might lead to some unfavourable positioning of the nitro group which doesn' t allow for good interactions.

Compounds with a methoxy group in the *meta*- position of the phenyl ring (**e2**, IC_{50} = 48.90 µM for AChE, IC_{50} = 59.56 µM for BuChE) exhibited higher inhibitory activity than that with the same substituent in the *ortho* or *para* positions (**e1**, IC_{50} = 60.97 µM for AChE, IC_{50} = 81.28 µM for BuChE; **e3**, IC_{50} = 52.47 µM for AChE, IC_{50} = 74.26 µM for BuChE) for both ChEs (Table 1). It is supposed that methoxy substituent can better act as H-bond acceptor binding more tightly to both enzymes finally enhancing the inhibitory effects.

Alternatively this favourable effect might be explained as a consequence of a different electron density which is lower in the *meta*- position on respect to that *ortho*- and *para*.

Overall, the inhibitory activity on AChE seems to be strongly dependent on the size and polarizability of the halogen substituent at the *para*-position of the phenyl ring (for size and polarizability, I > Br > Cl > F; for AChE inhibitory activity, **e16** (R_2=4-I, IC_{50} = 21.35 µM) > **e15** (R_2=4-Br, IC_{50} = 32.82 µM) > **e13** (R_2=4-Cl, IC_{50} = 42.55 µM) > **e11** (R_2=4-F, IC_{50} = 55.03 µM); **e31** (R_2=4-I, IC_{50} = 6.42 µM) > **e30** (R_2=4-Br, IC_{50} = 11.94 µM) > **e29** (R_2=4-Cl, IC_{50} = 22.23 µM) > **e27** (R_2=4-F, IC_{50} = 35.62 µM); **e38** (R_2=4-I, IC_{50} = 5.53 µM) > **e37** (R_2=4-Br, IC_{50} = 28.19 µM) > **e36** (R_2=4-Cl, IC_{50} = 30.56 µM) > **e35** (R_2=4-F, IC_{50} = 41.13 µM). This relationship was not observed for BuChE.

Hydrophobic contacts and π-π stacking interactions between the phenyl, thiazole and benzofuran rings of the synthesized compounds and CAS or PAS of AChE might take place. A hydrogen bond might form between urea moiety and Tyr70 or His447 in the active site.

2.2.2. Docking studies

AChE and BuChE share the 65% of amino acid sequence homology and overall have a similar structure [37]. Six of the fourteen aromatic amino acid residues that constitute the active site gorge of AChE are replaced by aliphatic amino acid residues in BuChE. Thereof the volume of the BuChE active site gorge is larger (~ 200 Å3) than that of AChE. The replacement of aromatic with aliphatic amino acids is also critical for the selectivity against different inhibitor of the two enzymes [38]. Docking studies performed on both ChEs reveal that all the title compounds have multiple binding modes. To reach a plausible positioning of the compounds into the active site of both ChEs, the allowed search space was restricted to the region between CAS and PAS sites of both AChE and BuChE. All the compounds gave a suitable occupation of the active binding site of the two enzymes, assuming different geometries stabilized by interactions with the side chains of CAS and PAS (Fig. 3). Overall, the thiazole ring has a critical role for its capacity to form H bond interaction with Tyr121 of AChE. Docking scores for compounds **e25** (IC_{50} = 3.85 µM

against AChE) and **e38** (IC_{50} = 2.03 μM against BuChE) are in agreement with the experimental *in vitro* data. In this regard, the former exhibits higher binding affinity for AChE whereas the latter gave a better scoring result for BuChE binding. 2D LigPlot diagrams [39] showing the interactions of the best poses for compounds **e25** and **e38** respectively into the active site of AChE site and BuChE as visualized by Python Molecular viewer [40], are shown in **Fig. 4** and **Fig. 5**. Thiazole ring of **e25** gives H bond interaction through its nitrogen that acts as acceptor towards the hydroxyl group of Tyr121 (hydrogen bond interaction energy, EH: -8.10) of AChE. Another H bond can be considered for nitrogen of the amidic moiety that acts as acceptor towards the hydroxyl group of Ser122 (EH: -7.95). Furthermore, favourable steric interactions can be established with Asp72, Gly117, Gly118, Gly123, Gly335, Phe330, Ser124, Trp279, Tyr116, Tyr121 and Tyr130 of AChE. The phenyl moiety of **e25** points toward the PAS pocket and gives *T*-stacking with the phenolic side chain of Tyr84 (π-π interaction). The benzofuran group stacks between the benzyl moiety of Phe331 (Steric Interaction Energy, ES: -15.56) and the phenolic one of Tyr334 (ES: -27.82), stabilizing the accommodation of compound **e25** at the entrance of the active binding site. Another *T*-stacking interaction can be found between the thiazole ring of **e25** and the benzyl side chain of Phe330 (ES: -9.44) [41].

Binding of **e38** into the BuChE gorge is characterized by the formation of the following three H bond interactions: (1) the nitrogen of thiazole ring as H-bond acceptor for Thr120, (2) the nitrogen of the nitro group as H-bond acceptor for Tyr128 hydroxyl group and (3) the oxygen of nitro group as H-bond acceptor for nitrogen of Gly115. This result can be due to the fact that BuChE binding site is bigger than the AChE one, therefore **e38** gains a better positioning into the BuChE binding site, finally leading to the formation of a more stable complex. *Orto*-Fluorine atom lies outside the gorge of BuChE. The two nitrogen atoms of the amidic moiety form a salt bridge with the side chain of Asp70. A strong π-π(pi-pi) interaction (ES: -35.21) is observed between the benzofuran ring and the Trp82 indolyl moiety. In addition, favourable steric interactions occur with the side chain of Asn68, Asn83, Gln71, Glu197, Gly116, Gly439, Ile69, Tyr114, Trp112 and His438.

2.3. Antioxidant activity assay

2.3.1. ABTS cation radical scavenging assay

The ABTS method is based on the ability of hydrogen or electron-donating antioxidants to decolourize the performed radical monocation of 2,2'-azino-bis(3-ethylbenzthiazoline-6-sulfonic acid) generated due to oxidation of ABTS with potassium persulfate [42]. Five of the synthesized

compounds exhibited good radical scavenging ability (Table 1). Particularly compounds **e2**, **e4** and **e11** (IC_{50}= 0.2, 0.5 and 1.13 µM, respectively) lacking of substituents on the benzofuran ring showed significantly better activity than quercetin (IC_{50}= 1.18 µM). Compounds **e18-e37,** containing NO_2- and Br- substituents at 5-position of the benzofuran ring, showed significantly less ABTS cation radical scavenging.

2.3.2. CUPRAC assay

CUPRAC assays have a distinct advantage over other electron-transfer based assays (e.g., Folin, FRAP, ABTS, DPPH). This advantage is its realistic pH close to that physiological, favourable redox potential, accessibility and stability of reagents and applicability to lipophilic antioxidants as well as hydrophilic ones [43]. The cupric reducing antioxidant capacities of the synthesized compounds (**e1-e38**) were determined according to a reported method [41] using quercetin as the reference compound. Among the synthesized compounds, **e17** ($A_{0.50}$ = 92.68 µM) showed the highest cupric reducing antioxidant activity. The synthesized compounds have lower CUPRAC activity than quercetin ($A_{0.50}$ = 1.45 µM) (Table 1).

The antioxidant results coming from the $ABTS^{+\cdot}$ and CUPRAC assays are, not comparable because of the differences in the methods. In fact, the interaction between an antioxidant and $ABTS^{+\cdot}$ is an indication of the ability of the hydroxyl or amine functional group to react with or scavenge free radicals. In addition, the trapping of $ABTS^{+\cdot}$ by hydroxyl or amine-type antioxidants can be regarded as a hydrogen atom transfer from O–H or N-H to $ABTS^{+\cdot}$ [44]. The CUPRAC method is based on reduction of Cu(II) to Cu(I) by reductants (antioxidants) present in a sample [45]. Compounds **e2** ($A_{0.50}$ = 104.46 µM), **e4** ($A_{0.50}$ = 192.91 µM), **e7** ($A_{0.50}$ >200 µM) and **e11** ($A_{0.50}$ = 110.31 µM)have a high electron or hydrogen atom transfer ability, but they don't have reducing ability of Cu(II) to Cu(I).

3. Conclusion

A series of 38 novel urea substituted benzofuranylthiazoles derivatives (**e1-e38**) was synthesized and their inhibitory activities on AChE and BuChE and antioxidant activities were evaluated. All the synthesized compounds inhibited AChE and BuChE. Among them, **e25** (IC_{50} = 3.85 µM against AChE) was found to be the most active as AChE inhibitor whereas **e38** (IC_{50} = 2.03 µM against BuChE) exhibited the strongest inhibition against BuChE with IC_{50} value of 2.03 µM, which was 8.5-fold more potent than that of galanthamine. Additionally, most of the synthesized compounds (**e2**, IC_{50} = 48.90 µM for AChE, IC_{50} = 59.56 µM for BuChE; **e4**, IC_{50} =10.40 µM for

AChE, IC_{50} = 56.32 µM for BuChE; **e7**, IC_{50} = 41.19 µM for AChE, IC_{50} = 26.81 µM for BuChE; **e9**, IC_{50} = 30.92 µM for AChE, IC_{50} = 41.66 µM for BuChE; **e11**, IC_{50} = 55.03 µM for AChE, IC_{50} = 7.45 µM for BuChE) exhibited good ABTS cation radical scavenging ability with **e2** (IC_{50} = 48.90 µM for AChE, IC_{50} = 59.56 µM for BuChE), **e4** (IC_{50} = 10.40 µM for AChE, IC_{50} = 56.32 µM for BuChE) and **e11** (IC_{50} = 55.03 µM for AChE, IC_{50} = 7.45 µM for BuChE) showing significantly better activity than quercetin. The SAR revealed that the inhibitory activity of the synthesized compounds could also be affected by the type and position of the halogen substituent on the phenyl ring.

Overall benzofuranylthiazole shows an interesting potential as a new chemotype to develop multifunctional agents in AD by properly modulating the substitution pattern.

4. Experimental section

4.1. Chemistry. General information

Melting points were taken on a Barnstead Electrothermal 9200. IR spectra were registered on a Shimadzu Prestige-21 (200 VCE) spectrometer. ^{1}H and ^{13}C NMR spectra (Supplementary Materials) were registered on a Varian Infinity Plus spectrometer at 300 and at 75 Hz, respectively. ^{1}H and ^{13}C chemical shifts are referenced to the internal deuterated solvent. Mass spectra were obtained using MICROMASS Quattro LC-MS-MS spectrometer. The elemental analyses were carried out with a Leco CHNS-932 instrument. Spectrophotometric analyses were performed by a BioTek Power Wave XS (BioTek, USA). The electric eel acetylcholinesterase (AChE, Type-VI-S, EC 3.1.1.7, 425.84 U/mg, Sigma) and horse serum butyrylcholinesterase (BuChE, EC 3.1.1.8, 11.4 U/mg, Sigma) were purchased from Sigma (Steinheim, Germany). The other chemicals and solvents were purchased from Fluka Chemie, Merck, Alfa Easer and Sigma-Aldrich.

4.1.1. General procedures of synthesis and spectral data

*4.1.1.1. Synthesis of 2-acetyl benzofuran derivatives (**b1-3**)*

2-Acetyl benzofuran derivatives were prepared in accordance with previously reported methods [35]. Salicylaldehydes (100 mmol) and KOH (100 mmol) were stirred in methanol (250 ml) for 30 minutes then chloroacetone (120 mmol) was dropped at 0–10°C. The mixture was refluxed for 2 h (or 48 hours for **b3**). Methanol was removed using a rotary evaporator, and the mixture was extracted with CH_2Cl_2 (3x 50 mL). The organic layer was dried over anhydrous Na_2SO_4 and removed using a rotary evaporator. The product was recrystallized from ethanol.

1-(Benzofuran-2-yl)ethanone (b1): 78% yield, mp. 76-77 °C (lit. [35] mp. 75°C); ^{1}H NMR (DMSO-d_6, 300 MHz) δ/ppm: 2.65 (3H, s), 7.31–7.34 (1H, m), 7.45–7.52 (2H, m), 7.60 (1H, d), 7.73 (1H, d); ^{13}C NMR (DMSO-d_6, 75 MHz) δ/ppm: 27.8, 111.8, 112.4, 124.6, 125.3, 127.4, 129.6, 151.8, 155.4, 187.2.

1-(5-Bromo-benzofuran-2-yl)ethanone (b2): 85% yield, mp. 110-111 °C (lit. [35] mp. 109–111°C); ^{1}H NMR (DMSO-d_6, 300 MHz) δ/ppm: 2.72 (3H, s), 7.49 (1H, s), 7.52 (1H, d), 7.57 (1H, d), 7.85 (1H, s); ^{13}C NMR (DMSO-d_6, 75 MHz) δ/ppm: 27.9, 111.7, 113.3, 116.9, 125.8, 129.3, 132.2, 153.9, 155.6, 188.8.

1-(5-Nitrobenzofuran-2-yl)ethanone (b3): 65% yield, mp. 174-176 °C (lit. [35] mp. 175–177°C); ^{1}H NMR (DMSO-d_6, 300 MHz) δ/ppm: 2.66 (3H, s), 7.62 (1H, s), 7.69 (1H, d), 8.38 (1H, d), 8.66 (1H, s); ^{13}C NMR (DMSO-d_6, 75 MHz) δ/ppm: 27.6, 111.8, 112.1, 118.8, 124.4, 126.7, 142.9, 154.8, 156.8, 187.5.

*4.1.1.2. Synthesis of 2-bromoacetylbenzofuran derivatives (**c1-3**)*

2-Bromoacetyl benzofuran derivatives were prepared in accordance with previously reported methods [46]. A solution of bromine (1 mol) in chloroform was added to a solution of 2-acetyl benzofuran (1 mol) in chloroform. The mixture was stirred at 50 °C for 15 min. The precipitate was filtered and washed with ether. The product was recrystallized from acetic acid.

1-(1-Benzofuran-2-yl)-2-bromoethanone (c1): 80% yield, mp. 90–92 °C; ^{1}H NMR (DMSO-d_6, 300 MHz) δ/ppm: 4.85 (2H, s), 7.40–7.45 (1H, t), 7.55–7.61 (1H, m), 7.88 (1H, t), 8.05 (1H, s), 8.12 (1H, s); ^{13}C NMR (DMSO-d_6, 75 MHz) δ/ppm: 49.7, 111.7, 117.1, 120.9, 122.5, 123.9, 135.5, 151.4, 154.8, 159.8, 185.8.

2-Bromo-1-(5-bromo-1-benzofuran-2-yl) ethanone (c2): 76% yield, mp. 140–142 °C; ^{1}H NMR (DMSO-d_6, 300 MHz) δ/ppm: 4.87 (2H, s), 7.52–7.62 (1H, m), 7.87 (1H, t), 8.07 (1H, s), 8.20 (1H, s); ^{13}C NMR (DMSO-d_6, 75 MHz) δ/ppm: 48.9, 112.5, 116.9, 117.2, 125.4, 130.1, 137.1, 153.3, 161.2, 185.0.

2-Bromo-1-(5-nitro-1-benzofuran-2-yl) ethanone (c3): 72% yield, mp. 211–213 °C; ^{1}H NMR (DMSO-d_6, 300 MHz) δ/ppm: 4.59 (2H, s), 7.68–7.82 (2H, m), 8.40 (1H, d), 8.71 (1H, s); ^{13}C NMR (DMSO-d_6, 75 MHz) δ/ppm: 50.1, 114.7, 117.2, 118.3, 121.4, 132.5, 147.1, 155.1, 169.0, 183.8.

*4.1.1.3. Synthesis of 4-(benzofuran-2-yl)thiazol-2-amine derivatives (**d1-3**)*

4-(benzofuran-2-yl)thiazol-2-amine derivatives were prepared in accordance with previously reported methods [47]. Thiourea (5 mmol) was added to a solution of 2-bromoacetylbenzofuran derivatives (5 mmol) in hot ethanol (20 mL). The mixture was refluxed for 1 hour and cooled.

The mixture was neutralized with aqueous ammonia. The precipitate was filtered and washed with ethanol. The product was recrystallized from ethanol.

4-(benzofuran-2-yl)thiazol-2-amine (d1): 85% yield; mp. 214–266 °C; ^{1}H NMR (DMSO-d_6, 300 MHz) δ/ppm: 6.96 (1H, s), 7.06 (1H, s), 7.22-7.32 (4H, m), 7.57 (1H, d), 7.63 (1H, d); ^{13}C NMR (DMSO-d_6, 75 MHz) δ/ppm: 102.1, 105.3, 110.7, 118.2, 121.3, 122.5, 126.1, 140.3, 151.3, 154.1, 164.3.

4-(5-bromobenzofuran-2-yl)thiazol-2-amine (d2): 85% yield; mp. 234–236 °C; ^{1}H NMR (DMSO-d6, 300 MHz) δ/ppm: 6.95 (1H, s), 7.10 (1H, s), 7.21 (2H, s), 7.42 (1H, d), 7.54 (1H, d), 7.84 (1H, d); ^{13}C NMR (DMSO-d_6, 75 MHz) δ/ppm: 102.2, 104.8, 112.1, 118.5, 122.4, 128.2, 129.5, 140.5, 151.1, 154.5, 164.7.

4-(5-nitrobenzofuran-2-yl)thiazol-2-amine (d3): 85% yield; mp. 244–256 °C; ^{1}H NMR (DMSO-d_6, 300 MHz) δ/ppm: 7.19 (2H, d), 7.36 (2H, s, NH_2), 7.81 (1H, d), 8.17-8.21 (1H, m), 8.61 (1H, d); ^{13}C NMR (DMSO-d_6, 75 MHz) δ/ppm: 103.3, 106.8, 112.4, 118.2, 120.8, 130.8, 140.9, 144.6, 155.7, 157.6, 169.8.

*4.1.1.4. Synthesis of urea substituted benzofuranylthiazole derivatives (**e1-e38**)*

Isocyanate derivatives (1 mmol) were added to a solution of thiazole derivatives (1 mmol) and triethyl amine (1 mL) in dry THF. The mixture was refluxed for 12 h. Tetrahydrofuran was removed using a rotary evaporator, and the mixture was washed with chloroform. The product was recrystallizated from ethanol. **e1**-**e38** were obtained in yields of 77-99%.

1-(4-(benzofuran-2-yl)thiazol-2-yl)-3-(2-methoxyphenyl)urea (e1): Yellowish powder, 64% yield, mp. 263-265 °C; IR: 3260, 3190, 3113, 2957, 1694, 1527, 1292, 1255 cm^{-1}; ^{1}H NMR (DMSO-d_6, 300 MHz) *δ*/ppm: 3.41 (3H, s, -OCH_3), 6.35-6.51 (4H, m, $H_{5,20,21,22}$), 6.73 (1H, d, *J*=8.8 Hz, H_6), 6.78 (1H, s, H_3), 6.97 (1H, s, H_{14}), 7.08 (1H, d, *J*=8.2 Hz, H_7), 7.43 (1H, d, *J*=7.6 Hz, H_{23}), 7.68 (1H, t, *J*=2,1 Hz, H_4), 8.21 (1H, s, NH), 10.68 (1H, s, NH); ^{13}C NMR (DMSO-d_6, 75 MHz) *δ*/ppm: 56.3(-OCH_3), 102.7(C-3), 104.8(C-14), 111.4(C-7), 111.6(C-20), 119.8 (C-4), 121.1(C-22), 121.9(C-23), 122.5(C-5), 123.8(C-18), 125.1(C-6), 129.2(C-21), 129.4(C-9), 141.9(C-14), 148.8(C-19), 152.9(C-2), 153.4(C-16), 154.6(C-8), 163.0(C-12); LC-MS (*m/z*): 366.17 [MH^+]. Anal. Calcd. for $C_{19}H_{15}N_3O_3S$: C, 62.45; H, 4.14; N, 11.50. Found: C, 62.73; H, 4.09; N, 11.33.

1-(4-(benzofuran-2-yl)thiazol-2-yl)-3-(3-methoxyphenyl)urea (e2): Cream powder, 80% yield, mp. 250-252 °C; IR: 3260, 3213, 3111, 2941, 1693, 1525, 1292, 1257 cm^{-1}; ^{1}H NMR (DMSO-d_6, 300 MHz) *δ*/ppm: 3.77 (3H, s, -OCH_3), 6.66 (1H, d, *J*=8.2 Hz, H_{21}), 7.01 (1H, d, *J*=8.0 Hz,

H_{23}), 7.16 (1H, s, H_3), 7.20–7.37 (4H, m, $H_{5,6,14,22}$), 7.58 (1H, s, H_{19}), 7.62 (1H, d, *J*=8.0 Hz, H_7), 7.69 (1H, d, *J*=7.3 Hz, H_4), 8.96 (1H, s, NH), 10.87 (1H, s, NH); ^{13}C NMR (DMSO-d_6, 75 MHz) *δ*/ppm: 55.7(-OCH_3), 103.1(C-3), 105.1(C-14), 109.0(C-19), 110.2(C-7), 111.7(C-23), 118.6(C-21), 122.0(C-4), 123.9(C-5), 125.3(C-6), 129.1(C-9), 130.4(C-22), 140.2(C-18), 140.9(C-10), 152.1(C-2), 152.4(C-16), 154.6(C-7), 154.8(C-20), 160.4(C-12); LC-MS (*m/z)*: 366.17 [MH^+]. Anal. Calcd. for $C_{19}H_{15}N_3O_3S$: C, 62.45; H, 4.14; N, 11.50; found: C, 62.82; H, 4.08; N, 11.27.

1-(4-(benzofuran-2-yl)thiazol-2-yl)-3-(4-methoxyphenyl)urea (e3): White powder, 68% yield, mp. 236-238 °C; IR: 3259, 3188, 3116, 2997, 1674, 1566, 1307, 1252 cm^{-1}; ^{1}H NMR (DMSO-d_6, 300 MHz) *δ*/ppm: 3.71 (3H, s, -OCH_3), 6.90 (2H, d, *J*=9.1 Hz, $H_{20,22}$), 7.11 (1H, s, H_3), 7.24-7.33 (2H, m, $H_{5,6}$), 7.38 (2H, d, *J*=8.8 Hz, $H_{19,23}$), 7.52 (1H, s, H_{14}), 7.59 (1H, d, *J*=7.6 Hz, H_7), 7.65 (1H, d, *J*=7.3 Hz, H_4), 8.73 (1H, s, NH), 10.80 (1H, s, NH); ^{13}C NMR (DMSO-d_6, 75 MHz) *δ*/ppm: 55.8(-OCH_3), 103.1(C-3), 110.1(C-14), 111.7(C-7), 114.7(C-20,22), 121.3(C-19,23), 122.0(C-4), 123.9(C-5), 125.3(C-6), 129.1(C-9), 131.9(C-18), 140.8(C-10), 152.3(C-2), 152.5(C-16), 154.8(C-8), 155.8(C-21), 160.7(C-12); LC-MS (*m/z)*: 366.12 [MH^+]. Anal. Calcd. for $C_{19}H_{15}N_3O_3S$: C, 62.45; H, 4.14; N, 11.50; found: C, 62.58; H, 4.17; N, 11.43.

1-(4-(benzofuran-2-yl)thiazol-2-yl)-3-(p-tolyl)urea (e4): Cream powder, 75% yield, mp. 269-271 °C; IR: 3323, 3271, 3121, 2916, 1687, 1556, 1288, 1242 cm^{-1}; ^{1}H NMR (DMSO-d_6, 300 MHz) *δ*/ppm2.24 (3H, s, 4-CH_3), 7.11 (2H, d, *J*=8.2 Hz, $H_{20,22}$) 7.12 (1H, s, H_3) 7.24 –7 34 (2H, m, $H_{5,6}$), 7.36 (2H, d, *J*=8.2 Hz, $H_{19,23}$), 7.53 (1H, s, H_{14}) 7.59 (1H, d, *J*= 7.9 Hz, H_7), 7.67 (1H, d, *J*=8.2 Hz, H_4), 8.82 (1H, s, NH), 10.81 (1H, s, NH); ^{13}C NMR (DMSO-d_6, 75 MHz) *δ*/ppm: 21.0(-CH_3), 103.1(C-3), 110.1(C-14), 111.7(C-7), 119.5(C-4), 122.0(C-19,23), 123.9(C-5), 125.3(C-6), 129.1(C-20,22), 130.0(C-9), 132.5(C-18), 136.4(C-21), 140.8(C-10), 152.1(C-2), 152.4(C-16), 154.8(C-8), 160.6(C-12);LC-MS (*m/z)*: 350.11 [MH^+]. Anal. Calcd. for $C_{19}H_{15}N_3O_2S$: C, 65.31; H, 4.33; N, 12.03; found: C, 65.44; H, 4.29; N, 12.08.

1-(4-(benzofuran-2-yl)thiazol-2-yl)-3-phenylurea (e5): White powder, 78% yield, mp. 283-285 °C; IR: 3209, 3132, 3034, 2949, 1681, 1512, 1269, 1255 cm^{-1}; ^{1}H NMR (DMSO-d_6, 300 MHz) *δ*/ppm: 7.04 (1H, t, *J*=7.3 Hz, H_{21}), 7.12(1H, s, H_3), 7.24-7.34 (4H, m, $H_{5,6,20,22}$), 7.50 (2H, d, *J*=11.5 Hz, $H_{19,23}$), 7.54 (1H, s, H_{14}), 7.59 (1H, d, *J*=8.2 Hz, H_7), 7.65 (1H, d, *J*= 7.3 Hz, H_4), 8.93 (1H, s, NH), 10.86 (1H, s, NH); ^{13}C NMR (DMSO-d_6, 75 MHz) *δ*/ppm: 103.1(C-3), 110.2(C-14), 111.7(C-7), 119.4(C-4), 122.0(C-19,23), 123.6(C-5), 123.9(C-6), 125.3(C-21), 129.1(C-20,22), 129.6(C-9), 139.0(C-18), 140.8(C-10), 152.2(C-2), 152.4(C-16), 154.8(C-8), 160.6(C-12); LC-

MS (*m/z*): 335.89 [MH^+]. Anal. Calcd. for $C_{18}H_{13}N_3O_2S$: C, 64.46; H, 3.91; N, 12.53; found: C, 64.57; H, 3.88; N, 12.50.

1-(4-(benzofuran-2-yl)thiazol-2-yl)-3-(2-nitrophenyl)urea (e6): Orange powder, 70% yield, mp. 253-255 °C; IR: 3323, 3286, 3126, 2953, 1697, 1492, 1332, 1266 cm^{-1}; ^1H NMR (DMSO-d_6, 300 MHz) δ/ppm: 7.12 (1H, s, H_3), 7.24-7.33 (3H, m, $H_{5,6,7}$), 7.57-7.60 (2H, m, $H_{13,21}$), 7.67 (1H, dd, J_1=1.2 Hz; J_2=7.0 Hz, H_4), 7.73 (1H, td, J_1=1.4 Hz; J_2=7.1 Hz, H_{22}), 8.12 (1H, dd, J_1=1.4 Hz; J_2=8.5 Hz, H_{20}), 8.32 (1H, dd, J_1=1.2 Hz; J_2=8.5 Hz, H_{23}), 9.92 (1H, s, NH), 12.18 (1H, s, NH); ^{13}C NMR (DMSO-d_6, 75 MHz) δ/ppm: 103.2(C-3), 110.5(C-14), 111.7(C-7), 119.8(C-23), 122.1(C-4), 123.6(C-5), 124.0(C-6), 125.4(C-20), 126.2(C-21), 129.1(C-9), 134.3(C-18), 135.8(C-22), 138.7(C-19), 141.1(C-10), 152.1(C-2), 152.3(C-16), 154.8(C-8), 160.4(C-12); LC-MS (*m/z*): 380.85 [MH^+]. Anal. Calcd. for $C_{18}H_{12}N_4O_4S$: C, 56.84; H, 3.18; N, 14.73; found: C, 56.92; H, 3.14; N, 14.77.

1-(4-(benzofuran-2-yl)thiazol-2-yl)-3-(3-nitrophenyl)urea (e7): Yellowish powder, 65% yield, mp. 257-259 °C; IR: 3325, 3210, 3151, 2980, 1691, 1527, 1344, 1294, 1246 cm^{-1}; ^1H NMR (DMSO-d_6, 300 MHz) δ/ppm: 7.16 (1H, s, H_3), 7.25-7.37 (2H, m, $H_{5,6}$), 7.59-7.65 (3H, m, $H_{7,14,22}$), 7.69 (1H, d, J=8.2 Hz, H_4), 7.82 (1H, d, J=8.2 Hz, H_{23}), 7.91 (1H, dd, J_1=1.5 Hz; J_2=8.2 Hz, H_{21}), 8.58 (1H, s, H_{19}), 9.46 (1H, s, NH), 11.20 (1H, s, NH); ^{13}C NMR (DMSO-d_6, 75 MHz) δ/ppm: 103.2(C-3), 110.5(C-14), 111.7(C-7), 113.4(C-19), 118.0(C-21), 122.1(C-4), 124.0(C-5), 125.4(C-9), 125.7(C-6), 129.1(C-23), 130.9(C-22), 140.4(C-18), 140.9(C-10), 148.7(C-20), 152.3(C-2), 152.4(C-16), 154.8(C-8), 160.3(C-12); LC-MS (*m/z*): 381.22 [MH^+]. Anal. Calcd. for $C_{18}H_{12}N_4O_4S$: C, 56.84; H, 3.18; N, 14.73; found: C, 56.90; H, 3.15; N, 14.70.

1-(4-(benzofuran-2-yl)thiazol-2-yl)-3-(4-nitrophenyl)urea (e8): Yellowish powder, 85% yield, mp. 304-306 °C; IR: 3466, 3213, 3126, 2976, 1693, 1560, 1512, 1330, 1298, 1253 cm^{-1}; ^1H NMR (DMSO-d_6, 300 MHz) δ/ppm: 7.16 (1H, s, H_3), 7.25-7.36 (2H, m, $H_{5,6}$), 7.60-7.63 (2H, m, $H_{7,14}$), 7.68 (1H, d, J=7.6 Hz, H_4), 7.75 (2H, d, J=9.1 Hz, $H_{19,23}$), 8.23 (2H, d, J=9.1 Hz, $H_{20,22}$), 9.63 (1H, s, NH), 11.16 (1H, s, NH); ^{13}C NMR (DMSO-d_6, 75 MHz) δ/ppm: 103.2(C-3), 110.7(C-14), 111.7(C-7), 118.9(C-19,23), 122.1(C-4), 124.0(C-5), 125.4(C-20,22), 125.8(C-6), 129.1(C-9), 141.2(C-10), 142.5(C-21), 145.6(C-18), 152.0(C-2), 152.3(C-16), 154.8(C-8), 160.1(C-12); LC-MS (*m/z*): 380.89 [MH^+]. Anal. Calcd. for $C_{18}H_{12}N_4O_4S$: C, 56.84; H, 3.18; N, 14.73; found: C, 56.89; H, 3.13; N, 14.76.

1-(4-(benzofuran-2-yl)thiazol-2-yl)-3-(2-fluorophenyl)urea (e9): Cream powder, 85% yield, mp. 273-275 °C; IR: 3203, 3113, 3087, 2954, 1701, 1519, 1280, 1257 cm^{-1}; ^{1}H NMR (DMSO-d_6, 300 MHz) δ/ppm: 7.10-7.23 (3H, m, $H_{3,21,22}$), 7.25-7.37 (3H, m, $H_{5,6,20}$), 7.59 (1H, s, H_{14}), 7.64 (1H, d, J=8.2 Hz, H_7), 7.69 (1H, d, J=7.9 Hz, H_4), 8.15 (1H, td, J_1=1.8 Hz; J_2=8.2 Hz, H_{23}), 8.99 (1H, s, NH), 11.15 (1H, s, NH); ^{13}C NMR (DMSO-d_6, 75 MHz) δ/ppm: 103.2(C-3), 110.3(C-14), 111.7(C-7), 115.7(C-20), 116.0(C-18), 121.5(C-4), 122.1(C-23), 124.0(C-5), 124.4(C-6), 125.4(C-9), 126.9(C-22), 127.1(C-21), 129.1(C-10), 140.9(C-2), 151.9(C-16), 152.3(C-8), 154.8(C-19), 160.4(C-12); LC-MS (*m/z)*: 354.20 [MH^+]. Anal. Calcd. for $C_{18}H_{12}FN_3O_2S$: C, 61.18; H, 3.42; N, 11.89; found: C, 61.23; H, 3.39; N, 11.87.

1-(4-(benzofuran-2-yl)thiazol-2-yl)-3-(3-fluorophenyl)urea (e10): Cream powder, 80% yield, mp. 293-295 °C; IR: 3258, 3205, 3116, 2962, 1689, 1573, 1516, 1294, 1255 cm^{-1}; ^{1}H NMR (DMSO-d_6, 300 MHz) δ/ppm: 6.86 (1H, td, J_1=1.8 Hz; J_2=8.2 Hz, H_{21}), 7.12 (1H, s, H_3), 7.17-7.38 (4H, m, $H_{5,6,14,23}$), 7.48 (1H, dt, J_1=2.0 Hz; J_2=11.4 Hz, H_{22}), 7.56 (1H, s, H_{19}), 7.59 (1H, d, J=8.5 Hz, H_7), 7.67 (1H, dd, J_1=1.2 Hz; J_2=8.5 Hz, H_4), 9.14 (1H, s, NH), 10.96 (1H, s, NH); ^{13}C NMR (DMSO-d_6, 75 MHz) δ/ppm: 103.2(C-3), 106.0(C-14), 106.3(C-7), 109.8(C-4), 110.4(C-19), 111.7(C-21), 115.2(C-23), 122.1(C-5), 124.0(C-6), 125.4(C-9), 129.1(C-22), 131.2(C-18), 131.3(C-10), 140.8(C-2), 152.1(C-16), 152.4(C-8), 154.8(C-20), 160.4(C-12); LC-MS (*m/z)*: 354.16 [MH^+]. Anal. Calcd. for $C_{18}H_{12}FN_3O_2S$: C, 61.18; H, 3.42; N, 11.89; found: C, 61.13; H, 3.45; N, 11.93.

1-(4-(benzofuran-2-yl)thiazol-2-yl)-3-(4-fluorophenyl)urea (e11): White powder, 80% yield, mp. 264-266 °C; IR: 3266, 3224, 3132, 2958, 1685, 1520, 1269, 1255 cm^{-1}; ^{1}H NMR (DMSO-d_6, 300 MHz) δ/ppm: 7.12 (1H, s, H_3), 7.17 (2H, d, J=8.8 Hz, $H_{20,22}$), 7.22-7.33 (2H, m, $H_{5,6}$), 7.41-7.52 (2H, m, $H_{19,23}$), 7.54 (1H, s, H_{14}), 7.59 (1H, d, J=8.2 Hz, H_7), 7.65 (1H, dd, J_1=0.9 Hz; J_2=7.5 Hz, H_4), 8.95 (1H, s, NH), 10.90 (1H, s, NH); ^{13}C NMR (DMSO-d_6, 75 MHz) δ/ppm: 103.1(C-3), 110.2(C-14), 111.7(C-7), 116.0(C-22), 116.3(C-20), 120.6(C-23), 121.4(C-19), 121.5(C-4), 122.1(C-5), 123.9(C-6), 125.3(C-9), 129.1(C-18), 135.3(C-10), 140.8(C-2), 152.3(C-16), 152.4(C-8), 154.8(C-21), 160.6(C-12); LC-MS (*m/z)*: 352.79 [M^+]. Anal. Calcd. for $C_{18}H_{12}FN_3O_2S$: C, 61.18; H, 3.42; N, 11.89; found: C, 61.21; H, 3.46; N, 11.91.

1-(4-(benzofuran-2-yl)thiazol-2-yl)-3-(3-chlorophenyl)urea (e12): White solid, 90% yield, mp. 244-246 °C; IR: 3441, 3192, 3110, 2989, 1693, 1573, 1286, 1259 cm^{-1}; ^{1}H NMR (DMSO-d_6, 300 MHz) δ/ppm: 7.06-7.10 (1H, m, H_{21}), 7.12 (1H, s, H_3), 7.24-7.33 (4H, m, $H_{5,6,22,23}$), 7.56 (1H,

s, H_{14}), 7.59 (1H, d, *J*=7.6 Hz, H_7), 7.65 (1H, dd, J_1=1.2 Hz; J_2=7.6 Hz, H_4), 7.70 (1H, s, H_{19}), 9.11 (1H, s, NH), 10.99 (1H, s, NH); ^{13}C NMR (DMSO-d_6, 75 MHz) *δ*/ppm: 103.2(C-3), 110.4(C-14), 111.7(C-7), 117.9(C-23), 118.8(C-4), 122.1(C-5), 123.2(C-19), 124.0(C-6), 125.4(C-21), 129.1(C-9), 131.2(C-22), 133.9(C-20), 140.6(C-18), 140.9(C-10), 152.2(C-2), 152.4(C-16), 154.8(C-8), 160.4(C-12); LC-MS (*m/z*): 370.09 [MH^+]. Anal. Calcd. for $C_{18}H_{12}ClN_3O_2S$: C, 58.46; H, 3.27; N, 11.36; found: C, 58.50; H, 3.24; N, 11.39.

1-(4-(benzofuran-2-yl)thiazol-2-yl)-3-(4-chlorophenyl)urea (e13): White powder, 80% yield, mp. 294-296 °C; IR: 3228, 3112, 3047, 2953, 1689, 1510, 1497, 1269, 1253 cm^{-1}; ^{1}H NMR (DMSO-d_6, 300 MHz) *δ*/ppm: 7.15 (1H, s, H_3), 7.25-7.37 (2H, m, $H_{5,6}$), 7.40 (2H, d, *J*=9.0 Hz, $H_{20,22}$), 7.55 (2H, d, *J*=8.8 Hz, $H_{19,23}$), 7.59 (1H, s, H_{14}), 7.62 (1H, dd, J_1=1.2 Hz; J_2=8.2 Hz, H_7), 7.69 (1H, dd, J_1=1.2 Hz; J_2=7.3 Hz, H_4), 9.09 (1H, s, NH), 10.97 (1H, s, NH); ^{13}C NMR (DMSO-d_6, 75 MHz) *δ*/ppm: 103.1(C-3), 110.3(C-14), 111.7(C-7), 121.0(C-19,23), 122.1(C-4), 123.9(C-5), 125.4(C-6), 127.1(C-20,22), 129.1(C-9), 129.4(C-21), 138.1(C-18), 140.8(C-10), 152.1(C-2), 152.4(C-16), 154.8(C-8), 160.4(C-12); LC-MS (*m/z*): 370.08 [MH^+]. Anal. Calcd. for $C_{18}H_{12}ClN_3O_2S$: C, 58.46; H, 3.27; N, 11.36; found: C, 58.52; H, 3.22; N, 11.34.

1-(4-(benzofuran-2-yl)thiazol-2-yl)-3-(3,4-dichlorophenyl)urea (e14): Cream powder, 85% yield, mp. 285-287 °C; IR: 3242, 3116, 3053, 2949, 1701, 1517, 1284, 1253 cm^{-1}; ^{1}H NMR (DMSO-d_6, 300 MHz) *δ*/ppm: 7.15 (1H, s, H_3), 7.24-7.36 (2H, m, $H_{5,6}$), 7.42 (1H, dd, J_1=2.4 Hz; J_2=8.8 Hz, H_{23}), 7.57 (1H, s, H_{14}), 7.60-7.63 (2H, m, $H_{7,22}$), 7.69 (1H, dd, J_1=0.9 Hz; J_2=6.7 Hz, H_4), 7.90 (1H, d, *J*=2.3 Hz H_{19}), 9.23 (1H, s, NH), 11.14 (1H, s, NH); ^{13}C NMR (DMSO-d_6, 75 MHz) *δ*/ppm: 103.2(C-3), 110.5(C-14), 111.7(C-7), 119.7(C-4), 120.6(C-22), 122.1(C-23), 124.0(C-5), 125.0(C-6), 125.4(C-9), 129.1(C-19), 131.4(C-21), 131.8(C-20), 139.3(C-18), 140.9(C-10), 152.1(C-2), 152.4(C-16), 154.8(C-8), 160.3(C-12); LC-MS (*m/z*): 404.10 [MH^+]. Anal. Calcd. for $C_{18}H_{11}Cl_2N_3O_2S$: C, 53.48; H, 2.74; N, 10.39; found: C, 53.53; H, 2.78; N, 10.37.

1-(4-(benzofuran-2-yl)thiazol-2-yl)-3-(4-bromophenyl)urea (e15): White powder, 80% yield, mp. 291-293 °C; IR: 3230, 3128, 3061, 2951, 1685, 1512, 1490, 1273, 1253 cm^{-1}; ^{1}H NMR (DMSO-d_6, 300 MHz) *δ*/ppm: 7.12 (1H, s, H_3), 7.22-7.33 (2H, m, $H_{5,6}$), 7.45 (2H, d, *J*=9.7 Hz, $H_{20,22}$), 7.50 (2H, d, *J*=9.7 Hz, $H_{19,23}$), 7.55 (1H, s, H_{14}), 7.59 (1H, d, *J*=7.9 Hz, H_7), 7.65 (1H, d, *J*=7.6 Hz, H_4), 9.06 (1H, s, NH), 10.94 (1H, s, NH); ^{13}C NMR (DMSO-d_6, 75 MHz) *δ*/ppm: 103.3(C-3), 110.5(C-14), 111.9(C-7), 115.3(C-21), 118.8(C-19), 118.9(C-23), 121.6(C-4), 122.3(C-20), 124.2(C-22), 125.6(C-6), 129.3(C-9), 132.5(C-5), 138.7(C-18), 141.1(C-10), 152.3(C-2),

152.6(C-16), 155.0(C-8), 160.6(C-12); LC-MS (*m/z)*: 414.13 [MH^+]. Anal. Calcd. for $C_{18}H_{12}BrN_3O_2S$: C, 52.19; H, 2.92; N, 10.14; found: C, 52.15; H, 2.95; N, 10.16.

1-(4-(benzofuran-2-yl)thiazol-2-yl)-3-(4-iodophenyl)urea (e16): White powder, 68% yield, mp. 254-256 °C; IR: 3228, 3113, 3055, 2955, 1687, 1512, 1495, 1292, 1255 cm^{-1}; ^{1}H NMR (DMSO-d_6, 300 MHz) δ/ppm: 7.14 (1H, s, H_3), 7.24-7.37 (4H, m, $H_{5,6,20,22}$), 7.57 (1H, s, H_{14}), 7.61 (2H, dd, J_1=2.6 Hz; J_2=8.2 Hz, $H_{4,7}$), 7.68 (2H, dd, J_1=2.4 Hz; J_2=8.5 Hz, $H_{19,23}$), 9.04 (1H, s, NH), 10.92 (1H, s, NH); ^{13}C NMR (DMSO-d_6, 75 MHz) δ/ppm: 86.8(C-21), 103.1(C-3), 110.3(C-14), 111.7(C-7), 121.6(C-4), 122.0(C-19,23), 123.9(C-5), 125.3(C-6), 129.1(C-9), 138.1(C-20,22), 139.0(C-18), 140.9(C-10), 152.1(C-2), 152.4(C-16), 154.8(C-8), 160.4(C-12); LC-MS (*m/z)*: 462.10 [MH^+]. Anal. Calcd. for $C_{18}H_{12}IN_3O_2S$: C, 46.87; H, 2.62; N, 9.11; found: C, 46.84; H, 2.65; N, 9.13.

1-(4-(5-bromobenzofuran-2-yl)thiazol-2-yl)-3-(2-methoxyphenyl)urea (e17): Greenish powder, 70% yield, mp. 271-273 °C; IR: 3242, 3120, 3060, 2935, 1697, 1523, 1282, 1257 cm^{-1}; ^{1}H NMR (DMSO-d_6, 300 MHz) δ/ppm: 3.87 (3H, s, -OCH_3), 6.89-7.06 (3H, m, $H_{20,21,22}$), 7.1 (1H, s, H_3), 7.44 (1H, dd, J_1=2.1 Hz; J_2=8.8 Hz, H_7), 7.57 (2H, t, J=4.1 Hz, $H_{6,14}$), 7.86 (1H, d, J=2.1 Hz, H_{23}), 8.10 (1H, d, J=9.0 Hz, H_4), 8.75 (1H, s, NH), 11.37 (1H, s, NH); ^{13}C NMR (DMSO-d_6, 75 MHz) δ/ppm: 56.5(-OCH_3), 102.6(C-3), 111.0(C-14), 111.6(C-20), 113.7(C-7), 116.2(C-5), 119.2(C-23), 121.3(C-22), 123.7(C-4), 124.4(C-18), 127.8(C-21), 128.1(C-6), 131.5(C-9), 140.3(C-10), 148.6(C-19), 152.0(C-2), 153.6(C-16), 153.7(C-8), 160.7(C-12); LC-MS (*m/z)*: 444.26 [MH^+]. Anal. Calcd. for $C_{19}H_{14}BrN_3O_3S$: C, 51.36; H, 3.18; N, 9.46; found: C, 51.33; H, 3.14; N, 9.49.

1-(4-(5-bromobenzofuran-2-yl)thiazol-2-yl)-3-(3-methoxyphenyl)urea (e18): Yellow powder, 78% yield, mp. 264-266 °C; IR: 3266, 3217, 3107, 2953, 1691, 1525, 1290, 1255 cm^{-1}; ^{1}H NMR (DMSO-d_6, 300 MHz) δ/ppm: 3.75 (3H, s, -OCH_3), 6.62 (1H, dd, J_1=2.3 Hz; J_2=8.2 Hz, H_{21}), 6.97 (1H, d, J=7.9 Hz, H_{23}), 7.10 (1H, s, H_3), 7.16 (1H, t, J=2.3 Hz, H_7), 7.21 (1H, t, J=8.2 Hz, H_{22}), 7.44 (1H, dd, J_1=2.0 Hz; J_2=8.8 Hz, H_6), 7.57 (1H, s, H_{14}), 7.60 (1H, s, H_{19}), 7.86 (1H, d, J=2.0 Hz, H_4), 8.94 (1H, s, NH), 10.84 (1H, s, NH); ^{13}C NMR (DMSO-d_6, 75 MHz) δ/ppm: 55.7(-OCH_3), 102.7(C-3), 105.2(C-14), 109.1(C-9), 111.2(C-7), 111.7(C-23), 113.7(C-5), 116.2(C-21), 118.6(C-4), 124.4(C-22), 127.9(C-6), 130.5(C-9), 131.4(C-18), 140.1(C-10), 140.3(C-2), 152.1(C-16), 153.6(C-8), 153.8(C-20), 160.3(C-12); LC-MS (*m/z)*: 444.08 [MH^+]. Anal. Calcd. for $C_{19}H_{14}BrN_3O_3S$: C, 51.36; H, 3.18; N, 9.46; found: C, 51.38; H, 3.20; N, 9.43.

1-(4-(5-bromobenzofuran-2-yl)thiazol-2-yl)-3-(4-methoxyphenyl)urea (e19): Cream powder, 75% yield, mp. 260-262 °C; IR: 3269, 3211, 3115, 2937, 1685, 1525, 1274, 1255 cm^{-1}; ^{1}H NMR (DMSO-d_6, 300 MHz) δ/ppm: 3.72 (3H, s, -OCH_3), 6.83 (1H, d, J=7.6 Hz, H_{19}), 6.89 (2H, d, J=7.9 Hz, $H_{20,22}$), 7.10 (1H, s, H_3), 7.31 (1H, d, J=7.9 Hz, H_{23}), 7.38 (1H, d, J=7.9 Hz, H_7), 7.43 (1H, d, J=8.8 Hz, H_6), 7.57 (1H, s, H_{14}), 7.86 (1H, s, H_4), 8.75 (1H, s, NH), 10.79 (1H, s, NH); ^{13}C NMR (DMSO-d_6, 75 MHz) δ/ppm: 55.8(-OCH_3), 102.6(C-3), 111.1(C-14), 113.7(C-7), 114.7(C-20,22), 116.2(C-5), 121.4(C-19,23), 124.4(C-4), 127.8(C-6), 131.5(C-9), 131.9(C-18), 133.7(C-10), 140.3(C-2), 152.3(C-16), 153.6(C-8), 155.9(C-21), 160.8(C-12); LC-MS (*m/z)*: 444.16 [MH^+]. Anal. Calcd. for $C_{19}H_{14}BrN_3O_3S$: C, 51.36; H, 3.18; N, 9.46; found: C, 51.39; H, 3.15; N, 9.49.

1-(4-(5-bromobenzofuran-2-yl)thiazol-2-yl)-3-(p-tolyl)urea (e20): Cream powder, 80% yield, mp. 277-279 °C; IR: 3259, 3199, 3113, 2914, 1685, 1520, 1319, 1295, 1257 cm^{-1}; ^{1}H NMR (DMSO-d_6, 300 MHz) δ/ppm: 2.24 (3H, s, 4-CH_3), 7.10 (1H, s, H_3), 7.12 (2H, d, J=8.5 Hz, $H_{20,22}$), 7.35 (2H, d, J=8.5 Hz, $H_{19,23}$), 7.44 (1H, dd, J_1=2.0 Hz; J_2=8.8 Hz, H_7), 7.57 (1H, s, H_{14}), 7.59 (1H, d, J=8.8 Hz, H_6), 7.86 (1H, d, J=2.0 Hz, H_4), 8.83 (1H, s, NH), 10.81 (1H, s, NH); ^{13}C NMR (DMSO-d_6, 75 MHz) δ/ppm: 21.0(-CH_3), 102.6(C-3), 111.2(C-5), 113.7(C19,23), 116.2(C-14), 119.5(C-7), 124.4(C-4), 127.8(C-20,22), 130.0(C-9), 131.5(C-6), 132.6(C-18), 136.4(C-21), 140.3(C-10), 152.1(C-2), 153.6(C-16), 153.7(C-8), 160.7(C-12); LC-MS (*m/z)*: 428.69 [MH^+]. Anal. Calcd. for $C_{18}H_{12}BrN_3O_2S$: C, 53.28; H, 3.29; N, 9.81; found: C, 53.25; H, 3.27; N, 9.85.

1-(4-(5-bromobenzofuran-2-yl)thiazol-2-yl)-3-phenylurea (e21): Cream powder, 72% yield, mp. 329-331 °C; IR: 3232, 3200, 3111, 2943, 1695, 1519, 1498, 1274, 1252 cm^{-1}; ^{1}H NMR (DMSO-d_6, 300 MHz) δ/ppm: 7.04 (1H, t, J=7.3 Hz, H_{21}), 7.10 (1H, s, H_3), 7.25-7.38 (2H, m, $H_{20,22}$), 7.41-7.53 (3H, m, $H_{7,19,23}$), 7.56 (1H, s, H_{14}), 7.59 (1H, s, H_6), 7.86 (1H, d, J=2.0 Hz, H_4), 8.92 (1H, s, NH), 10.83 (1H, s, NH); ^{13}C NMR (DMSO-d_6, 75 MHz) δ/ppm: 102.6(C-3), 111.2(C-14), 113.7(C-7), 116.2(C-5), 119.4(C-19,23), 123.6(C-4), 124.4(C-21), 127.8(C-20,22), 129.6(C-6), 131.5(C-9), 139.0(C-18), 140.3(C-10), 152.1(C-2), 153.6(C-16), 153.7(C-8), 160.7(C-12); LC-MS (*m/z)*: 414.77[MH^+]. Anal. Calcd. for $C_{18}H_{12}BrN_3O_2S$: C, 52.19; H, 2.92; N, 10.14; found: C, 52.28; H, 2.87; N, 10.11.

1-(4-(5-bromobenzofuran-2-yl)thiazol-2-yl)-3-(2-nitrophenyl)urea (e22): Greenish powder, 82 % yield, mp. 337-339 °C; IR: 3254, 3206, 3115, 2960, 1695, 1525, 1348, 1280, 1259 cm^{-1}; ^{1}H NMR (DMSO-d_6, 300 MHz) δ/ppm: 7.11 (1H, s, H_3), 7.28 (1H, t, J=7.3 Hz, H_{21}), 7.44 (1H, dd,

J_1=2.0 Hz; J_2=8.8 Hz, H_7), 7.57 (1H, d, J=8.8 Hz, H_6), 7.64 (1H, s, H_{14}), 7.74 (1H, t, J=7.3 Hz, H_{22}), 7.87 (1H, d, J=1.8 Hz, H_4), 8.12 (1H, d, J=8.2 Hz, H_{20}), 8.30 (1H, d, J=8.2 Hz, H_{23}), 9.91 (1H, s, NH), 12.18 (1H, s, NH); ^{13}C NMR (DMSO-d_6, 75 MHz) δ/ppm: 102.6(C-3), 111.2(C-14), 113.7(C-7), 116.2(C-5), 119.4 (C-6), 123.6(C-18), 124.4(C-4), 127.8(C-21), 129.6(C-20,22), 131.5(C-9), 139.0(C-19,23), 140.3(C-10), 152.1(C-2), 153.6(C-16), 153.7(C-8), 160.7(C-12); LC-MS (*m/z*): 459.02 [MH^+]. Anal. Calcd. for $C_{18}H_{11}BrN_4O_4S$: C, 47.07; H, 2.41; N, 12.20; found: C, 47.18; H, 2.45; N, 12.22.

1-(4-(5-bromobenzofuran-2-yl)thiazol-2-yl)-3-(3-nitrophenyl)urea (e23): Cream powder, 80% yield, mp. 292-294 °C; IR: 3331, 3280, 3095, 2940, 1699, 1552, 1520, 1325, 1284, 1247 cm^{-1}; ^{1}H NMR (DMSO-d_6, 300 MHz) δ/ppm: 7.10 (1H, s, H_3), 7.42 (1H, dd, J_1=1.8 Hz; J_2=8.5 Hz, H_7), 7.57 (2H, d, J=8.5 Hz, $H_{6,21}$), 7.62 (1H, s, H_{14}), 7.73-7.89 (3H, m, $H_{4,22,23}$), 8.53 (1H, s, H_{19}), 9.42 (1H, s, NH), 11.11 (1H, s, NH); ^{13}C NMR (DMSO-d_6, 75 MHz) δ/ppm: 102.7(C-3), 111.5(C-14), 113.4(C-7), 113.7(C-19), 116.2(C-5), 118.0(C-21), 124.4(C-4), 125.3(C-23), 125.6(C-22), 127.8(C-6), 130.8(C-9), 131.4(C-18), 140.4(C-10), 148.7(C-20), 152.2(C-2), 153.0(C-16), 153.6(C-8), 160.6(C-12); LC-MS (*m/z*): 459.07 [MH^+]. Anal. Calcd. for $C_{18}H_{11}BrN_4O_4S$: C, 47.07; H, 2.41; N, 12.20; found: C, 47.14; H, 2.43; N, 12.25.

1-(4-(5-bromobenzofuran-2-yl)thiazol-2-yl)-3-(4-nitrophenyl)urea (e24): Orange powder, 85% yield, mp. 337-339 °C; IR: 3367, 3338, 3122, 2962, 1703, 1517, 1506, 1295, 1255 cm^{-1}; ^{1}H NMR (DMSO-d_6, 300 MHz) δ/ppm: 7.11 (1H, s, H_3), 7.42 (1H, dd, J_1=2.0 Hz; J_2=8.5 Hz, H_7), 7.55 (1H, d, J=8.8 Hz, H_6), 7.63 (1H, s, H_{14}), 7.70 (2H, d, J=9.0 Hz, $H_{19,23}$), 7.84 (1H, d, J=2.0 Hz, H_4), 8.18 (2H, d, J=9.0 Hz, $H_{20,22}$), 9.60 (1H, s, NH), 11.08 (1H, s, NH); ^{13}C NMR (DMSO-d_6, 75 MHz) δ/ppm: 102.7(C-3), 111.5(C-14), 113.5(C-7), 113.7(C-5), 116.2(C-19,23), 118.0(C-4), 124.5(C-20,22), 125.7(C-6), 127.9(C-9), 130.9(C-10), 131.5(C-21), 140.4(C-2), 148.7(C-18), 152.3(C-16), 153.6(C-8), 160.4(C-12); LC-MS (*m/z*): 459.59 [MH^+]. Anal. Calcd. for $C_{18}H_{11}BrN_4O_4S$: C, 47.07; H, 2.41; N, 12.20; found: C, 47.16; H, 2.40; N, 12.23.

1-(4-(5-bromobenzofuran-2-yl)thiazol-2-yl)-3-(2-fluorophenyl)urea (e25): White powder, 87% yield, mp. 346-348 °C; IR: 3270, 3209, 3113, 2947, 1689, 1521, 1284, 1257 cm^{-1}; ^{1}H NMR (DMSO-d_6, 300 MHz) δ/ppm: 7.07-7.17 (3H, m, $H_{3,21,22}$), 7.27 (1H, td, J_1=1.5 Hz; J_2=8.2 Hz, H_{20}), 7.43 (1H, dd, J_1=2.0 Hz; J_2=8.5 Hz, H_7), 7.58 (1H, d, J=8.8 Hz, H_6), 7.61 (1H, s, H_{14}), 7.86 (1H, d, J=2.0 Hz, H_4), 8.11 (1H, td, J_1=1.8 Hz; J_2=8.2 Hz, H_{23}), 8.94 (1H, s, NH), 11.09 (1H, s, NH); ^{13}C NMR (DMSO-d_6, 75 MHz) δ/ppm: 102.8(C-3), 111.7(C-14), 113.7(C-7), 116.3(C-20),

118.6(C-5), 118.9(C-18), 124.5(C-23), 125.8(C-4), 127.9(C-22), 131.5(C-21), 140.5(C-6), 142.2(C-9), 142.5(C-10), 145.6(C-2), 146.3(C-16), 152.3(C-8), 153.7(C-19), 160.3(C-12); LC-MS (*m/z)*: 431.83 [MH^+]. Anal. Calcd. for $C_{18}H_{11}BrFN_3O_2S$: C, 50.01; H, 2.56; N, 9.72; found: C, 50.12; H, 2.50; N, 9.70.

1-(4-(5-bromobenzofuran-2-yl)thiazol-2-yl)-3-(3-fluorophenyl)urea (e26): Cream powder, 65% yield, mp. 272-274 °C; IR: 3271, 3207, 3113, 2953, 1701, 1519, 1294, 1257 cm^{-1}; ^1H NMR (DMSO-d_6, 300 MHz) δ/ppm: 6.86 (1H, td, J_1=2.0 Hz; J_2=8.5 Hz, H_{21}), 7.10 (1H, s, H_3), 7.18 (1H, d, J=8.2 Hz, H_{23}), 7.34 (1H, q, J=7.6 Hz, H_{22}), 7.41-7.50 (2H, m, $H_{7,19}$), 7.58 (1H, d, J=8.5 Hz, H_6), 7.60 (1H, s, H_{14}), 7.86 (1H, d, J=1.8 Hz, H_4), 9.14 (1H, s, NH), 10.95 (1H, s, NH); ^{13}C NMR (DMSO-d_6, 75 MHz) δ/ppm: 102.7(C-3), 106.0(C-14), 106.3(C-7), 109.9(C-19), 110.1(C-21), 111.3(C-5), 113.7(C-23), 115.2(C-4), 116.2(C-22), 124.4(C-6), 127.8(C-9), 131.1(C-18), 131.4(C-10), 140.3(C-2), 140.9(C-16), 152.1(C-8), 153.6(C-20), 160.5(C-12); LC-MS (*m/z)*: 432.19 [MH^+]. Anal. Calcd. for $C_{18}H_{11}BrFN_3O_2S$: C, 50.01; H, 2.56; N, 9.72; found: C, 50.09; H, 2.53; N, 9.89.

1-(4-(5-bromobenzofuran-2-yl)thiazol-2-yl)-3-(4-fluorophenyl)urea (e27): White powder, 62% yield, mp. 258-260 °C; IR: 3278, 3109, 3080, 2951, 1697, 1527, 1276, 1259, 1207 cm^{-1}; ^1H NMR (DMSO-d_6, 300 MHz) δ/ppm: 7.08-7.21 (3H, m, $H_{3,20,22}$), 7.41-7.55 (3H, m, $H_{7,19,23}$), 7.61 (1H, s, H_{14}), 7.89 (1H, d, J=2.0 Hz, H_6), 8.75 (1H, s, H_4), 9.06 (1H, s, NH), 10.97 (1H, s, NH); ^{13}C NMR (DMSO-d_6, 75 MHz) δ/ppm: 102.6(C-3), 111.2(C-14), 113.7(C-7), 116.0(C-5), 116.3(C-19,23), 121.4(C-4), 121.5(C-20,22), 124.5(C-9), 127.9(C-6), 131.5(C-21), 135.4(C-18), 140.3(C-10), 152.3(C-2), 153.7(C-16), 157.1(C-8), 160.7(C-12); LC-MS (*m/z)*: 431.75 [MH^+]. Anal. Calcd. for $C_{18}H_{11}BrFN_3O_2S$: C, 50.01; H, 2.56; N, 9.72; found: C, 50.10; H, 2.51; N, 9.70.

1-(4-(5-bromobenzofuran-2-yl)thiazol-2-yl)-3-(3-chlorophenyl)urea (e28): Orange powder, 72% yield, mp. 290-292 °C; IR: 3261, 3113, 3084, 2951, 1693, 1519, 1274, 1257 cm^{-1}; ^1H NMR (DMSO-d_6, 300 MHz) δ/ppm: 7.10 (1H, s, H_3), 7.26-7.33 (3H, m, $H_{21,22,23}$), 7.43 (1H, dd, J_1=2.0 Hz; J_2=8.8 Hz, H_7), 7.57 (1H, d, J=8.8 Hz, H_6), 7.61 (1H, s, H_{14}), 7.70 (1H, s, H_4), 7.86 (1H, d, J=1.8 Hz, H_{19}), 9.11 (1H, s, NH), 10.99 (1H, s, NH); ^{13}C NMR (DMSO-d_6, 75 MHz) δ/ppm: 102.7(C-3), 111.3(C-14), 111.4(C-7), 113.7(C-5), 116.2(C-23), 117.9(C-19), 118.6(C-4), 118.8(C-21), 123.2(C-22), 124.4(C-6), 127.8(C-9), 131.2(C-20), 131.4(C-18), 133.9(C-10), 140.6(C-2), 152.2(C-16), 153.6(C-8), 160.5(C-12); LC-MS (*m/z)*: 447.74 [MH^+]. Anal. Calcd. for $C_{18}H_{11}BrClN_3O_2S$: C, 48.18; H, 2.47; N, 9.36; found: C, 48.12; H, 2.45; N, 9.33.

1-(4-(5-bromobenzofuran-2-yl)thiazol-2-yl)-3-(4-chlorophenyl)urea (e29): White powder, 58% yield, mp. 306-308 °C; IR: 3269, 3196, 3128, 2997, 1693, 1610, 1525, 1282, 1242 cm^{-1}; ^{1}H NMR (DMSO-d_6, 300 MHz) δ/ppm: 7.10 (1H, s, H_3), 7.36 (2H, d, J=8.8 Hz, $H_{20,22}$), 7.44 (1H, td, J_1=1.8 Hz; J_2=8.5 Hz, H_7), 7.51 (2H, d, J=8.8 Hz, $H_{19,23}$), 7.56 (1H, d, J=8.5 Hz, H_6), 7.60 (1H, s, H_{14}), 7.85 (1H, d, J=1.8 Hz, H_4), 9.07 (1H, s, NH), 10.92 (1H, s, NH); ^{13}C NMR (DMSO-d_6, 75 MHz) δ/ppm: 102.7(C-3), 111.3(C-14), 113.7(C-7), 116.2(C-5), 121.0(C-19,23), 124.4(C-4), 127.2(C-20,22), 127.8(C-6), 128.4(C-9), 131.5(C-21), 138.0(C-18), 140.3(C-10), 152.1(C-2), 153.6(C-16), 153.7(C-8), 160.6(C-12); LC-MS (*m/z*): 447.77 [MH^+]. Anal. Calcd. for $C_{18}H_{11}BrClN_3O_2S$: C, 48.18; H, 2.47; N, 9.36; found: C, 48.10; H, 2.44; N, 9.39.

1-(4-(5-bromobenzofuran-2-yl)thiazol-2-yl)-3-(4-bromophenyl)urea (e30): Yellowish powder, 76% yield, mp. 315-317 °C; IR: 3242, 3190, 3107, 2947, 1693, 1521, 1497, 1311, 1276, 1257 cm^{-1}; ^{1}H NMR (DMSO-d_6, 300 MHz) δ/ppm: 7.10 (1H, s, H_3), 7.42 (1H, d, J=2.0 Hz, H_7), 7.46 (2H, d, J=8.8 Hz, $H_{20,22}$), 7.50 (2H, d, J=8.8 Hz, $H_{19,23}$), 7.58 (1H, d, J=8.8 Hz, H_6), 7.61 (1H, s, H_{14}), 7.86 (1H, d, J=2.0 Hz, H_4), 9.08 (1H, s, NH), 10.95 (1H, s, NH); ^{13}C NMR (DMSO-d_6, 75 MHz) δ/ppm: 102.7(C-3), 107.5(C-21), 111.3(C-14), 113.7(C-7), 115.1(C-5), 116.2(C-19,23), 121.4(C-4), 124.5(C-6), 127.9(C-20,22), 131.5(C-9), 132.3(C-18), 138.5(C-10), 140.3(C-2), 152.1(C-16), 153.6(C-8), 160.6(C-12); LC-MS (*m/z*): 491.48 [MH^+]. Anal. Calcd. for $C_{18}H_{11}Br_2N_3O_2S$: C, 43.84; H, 2.25; N, 8.52; found: C, 43.89; H, 2.20; N, 8.50.

1-(4-(5-bromobenzofuran-2-yl)thiazol-2-yl)-3-(4-iodophenyl)urea (e31): White powder, 67% yield, mp. 311-313 °C; IR: 3252, 3192, 3118, 2967, 1695, 1525, 1350, 1278, 1252 cm^{-1}; ^{1}H NMR (DMSO-d_6, 300 MHz) δ/ppm: 7.13 (1H, s, H_3), 7.30 (2H, d, J=8.8 Hz, $H_{20,22}$), 7.46 (1H, dd, J_1=2.0 Hz; J_2=8.8 Hz, H_7), 7.60 (2H, d, J=8.8 Hz, $H_{19,23}$), 7.64 (1H, s, H_{14}), 7.67 (1H, d, J=8.8 Hz, H_6), 7.89 (1H, d, J=2.0 Hz, H_4), 9.05 (1H, s, NH), 10.92 (1H, s, NH); ^{13}C NMR (DMSO-d_6, 75 MHz) δ/ppm: 86.9(C-21), 102.7(C-3), 111.3(C-14), 113.7(C-7), 116.2(C-5), 121.6(C-19,23), 124.4(C-4), 127.8(C-6), 131.4(C-9), 138.1(C-20,22), 138.9(C-18), 140.3(C-10), 152.0(C-2), 153.6(C-16), 153.7(C-8), 160.5(C-12); LC-MS (*m/z*): 539.68 [MH^+]. Anal. Calcd. for $C_{18}H_{11}BrIN_3O_2S$: C, 40.02; H, 2.05; N, 7.78; found: C, 40.10; H, 2.01; N, 7.82.

1-(4-methoxyphenyl)-3-(4-(5-nitrobenzofuran-2-yl)thiazol-2-yl)urea (e32): Brown powder, 60% yield, mp. 266-268 °C; IR: 3310, 3225, 3116, 2990, 1695, 1555, 1527, 1340, 1292, 1247 cm^{-1}; ^{1}H NMR (DMSO-d_6, 300 MHz) δ/ppm: 3.70 (3H, s, -OCH_3), 6.88 (2H, d, J=9.0 Hz, $H_{20,22}$), 7.29 (1H, s, H_3), 7.36 (2H, d, J=9.0 Hz, $_{19,23}$), 7.61 (1H, s, H_{14}), 7.80 (1H, d, J=9.1 Hz, H_7), 8.16 (1H,

d, *J*=9.1 Hz, H_6), 8.57 (1H, d, *J*=2.4 Hz, H_4), 9.31 (1H, s, NH), 10.98 (1H, s, NH); ^{13}C NMR (DMSO-d_6, 75 MHz) *δ*/ppm: 55.8(-OCH_3), 103.6(C-3), 111.9(C-14), 112.5(C-7), 114.7(C-20,22), 118.3(C-4), 120.3(C-19,23), 121.1(C-6), 129.9(C-9), 132.0(C-18), 133.6(C-10), 139.7(C-5), 144.5(C-2), 152.3(C-16), 155.3(C-21), 157.5(C-8), 160.9(C-12); LC-MS (*m/z*): 411.17 [MH^+]. Anal. Calcd. for $C_{19}H_{14}N_4O_5S$: C, 55.60; H, 3.44; N, 13.65; found C, 55.68; H, 3.47; N, 13.62.

1-(4-(5-nitrobenzofuran-2-yl)thiazol-2-yl)-3-phenylurea (e33): Brown powder, 65% yield, mp. 264-266 °C; IR: 3325, 3260, 3121, 2952, 1701, 1497, 1330, 1310, 1276 cm^{-1}; ^{1}H NMR (DMSO-d_6, 300 MHz) *δ*/ppm: 7.01 (1H, d, *J*=8.8 Hz, H_3), 7.30-7.39 (2H, m, $H_{20,21}$), 7.41-7.48 (3H, m, $H_{19,22,23}$), 7.64 (1H, s, H_{14}), 7.82 (1H, d, *J*=8.8 Hz, H_7), 8.18 (1H, d, *J*=8.8 Hz, H_6), 8.57 (1H, s, H_4), 9.97 (1H, s, NH), 10.99 (1H, s, NH); ^{13}C NMR (DMSO-d_6, 75 MHz) *δ*/ppm: 102.8(C-3), 111.6(C-14), 113.8(C-7), 116.3(C-4), 118.2(C-6), 124.5(C-19), 125.7(C-23), 127.9(C-9), 129.0(C-21), 131.0(C-20), 131.5(C-22), 137.2(C-18), 140.4(C-10), 145.5(C-5), 148.8(C-2), 153.6(C-16), 153.7(C-8), 161.9(C-12); LC-MS (*m/z*): 381.15 [MH^+]. Anal. Calcd. for $C_{18}H_{12}N_4O_4S$: C, 56.84; H, 3.18; N, 14.73; found C, 56.80; H, 3.14; N, 14.78.

1-(4-(5-nitrobenzofuran-2-yl)thiazol-2-yl)-3-(4-nitrophenyl)urea (e34): Brown powder, 58% yield, mp. 286-288 °C; IR: 3418, 3223, 3128, 2966, 1697, 1512, 1337, 1320, 1298, 1270 cm^{-1}; ^{1}H NMR (DMSO-d_6, 300 MHz) *δ*/ppm: 7.33 (1H, s, H_3), 7.71 (2H, d, *J*=8.5 Hz, $H_{19,23}$), 7.81 (1H, d, *J*=8.5 Hz, H_7), 7.93 (1H, s, H_{14}), 8.16-8.22 (3H, m, $H_{6,20,22}$), 8.60 (1H, d, *J*=2.4 Hz, H_4), 9.96 (1H, s, NH), 11.25 (1H, s, NH); ^{13}C NMR (DMSO-d_6, 75 MHz) *δ*/ppm: 102.8(C-3), 111.7(C-14), 113.8(C-7), 116.3(C-4), 118.6(C-19,23), 124.5(C-6), 125.8(C-20,22), 127.9(C-9), 131.5(C-10), 142.2(C-21), 142.5(C-18), 145.7(C-5), 152.0(C-2), 152.5(C-16), 153.7(C-8), 160.3(C-12); LC-MS (*m/z*): 426.10 [MH^+]. Anal. Calcd. for $C_{18}H_{11}N_5O_6S$: C, 50.82; H, 2.61; N, 16.46; found C, 50.89; H, 2.63; N, 16.42.

1-(4-fluorophenyl)-3-(4-(5-nitrobenzofuran-2-yl)thiazol-2-yl)urea (e35): Yellowish powder, 54% yield, mp. 213-215 °C; IR: 3410, 3270, 3113, 2976, 1697, 1517, 1338, 1278, 1257 cm^{-1}; ^{1}H NMR (DMSO-d_6, 300 MHz) *δ*/ppm: 7.14 (1H, t, *J*=8.2 Hz, H_{22}), 7.26-7.39 (2H, m $H_{3,20}$), 7.46-7.51 (2H, m, $H_{19,23}$), 7.65 (1H, s, H_{14}), 7.82 (1H, d, *J*=8.8 Hz, H_7), 8.18 (1H, d, *J*=8.8 Hz, H_6), 8.58 (1H, s, H_4), 10.32 (1H, s, NH), 11.25 (1H, s, NH); ^{13}C NMR (DMSO-d_6, 75 MHz) *δ*/ppm: 102.6(C-3), 111.5(C-14), 113.2(C-7), 116.1(C-20,22), 117.3(C-4), 118.4(C-19,23), 121.2(C-6), 122.8(C-9), 128.7(C-18), 139.1(C-10), 143.1(C-5), 144.2(C-2), 151.2(C-16), 152.4(C-8),

155.6(C-21), 160.8(C-12); LC-MS (*m/z*): 399.11 [MH^+]. Anal. Calcd. for $C_{18}H_{11}FN_4O_4S$: C, 54.27; H, 2.78; N, 14.06; found C, 54.21; H, 2.75; N, 14.09.

1-(4-chlorophenyl)-3-(4-(5-nitrobenzofuran-2-yl)thiazol-2-yl)urea (e36): Yellowish powder, 68% yield, mp. 294-296 °C; IR: 3396, 3219, 3128, 2953, 1695, 1525, 1340, 1292, 1251 cm^{-1}; ^1H NMR (DMSO-d_6, 300 MHz) δ/ppm7.31 (1H, s, H_3), 7.35 (2H, d, J=8.8 Hz, $H_{20,22}$), 7.50 (2H, d, J=8.8 Hz, $H_{19,23}$), 7.66 (1H, s, H_{14}), 7.82 (1H, d, J=9.1 Hz, H_7), 8.17 (1H, d, J=9.1 Hz, H_6), 8.59 (1H, s, H_4), 9.83 (1H, s, NH), 11.15 (1H, s, NH); ^{13}C NMR (DMSO-d_6, 75 MHz) δ/ppm: 103.7(C-3), 112.1(C-14), 112.5(C-7), 118.3(C-4), 120.3(C-6), 120.9(C-19,23), 127.0(C-9), 129.4(C-20,22), 129.9(C-21), 138.2(C-18), 139.8(C-10), 144.5(C-5), 152.2(C-2), 155.3(C-16), 157.7(C-8), 160.6(C-12); LC-MS (*m/z*): 415.08 [MH^+]. Anal. Calcd. for $C_{18}H_{11}ClN_4O_4S$: C, 52.12; H, 2.67; N, 13.51; found C, 52.19; H, 2.64; N, 13.54.

1-(4-bromophenyl)-3-(4-(5-nitrobenzofuran-2-yl)thiazol-2-yl)urea (e37): Dark brown powder, 54% yield, mp. 234-236 °C; IR: 3466, 3230, 3121, 2982, 1701, 1550, 1515, 1342, 1292, 1253 cm^{-1}; ^1H NMR (DMSO-d_6, 300 MHz) δ/ppm: 7.32 (1H, s, H_3), 7.44 (2H, d, J=7.0 Hz, $H_{20,22}$), 7.50 (2H, d, J=7.0 Hz, $H_{19,23}$), 7.77 (1H, s, H_{14}), 7.94 (1H, d, J=9.0 Hz, H_7), 8.14 (1H, d, J=9.0 Hz, H_6), 8.55 (1H, s, H_4), 9.56 (1H, s, NH), 10.28 (1H, s, NH); ^{13}C NMR (DMSO-d_6, 75 MHz) δ/ppm: 92.6(C-21), 103.8(C-3), 112.2(C-14), 112.5(C-7), 114.8(C-4), 118.3(C-6), 120.5(C-19,23), 121.0(C-9), 129.9(C-20,22), 132.3(C-18), 139.8(C-10), 144.6(C-5), 152.3(C-2), 155.3(C-16), 157.7(C-8), 160.5(C-12); LC-MS (*m/z*): 459.04 [MH^+]. Anal. Calcd. for $C_{18}H_{11}BrN_4O_4S$: C, 47.07; H, 2.41; N, 12.20; found C, 47.13; H, 2.45; N, 12.22.

1-(4-iodophenyl)-3-(4-(5-nitrobenzofuran-2-yl)thiazol-2-yl)urea (e38): Brown powder 60% yield, mp. 239-241 °C; IR: 3418, 3211, 3121, 2967, 1695, 1512, 1340, 1278, 1255 cm^{-1}; ^1H NMR (DMSO-d_6, 300 MHz) δ/ppm: 7.17 (1H, d, J=1.4 Hz, H_3), 7.27-7.32 (2H, m, $H_{20,22}$), 7.28 (2H, dd, J_1=1.2 Hz; J_2=8.8 Hz, $H_{19,23}$), 7.57 (1H, d, J=1.2 Hz, H_{14}), 7.79 (1H, d, J=8.2 Hz, H_7), 8.18 (1H, dt, J_1=1.2 Hz; J_2=8.0 Hz, H_6), 8.51 (1H, s, NH), 8.59 (1H, d, J=1.2 Hz, H_4), 8.83 (1H, s, NH); ^{13}C NMR (DMSO-d_6, 75 MHz) δ/ppm: 85.0(C-21), 103.3(C-3), 106.8(C-14), 112.4(C-7), 118.2(C-4), 120.8(C-6), 121.2(C-23), 122.4(C-19), 130.1(C-9), 137.5(C-22), 138.0(C-20), 140.9(C-18), 141.4(C-10), 144.6(C-5), 155.2(C-2), 155.8(C-16), 157.7(C-8), 160.6(C-12); LC-MS (*m/z*): 507.04 [MH^+]. Anal. Calcd. for $C_{18}H_{11}IN_4O_4S$: C, 42.70; H, 2.19; N, 11.07; found C, 42.78; H, 2.15; N, 11.01.

4.2. Anticholinesterase activity assays

Acetyl- (AChE) and butyryl-cholinesterase (BuChE) inhibitory activities of the synthesized compounds were determined as previously reported [36]. The IC_{50} of each substance was determined by constructing an absorbance and/or inhibition (%) curve at five different concentrations (12.5, 25, 50, 100 and 200 μM). IC_{50} values were calculated for a given antagonist by determining the concentration needed to inhibit half of the maximum biological response of the agonist. The substrates of the reaction were acetylthiocholine iodide and butyrylthiocholine iodide. 5,5'-dithio-bis(2-nitrobenzoic) acid (DTNB) was used to measure anticholinesterase activity. Stock solutions of the compounds and galanthamine in n-propanol were prepared at a concentration of 4000 μg/mL. Aliquots of 150 μL of 100 mM phosphate buffer (pH 8.0), 10 μL of sample solution and 20 μL AChE ($2.476x10^{-4}$ U/μL) (or $3.1813x10^{-4}$ U/μL BChE) solution were mixed and incubated for 15 min at 25ºC. 10 μL of DTNB solution was prepared by adding 2.0 mL of pH 7.0 and 4.0 mL of pH 8.0 phosphate buffers to a mixture of 1.0 mL of 16 mg/mL DTNB and 7.5 mg/mL $NaHCO_3$ in pH 7.0 phosphate buffers. The reaction was initiated by the addition of 10 μL (7.1 mM) acetylthiocholine iodide (or 0.79 mM butyrylthiocholine iodide). In this method, the activity was measured by following the yellow colour produced as a result of the thio anion produced by reacting the enzymatic hydrolysis of the substrate with DTNB. The samples were prepared at an initial concentration of 4000 μM then were diluted with propyl alcohol which was also, used as a control solvent. The hydrolysis of the substrates was monitored using a BioTek Power Wave XS at 412 nm.

4.3. Antioxidant activity assays

In the CUPRAC assay, absorbance values were used to calculate the $A_{0.50}$, whereas inhibition (%) values were used in the in ABTS assay to calculate the IC_{50}.

$ABTS^{\cdot+}$ scavenging activities of the synthesized compounds were determined as previously reported [42]. The solution of $ABTS^{\cdot+}$ radical was generated by dissolving 19.2 mg of 2,2'-azino-bis(3-ethylbenzothiazoline-6-sulphonic acid) (7 mM ABTS) and 3.3 mg $K_2S_2O_3$ in distilled water (5 mL). This solution was kept in dark for 24 hours at room temperature, and absorbance of the solution was fixed to ~0.70 at 734 nm by dilution. Solutions of the samples were prepared in n-propanol at a concentration of 1000 μg/mL. Absorbance was measured at room temperature at 734 nm, after 6 minutes from $ABTS^{\cdot+}$ addition. Decrease in the absorption was used to calculate the activities. The results were expressed as IC_{50}. Propyl alcohol was used as a control solvent.

Cupric reducing antioxidant capacities of the synthesized compounds were determined in accordance with the literature method [43]. Solutions of the compounds and standards were

prepared in n-propanol at a concentration of 1000 µg/mL. Different volumes (1000 mg/L and 54.5 mL) of the sample were added to a solution prepared by adding 61.0 µL of 10 mM $CuCl_2$, 61.0 µL 7.5 mM neocuproine and 61.0 µL of 1.0 mM NH_4CH_3COO buffer (pH 7), respectively. Absorbance was measured at room temperature at 450 nm, after an hour. The results were calculated as $A_{0.50}$. Propyl alcohol was used as a controls.

4.4. Docking

3D structures of the ligands were built and energy-minimized using Sybyl v8.1 (Tripos, Inc., St. Louis, MO) on an Intel (Xeon 4 core, HP Z820) using Linux 6 operating system. The crystal structures of *torpedo califonica* AchE protein (PDB code: 1ACJ) and human BuchE (pdb code: 1P0M) were retrieved from the Protein Data Bank. Docking and scoring *per se* were performed using MolDock Optimizer and MolDock Grid, respectively, as implemented within Molegro Virtual Docker (version 6). The hardware used was Intel Core i7, with 16 GB ram memory using Linux/Ubuntu 10.04 operating system [48]. Only side-chain torsional angles were allowed to relax during energy minimization. The protein backbone was kept rigid and a new receptor conformation was generated for each pose after docking with flexible side chains. 30 runs for each molecule were carried out with a population size of 50, maximum iteration of 2000, scaling factor of 0.50, crossover rate of 0.90 and a variation-based termination scheme.

Acknowledgments

This work was supported by the Sakarya Research Fund of the Sakarya University. Project Number: 2014-50-02-003.

References

[1] O. di Pietro, E. Viayna, E.V. Garcia, M. Bartolini, R. Ramon, J.J. Jimenez, M.V. Clos, B. Perez, V. Andrisano, F.J. Luque, R. Lavilla, D.M. Torrero, 1,2,3,4-Tetrahydrobenzo[h][1,6]naphthyridines as a new family of potent peripheral-to-midgorge-site inhibitors of acetylcholinesterase: Synthesis, pharmacological evaluation and mechanistic studies, Eur. J. Med. Chem. 73 (2014) 141-152.

[2] P.M. Ruiz, L. Rubio, E.G. Palomero, I. Dorronsoro, M.M. Millan, R. Valenzuela, P. Usan, C. de Austria, M. Bartolini, V. Andrisano, A.B. Chanal, M. Orozco, F.J. Luque, M. Medina, A. Martinez, Design, synthesis, and biological evaluation of dual binding site acetylcholinesterase inhibitors: New disease-modifying agents for alzheimer's disease, J. Med. Chem. 48 (2005) 7223-7233.

[3] M. Ignasik, M. Bajda, N. Guzior, M. Prinz, Ul. Holzgrabe, B. Malawska, Design, synthesis and evaluation of novel 2-(aminoalkyl)-isoindoline-1,3-dione derivatives as dual-binding site acetylcholinesterase inhibitors, Arch. Pharm. Chem. Life Sci. 345 (2012) 509-516.

[4] F.C. Meng, F. Mao, W.J. Shan, F. Qin, L. Huang, X.S. Li, Design, synthesis, and evaluation of indanone derivatives as acetylcholinesterase inhibitors and metal-chelating agents, Bioorg. Med. Chem. Lett. 22 (2012) 4462–4466.

[5] S.S. Xie, X.B. Wang, J.Y. Li, L. Yang, L.Y. Kong, Design, synthesis and evaluation of novel tacrineecoumarin hybrids as multifunctional cholinesterase inhibitors against Alzheimer's disease, Eur. J. Med. Chem. 64 (2013) 540-553.

[6] W.J. Shan, L. Huang, Q. Zhou, F.C. Meng, X.S. Li, Synthesis, biological evaluation of 9-N-substituted berberine derivatives as multi-functional agents of antioxidant, inhibitors of acetylcholinesterase, butyrylcholinesterase and amyloid-β aggregation, Eur. J. Med. Chem. 46 (2011) 5885-5893.

[7] Q. Yu, H.W. Holloway, T. Utsuki, A. Brossi, N.H. Greig, Synthesis of novel phenserine-based-selective inhibitors of butyrylcholinesterase for alzheimer's disease, J. Med. Chem. 42 (1999) 1855-1861.

[8] Z.P. Wu, X.W. Wu, T. Shen, Y.P. Li, X. Cheng, L.Q. Gu, Z.S. Huang, L.K. An, Synthesis and acetylcholinesterase and butyrylcholinesterase inhibitory activities of 7-alkoxyl substituted indolizinoquinoline-5,12-dione derivatives, Arch. Pharm. Chem. Life Sci. 345 (2012) 175–184.

[9] N. Chitranshi, S. Gupta, P.K. Tripathi, P.K. Seth, New molecular scaffolds for the design of Alzheimer's acetylcholinesterase inhibitors identified using ligand- and receptor-based virtual screening, Med. Chem. Res. 22 (2013) 2328–2345.

[10] C. Guillou, A. Mary, D.Z. Renko, E. Gras, C. Thal, Potent acetylcholinesterase inhibitors: design, synthesis and structure-activity relationships of alkylene linked bis-galanthamine and galanthamine-galanthaminium salts, Bioorg. Med. Chem. Lett. 10 (2000) 637-639.

[11] P. Camps, R. el Achab, D.M. Gorbig, J. Morral, D.M. Torrero, A. Badia, J.E. Banos, N.M. Vivas, X. Barril, M. Orozcor, F.J. Luque, Synthesis, in vitro pharmacology, and molecular modeling of very potent tacrine-huperzine a hybrids as acetylcholinesterase inhibitors of potential interest for the treatment of alzheimer's disease, J. Med. Chem. 42 (1999) 3227-3242.

[12] M. Pohanka, Acetylcholinesterase inhibitors: a patent review (2008-present), Expert Opin. Ther. Pat. 22 (2012) 871-886.

[13] F. Leonetti, M. Catto, O. Nicolotti, L. Pisani, A. Cappa, A. Stefanachi, A. Carotti, Homo- and hetero-bivalent edrophonium-like ammonium salts as highly potent, dual binding site AChE inhibitors, Bioorg. Med. Chem. 16 (2008) 7450–7456.

[14] J.L. Sussman, M. Harel, F. Frolow, C. Oefner, A. Goldman, L. Toker, I. Silman, Atomic structure of acetylcholinesterase from Torpedo californica: a prototypic acetylcholine-binding protein, Science 253 (1991) 872-879.

[15] A. Mary, D.Z. Renko, C. Guillou, C. Thal, Potent acetylcholinesterase inhibitors: Design, synthesis, and structure-activity relationships of bis-interacting ligands in the galanthamine series, Bioorg. Med. Chem. 6 (1998) 1835-1850.

[16] A. Asadipour, M. Alipour, M. Jafari, M. Khoobi, S. Emami, H. Nadri, A. Sakhteman, A. Moradi, V. Sheibani, F.H. Moghadam, A. Shafiee, A. Foroumadi, Novel coumarin-3-carboxamides bearing N-benzylpiperidine moiety as potent acetylcholinesterase inhibitors, Eur. J. Med. Chem. 70 (2013) 623-630.

[17] I.W. Wyman, D.H. Macartney, Host-Guest complexes and pseudorotaxanes of cucurbit[7]uril with acetylcholinesterase inhibitors, J. Org. Chem. 74 (2009) 8031–8038.

[18] S. Rizzo, C. Riviere, L. Piazzi, A. Bisi, S. Gobbi, M. Bartolini, V. Andrisano, F. Morroni, A. Tarozzi, J.P. Monti, A. Rampa, Benzofuran-based hybrid compounds for the inhibition of cholinesterase activity, β-amyloid aggregation, and Aβ neurotoxicity, J. Med. Chem. 51, (2008), 2883–2886.

[19] S. Rizzo, A. Tarozzi, M. Bartolini, G. da Costa, A. Bisi, S. Gobbi, F. Belluti, A. Ligresti, M. Allara, J.P. Monti, V. Andrisano, V. di Marzo, P. Hrelia, A. Rampa, 2-Arylbenzofuran-based molecules as multipotent Alzheimer's disease modifying agents, Eur. J. Med. Chem. 58 (2012) 519-532.

[20] J.L. Vidaluc, F. Calmel, D.C. Bigg, E. Carilla, M. Briley, Flexible 1-[(2-Aminoethoxy) alkyl]-3-ar (o) yl (thio) ureas as novel acetylcholinesterase inhibitors. Synthesis and biochemical evaluation, J. Med. Chem. 38 (1995) 2969-2973.

[21] V. Lakshmi, V.S. Kannan, R. Boopathy, Identification of potential bivalent inhibitors from natural compounds for acetylcholinesterase through in silico screening using multiple pharmacophores, J. Mol. Graph. Model. 40 (2013) 72-79.

[22] T. Mohamed, W. Osman, G. Tin, P.P.N. Rao, Selective inhibition of human acetylcholinesterase by xanthine derivatives: In vitro inhibition and molecular modelling investigations, Bioorg. Med. Chem. Lett. 23 (2013) 4336–4341.

[23] B. Kaboudin, M. Arefi, S. Emadi, V.S. Hasani, Synthesis and inhibitory activity of ureidophosphonates, against acetylcholinesterase: Pharmacological assay and molecular modelling, Bioorg. Chem. 41-42 (2012) 22–27.

[24] P. Anand, B. Singh, Synthesis and evaluation of novel carbamate-substituted flavanone derivatives as potent acetylcholinesterase inhibitors and anti-amnestic agents, Med. Chem. Res. 22 (2013) 1648–1659.

[25] H.R. Girisha, J.N.N.S. Chandra, S. Boppana, M. Malviya, C.T. Sadashiva, K.S. Rangappa, Active site directed docking studies: Synthesis and pharmacological evaluation of cis-2,6-dimethyl piperidine sulfonamides as inhibitors of acetylcholinesterase, Eur. J. Med. Chem. 44 (2009) 4057–4062.

[26] L. Fang, B. Kraus, J. Lehmann, J. Heilmann, Y. Zhang, M. Decker, Design and synthesis of tacrine–ferulic acid hybrids as multi-potent anti-Alzheimer drug candidates, Bioorg. Med. Chem. Lett. 18 (2008) 2905-2909.

[27] L. Fang, X. Fang, S. Gou, A. Lupp, I. Lenhardt, Y. Sun, Z. Huang, Y. Chen, Y. Zhang, C. Fleck, Design, synthesis and biological evaluation of D-ring opened galantamine analogs as multifunctional anti-Alzheimer agents, Eur. J. Med. Chem. 76 (2014) 376-386.

[28] J.T. Ferrara, L.M. Cano, M.E. Fonseca, Synthesis, anticholinesterase activity and structure–activity relationships of m-aminobenzoic acid derivatives, Bioorg. Med. Chem. Lett. 13 (2003) 1825–1827.

[29] M.L. Bolognesi, A. Cavalli, L. Valgimigli, M. Bartolini, M. Rosini, V. Andrisano, M. Recanatini, C. Melchiorre, Multi-Target-Directed drug design strategy: From a dual binding site acetylcholinesterase inhibitor to a trifunctional compound against alzheimer's disease, J. Med. Chem. 50 (2007) 6446–6449.

[30] B. Tasso, M. Catto, O. Nicolotti, F. Novelli, M. Tonelli, I. Giangreco, L. Pisani, A. Sparatore, V. Boido, A. Carotti, F. Sparatore, Quinolizidinyl derivatives of bi- and tricyclic systems as potent inhibitors of acetyl- and butyrylcholinesterase with potential in Alzheimer's disease, Eur. J. Med. Chem. 46 (2011) 2170-2184.

[31] H. Akrami, B.F. Mirjalili, M. Khoobi, H. Nadri, A. Moradi, A. Sakhteman, S. Emami, A. Foroumadi, A. Shafiee, Indolinone-based acetylcholinesterase inhibitors: Synthesis, biological activity and molecular modelling, Eur. J. Med. Chem. 84 (2014) 375-381.

[32] M. Kliachyna, G. Santoni, V. Nussbaum, J. Renou, B. Sanson, J.P. Colletier, M. Arboléas, M. Loiodice, M. Weik, L. Jean, P.Y. Renard, F. Nachon, R. Baati, Design, synthesis and biological evaluation of novel tetrahydroacridine pyridine-aldoxime and -amidoxime hybrids as efficient uncharged reactivators of nerve agent-inhibited human acetylcholinesterase, Eur. J. Med. Chem. 78 (2014) 455-467.

[33] A.L.C. Otero, L.Y.V. Méndez, J.E. Duque L., V.V. Kouznetsov, Design, synthesis, acetylcholinesterase inhibition and larvicidal activity of girgensohnine analogs on Aedes aegypti, vector of dengue fever, Eur. J. Med. Chem. 78 (2014) 392-400.

[34] S. Liu, R. Shang, L. Shi, D.C.C. Wan, H. Lin, Synthesis and biological evaluation of 7H-thiazolo[3,2-b]-1,2,4-triazin-7-one derivatives as dual binding site acetylcholinesterase inhibitors, Eur. J. Med. Chem. 81 (2014) 237-244.

[35] C. Paizs, M. Tos¸, C. Majdik, P. Moldovan, L. Novak, P. Kolonits, A. Marcovici, F.D. Irimie, L. Poppe, Optically active 1-(benzofuran-2-yl)ethanols and ethane-1,2-diols by enantiotopic selective bioreductions, Tetrahedron: Asymmetry 14 (2003) 1495–1501.

[36] G.L. Ellman, K.D. Courtney, V. Andres, R.M. Featherstone, A new and rapid colorimetric determination of acetylcholinesterase activity, Biochem. Pharmacol. 7 (1961) 88–95.

[37] B. Brus, U. Kosăk, S. Turk, A. Pislar, N. Coquelle, J. Kos, J. Stojan, J.P. Colletier, S. Gobec, Discovery, biological evaluation, and crystal structure of a novel nanomolar selective butyrylcholinesterase inhibitor, J. Med. Chem. 57 (2014) 8167-8179.

[38] Y. Nicolet, O. Lockridge, P. Masson, J.C. Fontecilla-Camps, F. Nachon, Crystal structure of human butyrylcholinesterase and of its complexes with substrate and products, J. Biol. Chem. 278 (2003) 41141-41147.

[39] R. A. Laskowski and M. B. Swindells, LigPlot+: Multiple Ligand–Protein Interaction Diagrams for Drug Discovery, J. Chem. Inf. Model, 51 (2011) 2778–2786.

[40] M. F. Sanner, Python: a programming language for software integration and development, J. Mol. Graph. Model. 17, (1999) 57–61.

[41] M. Swart, T.V. Wijst, C.F. Guerra, F.M. Bickelhaupt, π-π stacking tackled with density functional theory, J. Mol. Model, 13 (2007) 1245-1257.

[42] R. Re, N. Pellegrini, A. Proteggente, A. Pannala, M. Yang, C.R. Evans, Antioxidant activity applying an improved ABTS radical cation decolorization assay, Free Radical Bio. Med. 26 (1999) 1231-1237.

[43] R. Apak, K. Guclu, M. Ozyurek, S.E. Karademir, Novel total antioxidant capacity index for dietary polyphenols and vitamins C and E, using their cupric ion reducing capability in the presence of neocuproine: CUPRAC method, J. Agr. Food Chem. 52 (2004) 7970–7981.

[44] Y.Z. Tang, Z.Q. Liu, Free-radical-scavenging effect of carbazole derivatives on DPPH and ABTS radicals, J. Am. Oil Chem. Soc. 84 (2007) 1095-1100.

[45] A. Karadag, B. Ozcelik, S. Saner, Review of methods to determine antioxidant capacities, Food Anal. Methods 2 (2009) 41-60.

[46] S. Laufer, H.G. Striegel, K. Neher, P. Zechmeister, C. Donat, K. Stolingwa, S. Baur, S. Tries, T. Kammermeier, G. Dannhardt, W. Kiefer, Synthesis and evaluation of a novel series of pyrrolizine derivatives as dual cyclooxygenase-1 and 5-lipoxygenase inhibitors, Arch. Pharm. Pharm. Med. Chem. 330 (1997) 307-312.

[47] D.I. Othman, A.M.M. Abdelal, M.A. El-Sayed, S.A.A. El Bialy, Novel benzofuran derivatives: synthesis and antitumor activity, Heterocycl. Commun. 19 (2013) 29–35.

[48] R. Thomsen, M.H. Christensen, MolDock: a new technique for high-accuracy molecular docking, J. Med. Chem. 49 (2006) 3315-3321.

Figure captions

Figure 1. Structures of well-known cholinesterase inhibitors.

Figure 2. Design strategy of the reported compounds.

Figure 3. Superimposition of the best binding modes of **e1-e38** into the gorge of AChE.

Figure 4. Best pose of **e25** in the AChE active site. (a) 2D diagram of **e25** and protein residue contacts by LigPlot (b) Side chain amino acids are shown as lines. **e25** is shown as stick by PyMol. In both figures H bond interactions are shown dotted lines.

Figure 5. Best pose of **e38** in the BuChE active site. (a) 2D diagram of **e38** and protein residue contacts by LigPlot (b) Side chain amino acids are shown as lines. **e38** is shown as stick by PyMol. In both figures H bond interactions are shown as dotted lines.

Tables

Table 1. In vitro inhibition IC_{50} and $A_{0.50}$ values (μM) and selectivity of compounds **e1-e38** for AChE and BuChE and antioxidant activities.

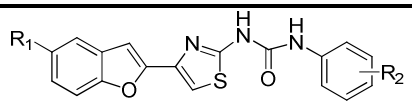

e1-e38

Compound	R_1	R_2	AChE IC_{50} (μM)[a]	BuChE IC_{50} (μM)[a]	Selectivity index[b]	$ABTS^{\cdot+}$ IC_{50} (μM)[a]	CUPRAC $A_{0.50}$ (μM)[c]
e1	H	2-OCH_3	60.97 ± 0.01	81.28 ± 0.02	1.33	47.43 ± 5.42	>200
e2	H	3-OCH_3	48.90 ± 0.01	59.56 ± 0.05	1.22	0.2 ± 0.03	104.46 ± 0.15
e3	H	4-OCH_3	52.47 ± 0.02	74.26 ± 0.03	1.42	17.37 ± 1.83	146.34 ± 0.02
e4	H	4-CH_3	10.40 ± 0.50	56.32 ± 0.10	5.41	0.5 ± 0.1	192.91 ± 0.01
e5	H	H	24.72 ± 0.23	21.26 ± 0.01	0.86	28.19 ± 1.74	132.00 ± 0.05
e6	H	2-NO_2	41.91 ± 0.42	79.93 ± 0.40	1.91	20.26 ± 0.14	100.33 ± 0.03
e7	H	3-NO_2	41.19 ± 0.02	26.81 ± 0.36	0.65	1.26 ± 0.5	>200
e8	H	4-NO_2	5.23 ± 1.86	3.44 ± 0.12	0.66	19.27 ± 5.66	>200
e9	H	2-F	30.92 ± 0.03	41.66 ± 0.23	1.35	2.63 ± 0.16	102.43 ± 0.06
e10	H	3-F	48.99 ± 0.21	17.98 ± 0.03	0.37	4.52 ± 0.58	126.52 ± 0.05
e11	H	4-F	55.03 ± 0.12	7.45 ± 0.15	0.14	1.13 ± 0.02	110.31 ± 0.04
e12	H	3-Cl	9.67 ± 0.54	21.52 ± 0.65	2.22	14.12 ± 2.17	>200
e13	H	4-Cl	42.55 ± 1.52	38.58 ± 2.27	0.91	11.23 ± 2.95	>200
e14	H	3,4-di-Cl	52.03 ± 0.23	75.60 ± 0.36	1.45	>200	>200
e15	H	4-Br	32.82 ± 0.03	55.18 ±0. 06	1.68	>200	>200
e16	H	4-I	21.35 ± 0.06	41.27 ± 0.03	1.93	61.98 ± 1.42	133.0 ± 0.06
e17	Br	2-OCH_3	78.85 ± 0.69	154.08 ± 0.32	1.95	77.23 ± 0.89	92.68 ± 0.06
e18	Br	3-OCH_3	29.42 ± 0.85	13.95 ± 0.28	0.47	>200	>200
e19	Br	4-OCH_3	32.75 ± 0.53	30.97 ± 0.98	0.95	>200	>200
e20	Br	4-CH_3	32.49 ± 0.07	5.65 ± 0.09	0.17	>200	>200
e21	Br	H	23.35 ± 0.36	35.03 ± 0.42	1.50	>200	>200
e22	Br	2-NO_2	8.82 ± 0.76	5.12 ± 0.08	0.58	165.92 ± 0.33	122.22 ± 0.03
e23	Br	3-NO_2	17.45 ± 0.32	78.97 ± 0.93	4.53	158.83 ± 0.80	>200
e24	Br	4-NO_2	4.78 ± 0.08	3.12 ± 0.04	0.65	>200	120.74 ± 0.05
e25	Br	2-F	3.85 ± 0.96	9.25 ± 0.65	2.40	>200	>200
e26	Br	3-F	29.38 ± 0.23	40.16 ± 0.32	1.37	>200	>200
e27	Br	4-F	35.62 ± 0.10	64.32 ± 0.22	1.81	>200	146.78 ± 0.04
e28	Br	3-Cl	7.93 ± 0.52	26.32 ± 0.78	3.32	>200	>200
e29	Br	4-Cl	22.23 ± 0.02	36.93 ± 0.03	1.66	>200	>200
e30	Br	4-Br	11.94 ± 0.05	35.81 ± 0.07	3.00	>200	>200
e31	Br	4-I	6.42 ± 0.12	43.63 ± 0.42	6.80	>200	>200
e32	NO_2	4-OCH_3	34.08 ± 0.03	49.24 ± 0.02	1.44	120.99 ± 0.20	>200
e33	NO_2	H	4.42 ± 0.05	2.26 ± 0.08	0.51	183.47 ± 0.00	>200
e34	NO_2	4-NO_2	25.20 ± 0.65	25.60 ± 0.03	1.02	100.44 ± 1.38	>200
e35	NO_2	4-F	41.13 ± 0.85	47.56 ± 0.05	1.16	123.04 ± 0.46	>200
e36	NO_2	4-Cl	30.56 ± 0.1	26.61 ± 0.52	0.87	116.54 ± 0.38	>200
e37	NO_2	4-Br	28.19 ± 0.36	34.50 ± 0.64	1.22	194.45 ± 0.56	>200
e38	NO_2	4-I	5.53 ± 0.44	2.03 ± 0.62	0.37	62.42 ± 0.41	>200
Quercetin	-	-	-	-	-	1.18 ± 0.03	1.45 ± 0.02
Galantamine	-	-	2.41 ± 0.12	17.38 ± 0.56	7.21	-	-
Donepezil[d]	-	-	0.03±0.0005	4.66±0.503	155.3	-	-
Rivastigmine[e]	-	-	3.01±0.21	0.30±0.01	0.10	-	-

[a] IC_{50} values represent the means ± S.E.M. of three parallel measurements ($p< 0.05$).

[b] Selectivity index = IC_{50} (BuChE) / IC_{50} (AChE).

[c] $A_{0.50}$ values represent the means ± S.E.M. of three parallel measurements ($p< 0.05$).

[d] From ref. [4]

[e] From ref. [30]

Figures

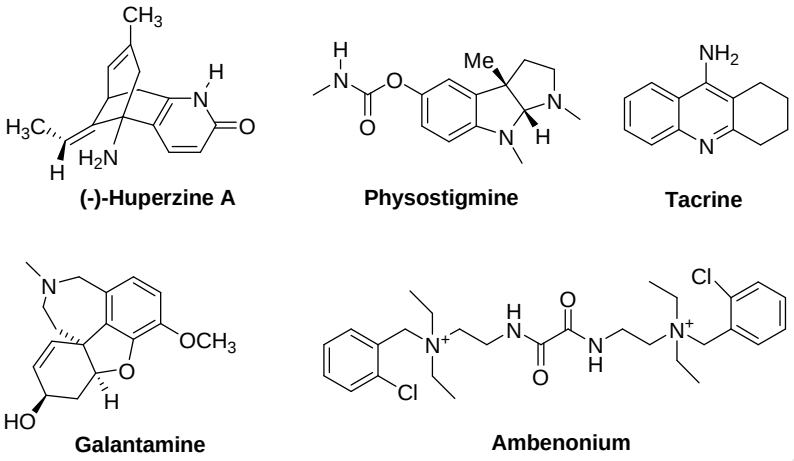

Fig. 1. Structures of well-known cholinesterase inhibitors.

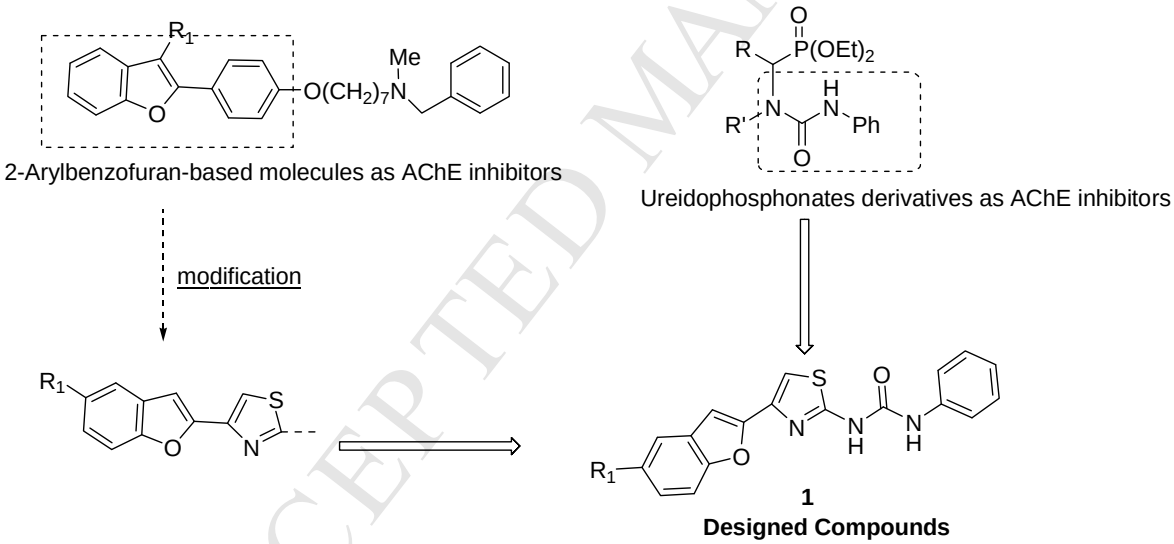

Fig. 2. Design strategy of the reported compounds.

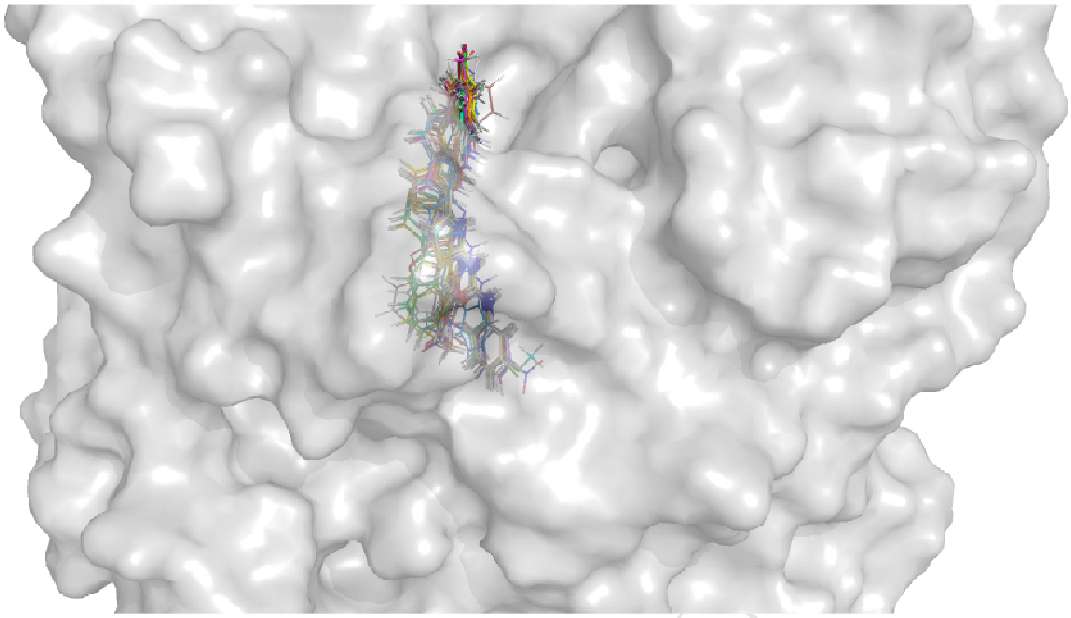

Fig. 3. Superimposition of the best binding modes of **e1-e38** into the gorge of AChE.

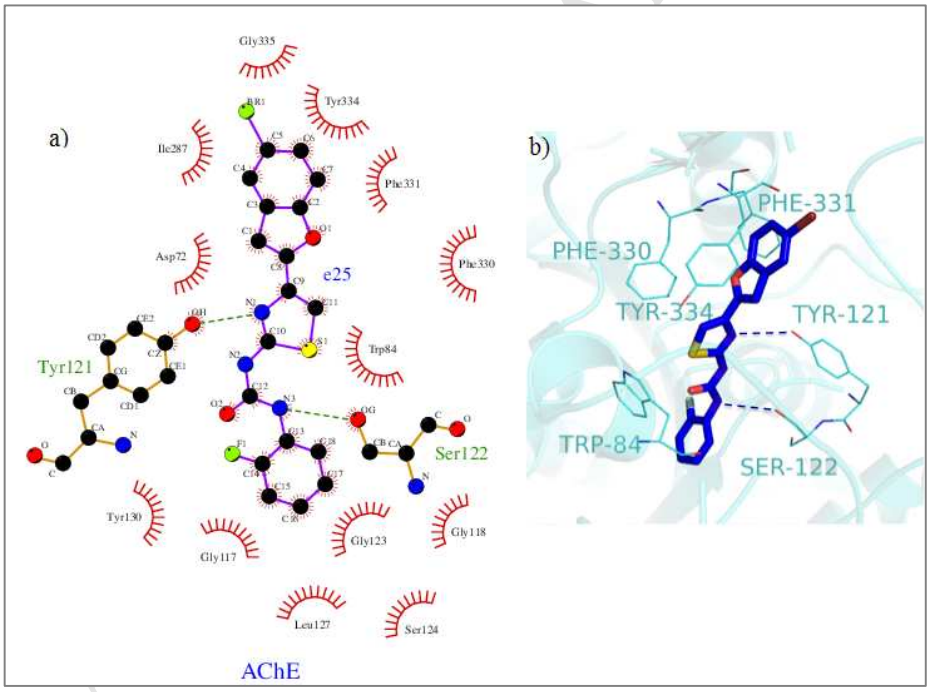

Figure 4. Best pose of **e25** in the AChE active site. (a) 2D diagram of **e25** and protein residue contacts by LigPlot+ (b) Side chain amino acids are shown as lines. **e25** is shown as stick by PyMol. In both figures H bond interactions are shown dotted lines.

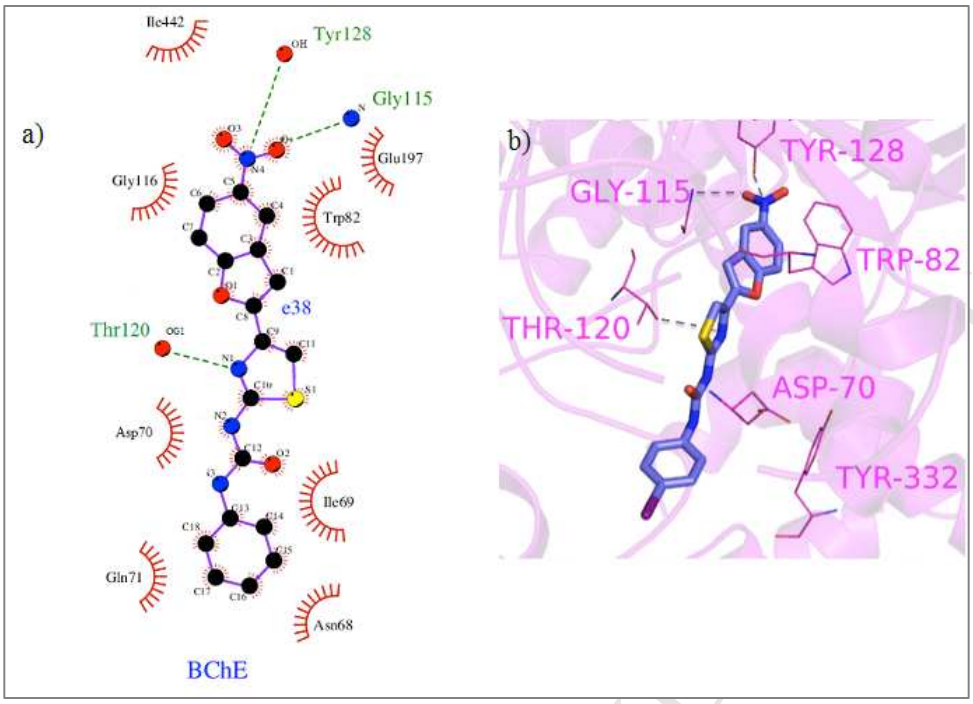

Figure 5. Best pose of **e38** in the BuChE active site. (a) 2D diagram of **e38** and protein residue contacts by LigPlot+. (b) Side chain amino acids are shown as lines. **e38** is shown as stick by PyMol. In both figures H bond interactions are shown as dotted lines.

Schemes

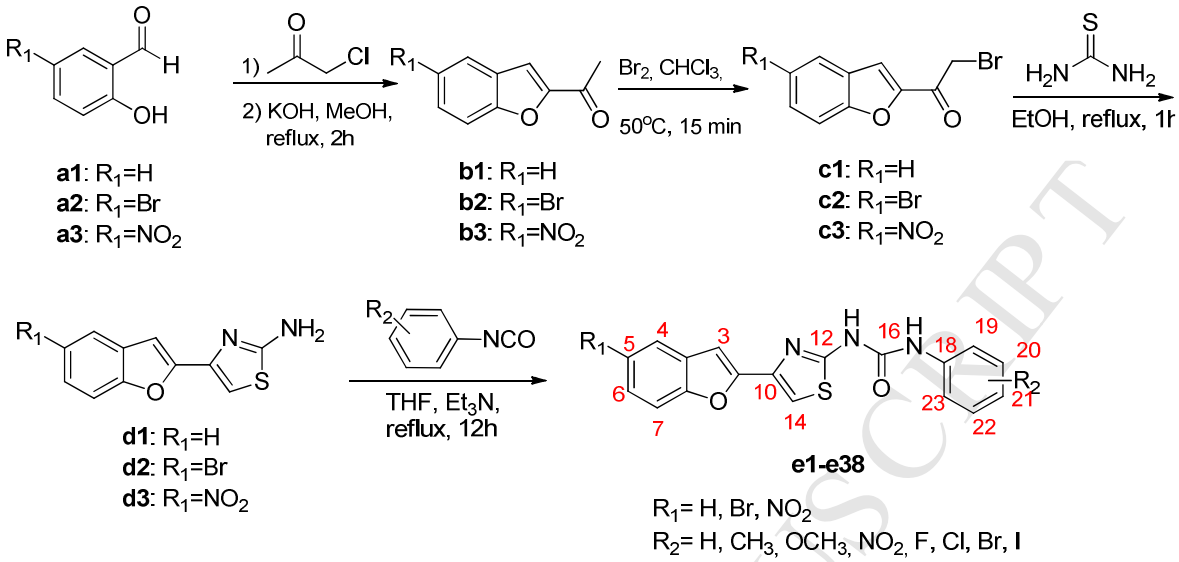

Scheme 1. Synthesis of new urea substituted benzofuranylthiazole derivatives.

HIGHLIGHTS:

- 38 new Benzofuranylthiazoles hybrids.
- Multitasking agents in AD.
- AChE and BuChE inhibition.
- Anti-oxidant activity.
- Docking studies.

Potential of Aryl-urea-Benzofuranylthiazoles hybrids as multitasking agents in Alzheimer's disease

Belma Zengin Kurt,[a] Isil Gazioglu,[a] Livia Basile,*[b] Fatih Sonmez,*[c] Tiziana Ginex,[d] Mustafa Kucukislamoglu[e] and Salvatore Guccione[b]

[a]*Bezmialem Vakif University, Faculty of Pharmacy, Department of Analytical and Medicinal Chemistry, 34093, Istanbul, TURKEY*

[b]*Department of Drug Sciences, University of Catania, Viale A. Doria 6 Ed. 2, Città Universitaria, I- 95125, Catania, ITALY*

[c]*Sakarya University, Pamukova Vocational High School, 54900, Sakarya, TURKEY*

[d]*Molecular Modelling Laboratory, Department of Food Science, University of Parma, Parco Area delle Scienze 17/A, Parma 43124, ITALY*

[e]*Sakarya University, Faculty of Arts and Science, Department of Chemistry, 54055, Sakarya, TURKEY*

*Corresponding authors: University of Catania, Department of Drug Sciences, Viale A. Doria 6 Ed. 2, Città Universitaria, I- 95125, Catania, ITALY. Tel. +39 095 738-4020; fax +39 095 738-4208; email address: basilelivia@gmail.com (L. Basile); Sakarya University, Pamukova Vocational High School, 54900, Sakarya, TURKEY. Tel.: +90-264-2953378; fax: +90-264-2953679; e-mail address: fsonmez@sakarya.edu.tr (F.Sonmez).

Supplementary Materials

^{1}H and ^{13}C NMR and MS spectra of the synthesized compounds are given below.

SM 1. ^{1}H and ^{13}C NMR and MS spectra of e1

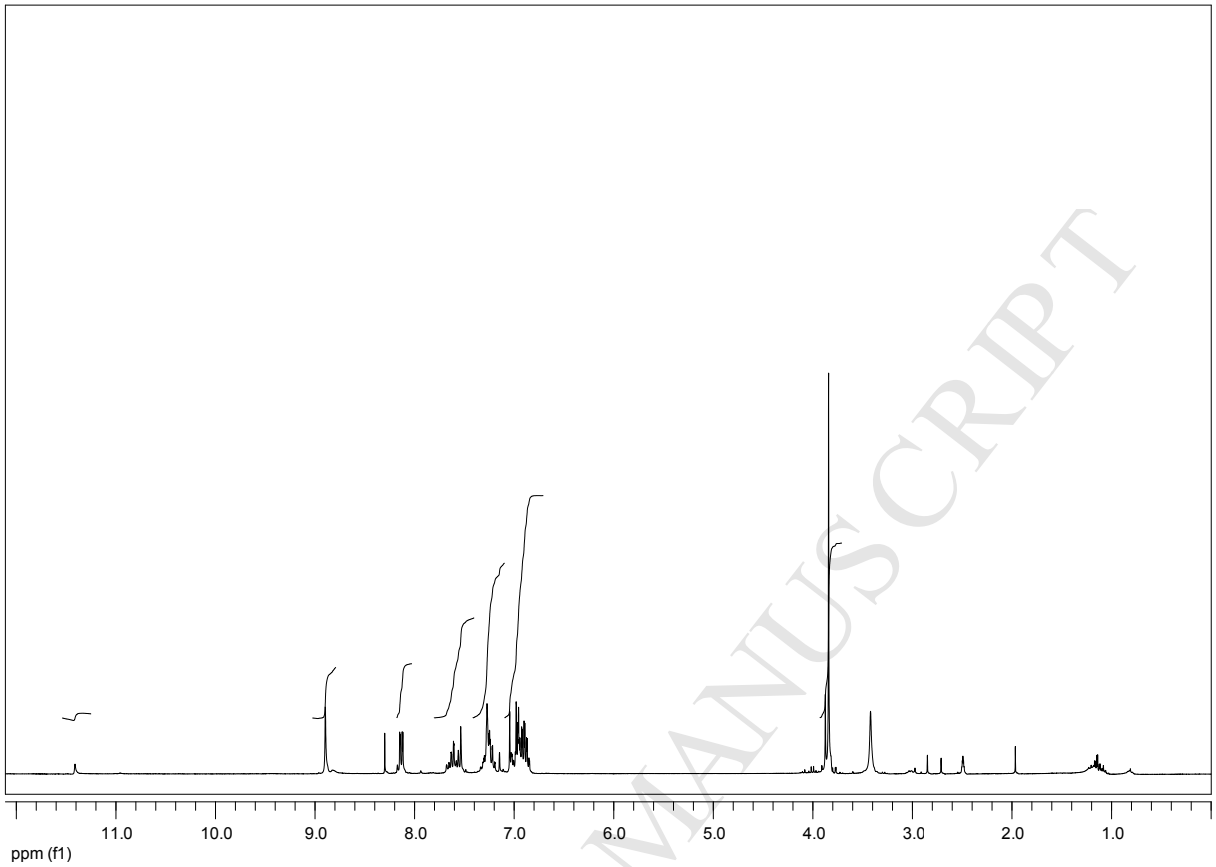

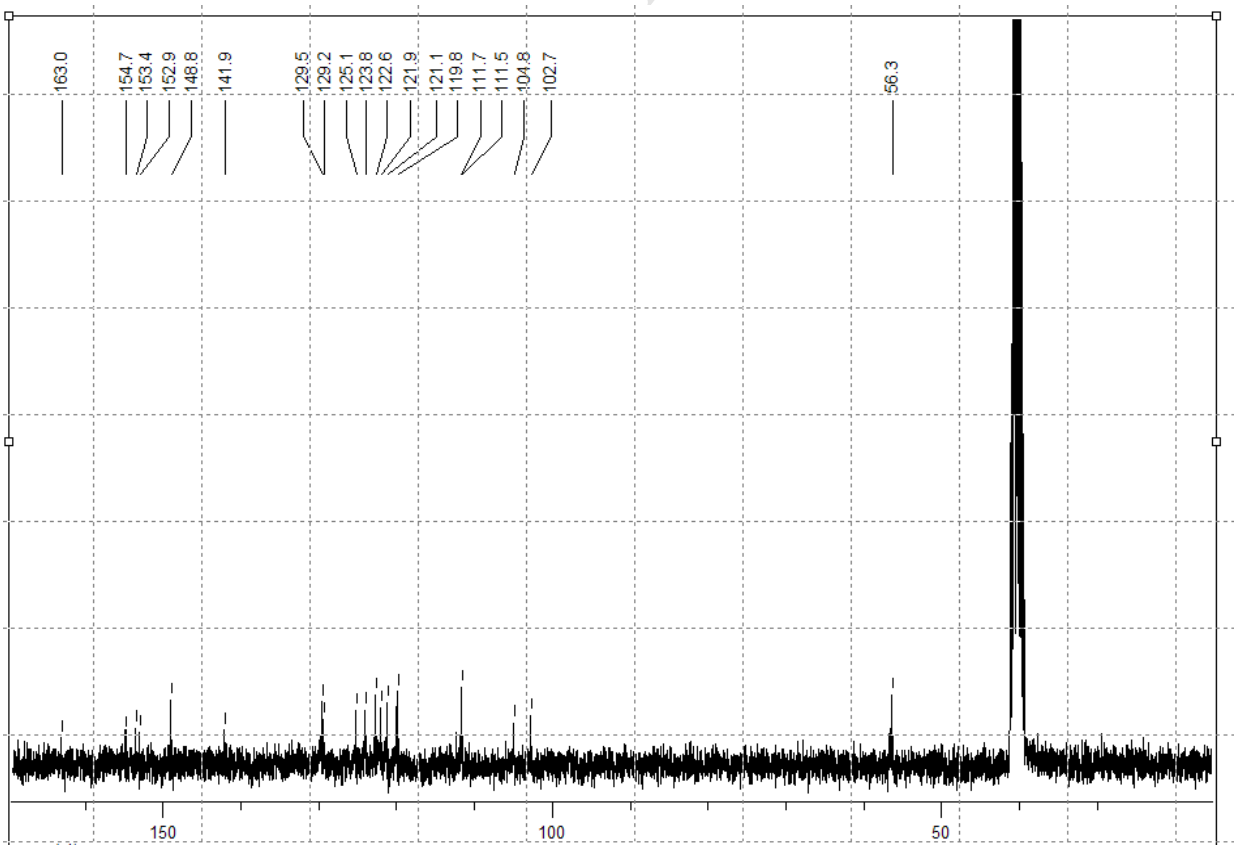

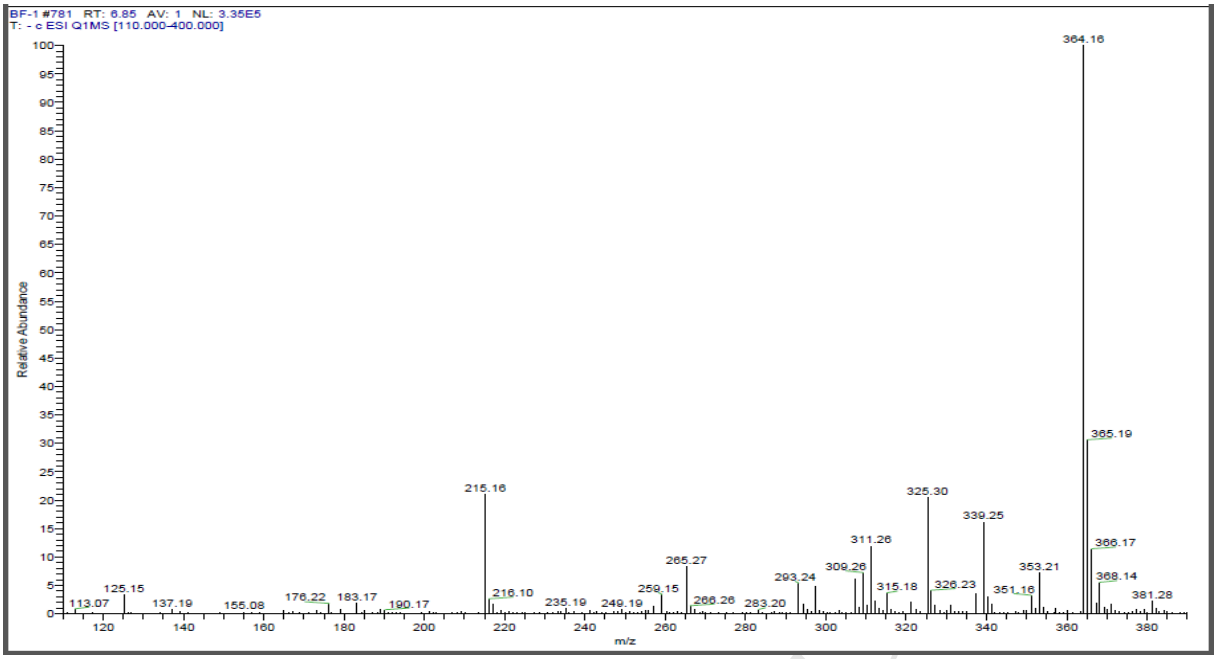

SM 2. ^{1}H and ^{13}C NMR and MS spectra of e2

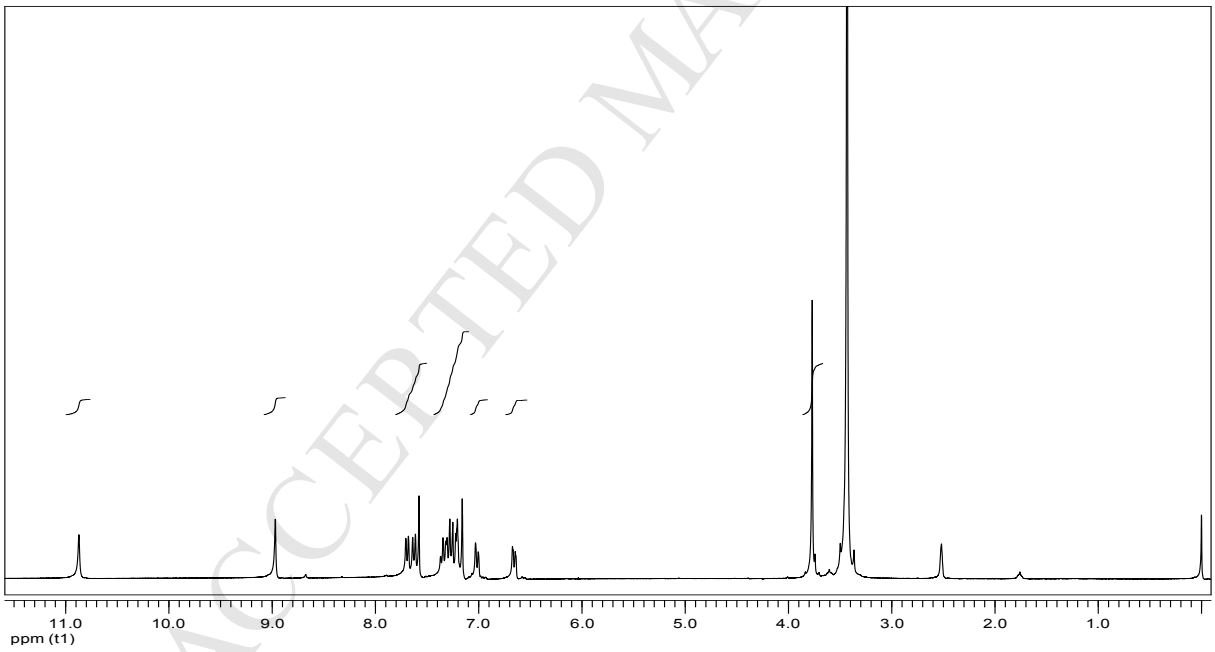

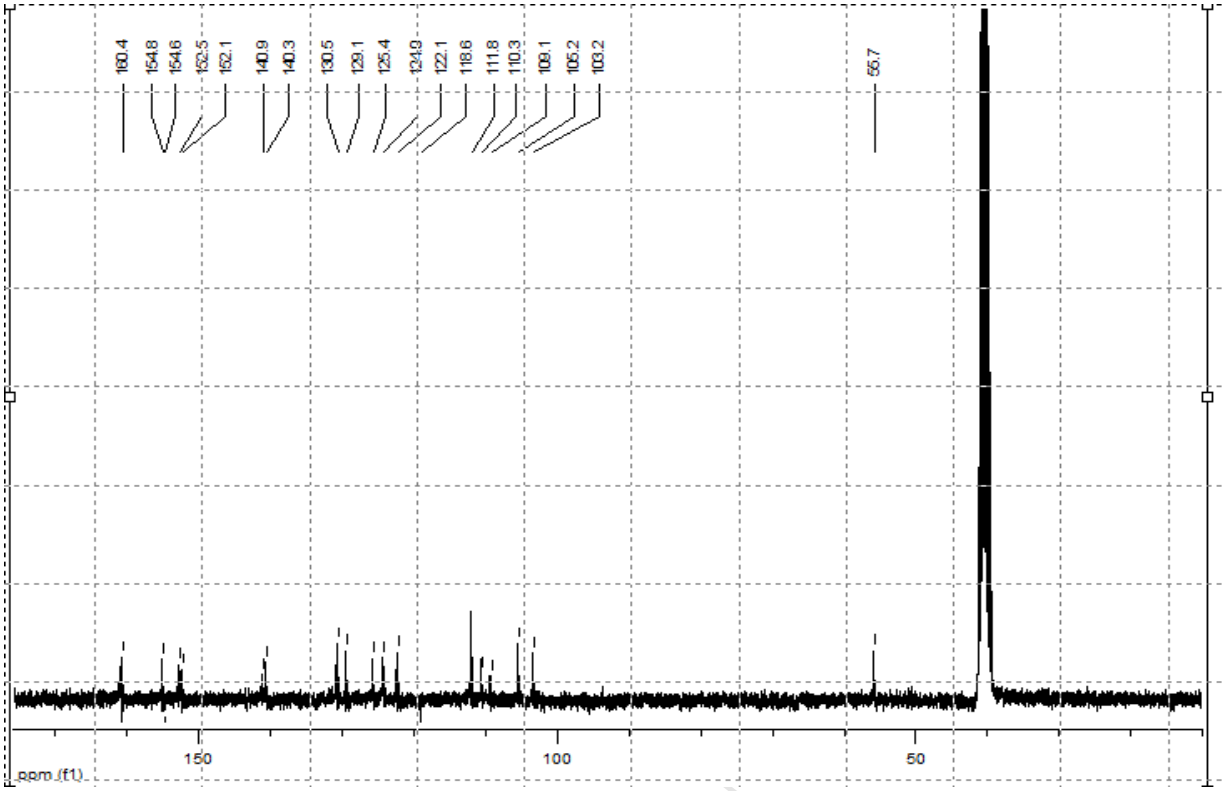
160.4
154.8
154.6
152.5
152.1
140.9
140.3
130.5
129.1
125.4
124.9
122.1
118.6
111.8
110.3
108.1
105.2
103.2
55.7
150
100
50
ppm (f1)

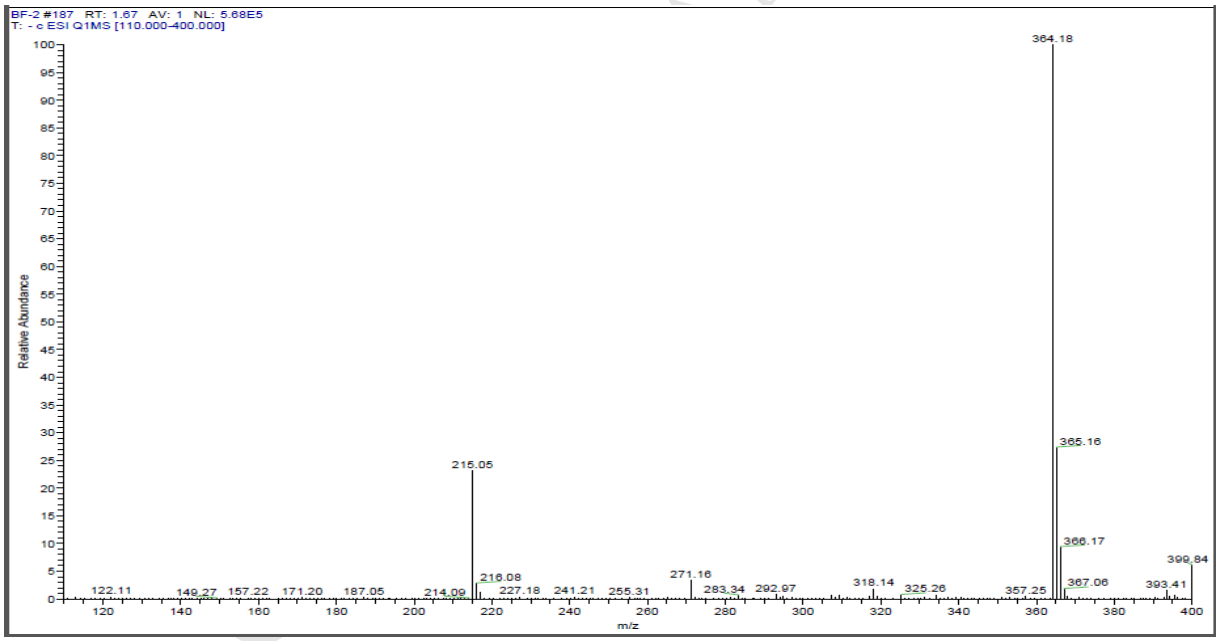
BF-2 #187 RT: 1.67 AV: 1 NL: 5.68E5
T: - c ESI Q1MS [110.000-400.000]
Relative Abundance
m/z
364.18
365.16
366.17
399.84
215.05
216.08
271.16
122.11
149.27
157.22
171.20
187.05
214.09
227.18
241.21
255.31
283.34
292.97
318.14
325.26
357.25
367.06
393.41

SM 3. ^{1}H and ^{13}C NMR and MS spectra of e3

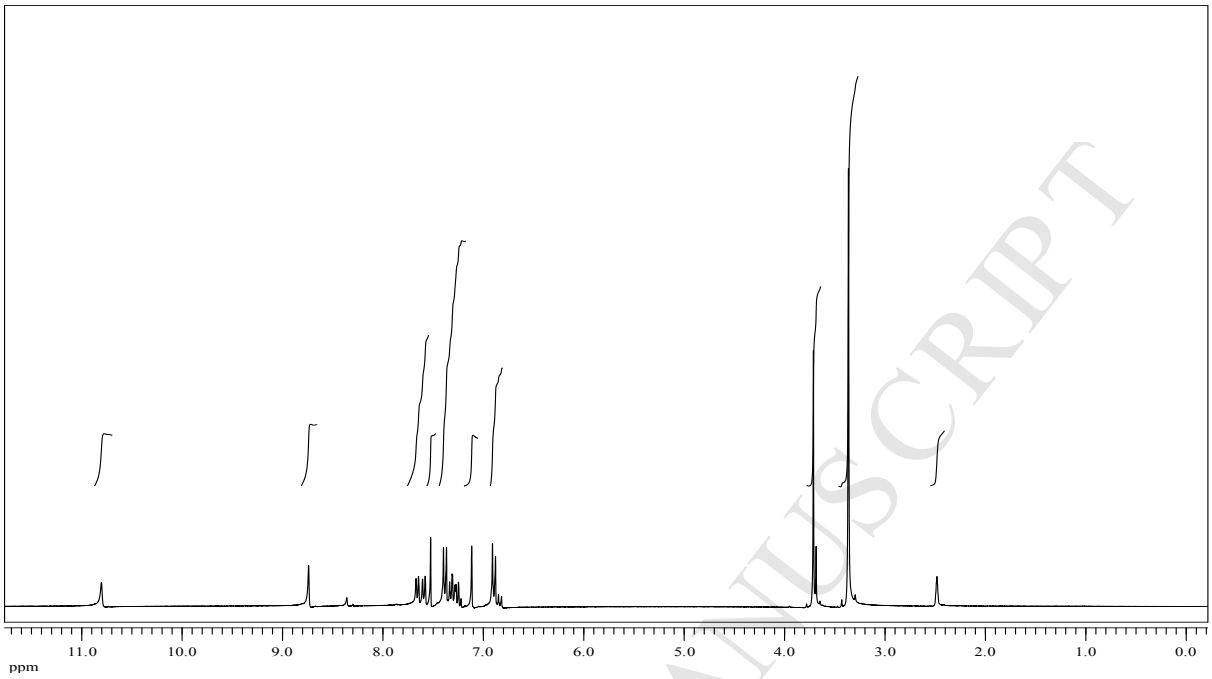

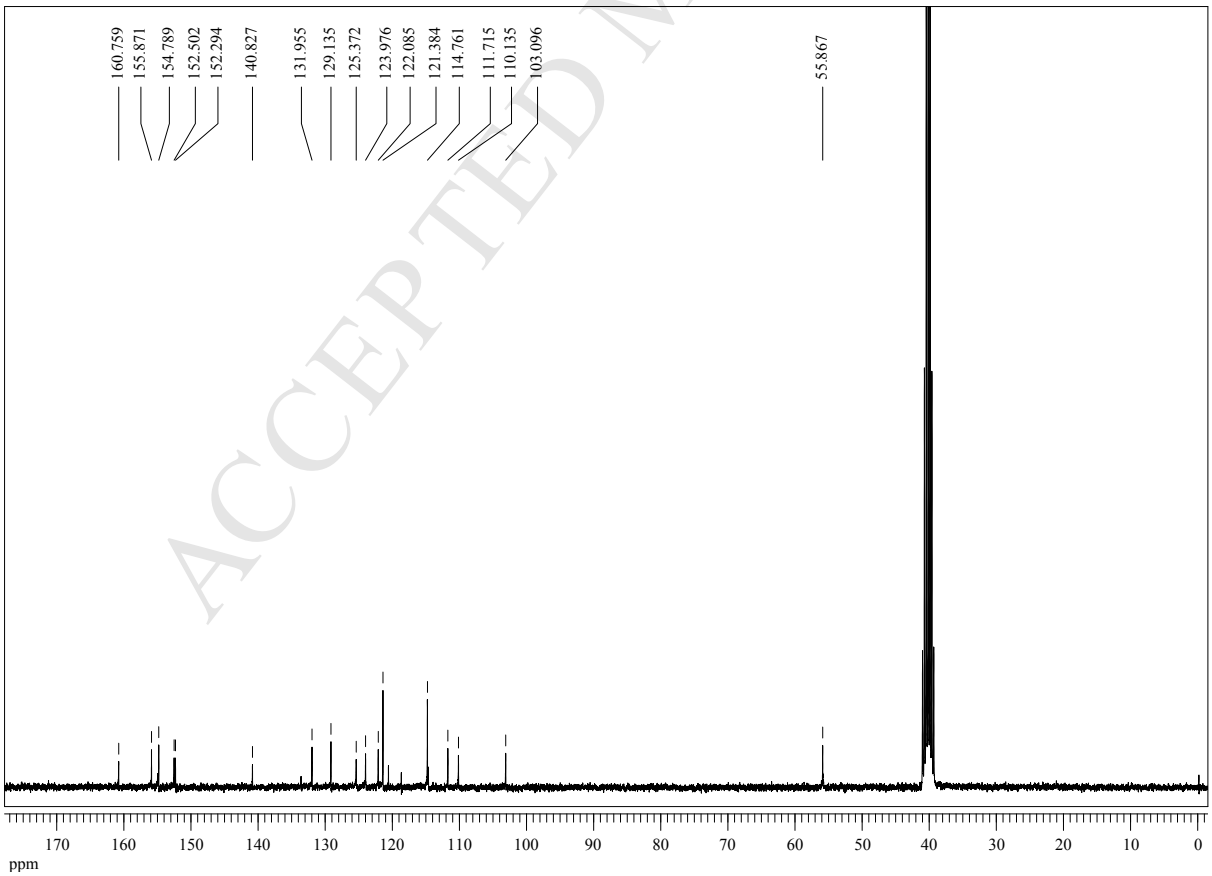

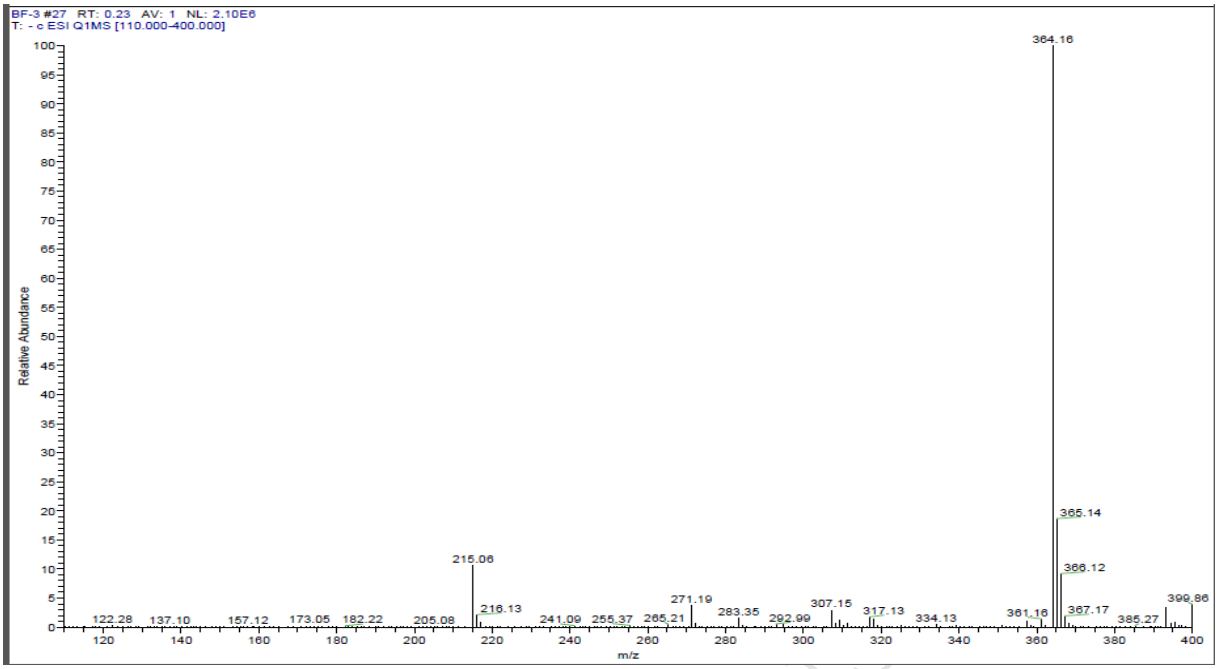

SM 4. ^{1}H and ^{13}C NMR and MS spectra of e4

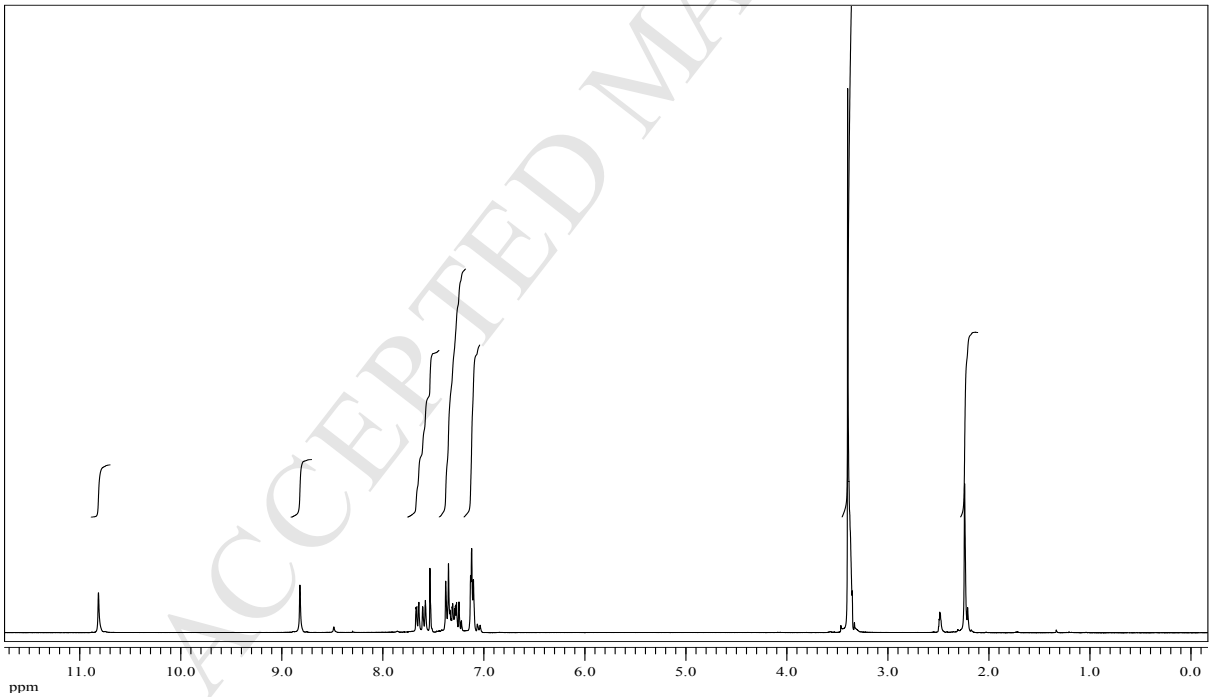

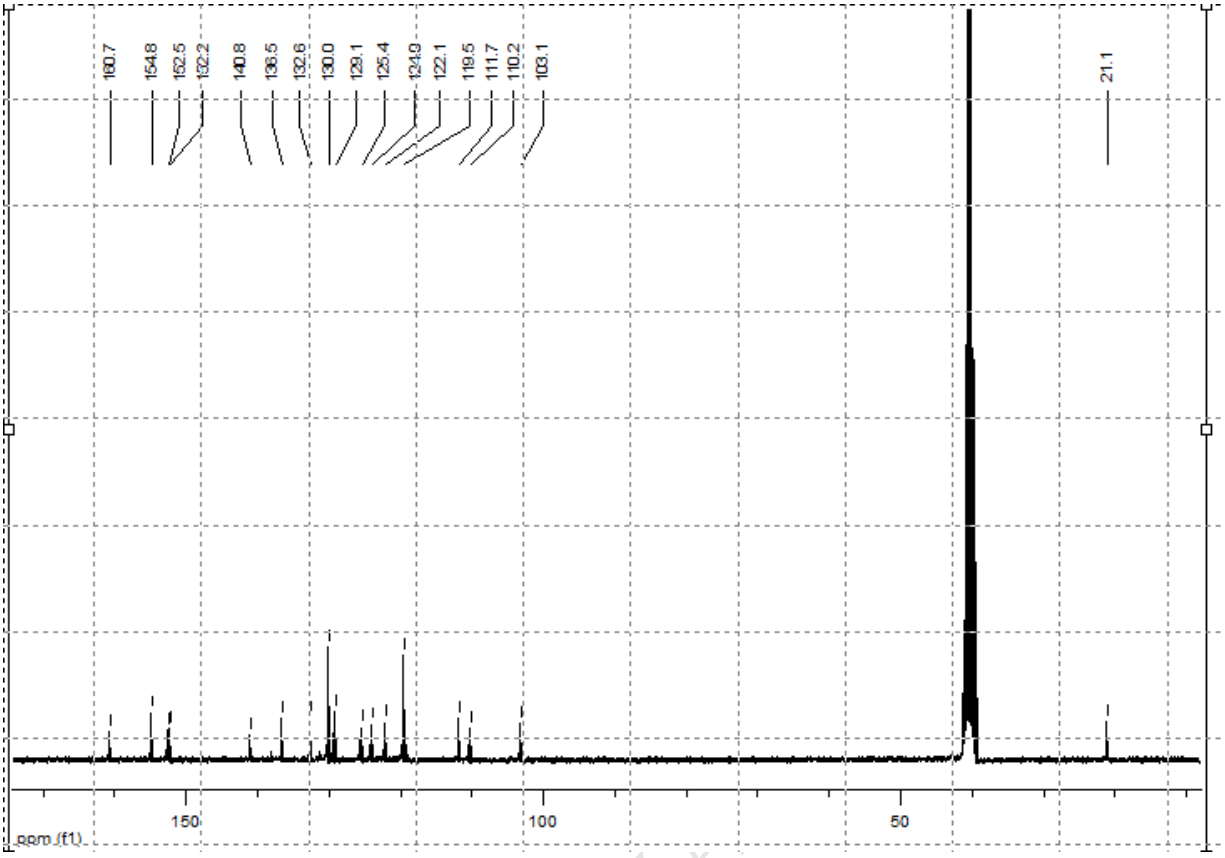
160.7
154.8
152.5
132.2
140.8
136.5
132.6
130.0
129.1
125.4
124.9
122.1
119.5
111.7
110.2
103.1
21.1
150
100
50
ppm (f1)

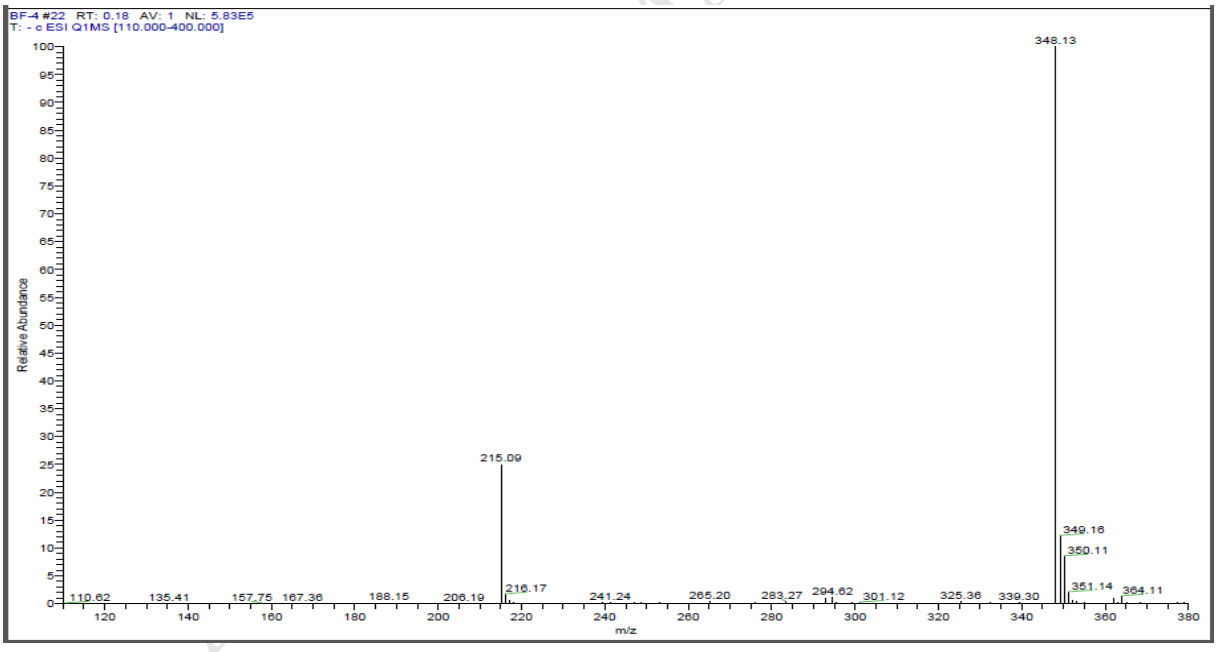
BF-4 #22 RT: 0.18 AV: 1 NL: 5.83E5
T: - c ESI Q1MS [110.000-400.000]
Relative Abundance
m/z
348.13
215.09
349.16
350.11
351.14
364.11
216.17
110.62
135.41
157.75
167.36
188.15
206.19
241.24
265.20
283.27
294.62
301.12
325.36
339.30

SM 5. ^{1}H and ^{13}C NMR and MS spectra of e5

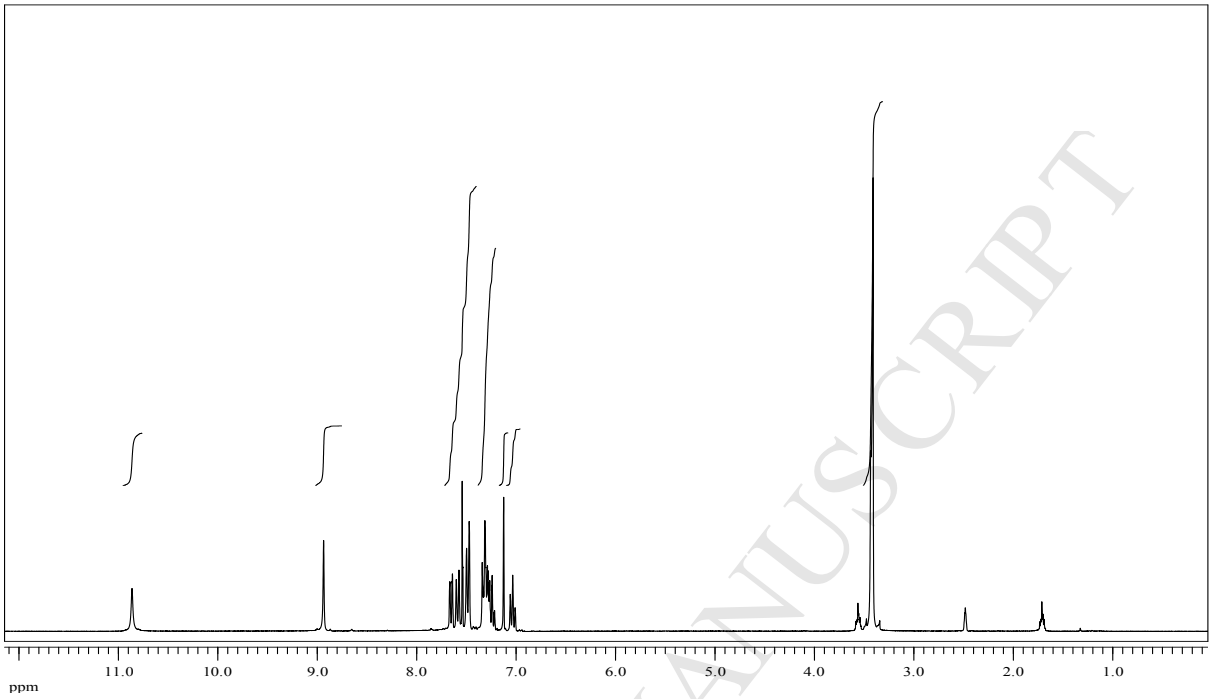

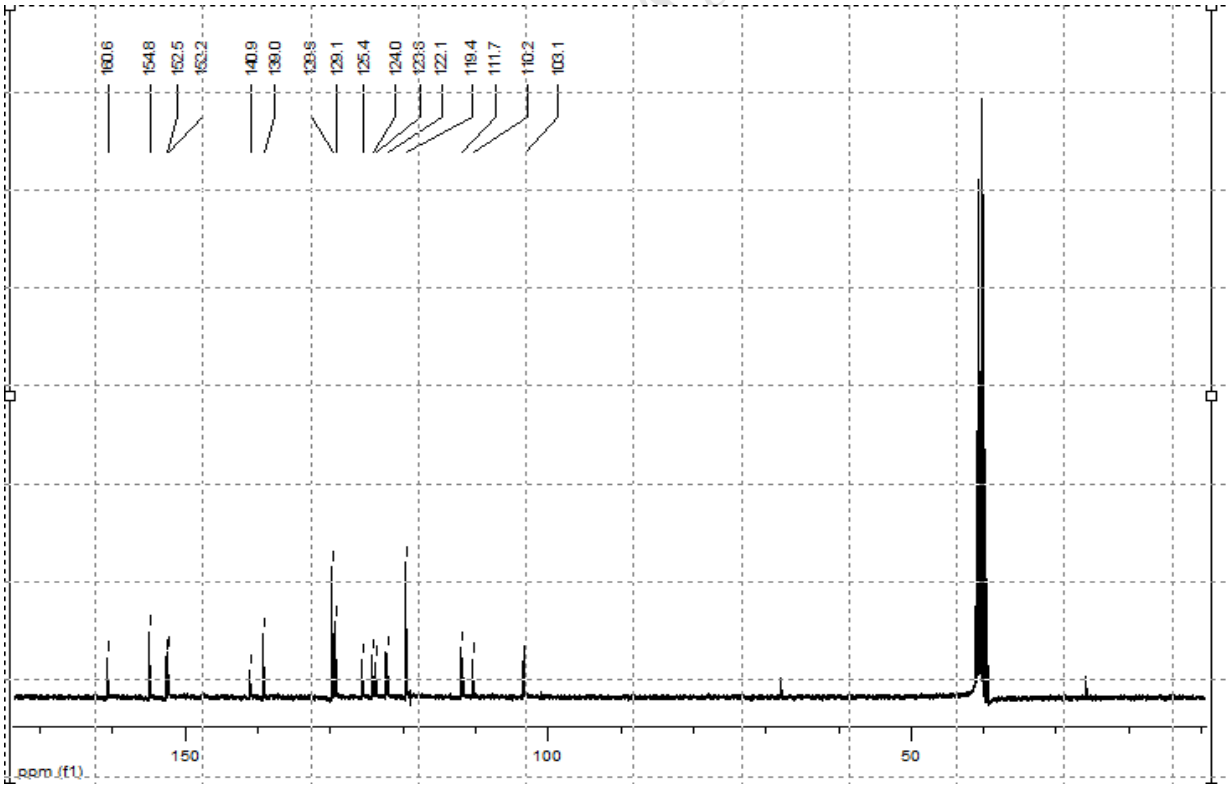

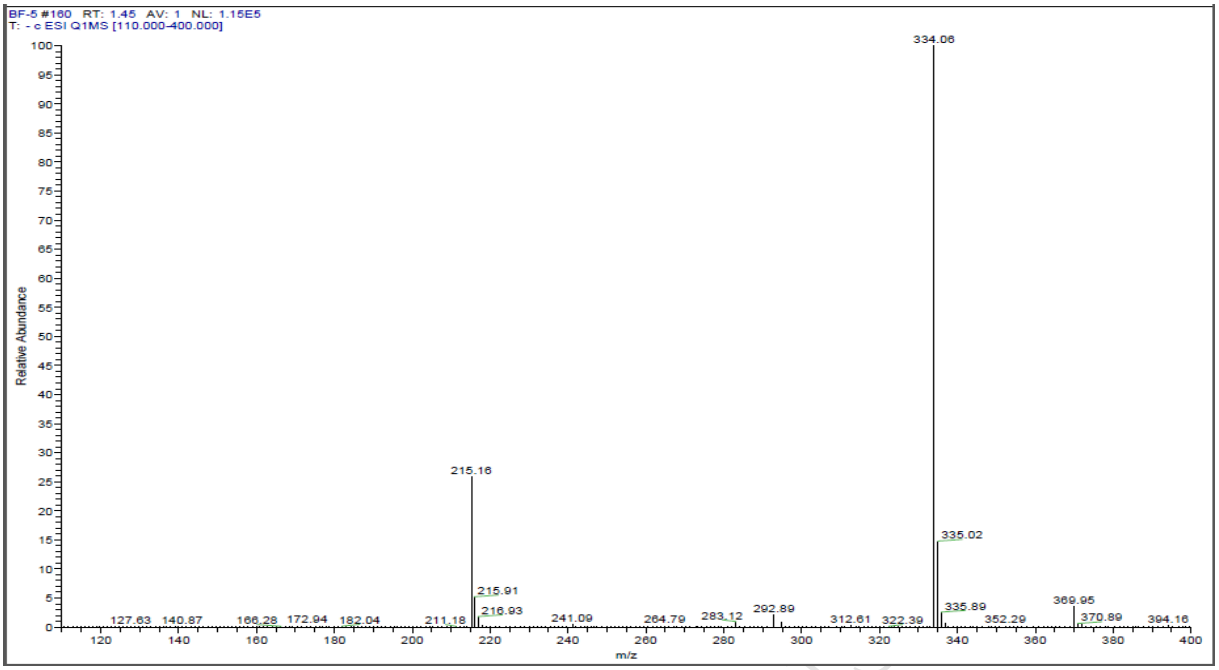

SM 6. ^{1}H and ^{13}C NMR and MS spectra of e6

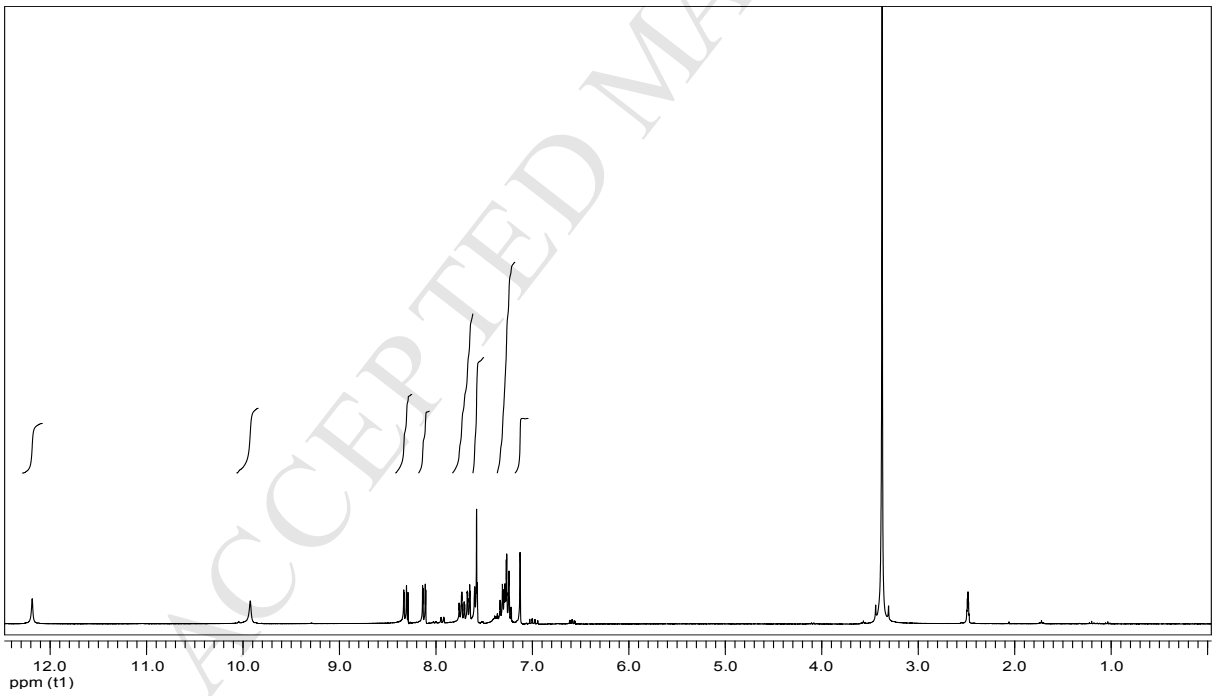

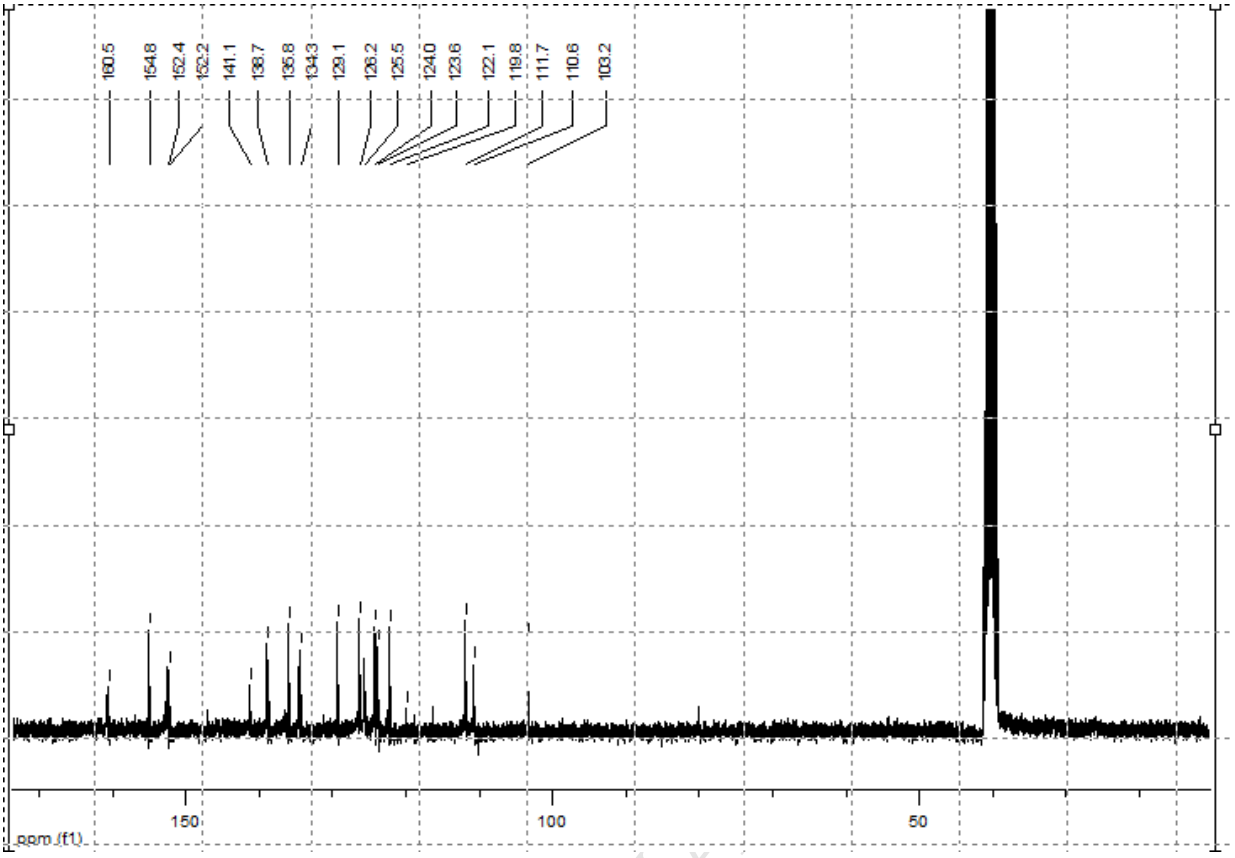
160.5
154.8
152.4
152.2
141.1
138.7
135.8
134.3
129.1
126.2
125.5
124.0
123.6
122.1
119.8
111.7
110.6
103.2
150
100
50
ppm (f1)

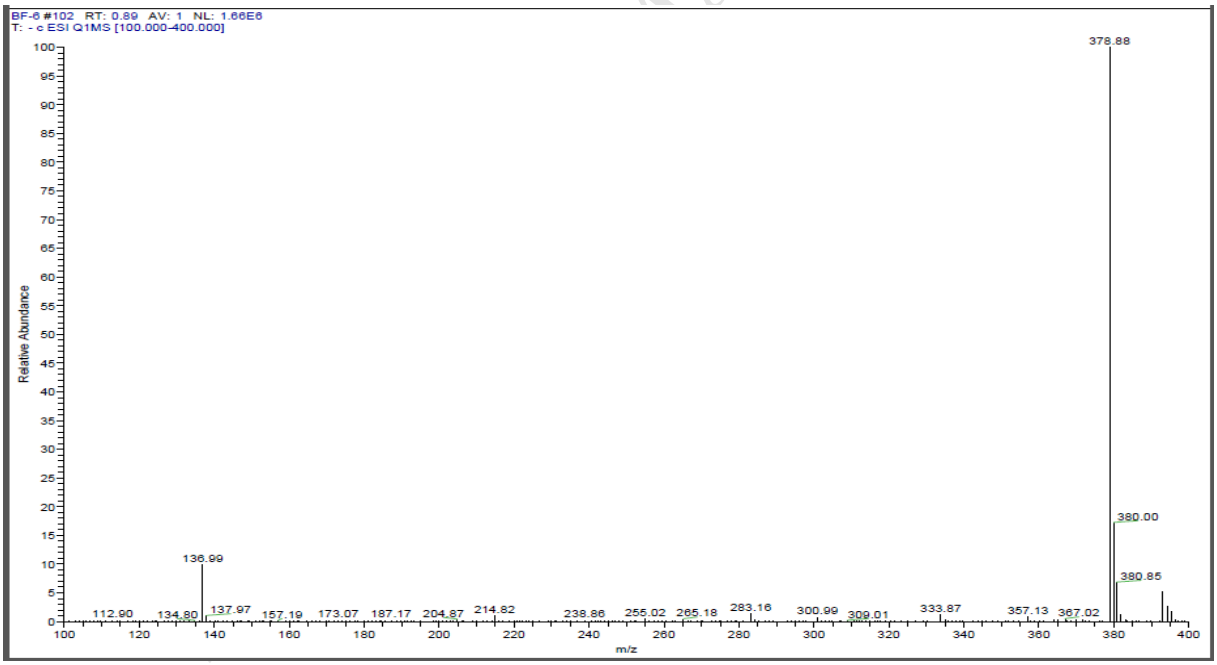
BF-6 #102 RT: 0.89 AV: 1 NL: 1.66E6
T: - c ESI Q1MS [100.000-400.000]
Relative Abundance
m/z
378.88
380.00
380.85
136.99
112.90
134.80
137.97
157.19
173.07
187.17
204.87
214.82
238.86
255.02
265.18
283.16
300.99
309.01
333.87
357.13
367.02

SM 7. ^{1}H and ^{13}C NMR and MS spectra of e7

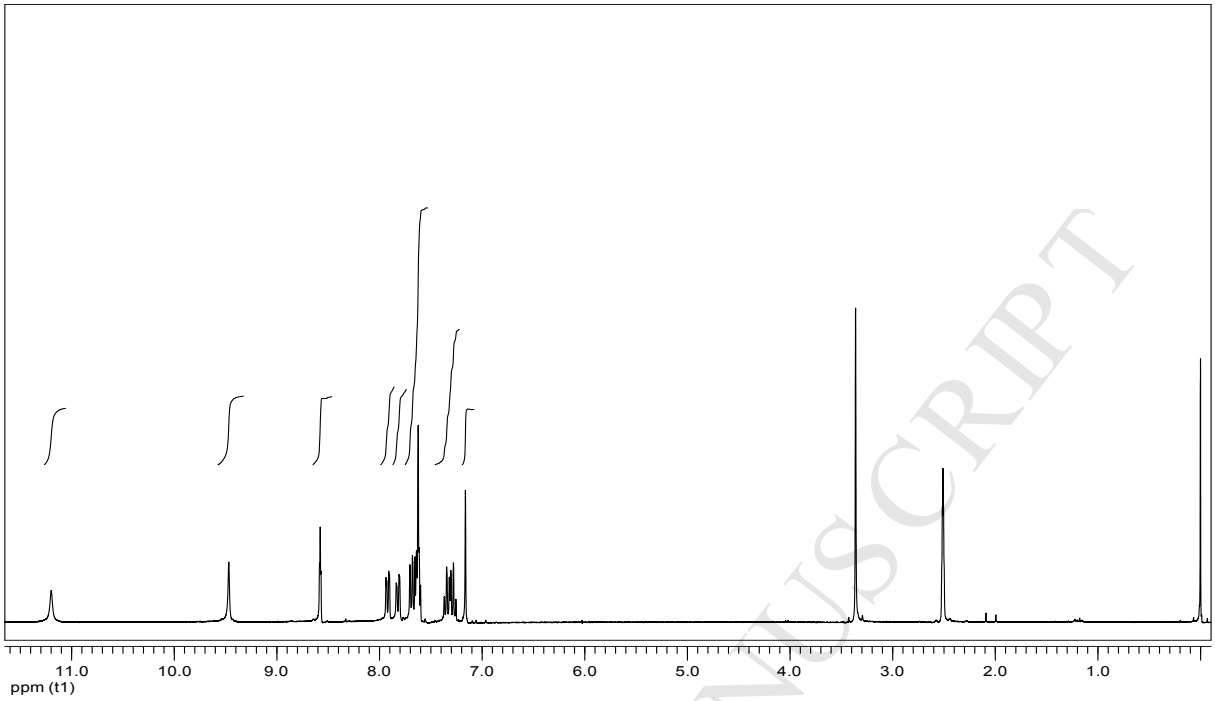

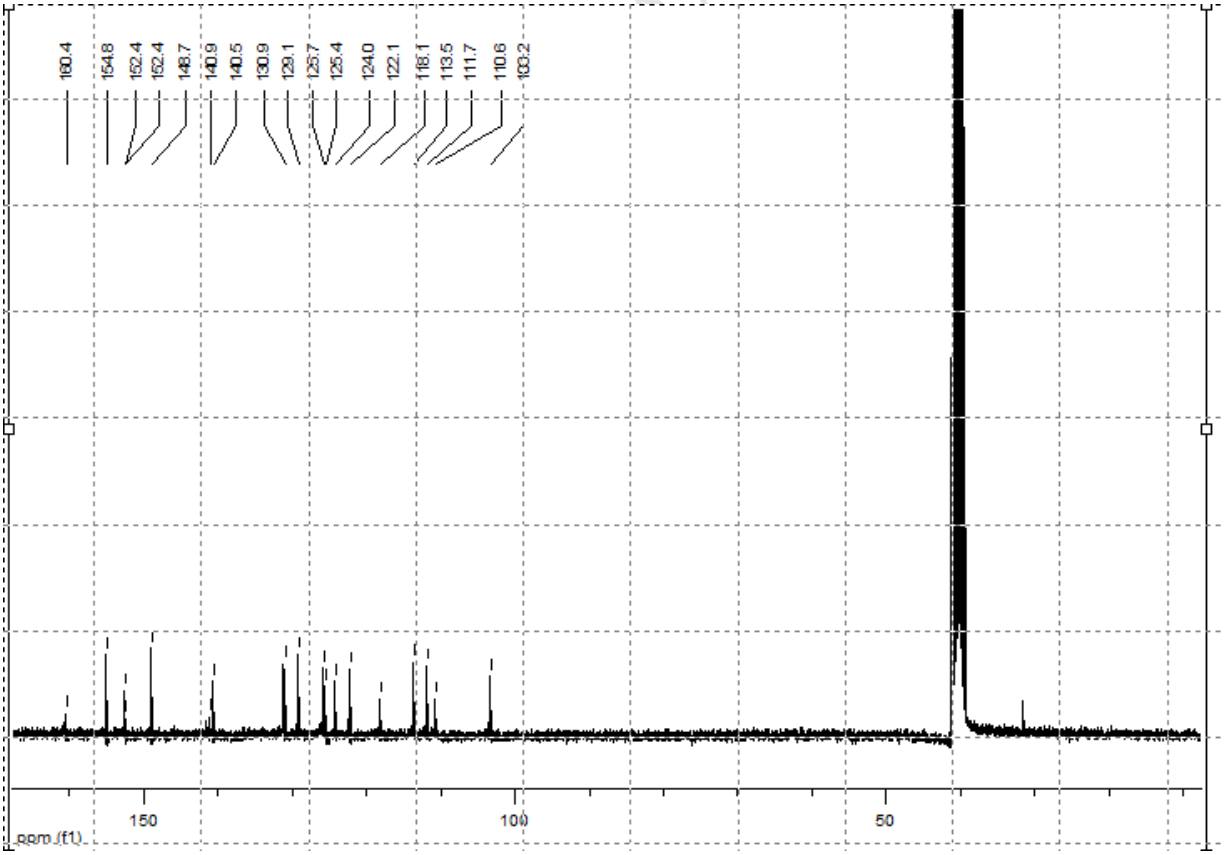

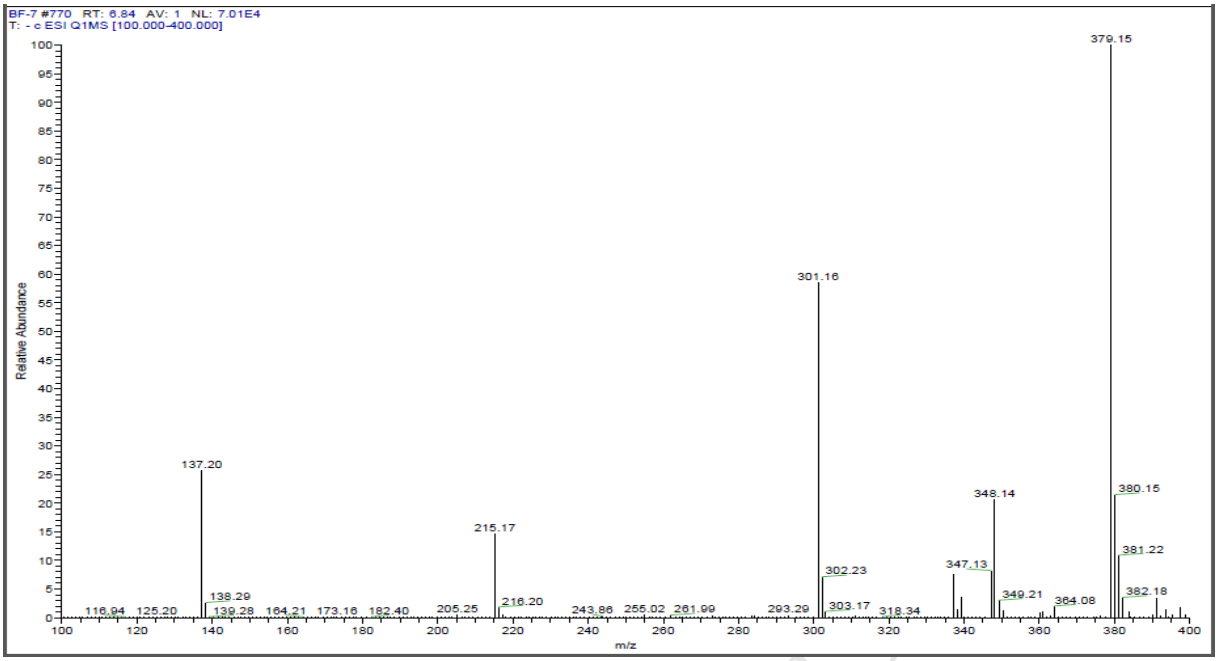

SM 8. ^{1}H and ^{13}C NMR and MS spectra of e8

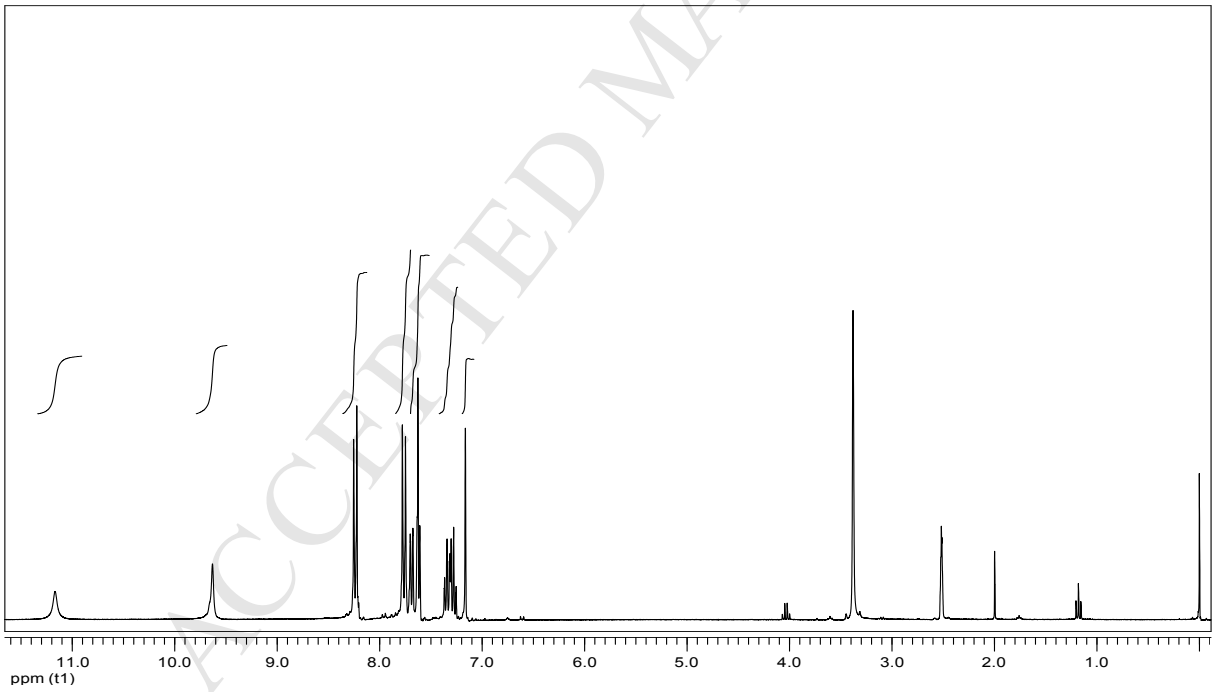

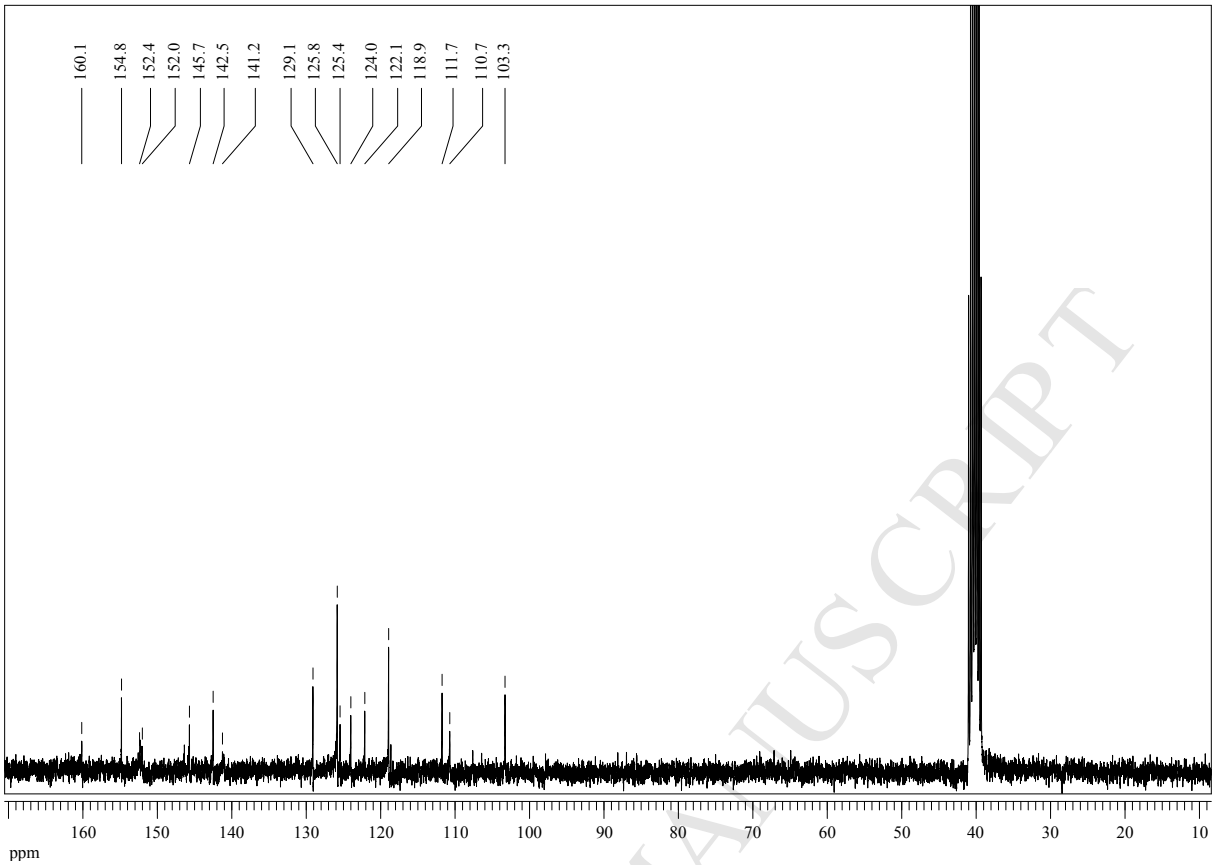
160.1
154.8
152.4
152.0
145.7
142.5
141.2
129.1
125.8
125.4
124.0
122.1
118.9
111.7
110.7
103.3
160
150
140
130
120
110
100
90
80
70
60
50
40
30
20
10
ppm

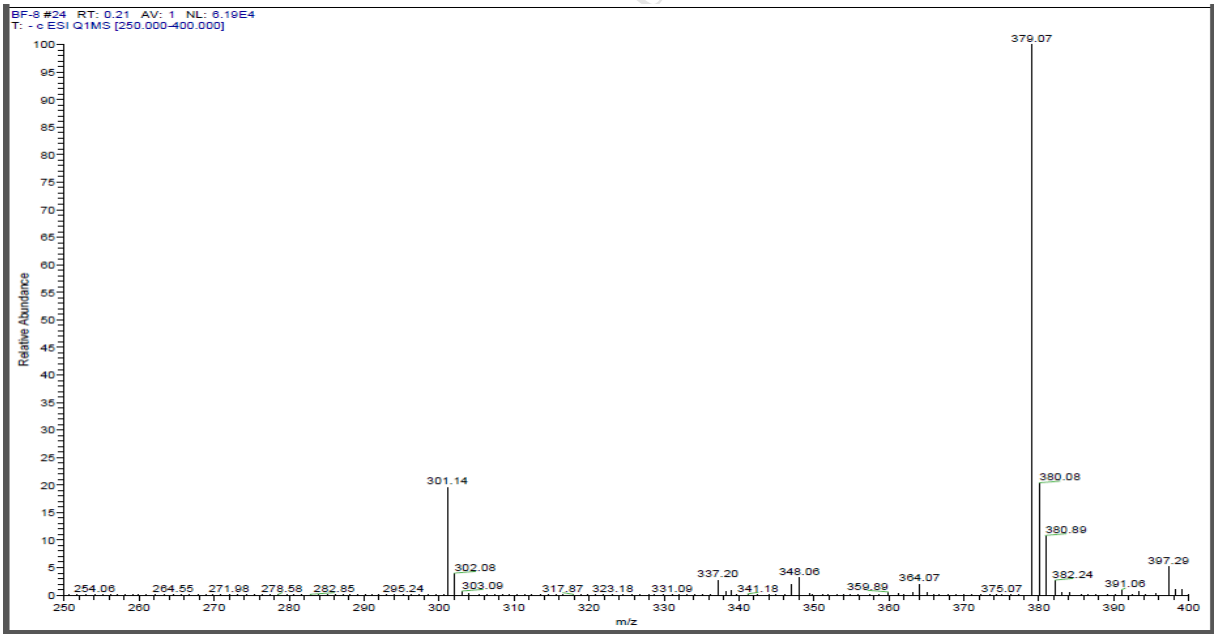
BF-8 #24 RT: 0.21 AV: 1 NL: 6.19E4
T: - c ESI Q1MS [250.000-400.000]
Relative Abundance
m/z
379.07
380.08
380.89
301.14
302.08
303.09
337.20
348.06
364.07
382.24
391.06
397.29
254.06
264.55
271.98
278.58
282.85
295.24
317.87
323.18
331.09
341.18
359.89
375.07

SM 9. ^{1}H and ^{13}C NMR and MS spectra of e9

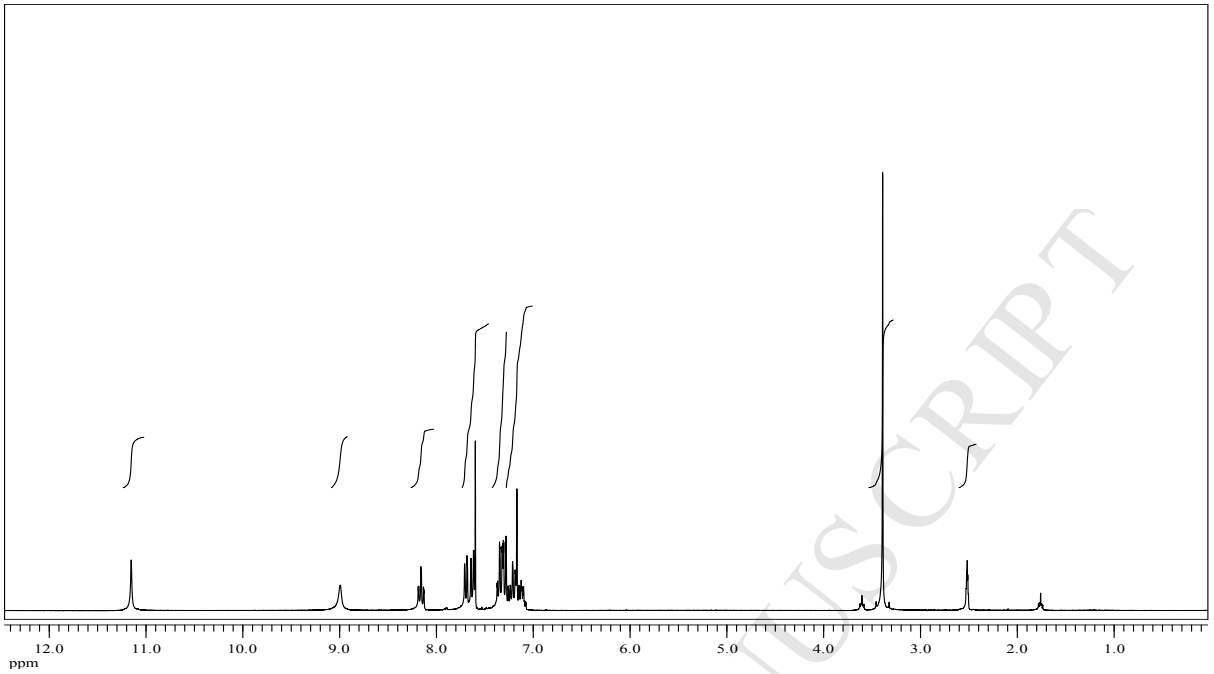

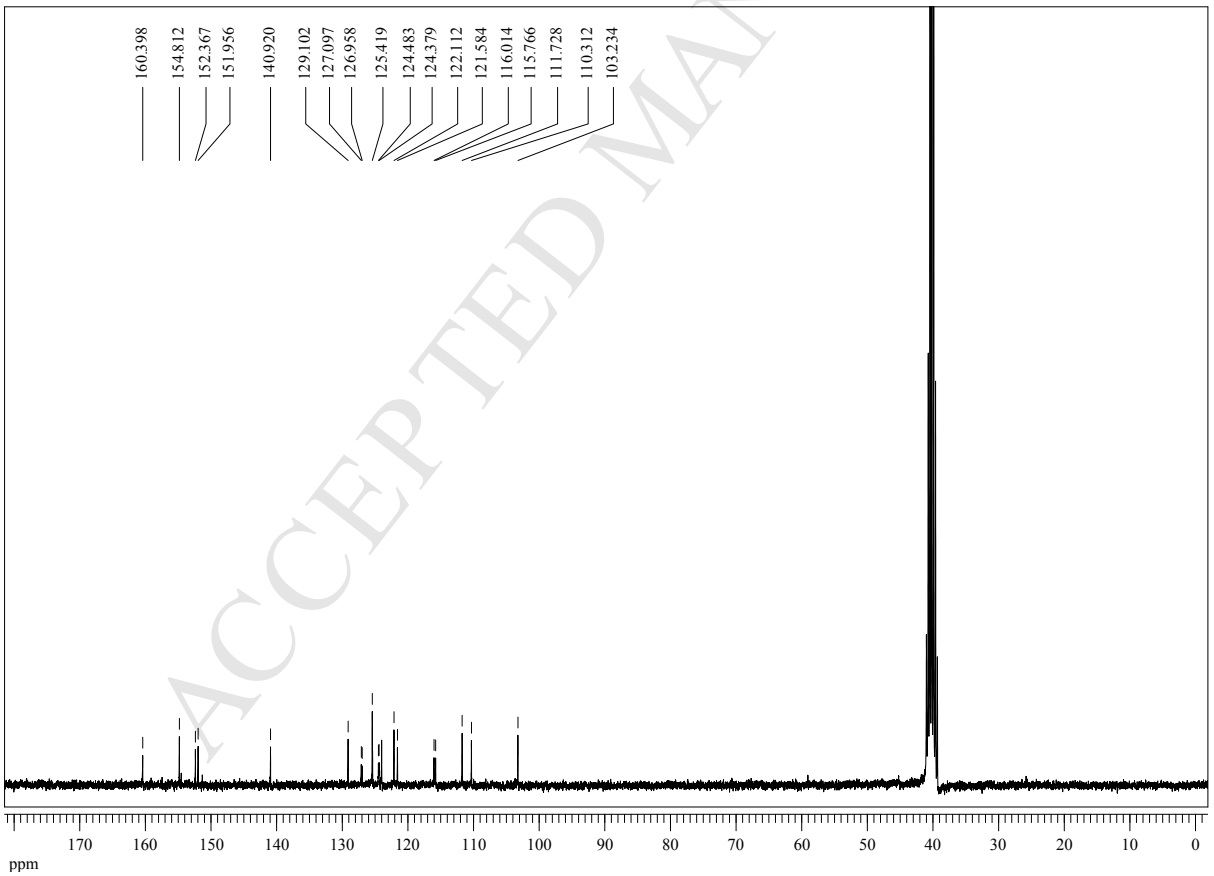

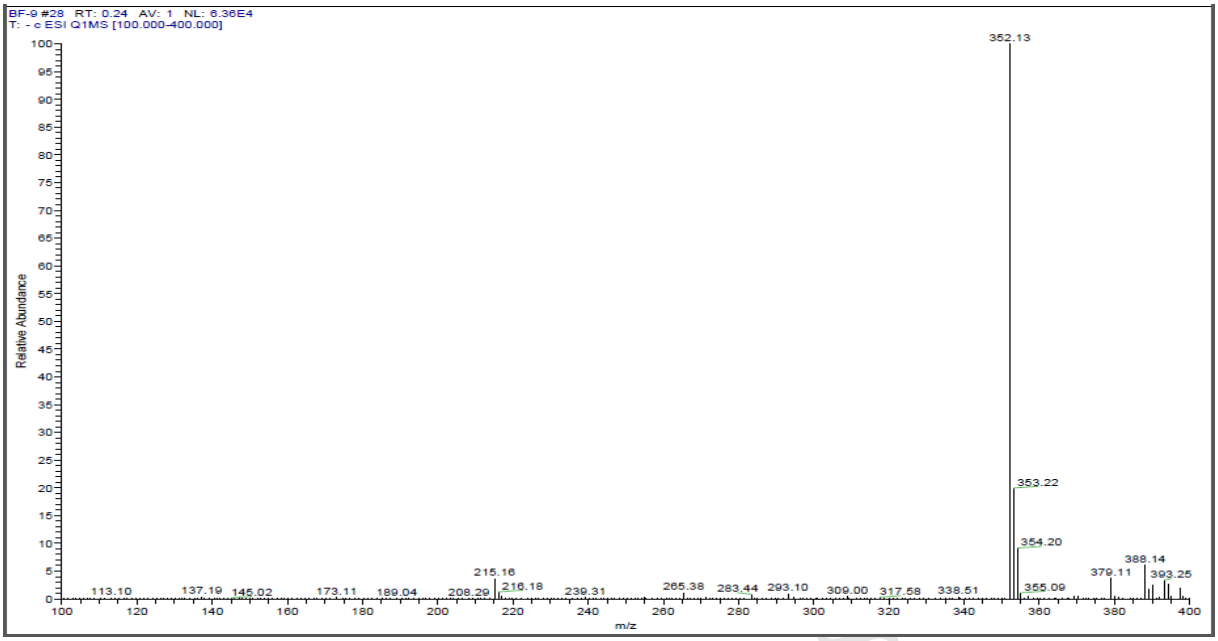

SM 10. ^{1}H and ^{13}C NMR and MS spectra of e10

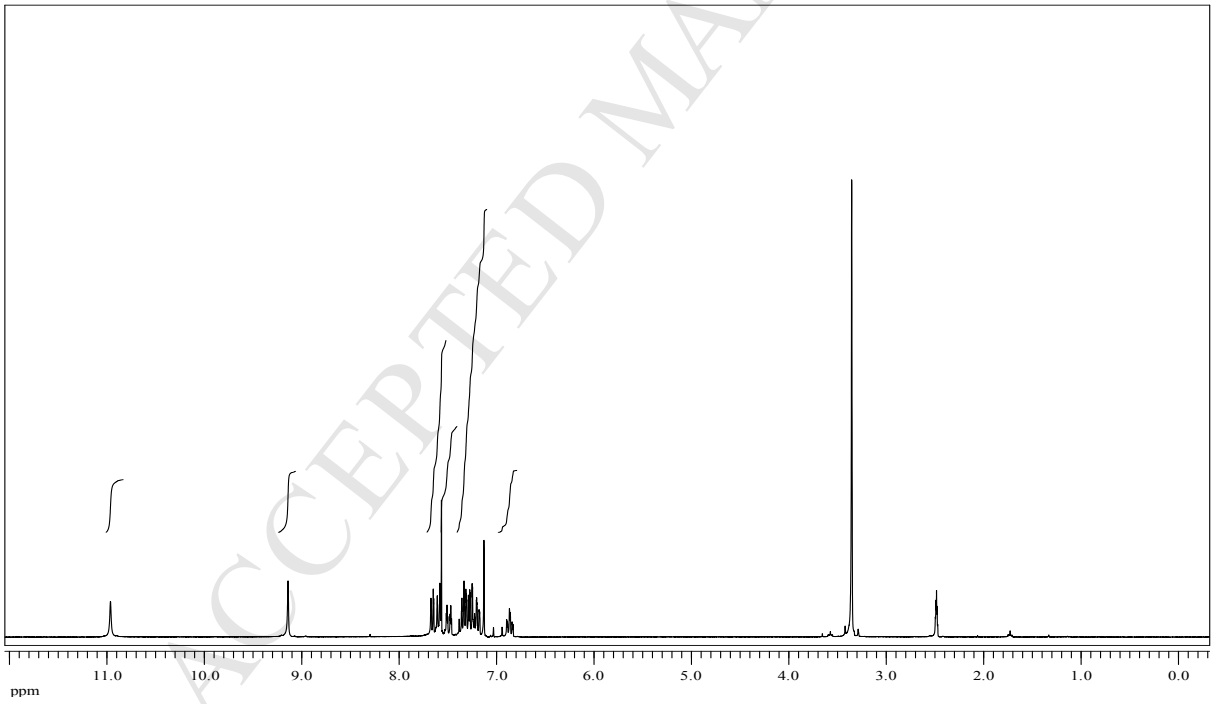

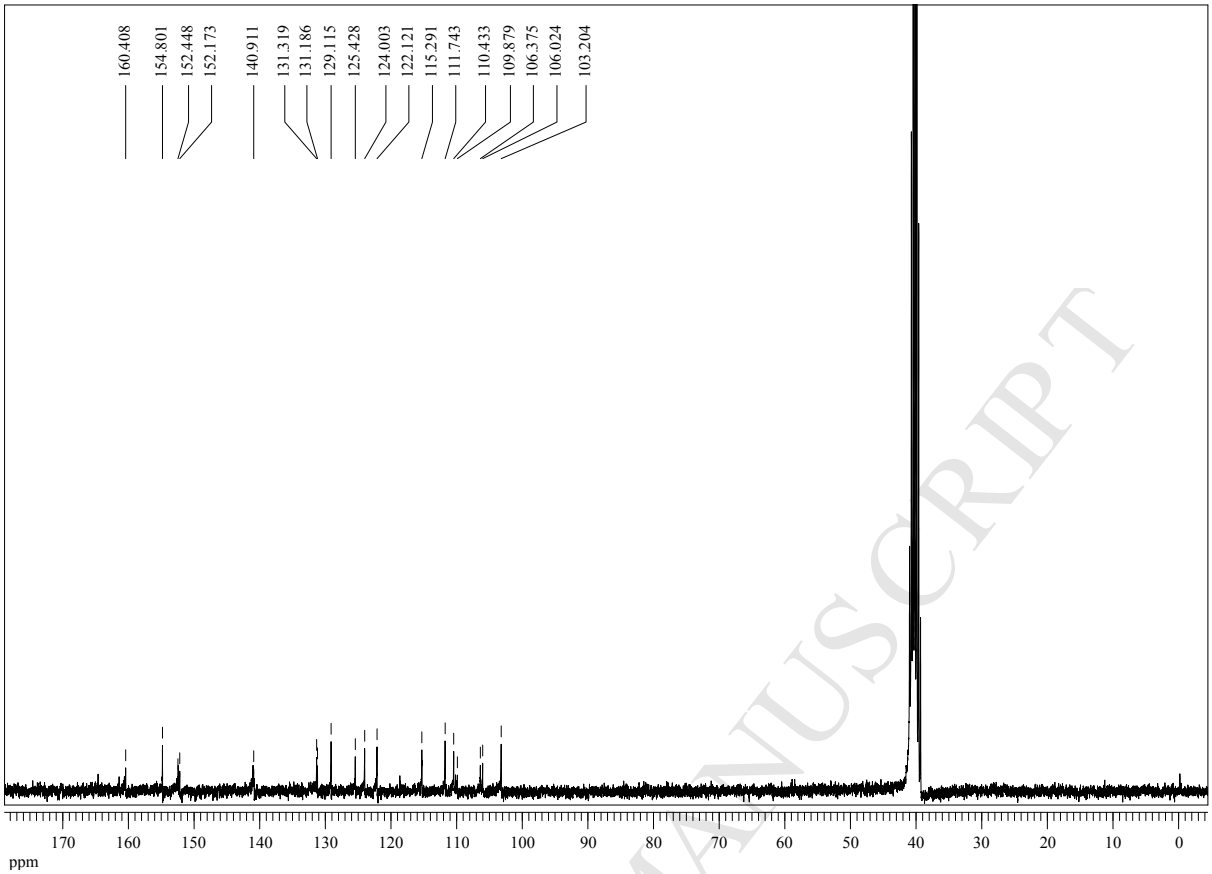
160.408
154.801
152.448
152.173
140.911
131.319
131.186
129.115
125.428
124.003
122.121
115.291
111.743
110.433
109.879
106.375
106.024
103.204
170
160
150
140
130
120
110
100
90
80
70
60
50
40
30
20
10
0
ppm

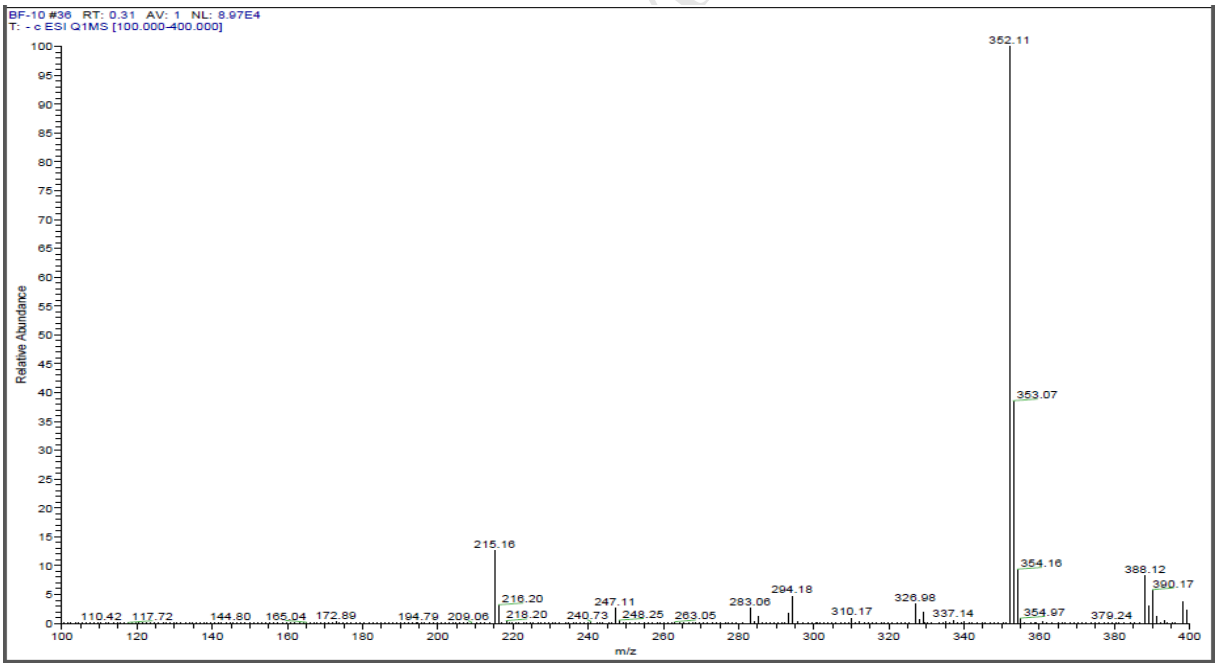
BF-10 #36 RT: 0.31 AV: 1 NL: 8.97E4
T: - c ESI Q1MS [100.000-400.000]
Relative Abundance
m/z
352.11
353.07
354.16
354.97
215.16
216.20
218.20
247.11
248.25
263.05
283.06
294.18
310.17
326.98
337.14
379.24
388.12
390.17
110.42
117.72
144.80
165.04
172.89
194.79
209.06
240.73

SM 11. ^{1}H and ^{13}C NMR and MS spectra of e11

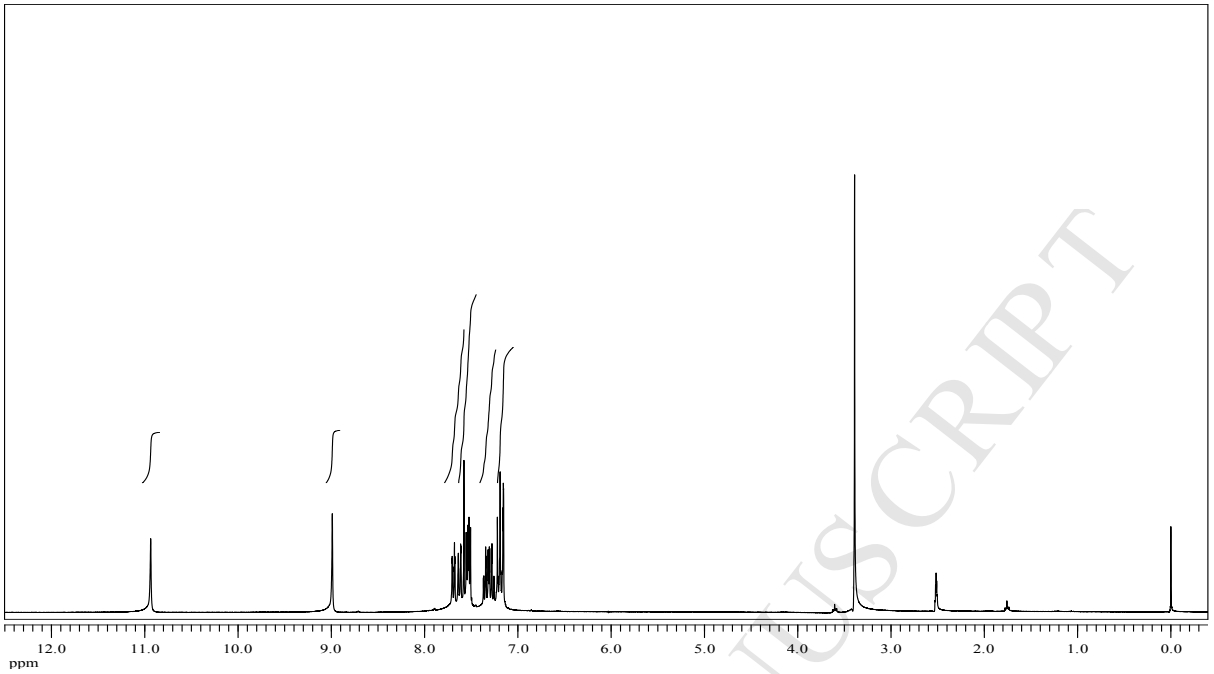

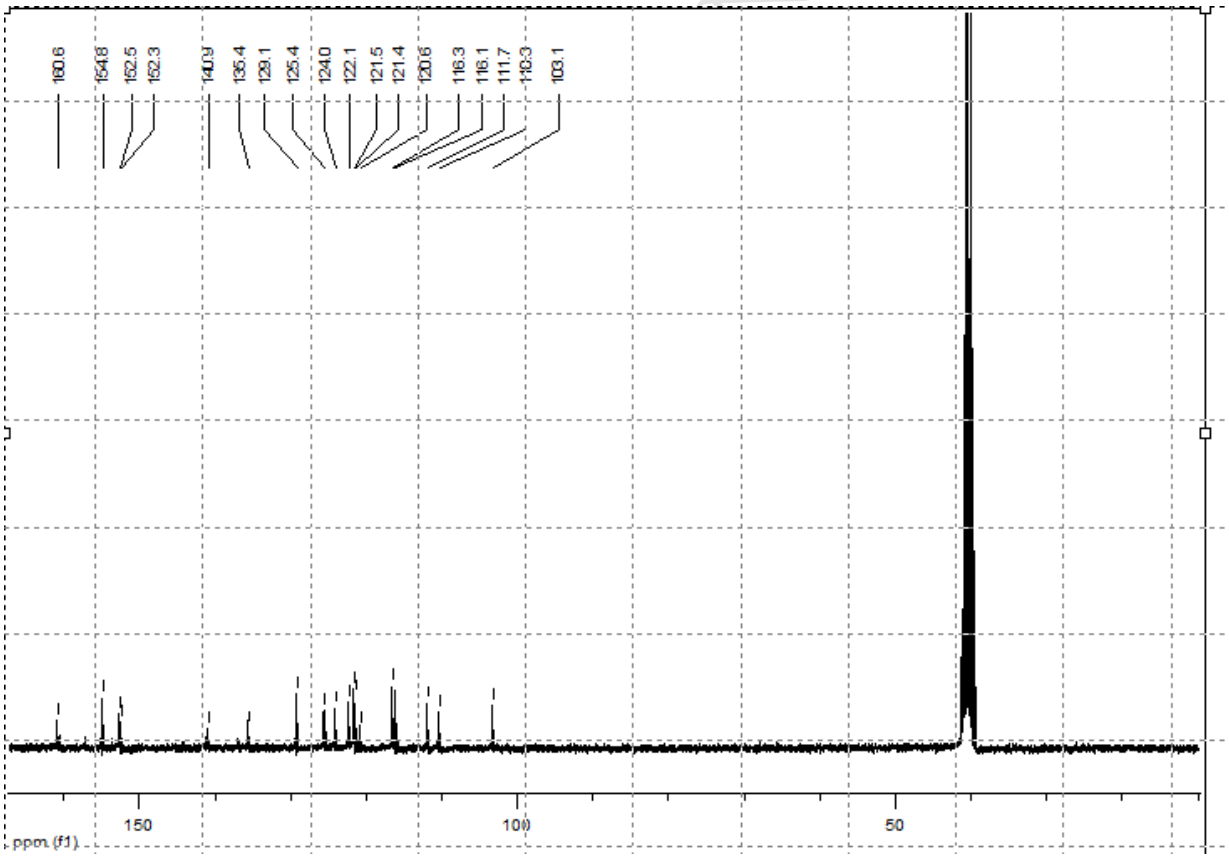

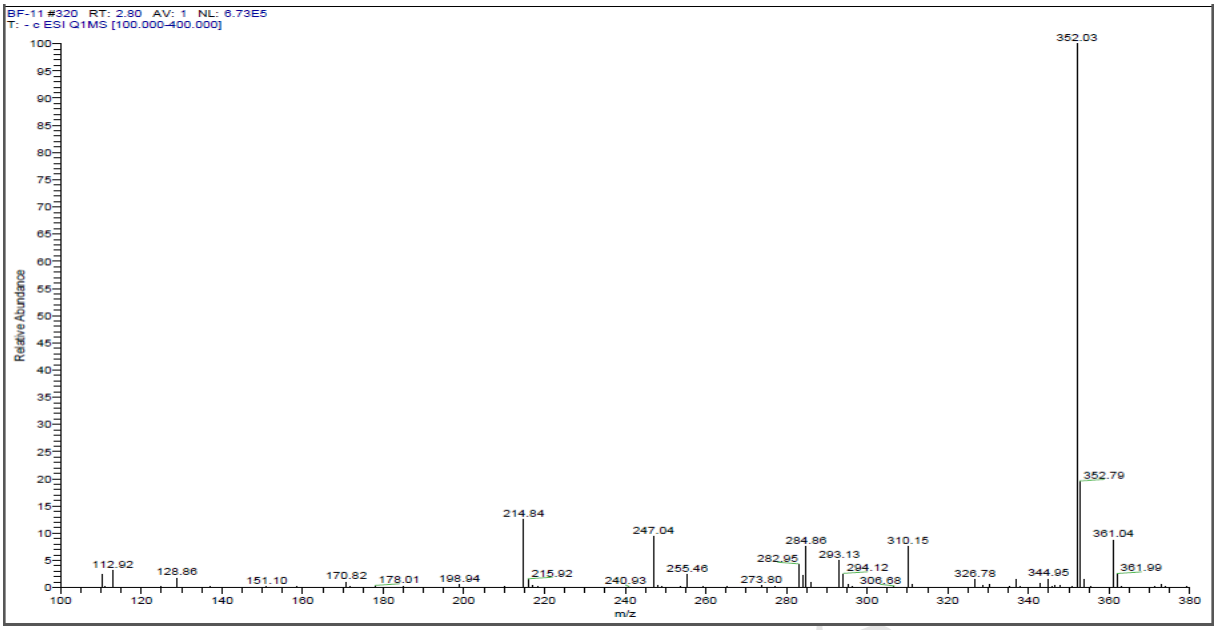

SM 12. ^{1}H and ^{13}C NMR and MS spectra of e12

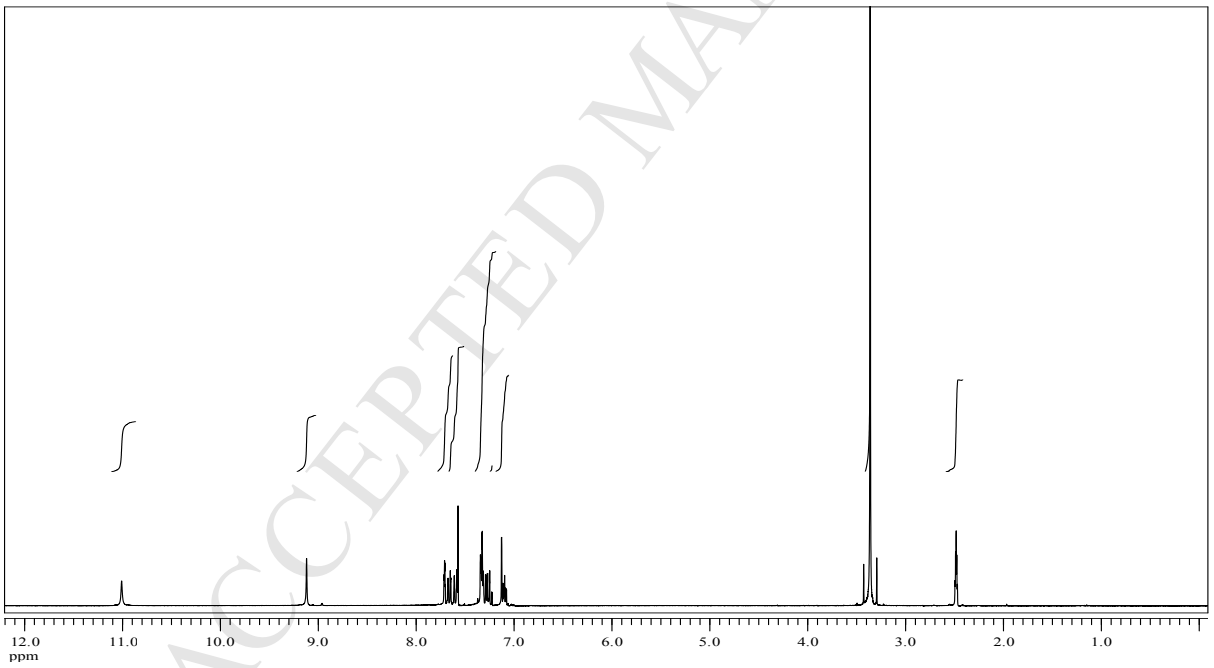

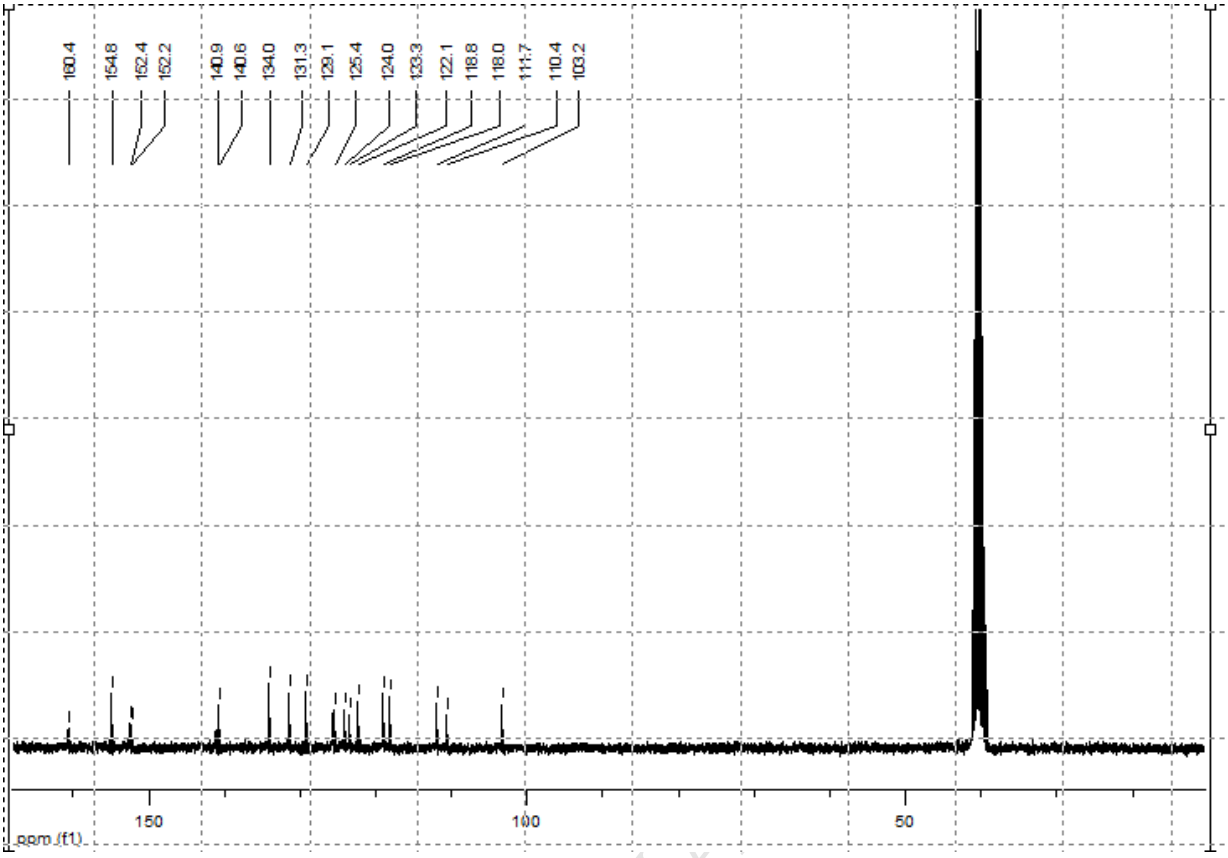
160.4
154.8
152.4
152.2
140.9
140.6
134.0
131.3
129.1
125.4
124.0
123.3
122.1
118.8
118.0
111.7
110.4
103.2
150
100
50
ppm (f1)

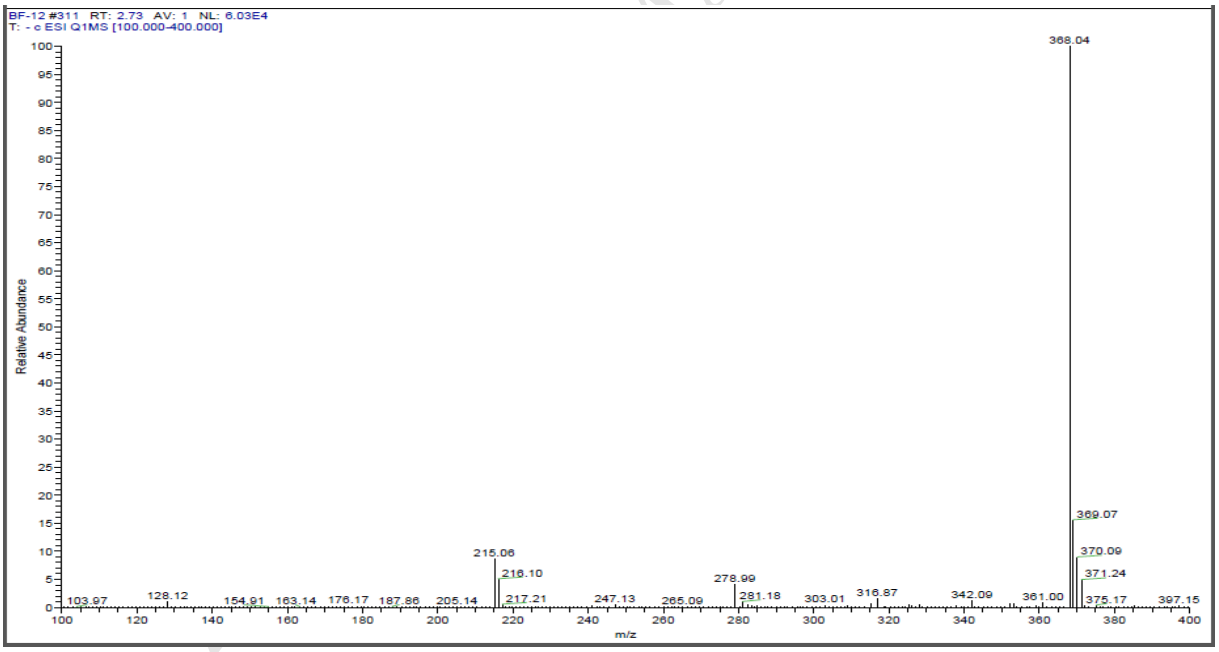
BF-12 #311 RT: 2.73 AV: 1 NL: 6.03E4
T: - c ESI Q1MS [100.000-400.000]
Relative Abundance
m/z
368.04
369.07
370.09
371.24
215.06
216.10
217.21
278.99
281.18
103.97
128.12
154.91
163.14
176.17
187.86
205.14
247.13
265.09
303.01
316.87
342.09
361.00
375.17
397.15

SM 13. ^{1}H and ^{13}C NMR and MS spectra of e13

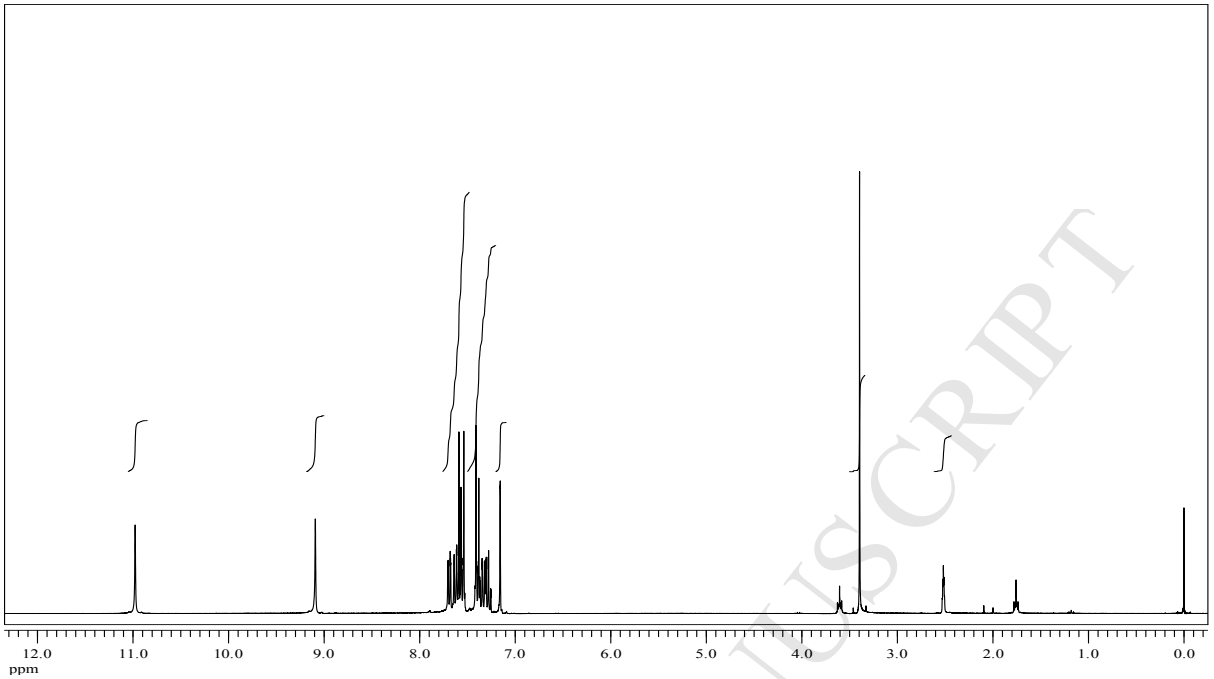

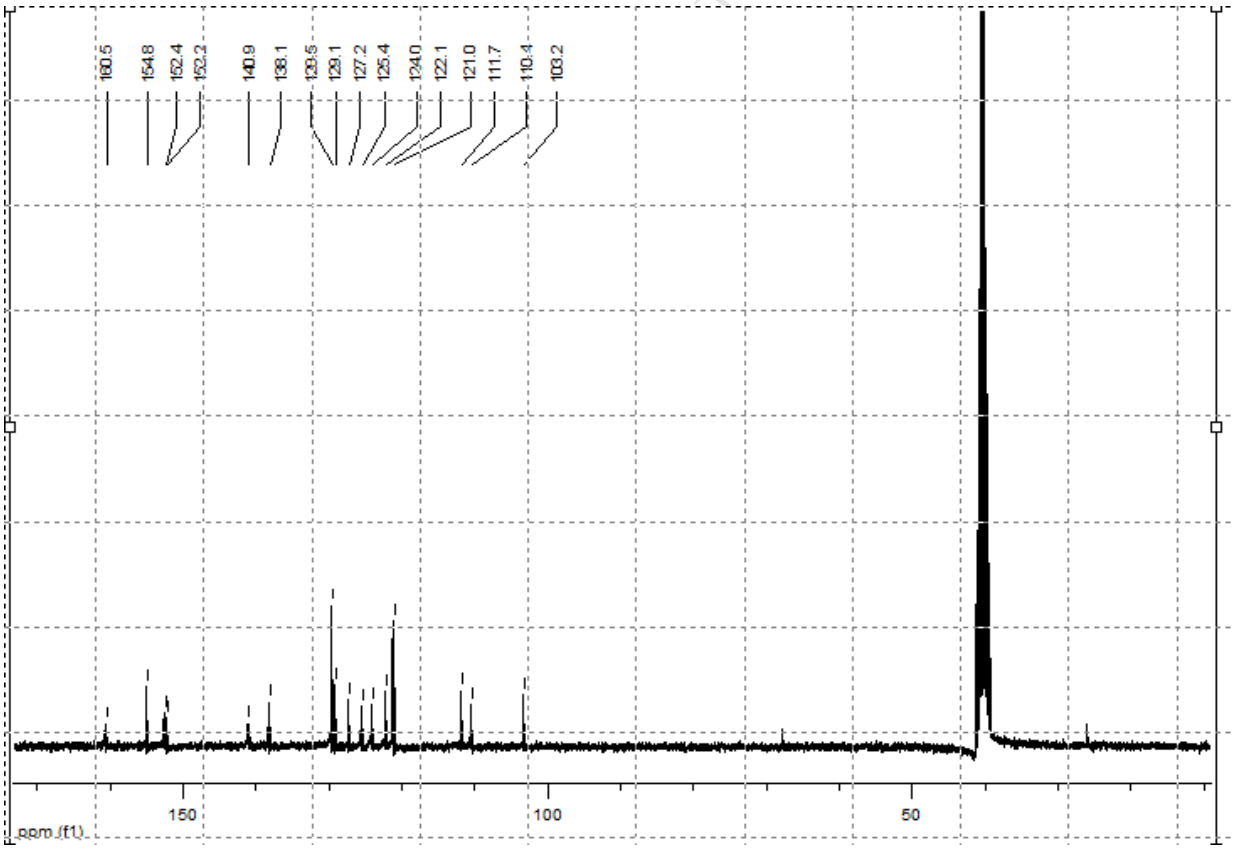

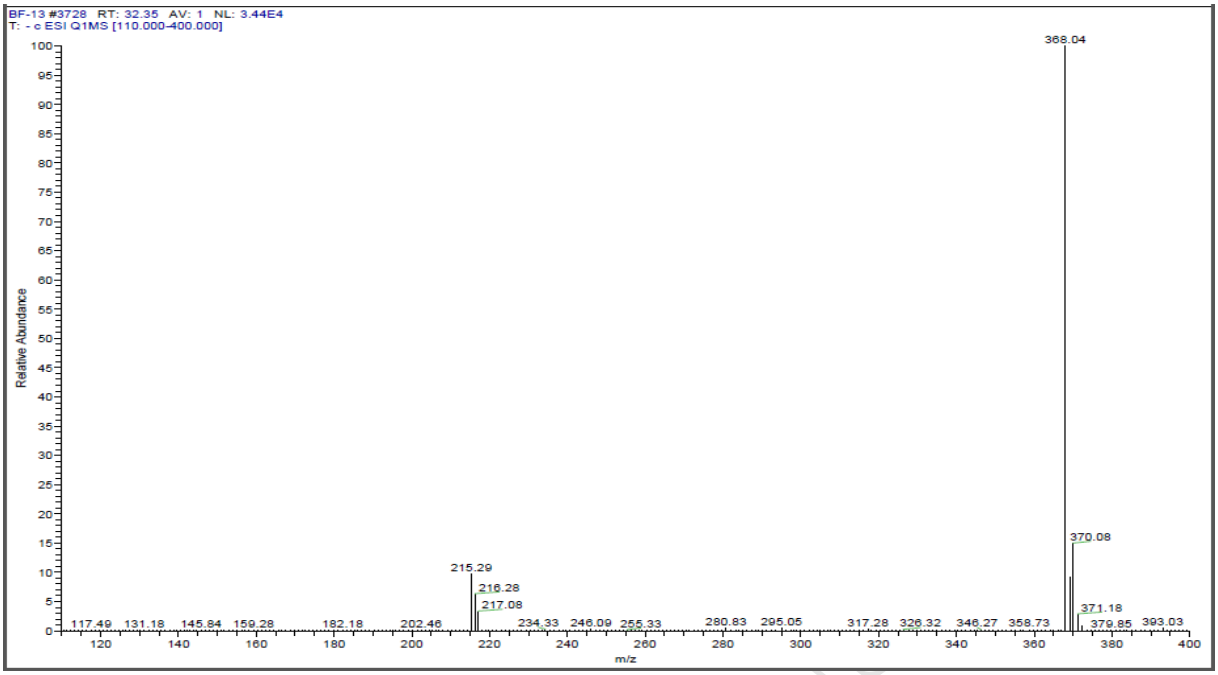

SM 14. ^{1}H and ^{13}C NMR and MS spectra of e14

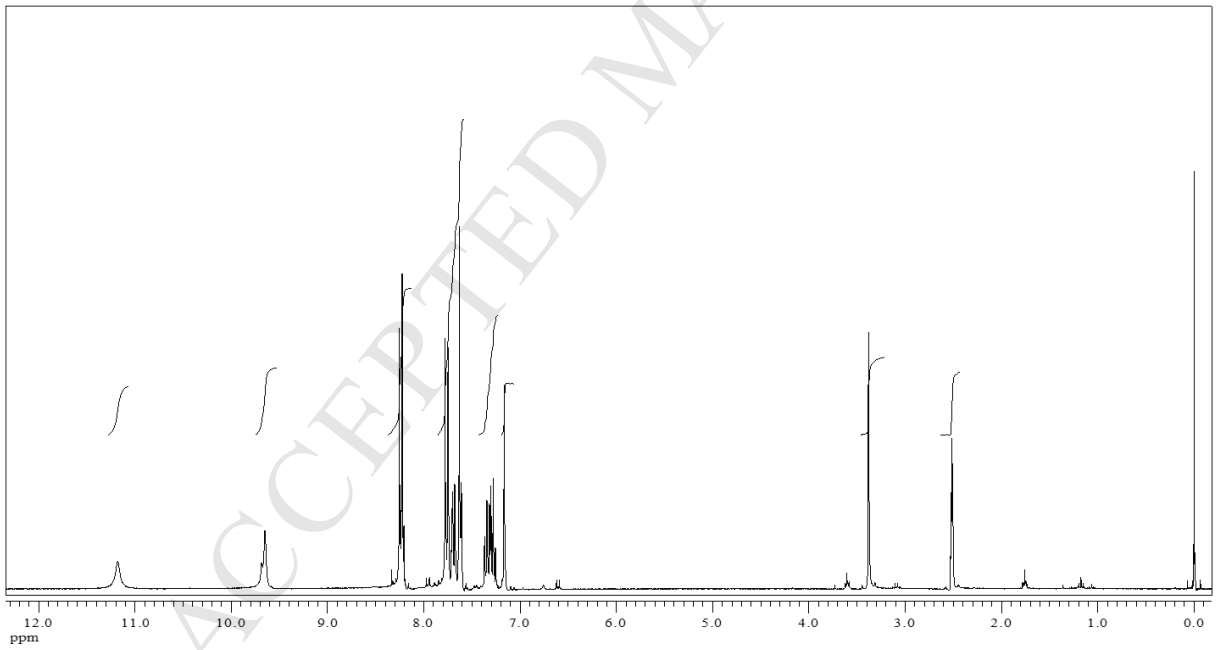

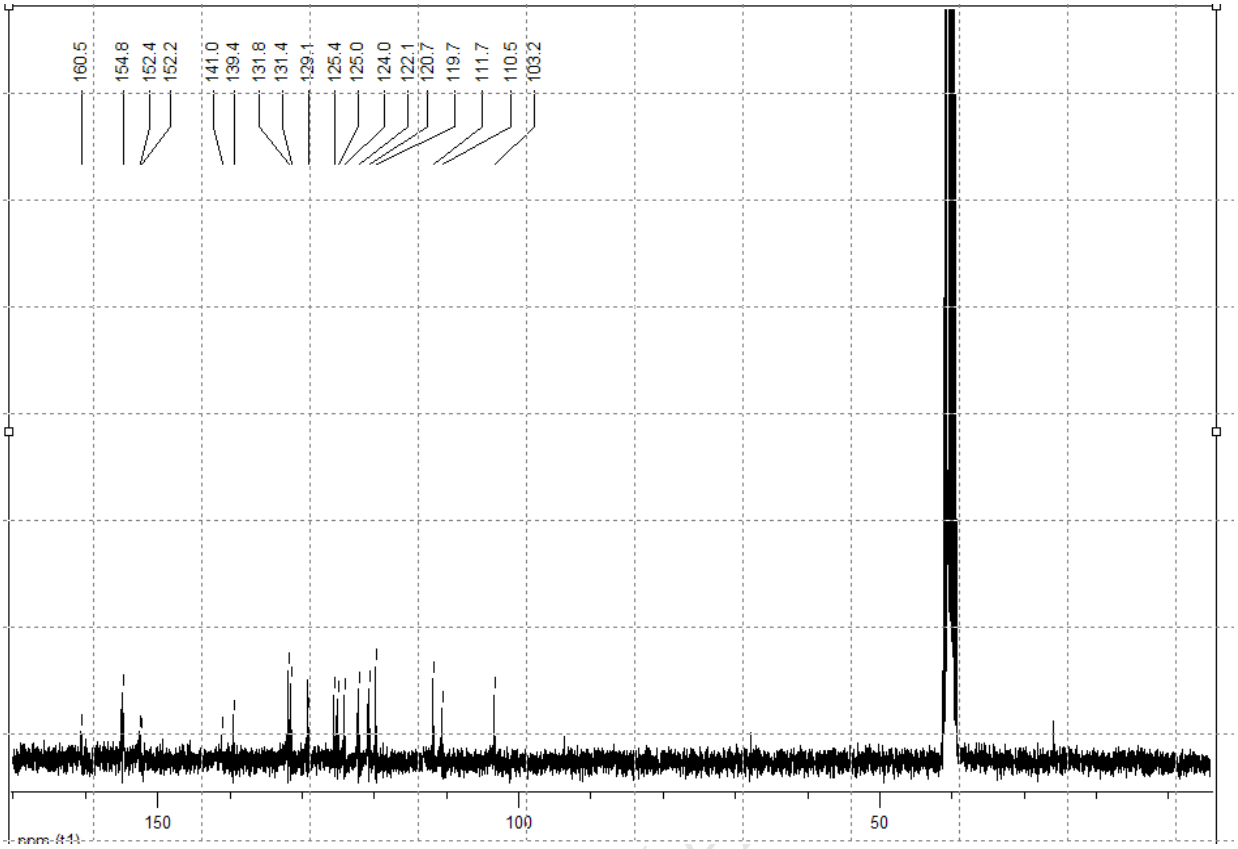
160.5
154.8
152.4
152.2
141.0
139.4
131.8
131.4
129.1
125.4
125.0
124.0
122.1
120.7
119.7
111.7
110.5
103.2
150
100
50
ppm (t1)

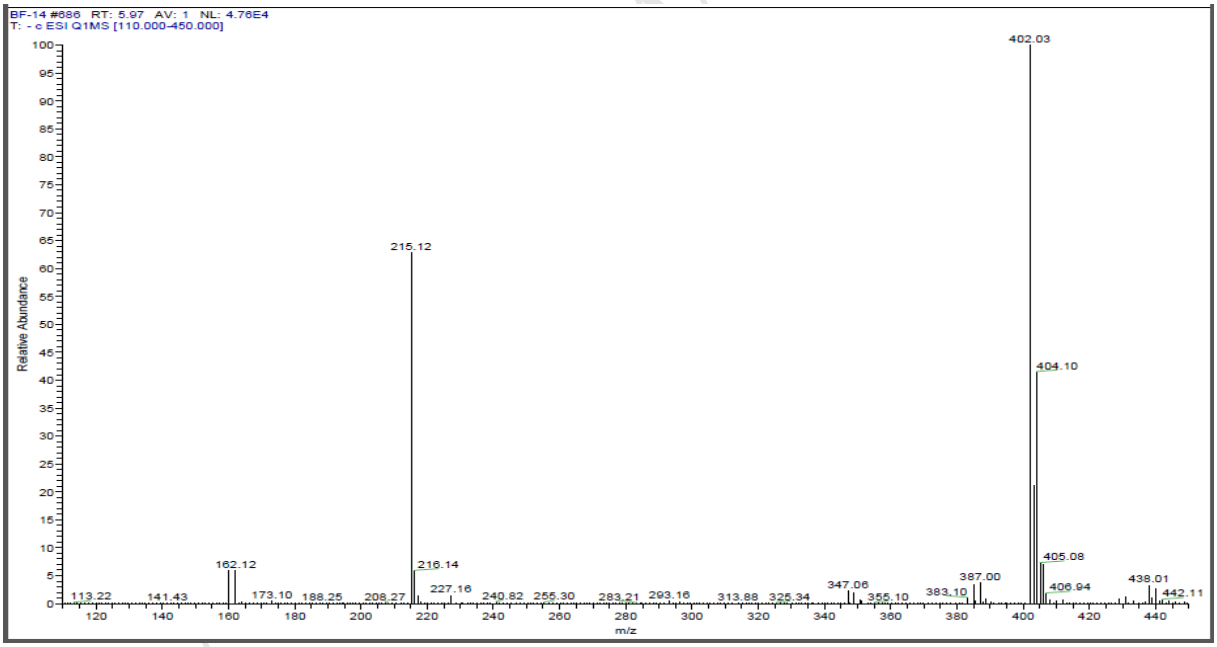
BF-14 #686 RT: 5.97 AV: 1 NL: 4.76E4
T: - c ESI Q1MS [110.000-450.000]
Relative Abundance
m/z
402.03
215.12
404.10
405.08
406.94
438.01
442.11
162.12
216.14
227.16
387.00
347.06
383.10
355.10
113.22
141.43
173.10
188.25
208.27
240.82
255.30
283.21
293.16
313.88
325.34

SM 15. ^{1}H and ^{13}C NMR and MS spectra of e15

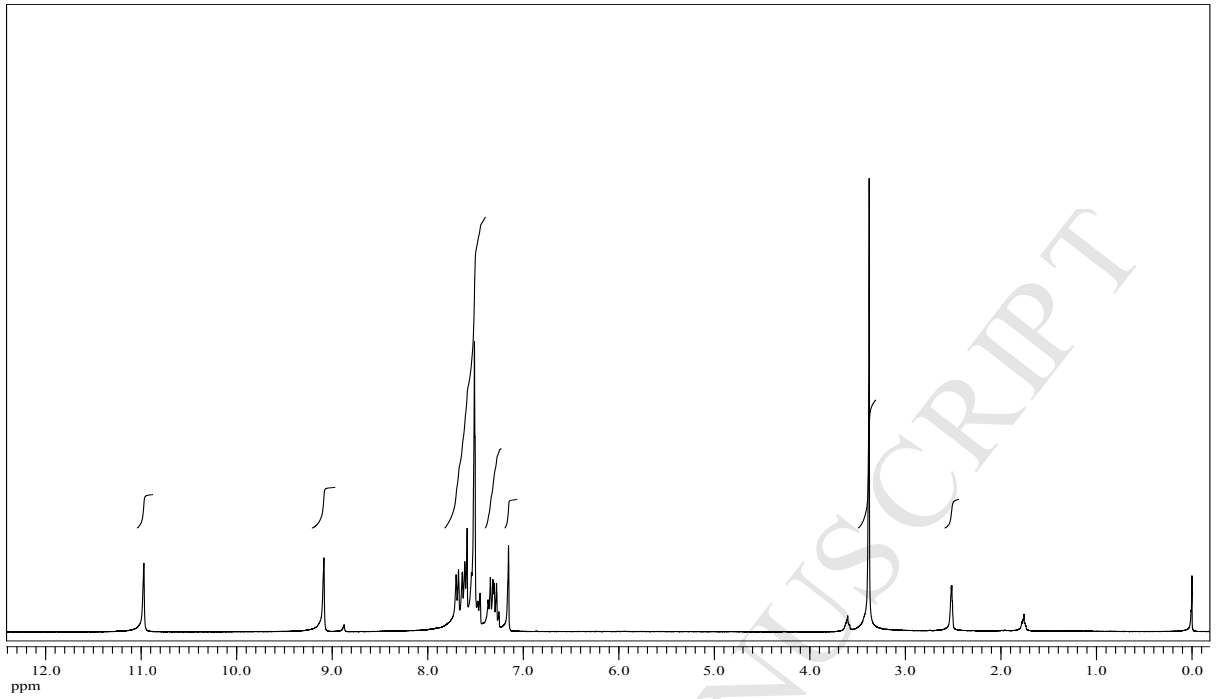

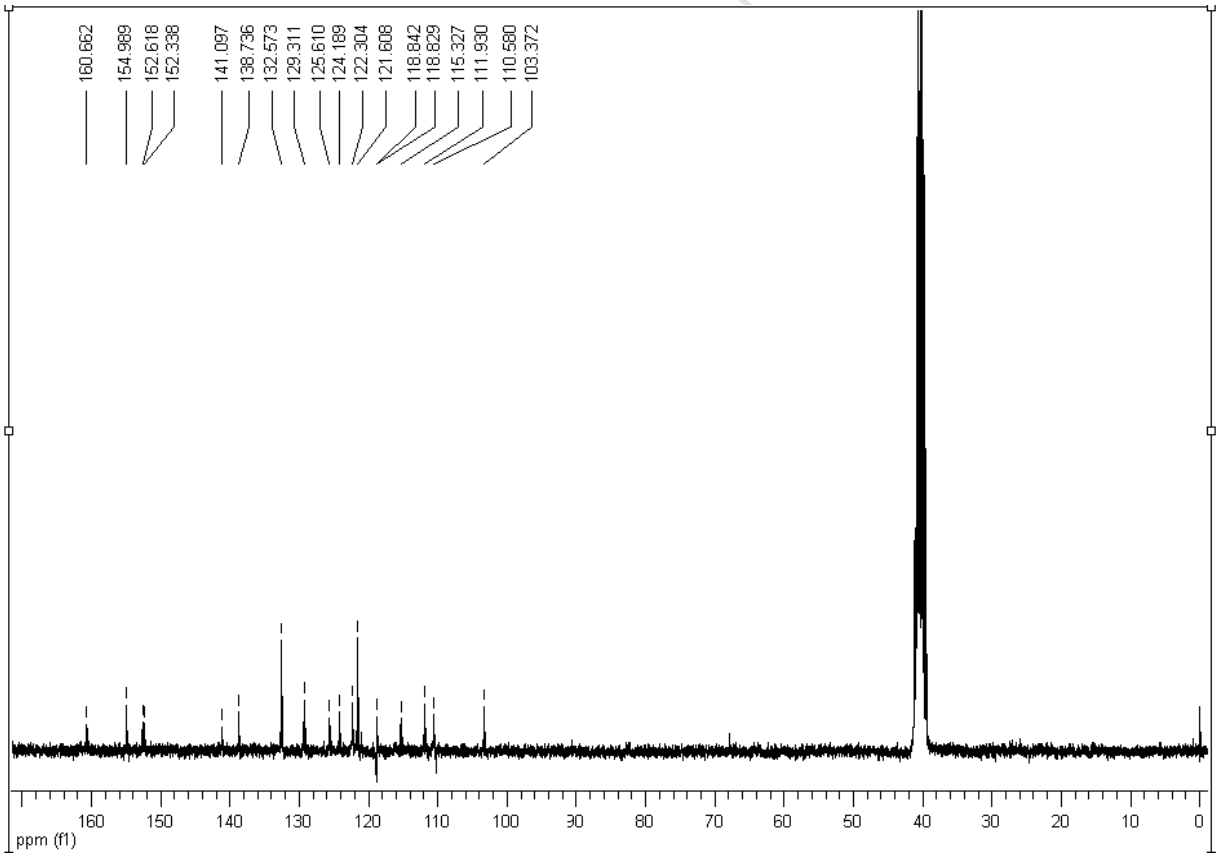

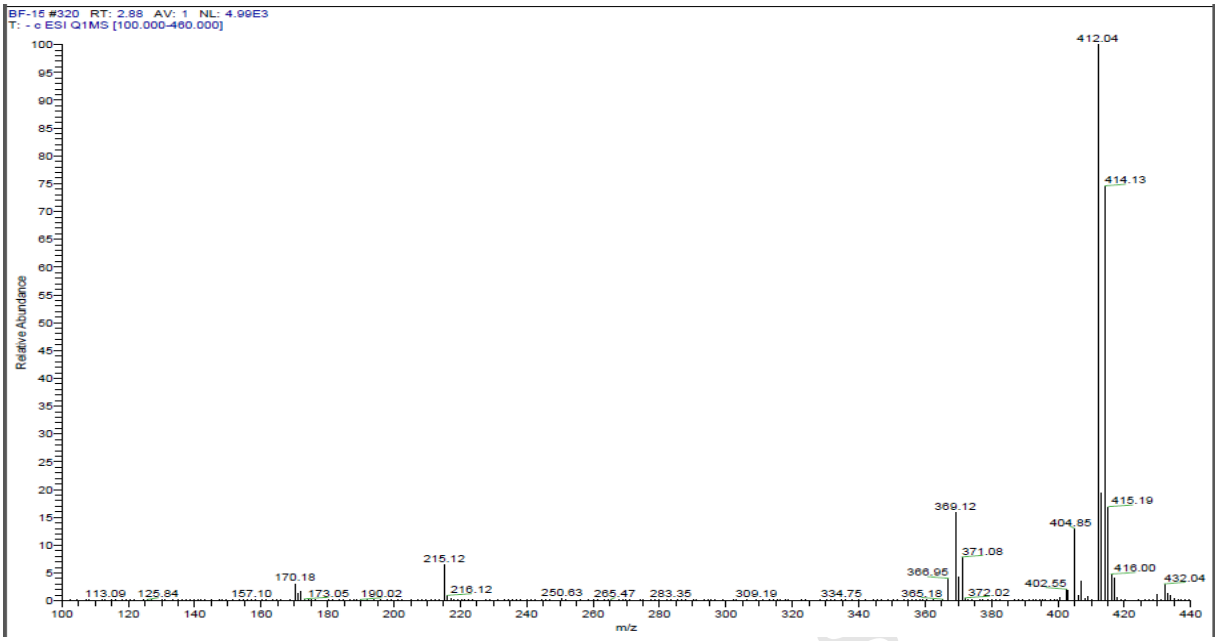

SM 16. ^{1}H and ^{13}C NMR and MS spectra of e16

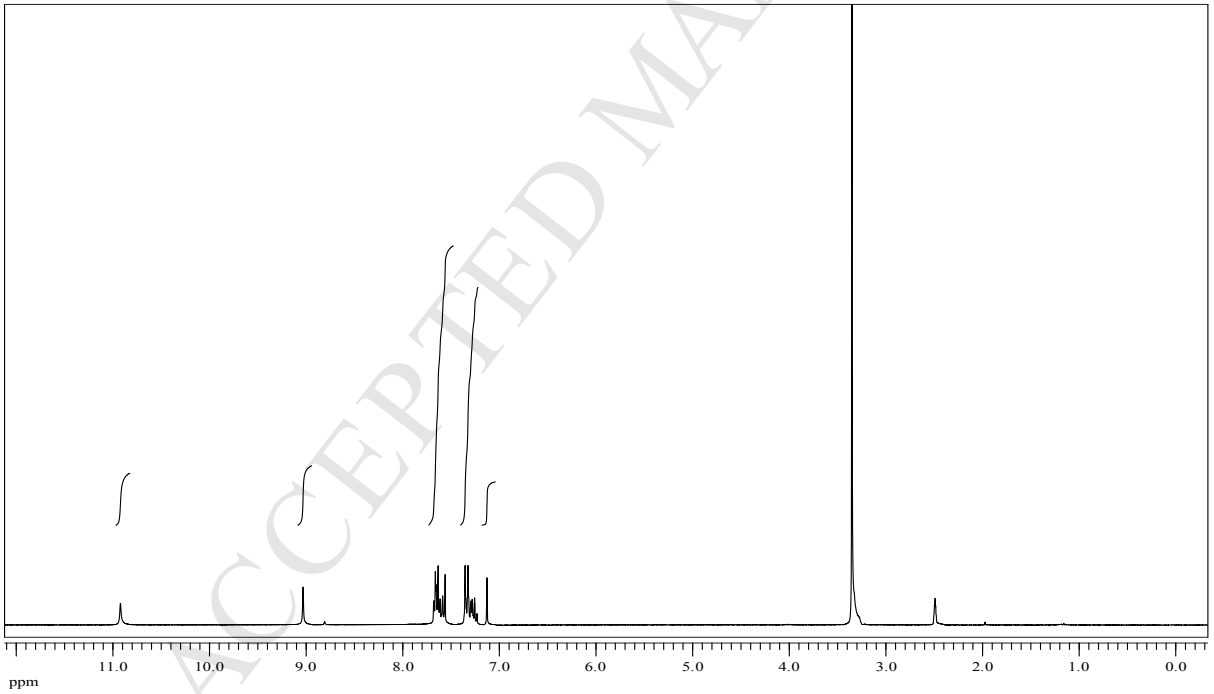

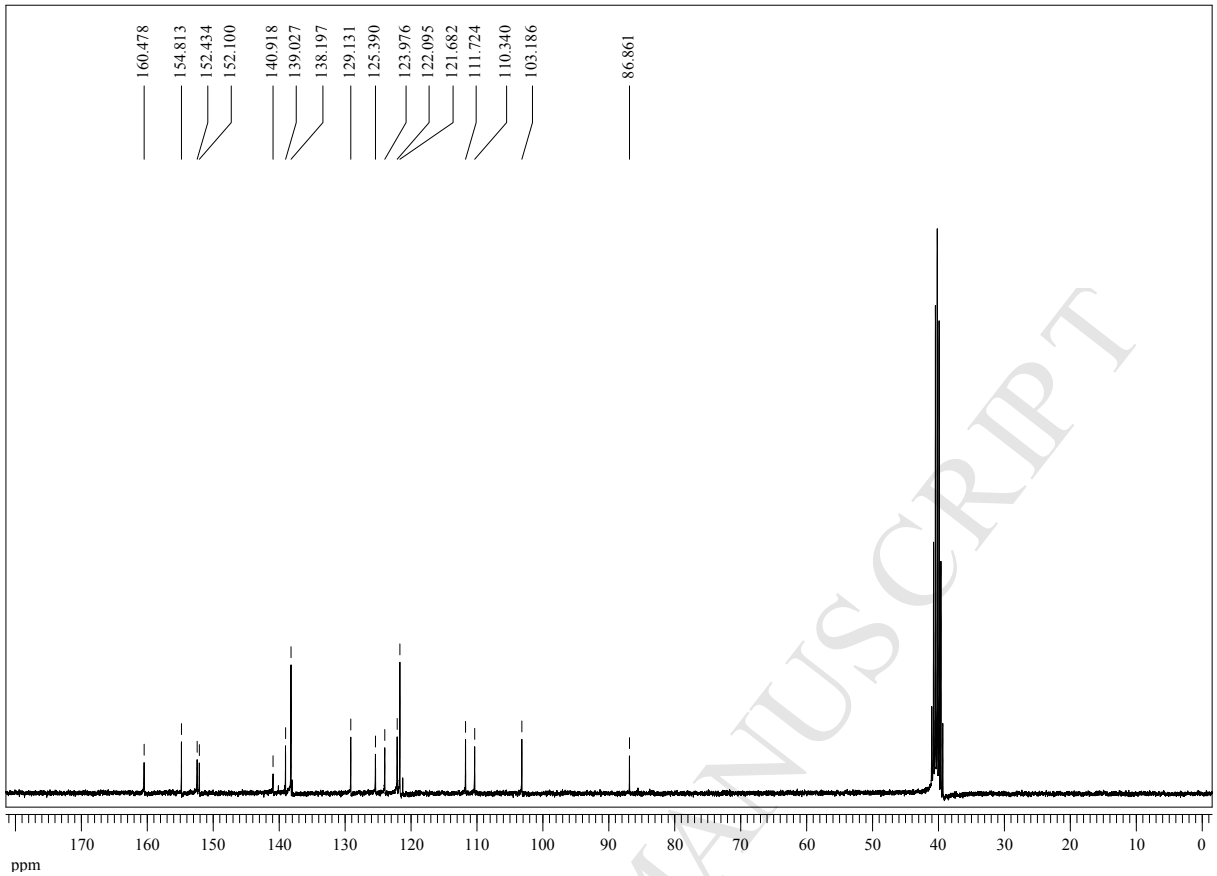
160.478
154.813
152.434
152.100
140.918
139.027
138.197
129.131
125.390
123.976
122.095
121.682
111.724
110.340
103.186
86.861
170
160
150
140
130
120
110
100
90
80
70
60
50
40
30
20
10
0
ppm

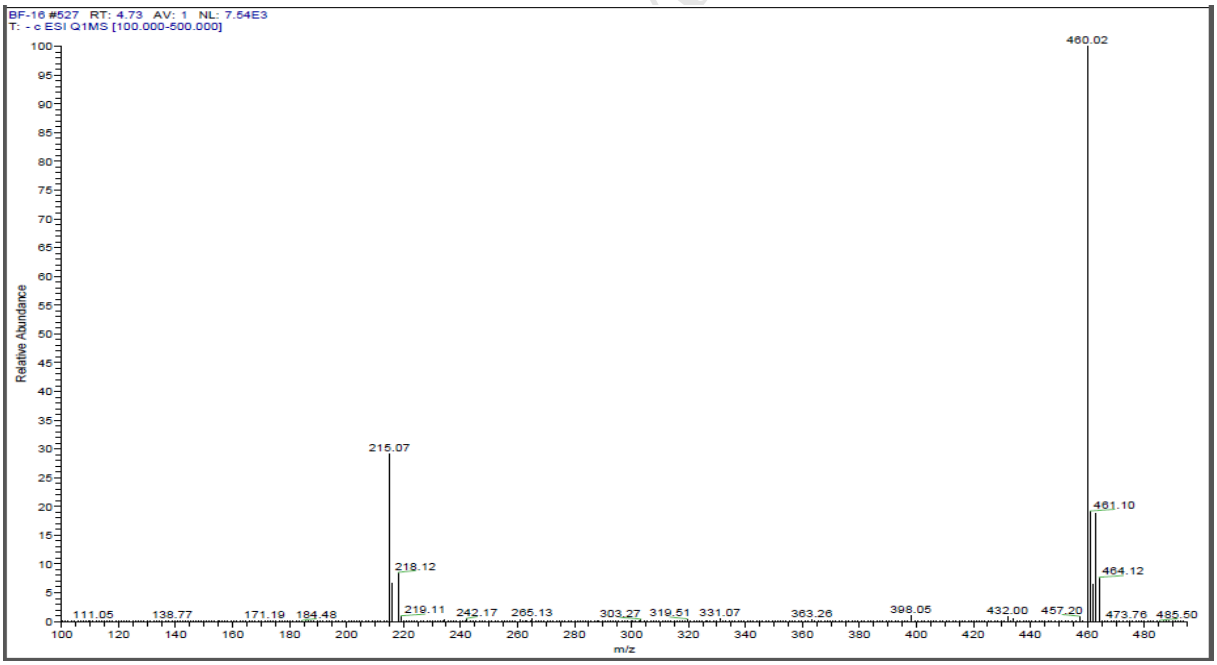
BF-16 #527 RT: 4.73 AV: 1 NL: 7.54E3
T: - c ESI Q1MS [100.000-500.000]
Relative Abundance
m/z
460.02
461.10
464.12
215.07
218.12
219.11
111.05
138.77
171.19
184.48
242.17
265.13
303.27
319.51
331.07
363.26
398.05
432.00
457.20
473.76
485.50

SM 17. ^{1}H and ^{13}C NMR and MS spectra of e17

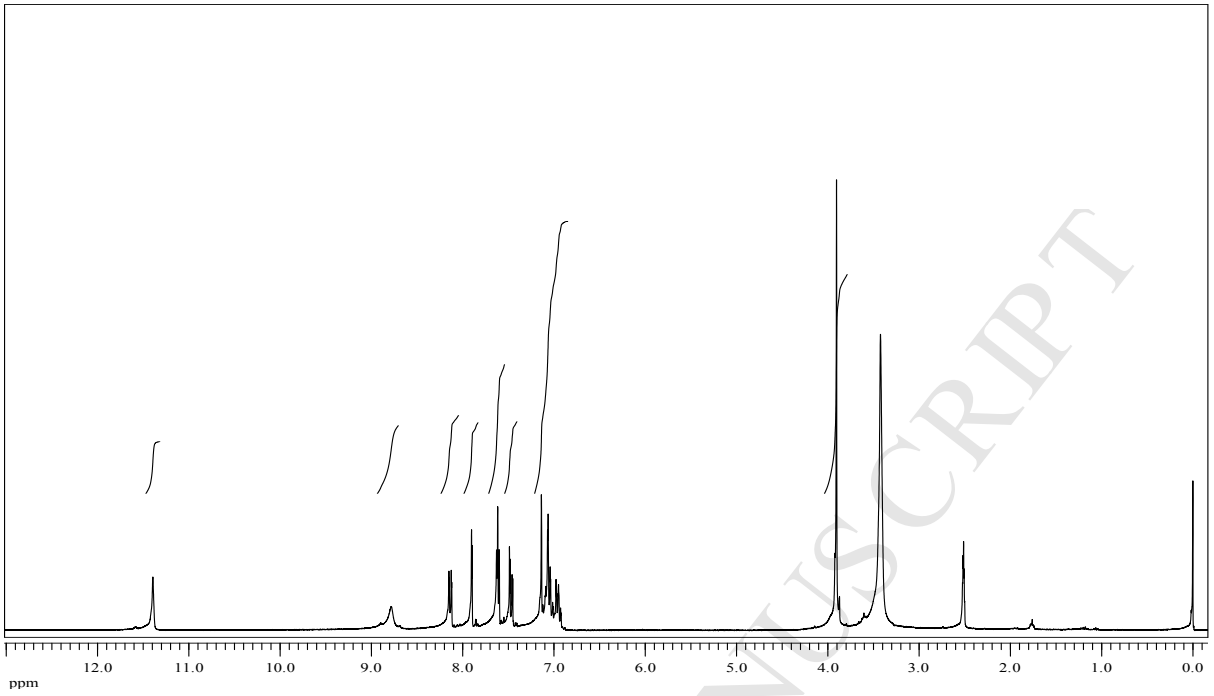

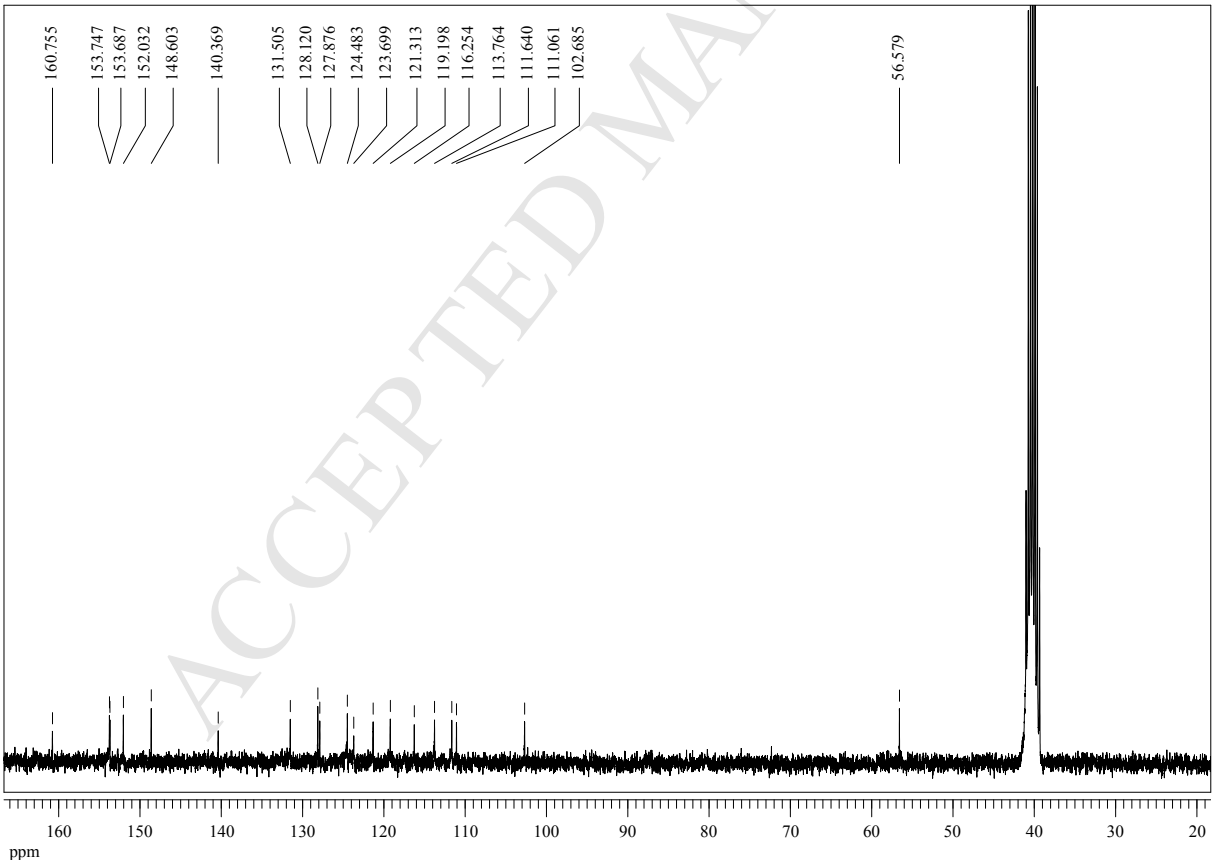

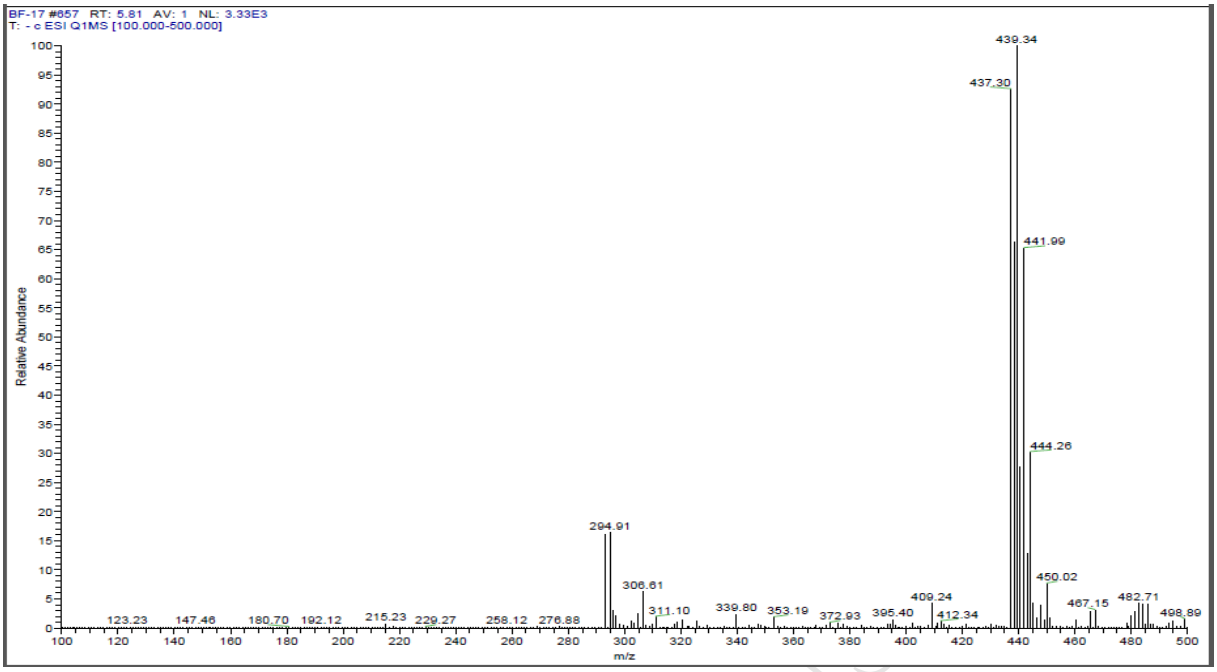

SM 18. ^{1}H and ^{13}C NMR and MS spectra of e18

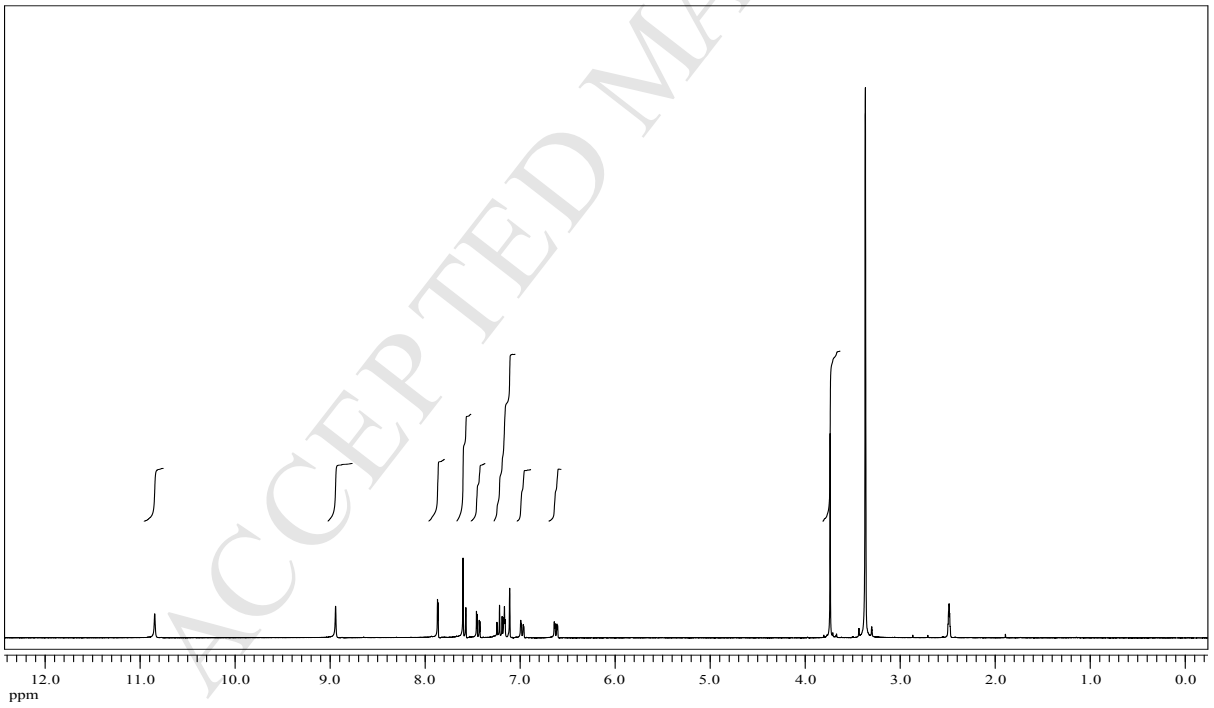

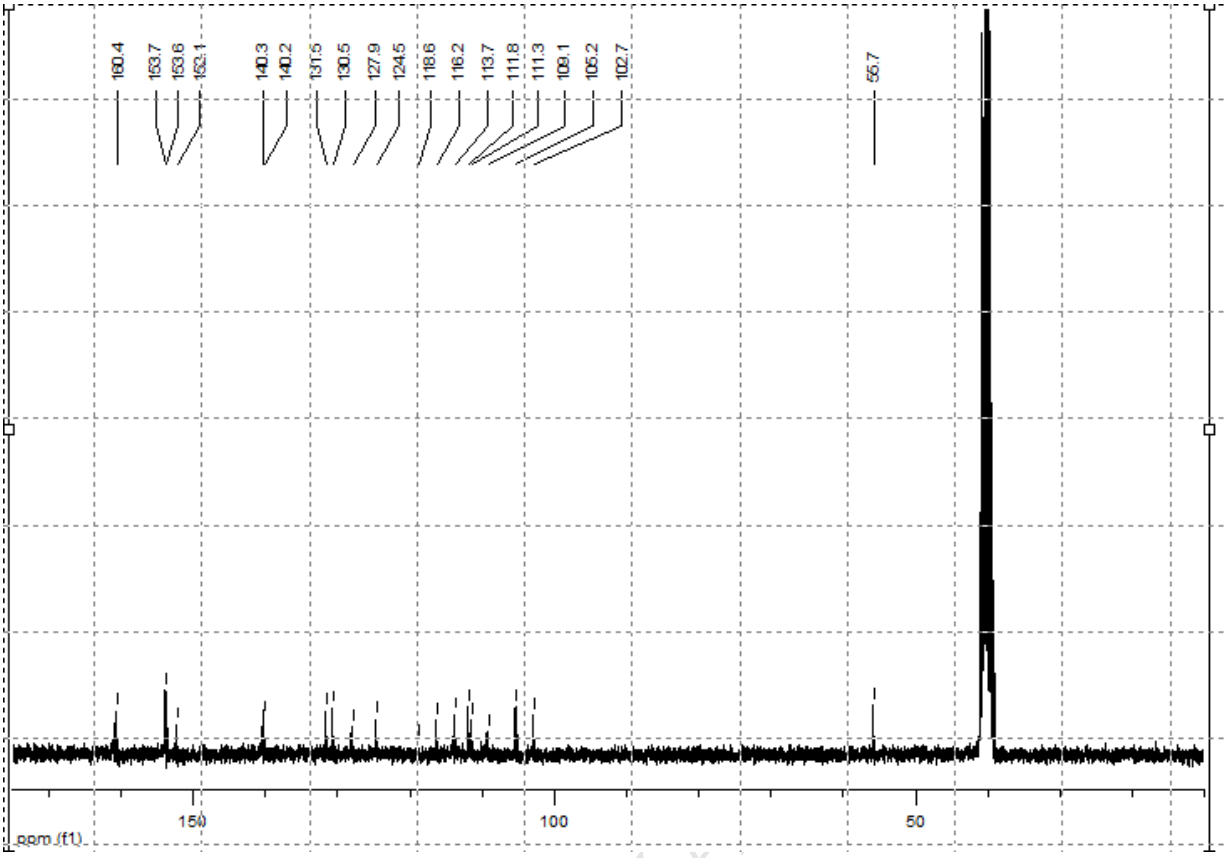
160.4
153.7
153.6
152.1
140.3
140.2
131.5
130.5
127.9
124.5
118.6
116.2
113.7
111.8
111.3
109.1
105.2
102.7
55.7
150
100
50
ppm (f1)

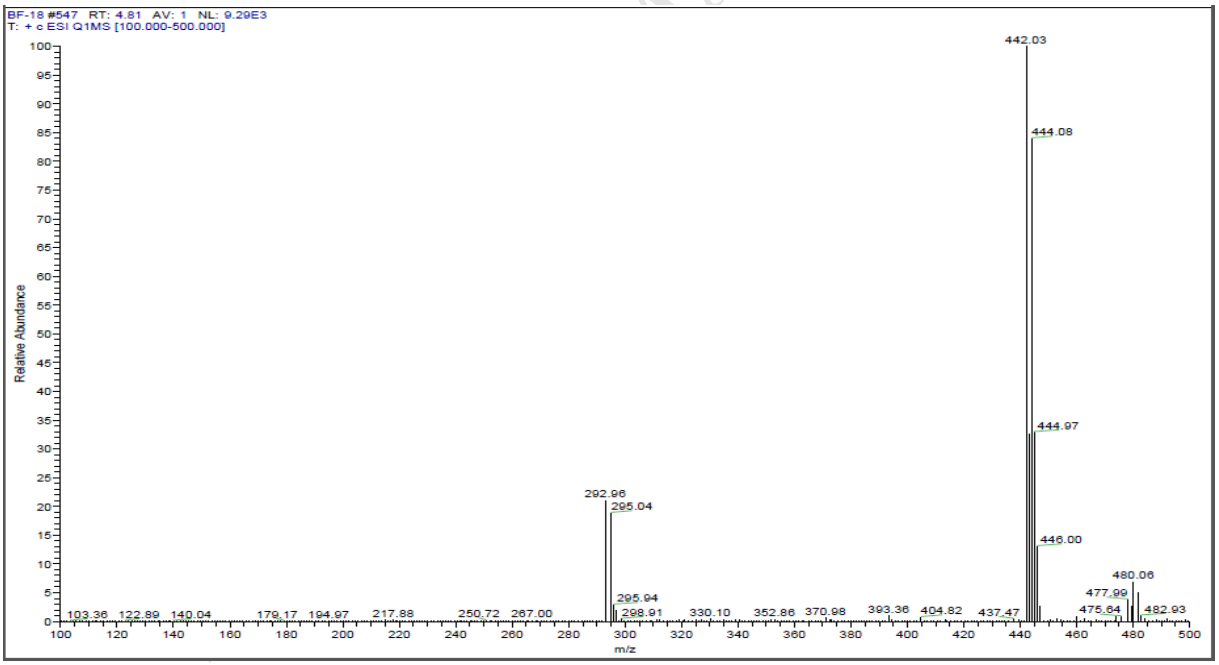
BF-18 #547 RT: 4.81 AV: 1 NL: 9.29E3
T: + c ESI Q1MS [100.000-500.000]
Relative Abundance
m/z
442.03
444.08
444.97
446.00
480.06
477.99
475.64
482.93
292.96
295.04
295.94
298.91
330.10
352.86
370.98
393.36
404.82
437.47
103.36
122.89
140.04
179.17
194.97
217.88
250.72
267.00

SM 19. ^{1}H and ^{13}C NMR and MS spectra of e19

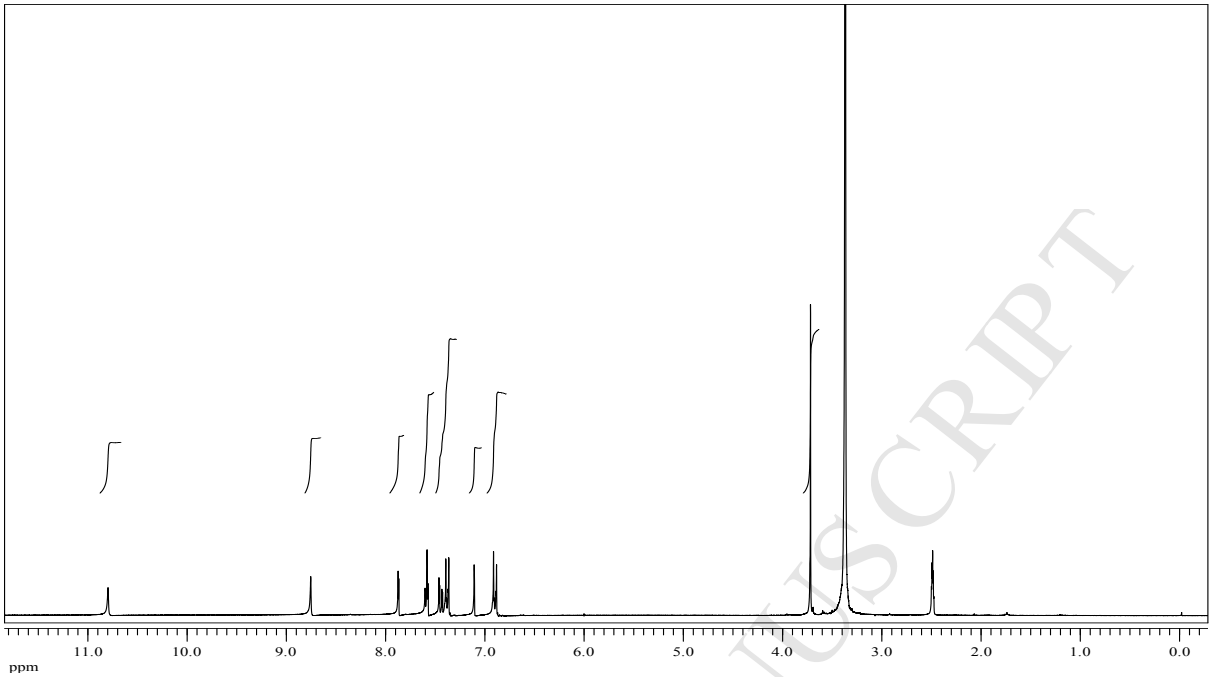

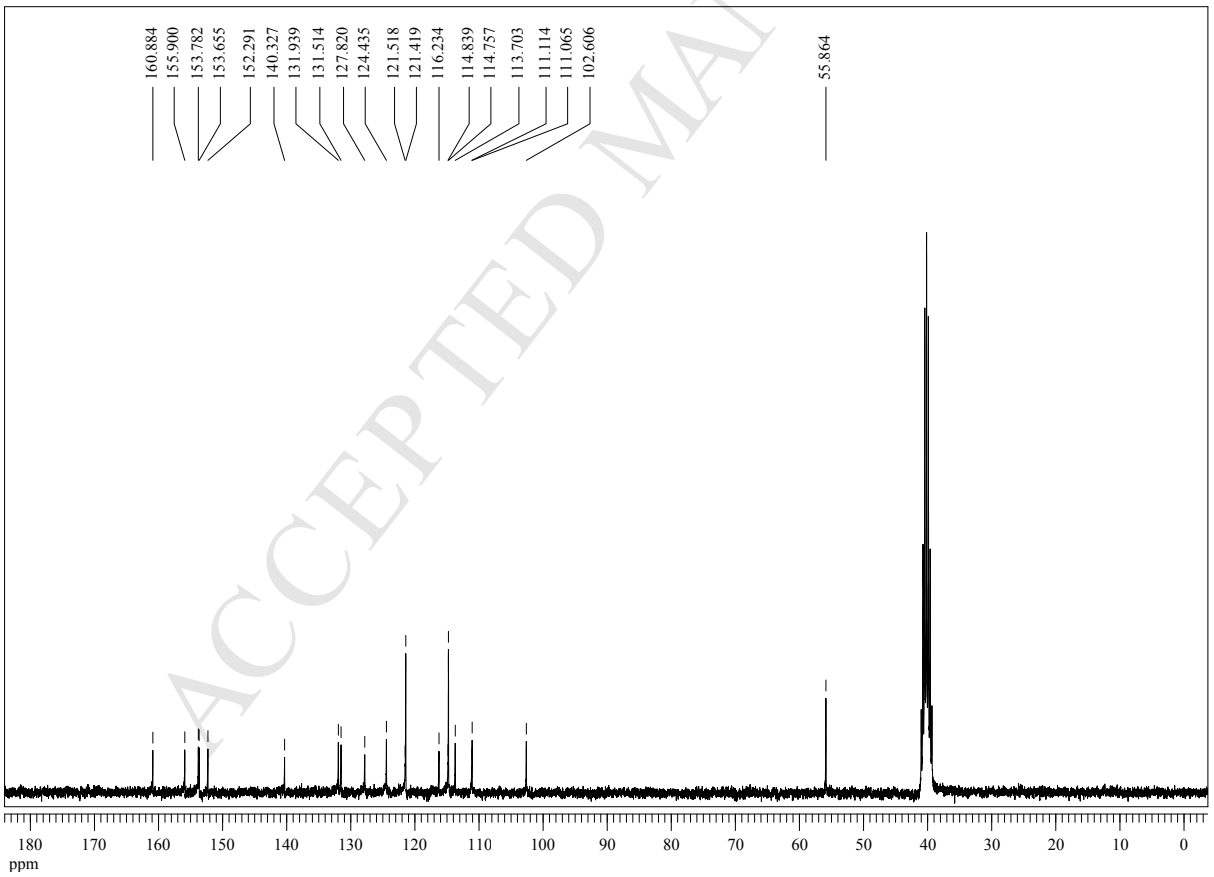

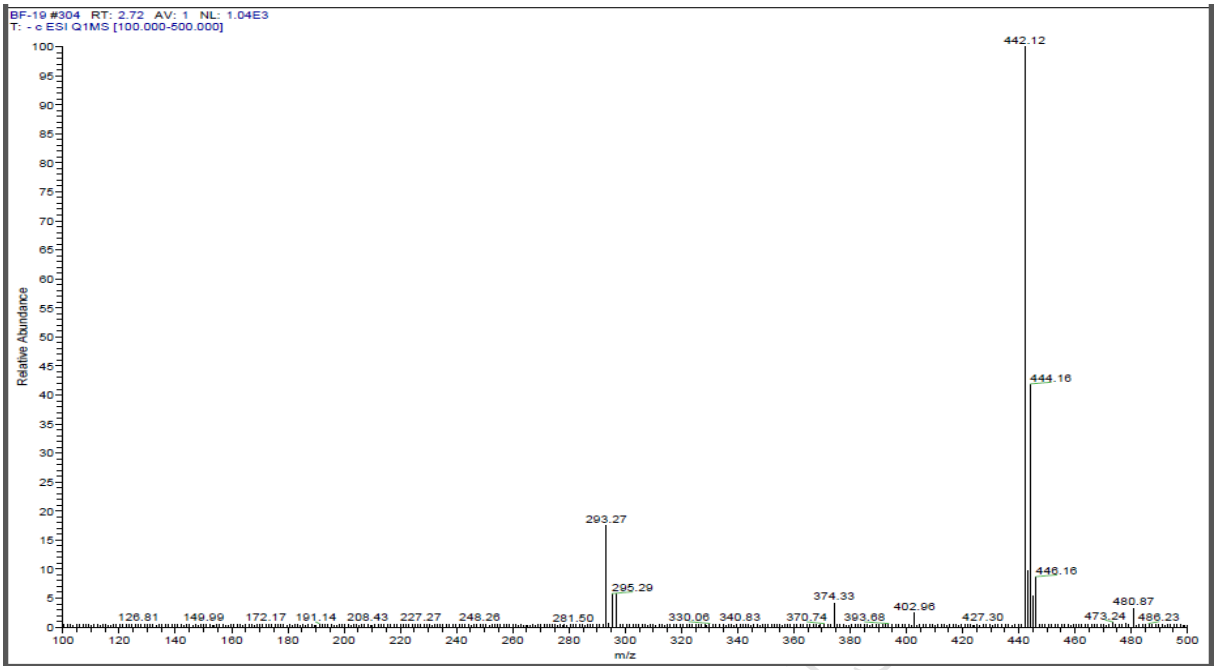

SM 20. ^{1}H and ^{13}C NMR and MS spectra of e20

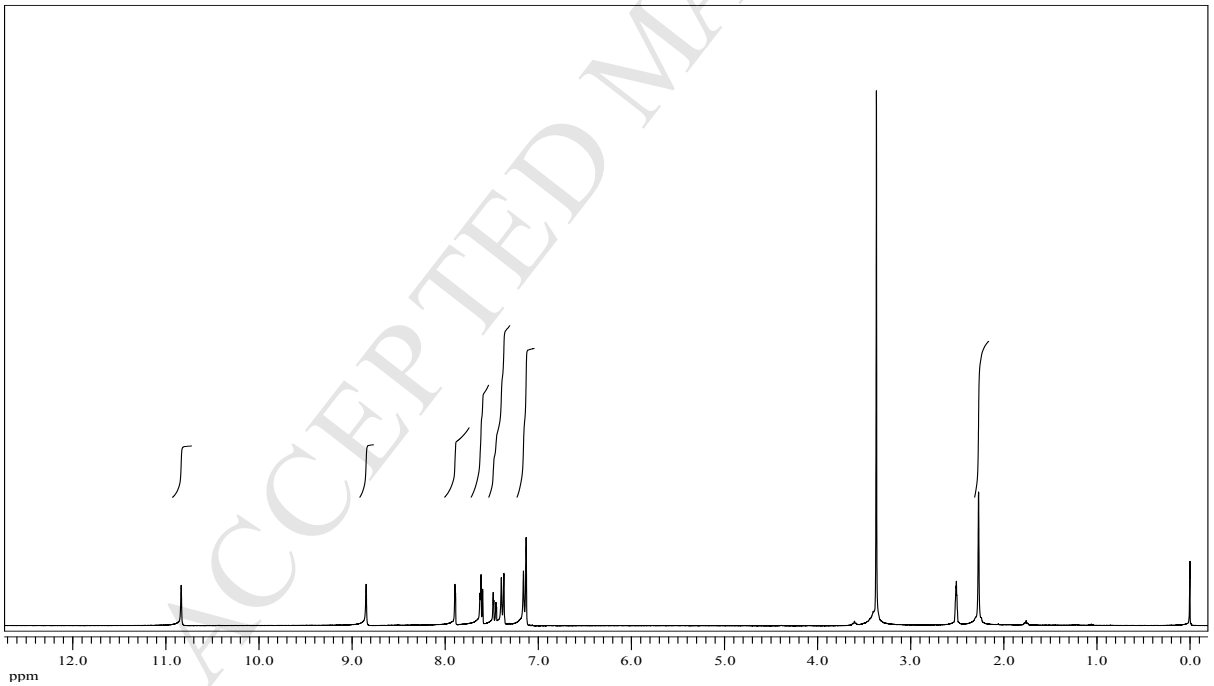

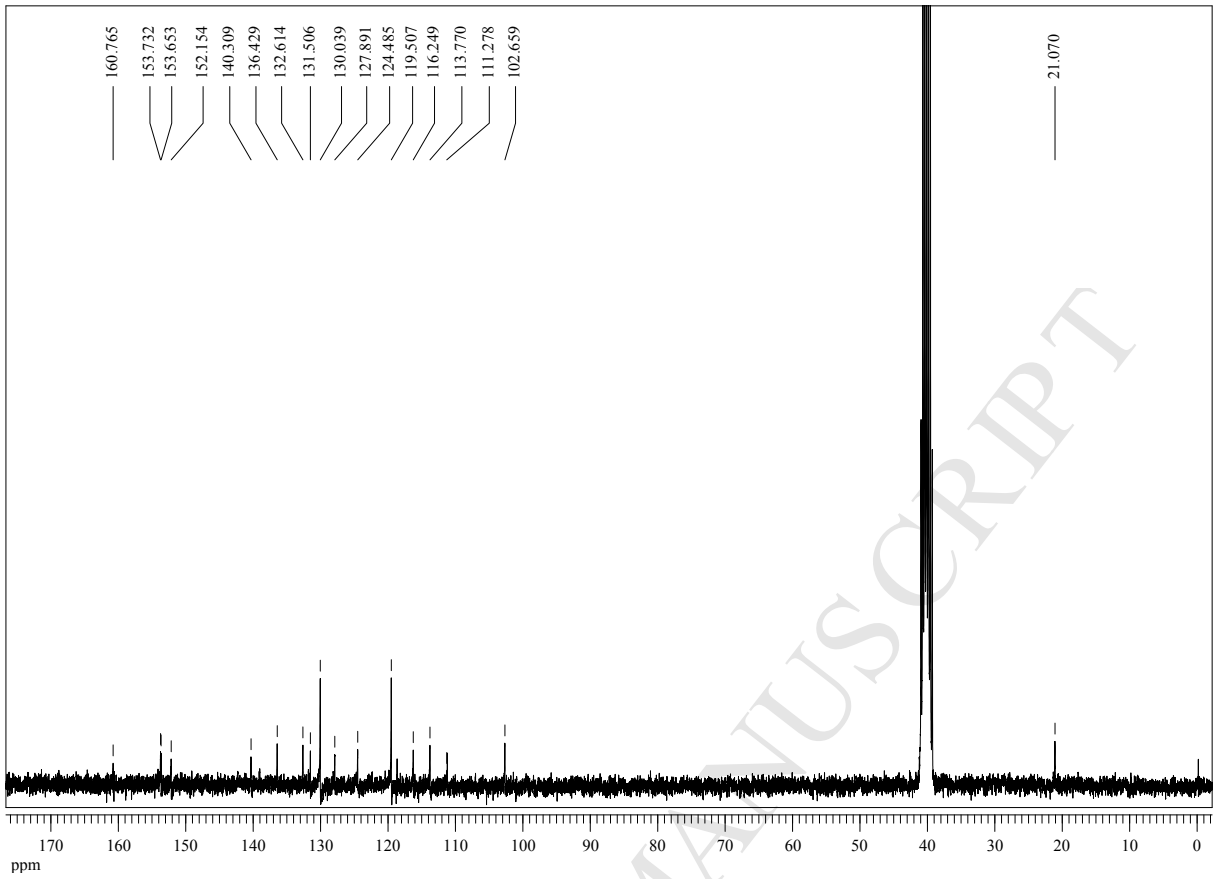
160.765
153.732
153.653
152.154
140.309
136.429
132.614
131.506
130.039
127.891
124.485
119.507
116.249
113.770
111.278
102.659
21.070
170
160
150
140
130
120
110
100
90
80
70
60
50
40
30
20
10
0
ppm

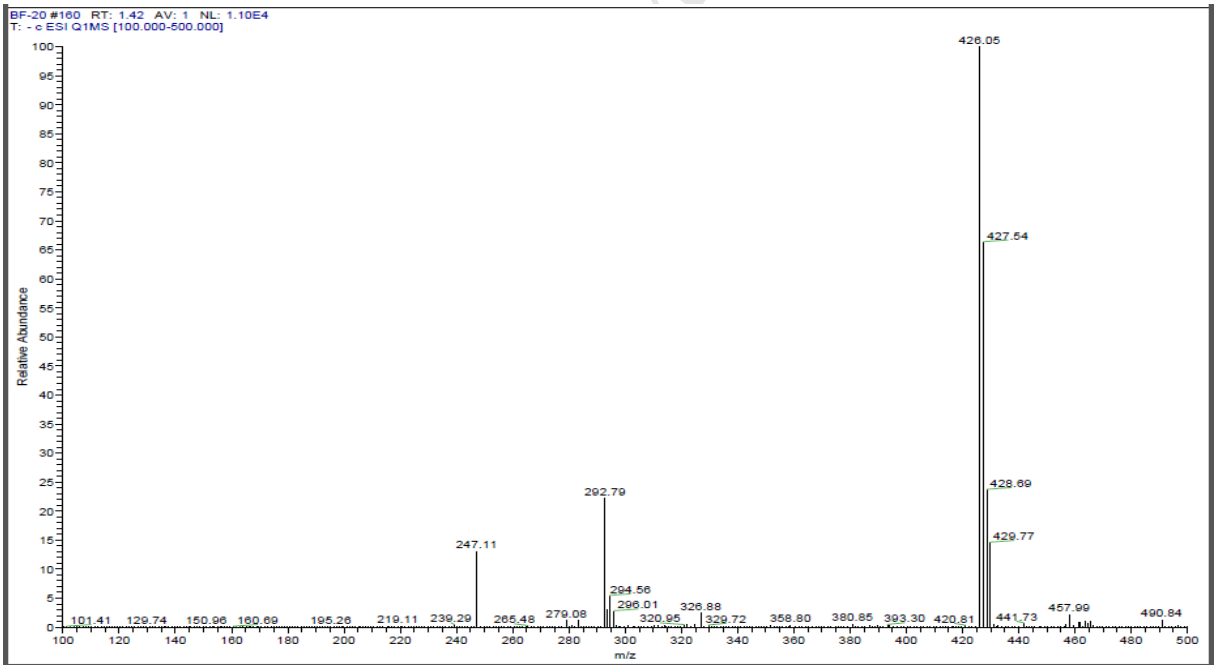
BF-20 #160 RT: 1.42 AV: 1 NL: 1.10E4
T: - c ESI Q1MS [100.000-500.000]
Relative Abundance
m/z
426.05
427.54
428.69
429.77
292.79
247.11
294.56
296.01
326.88
320.95
329.72
101.41
129.74
150.96
160.69
195.26
219.11
239.29
265.48
279.08
358.80
380.85
393.30
420.81
441.73
457.99
490.84

SM 21. ^{1}H and ^{13}C NMR and MS spectra of e21

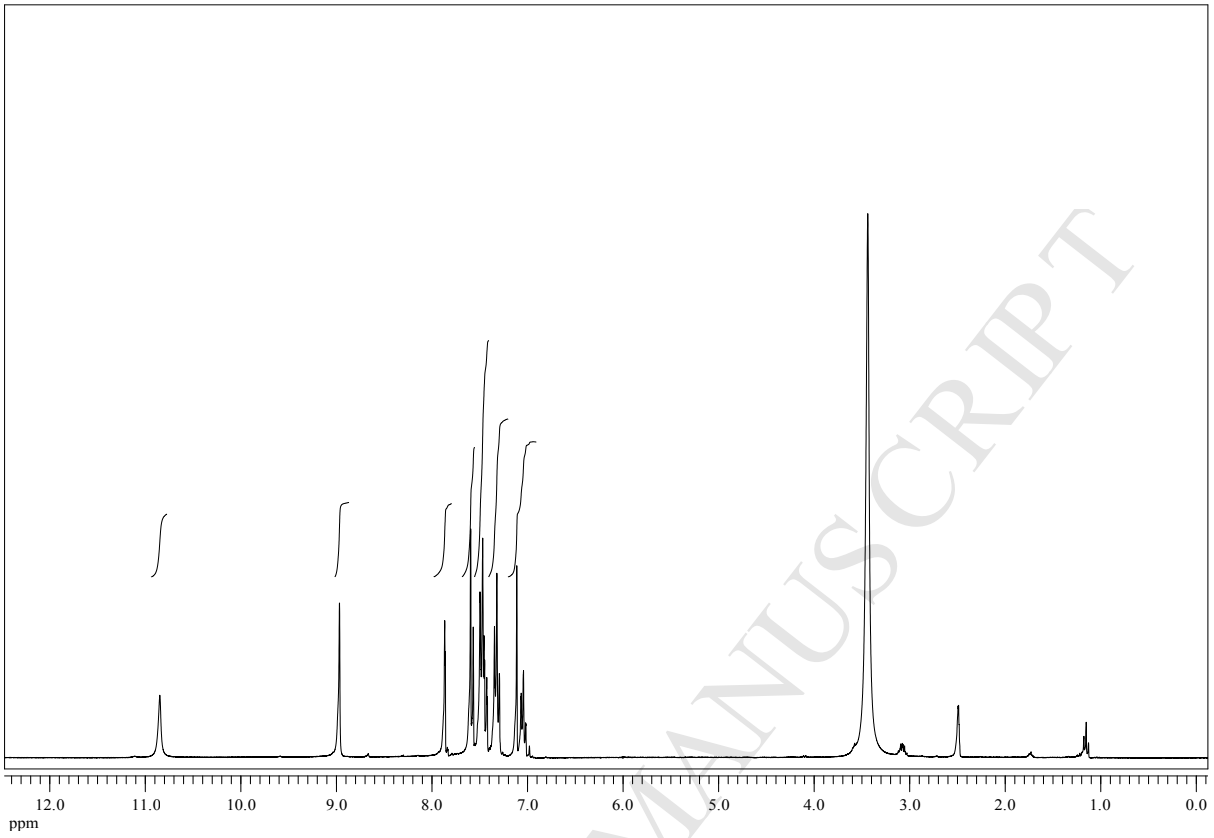

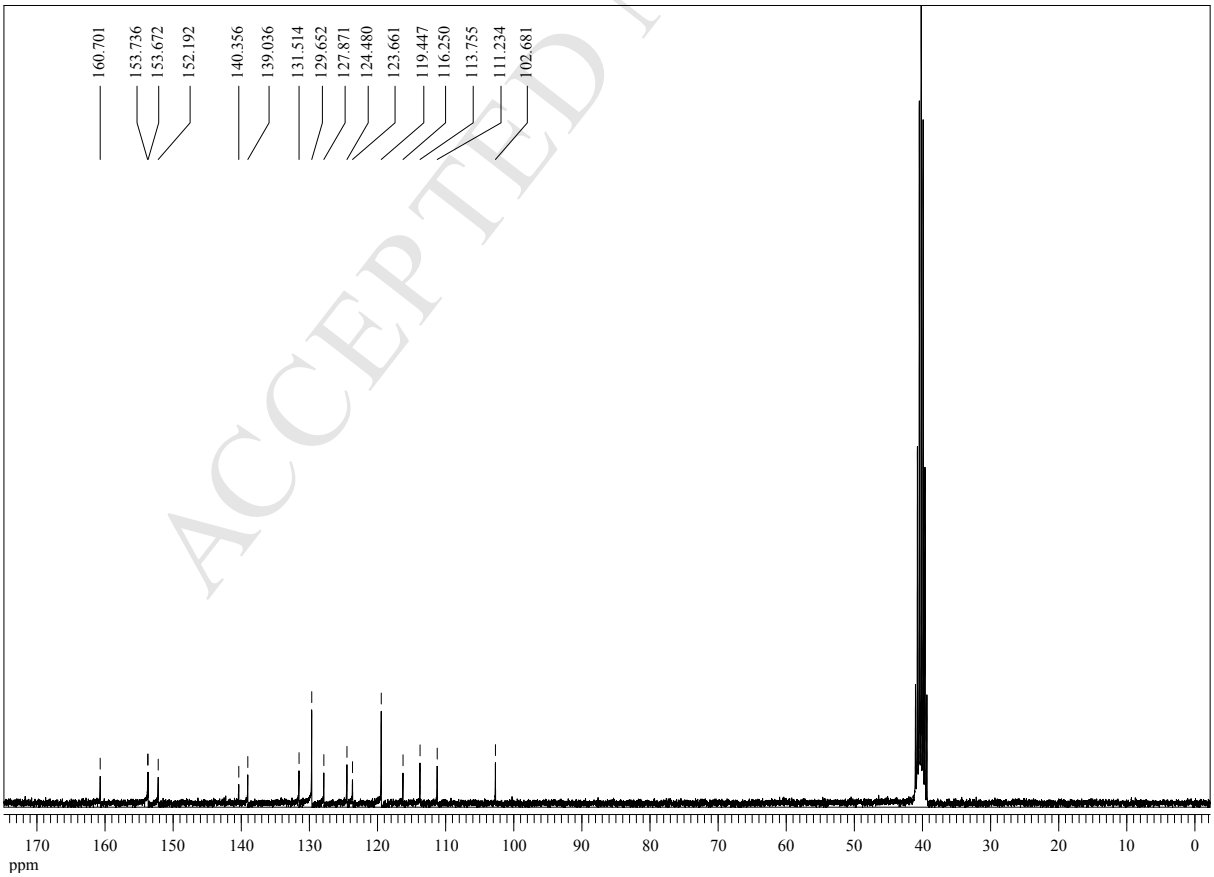

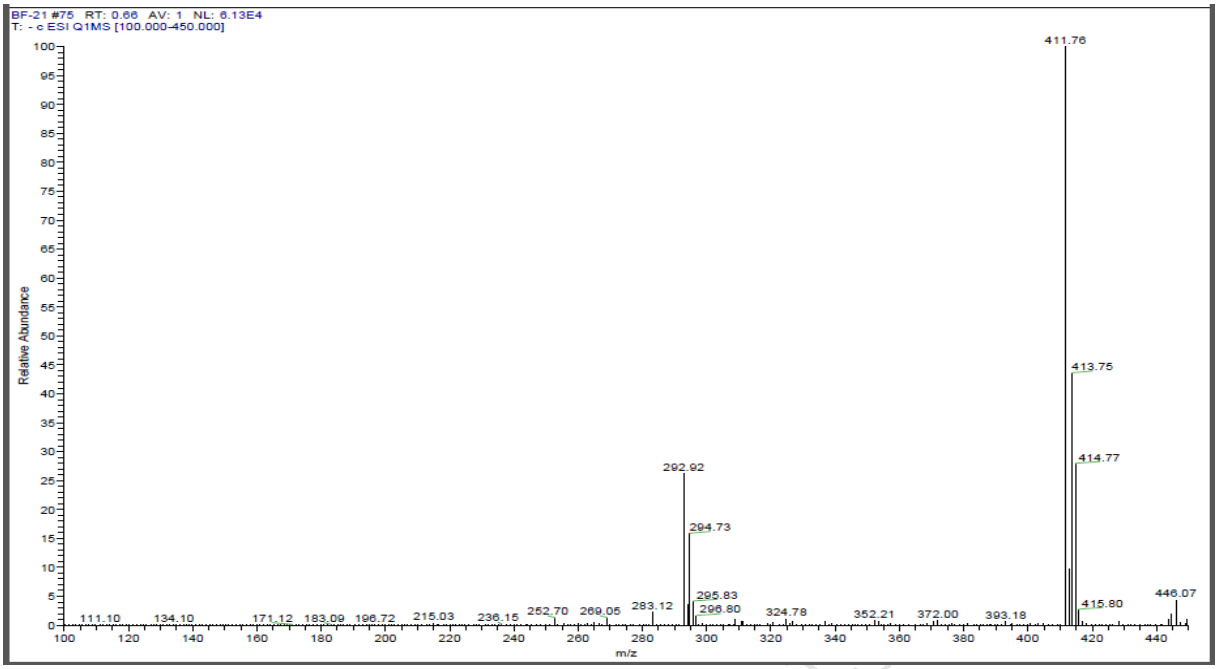

SM 22. ^{1}H and ^{13}C NMR and MS spectra of e22

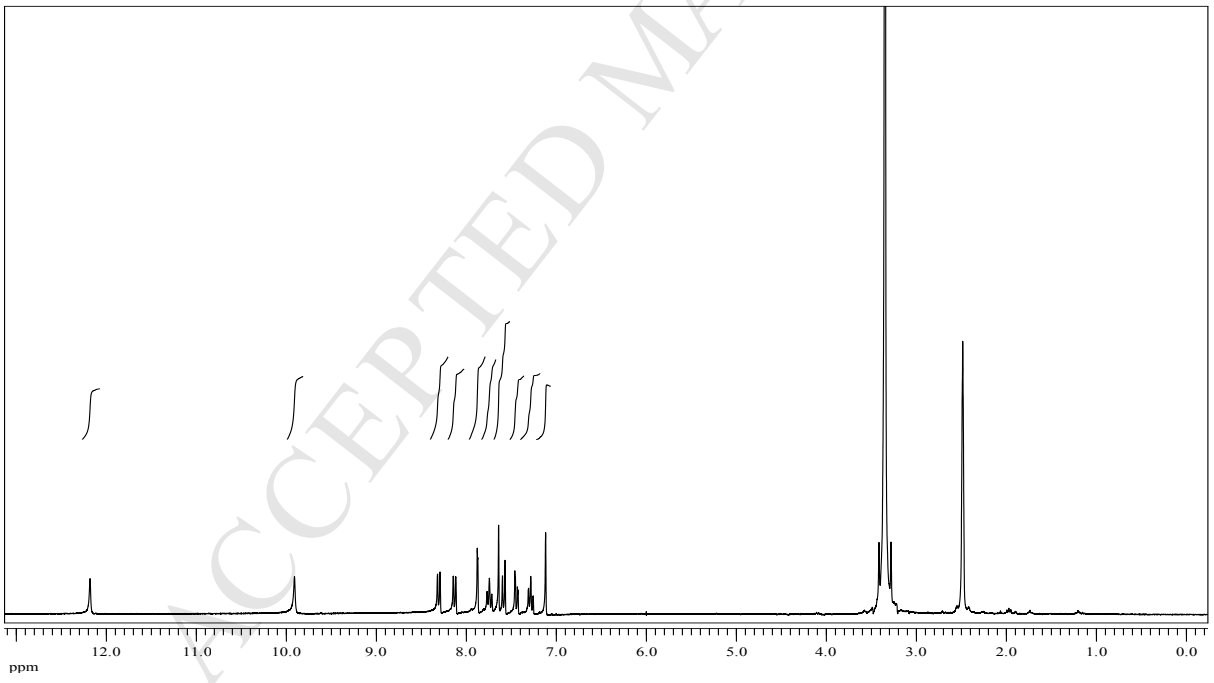

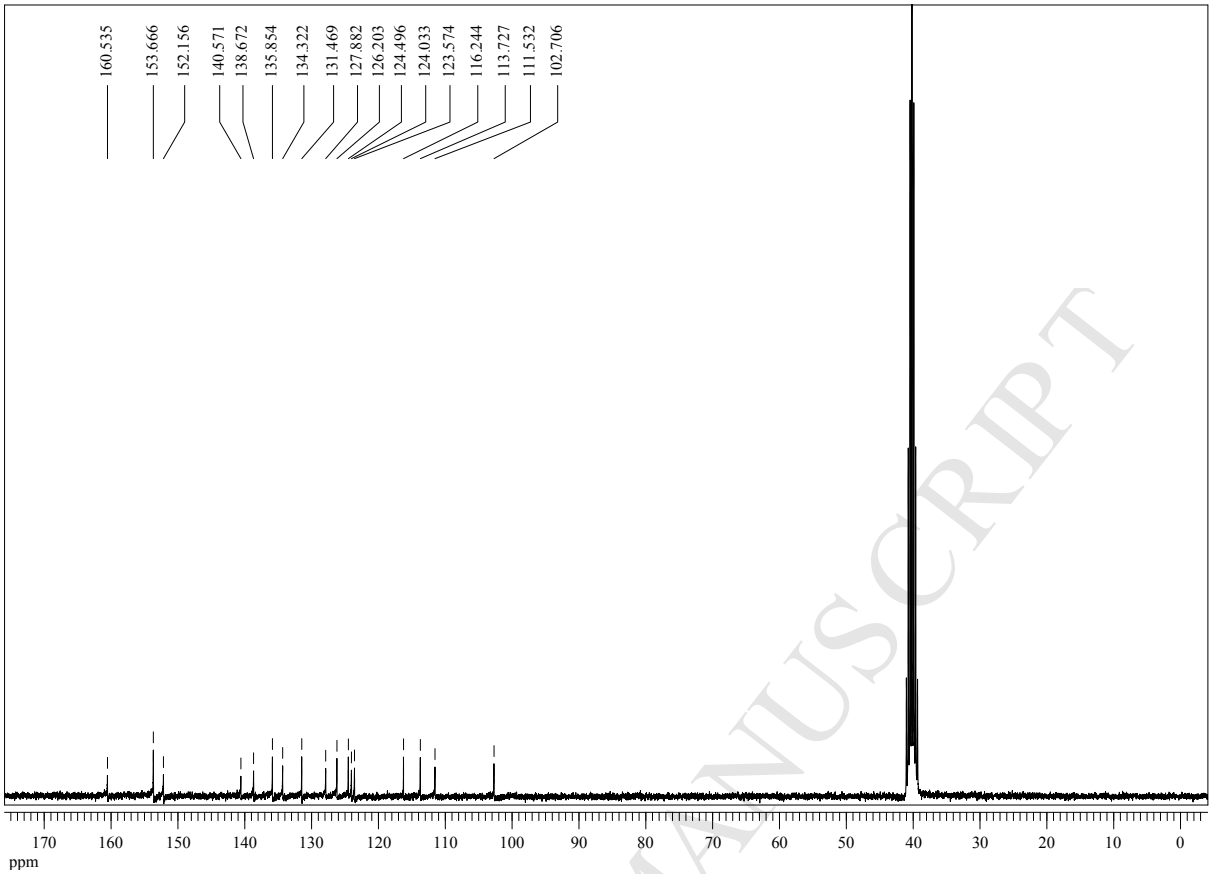
160.535
153.666
152.156
140.571
138.672
135.854
134.322
131.469
127.882
126.203
124.496
124.033
123.574
116.244
113.727
111.532
102.706
170 160 150 140 130 120 110 100 90 80 70 60 50 40 30 20 10 0
ppm

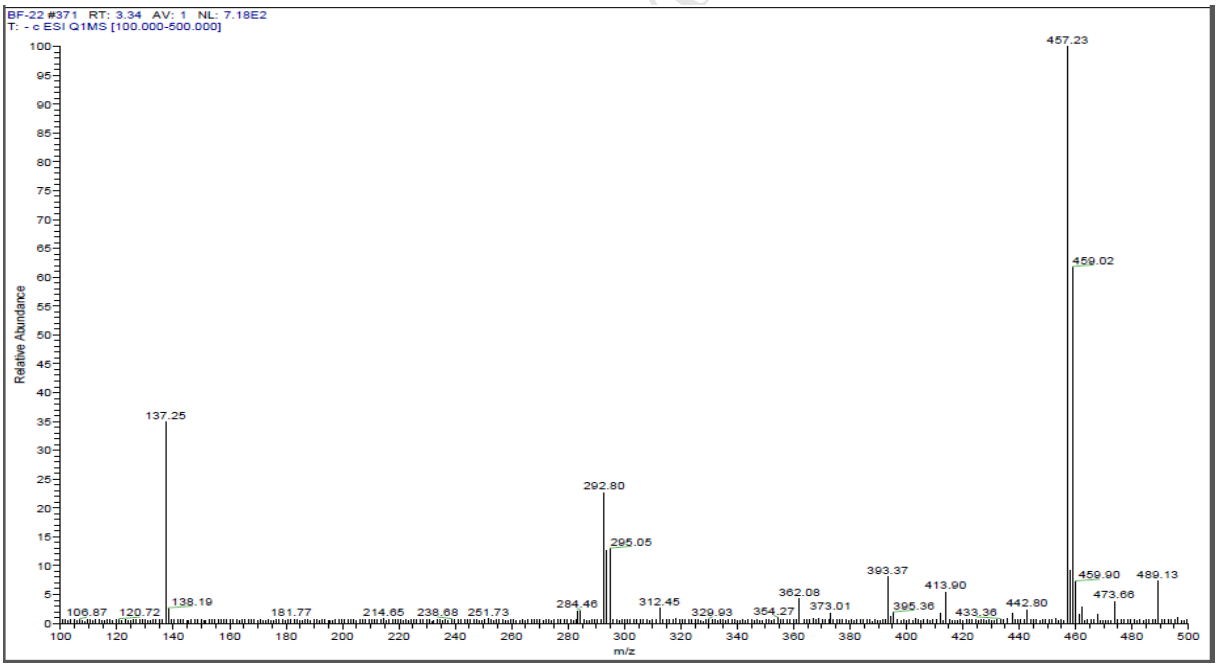
BF-22 #371 RT: 3.34 AV: 1 NL: 7.18E2
T: - c ESI Q1MS [100.000-500.000]
Relative Abundance
m/z
457.23
459.02
137.25
292.80
295.05
393.37
413.90
459.90
489.13
473.66
362.08
373.01
395.36
433.36
442.80
106.87
120.72
138.19
181.77
214.65
238.68
251.73
284.46
312.45
329.93
354.27

SM 23. ^{1}H and ^{13}C NMR and MS spectra of e23

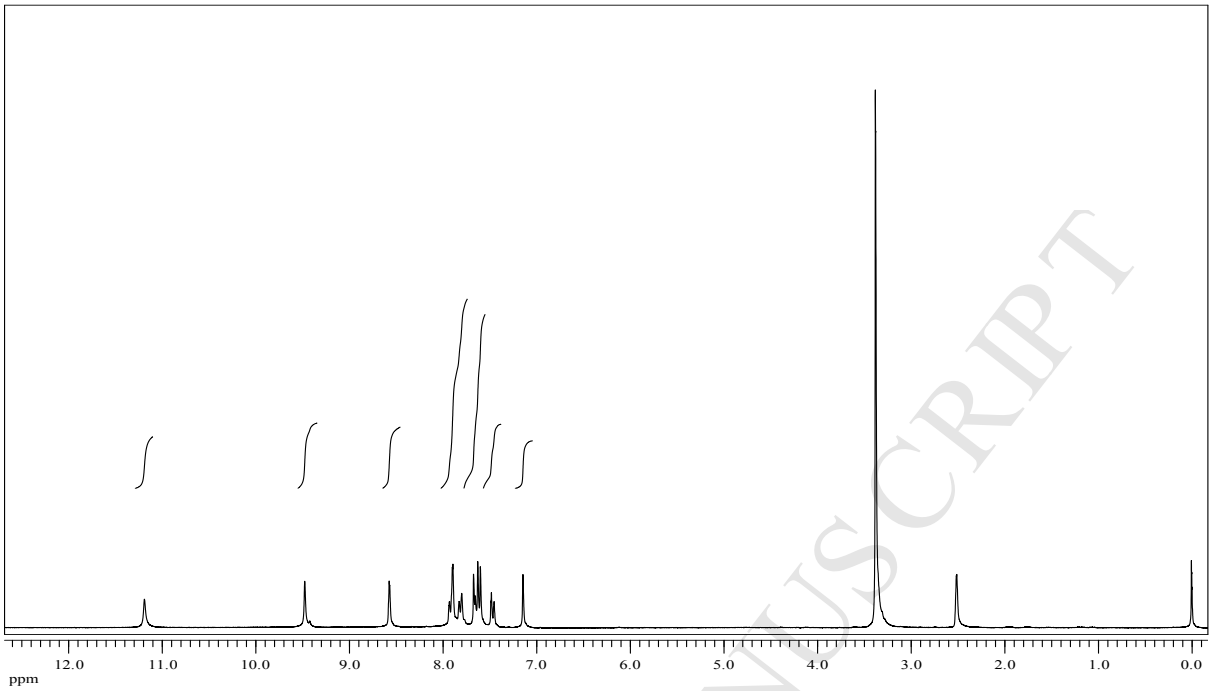

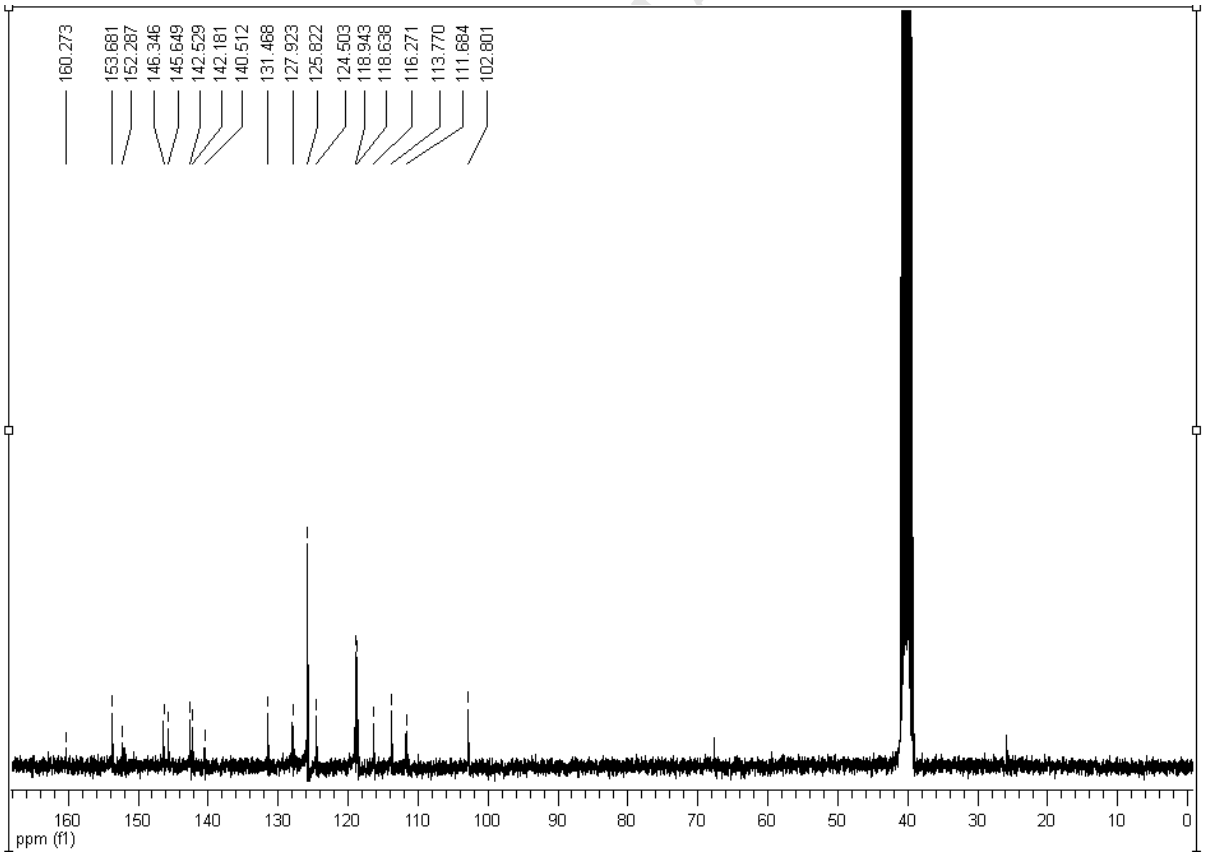

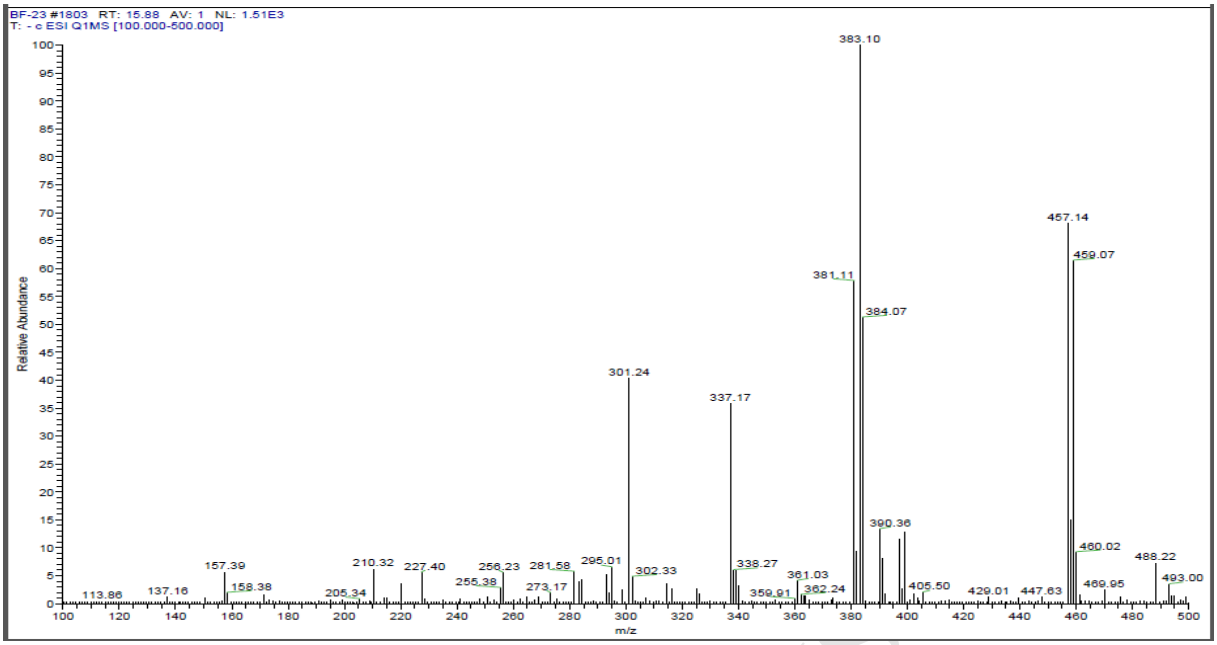

SM 24. ^{1}H and ^{13}C NMR and MS spectra of e24

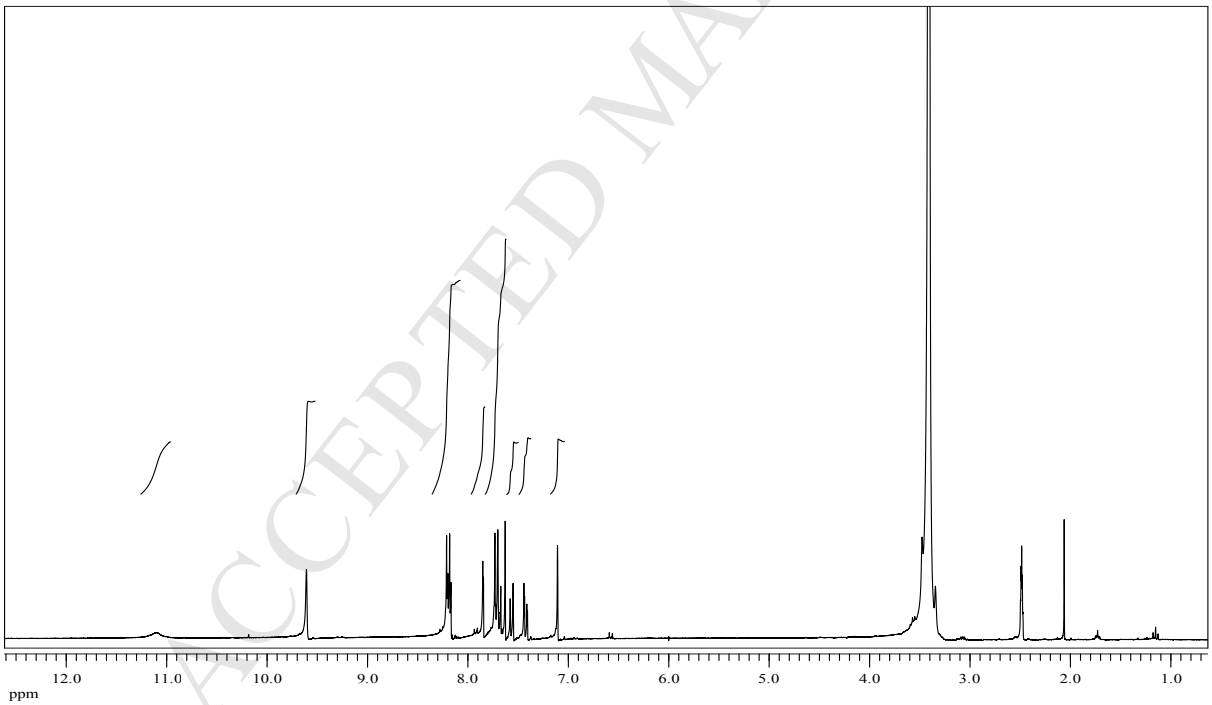

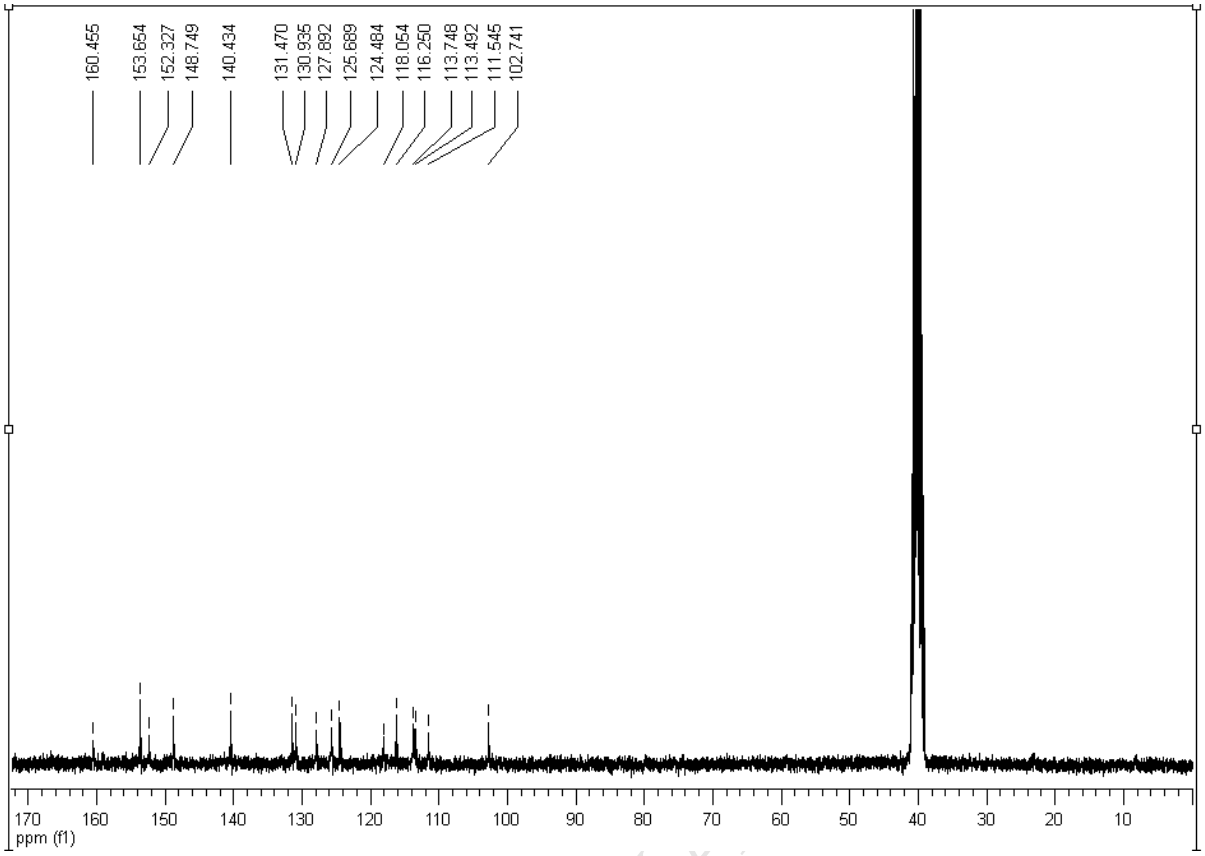
160.455
153.654
152.327
148.749
140.434
131.470
130.935
127.892
125.689
124.484
118.054
116.250
113.748
113.492
111.545
102.741
170 160 150 140 130 120 110 100 90 80 70 60 50 40 30 20 10
ppm (f1)

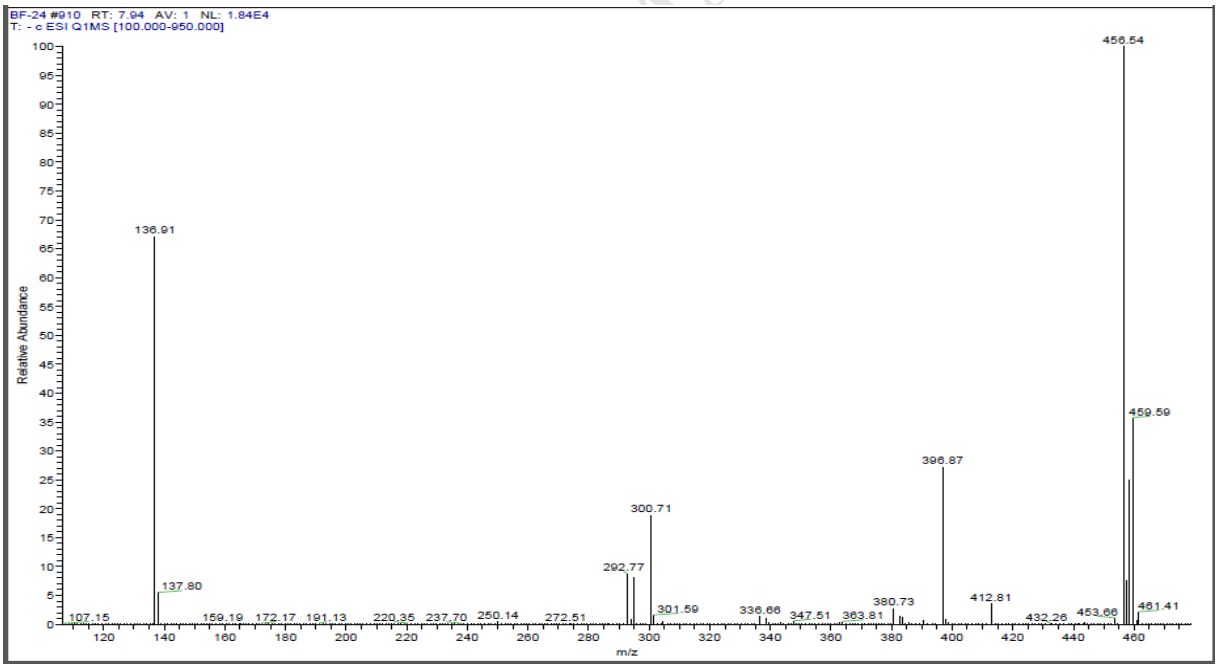
BF-24 #910 RT: 7.94 AV: 1 NL: 1.84E4
T: - c ESI Q1MS [100.000-950.000]
Relative Abundance
m/z
456.54
459.59
396.87
300.71
136.91
137.80
292.77
301.59
380.73
412.81
461.41
107.15
159.19
172.17
191.13
220.35
237.70
250.14
272.51
336.66
347.51
363.81
432.26
453.66

SM 25. ^{1}H and ^{13}C NMR and MS spectra of e25

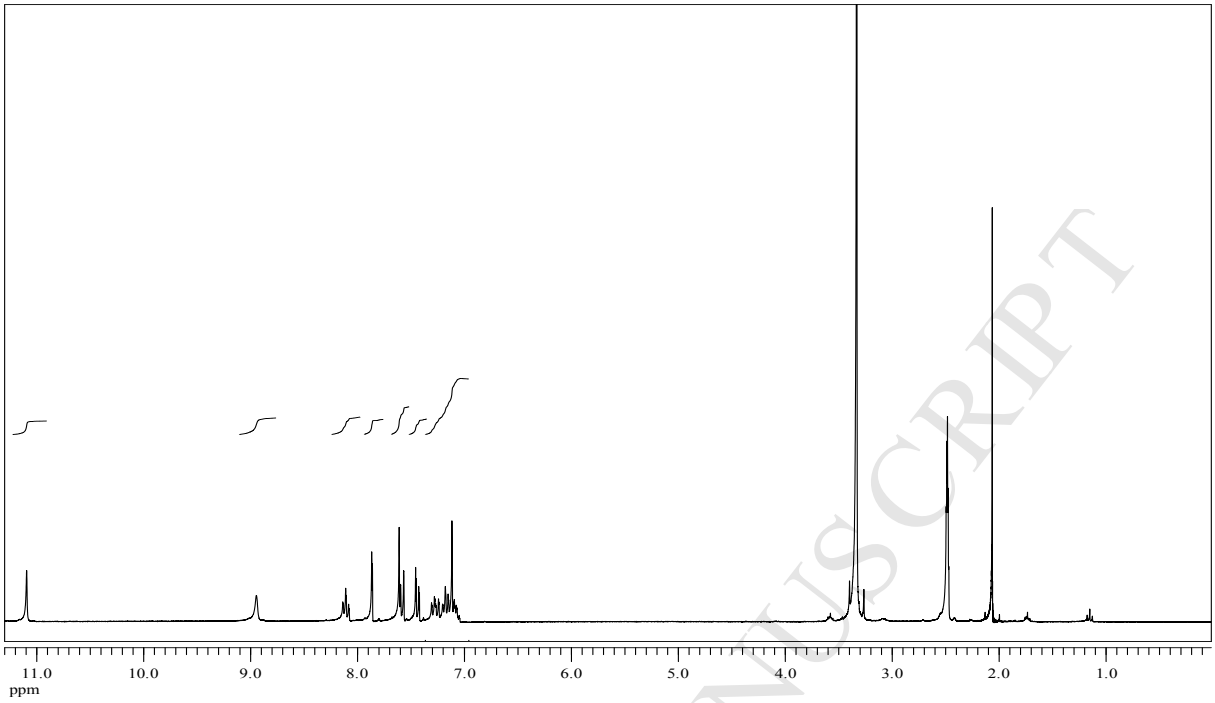

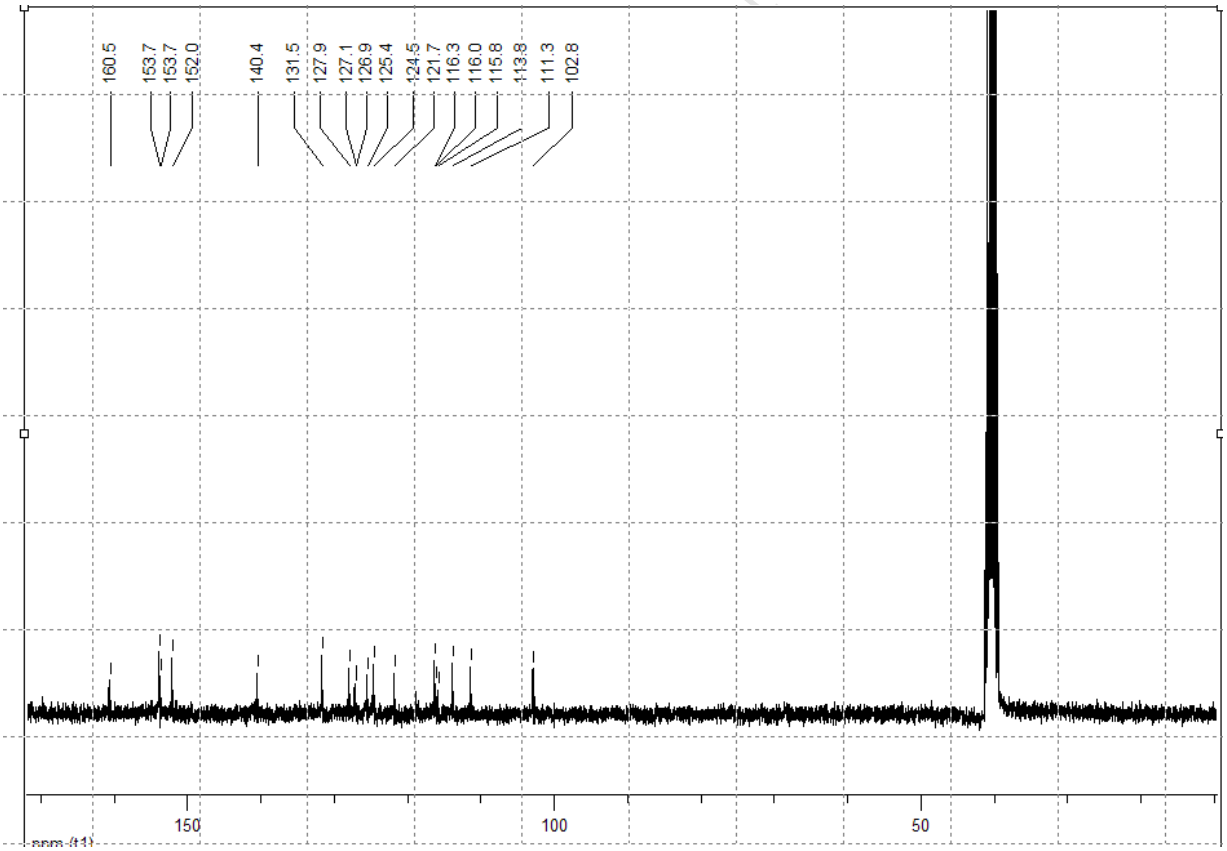

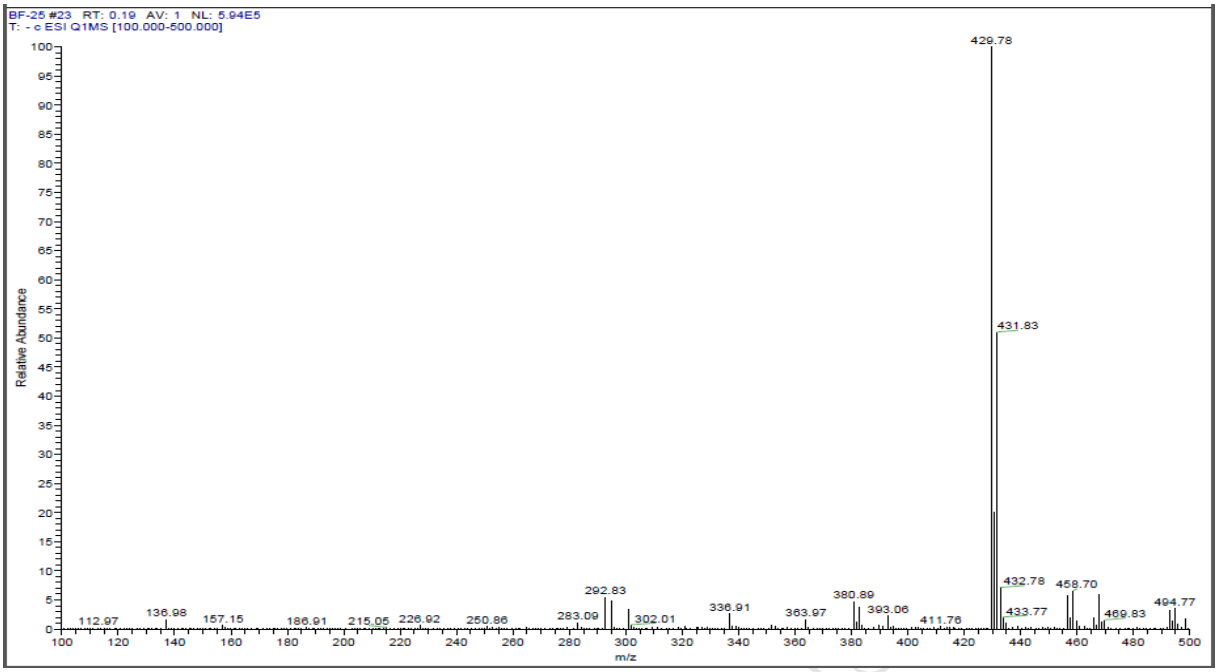

SM 26. ^{1}H and ^{13}C NMR and MS spectra of e26

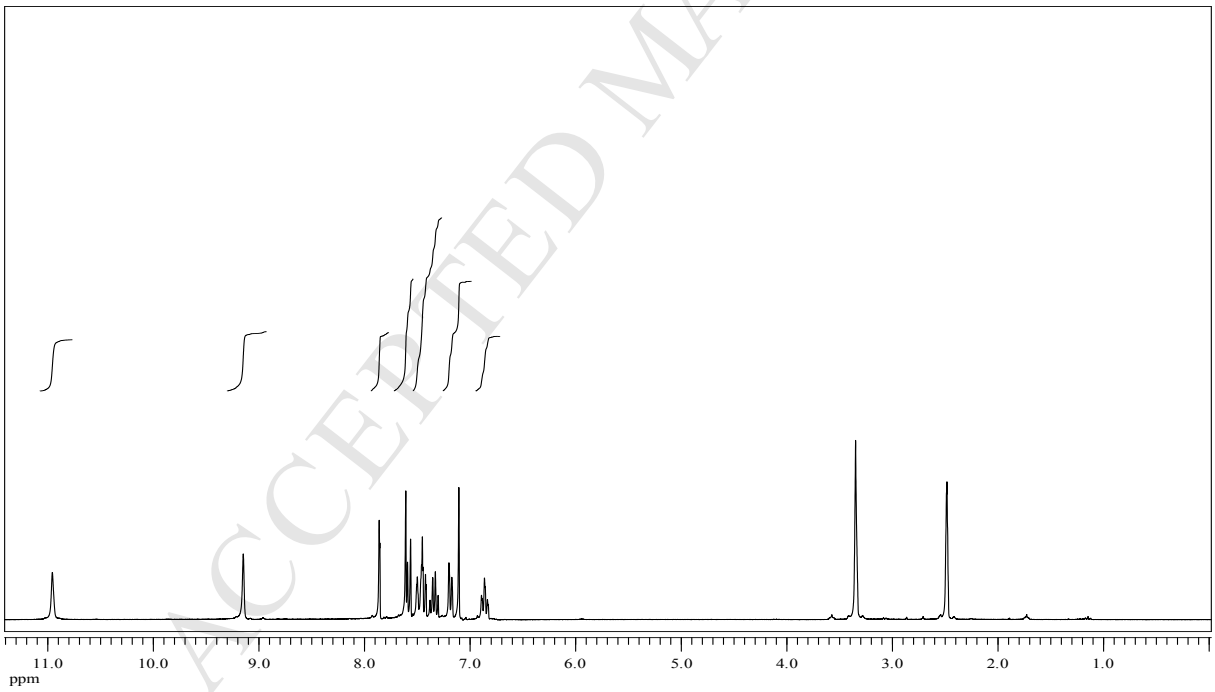

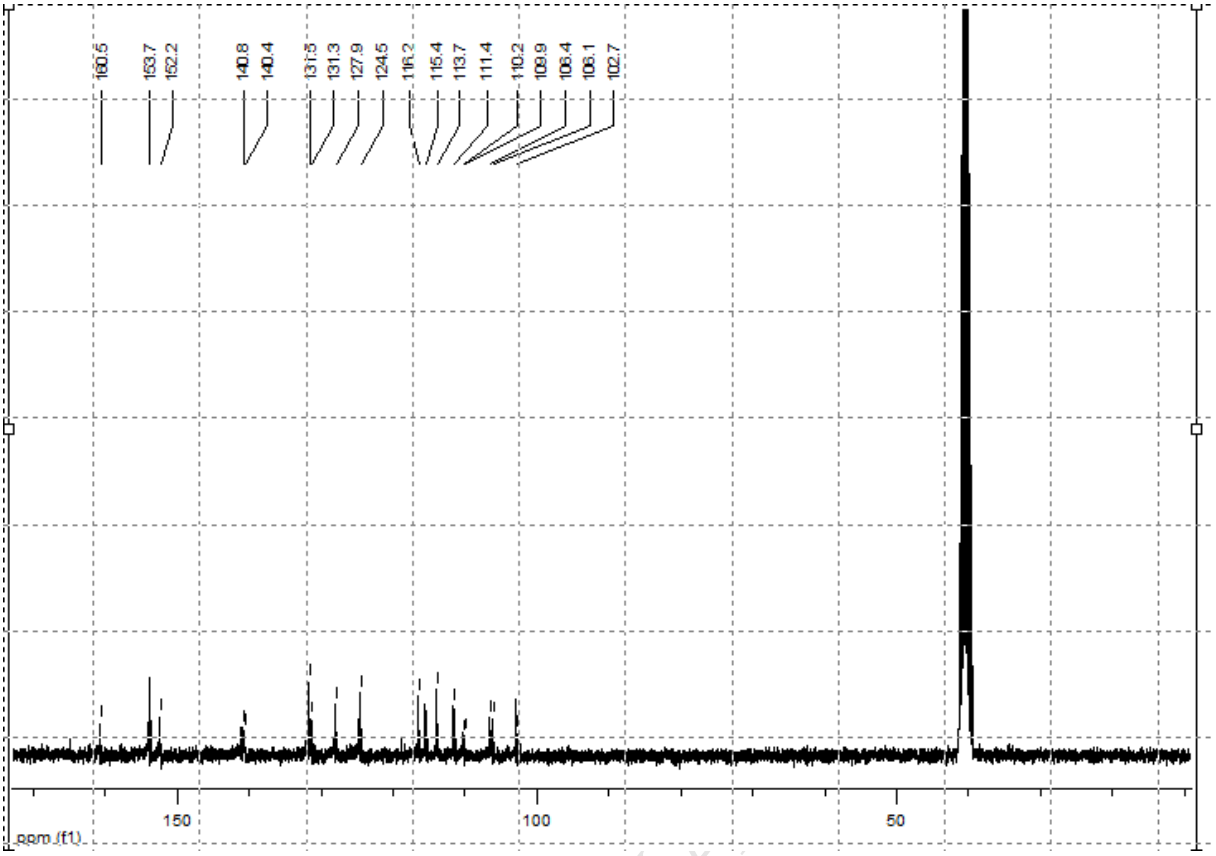
160.5
153.7
152.2
140.8
140.4
131.3
131.3
127.9
124.5
116.2
115.4
113.7
111.4
110.2
109.9
106.4
106.1
102.7
150
100
50
ppm (f1)

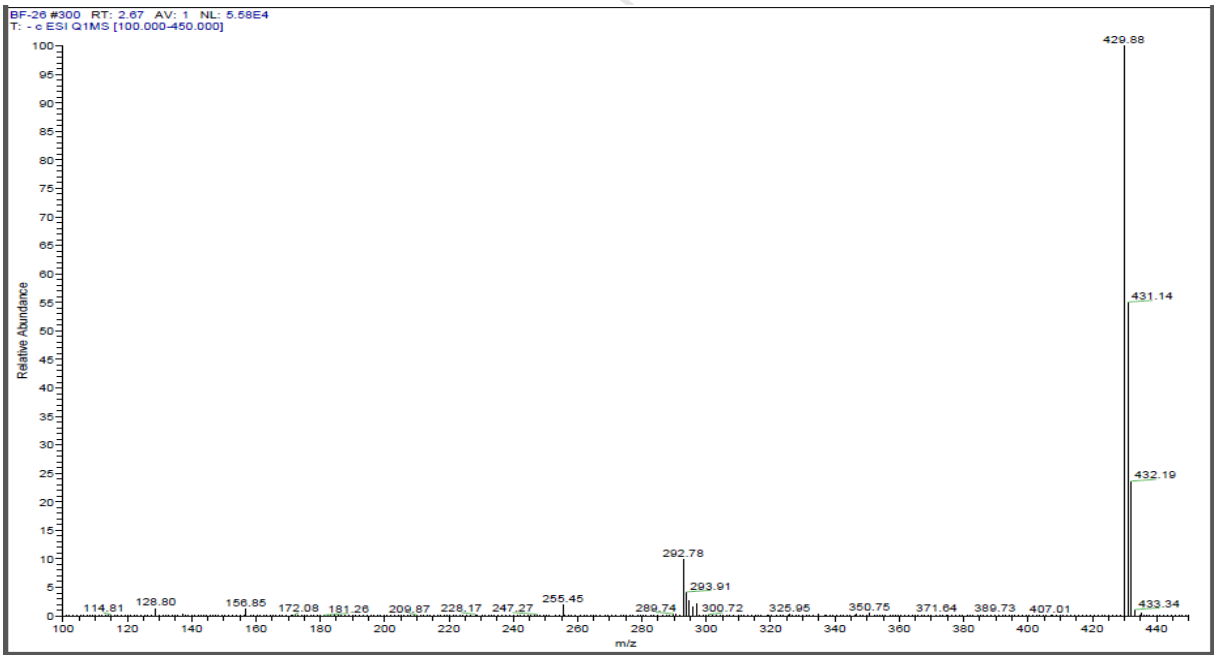
BF-26 #300 RT: 2.67 AV: 1 NL: 5.58E4
T: - c ESI Q1MS [100.000-450.000]
Relative Abundance
m/z
429.88
431.14
432.19
433.34
292.78
293.91
114.81
128.80
156.85
172.08
181.26
209.87
228.17
247.27
255.45
289.74
300.72
325.95
350.75
371.64
389.73
407.01

SM 27. ^{1}H and ^{13}C NMR and MS spectra of e27

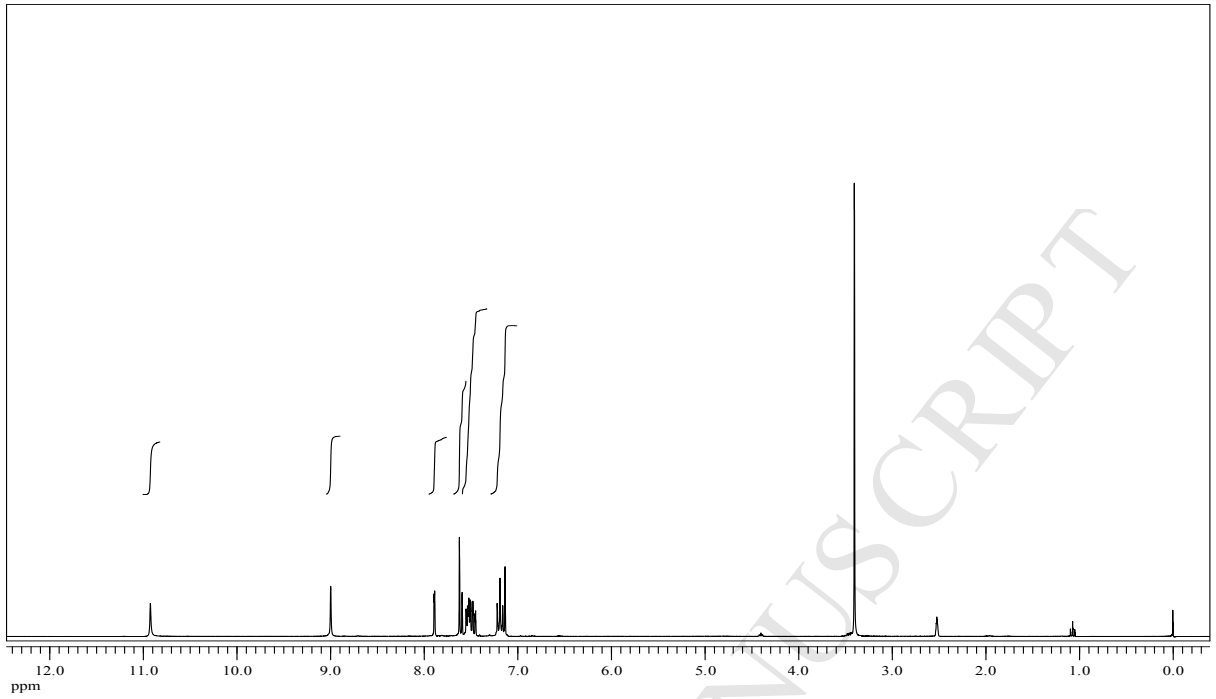

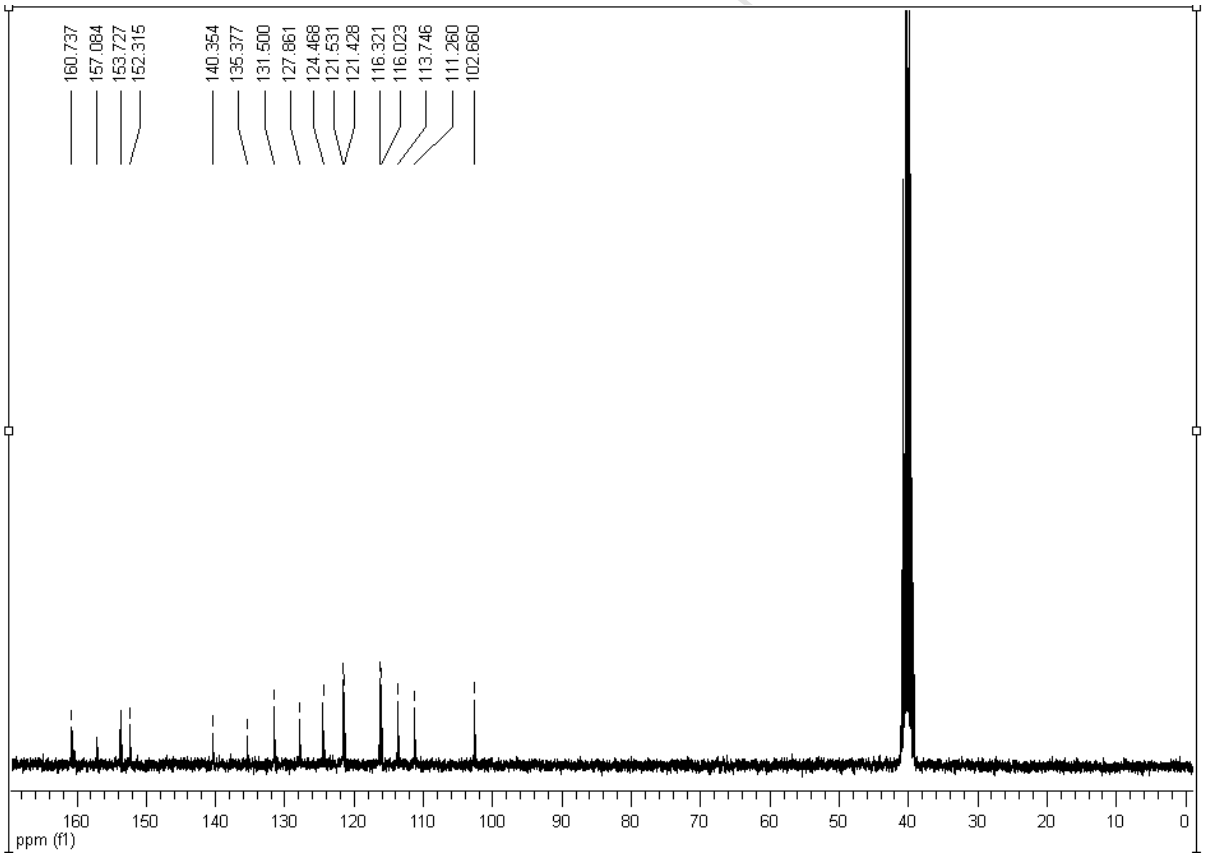

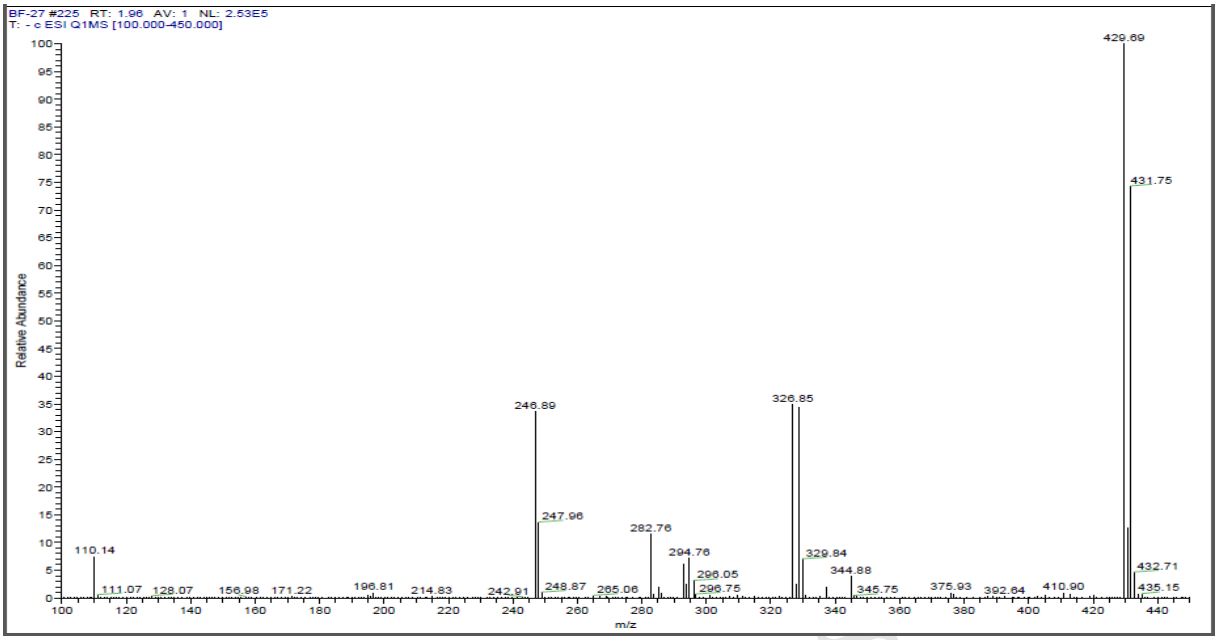

SM 28. ^{1}H and ^{13}C NMR and MS spectra of e28

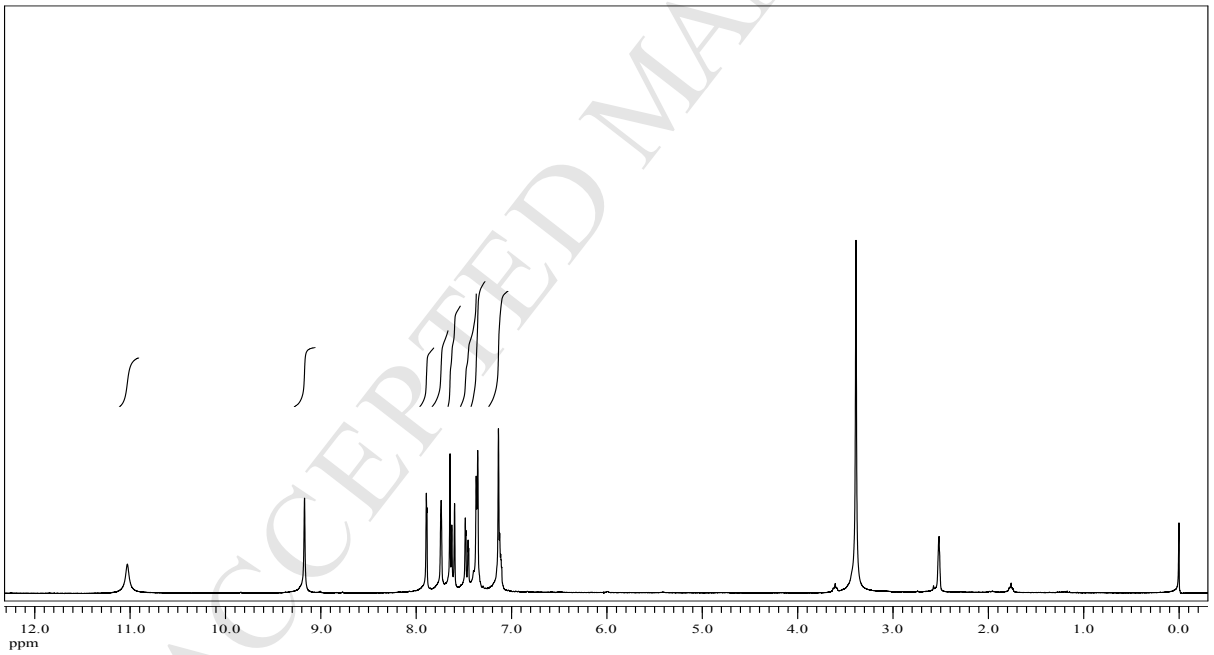

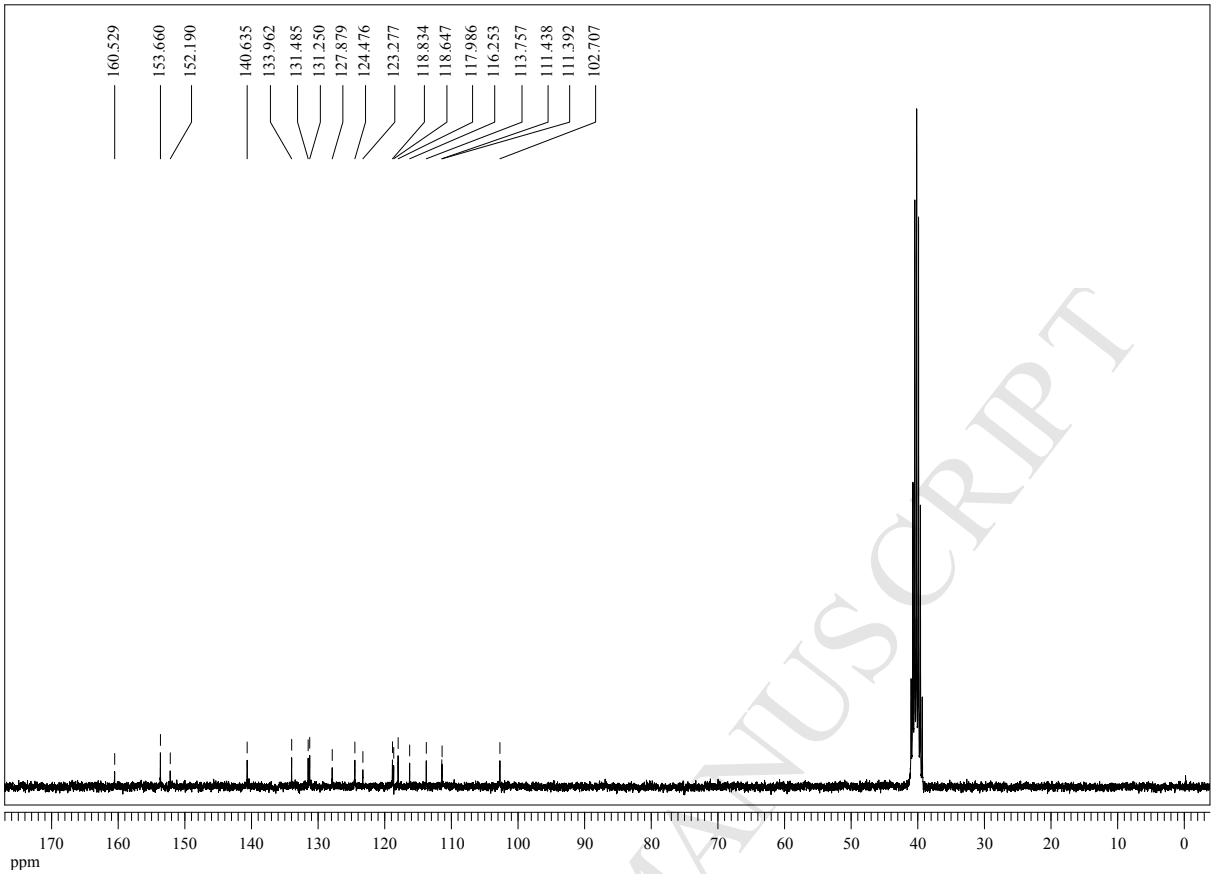
160.529
153.660
152.190
140.635
133.962
131.485
131.250
127.879
124.476
123.277
118.834
118.647
117.986
116.253
113.757
111.438
111.392
102.707
170
160
150
140
130
120
110
100
90
80
70
60
50
40
30
20
10
0
ppm

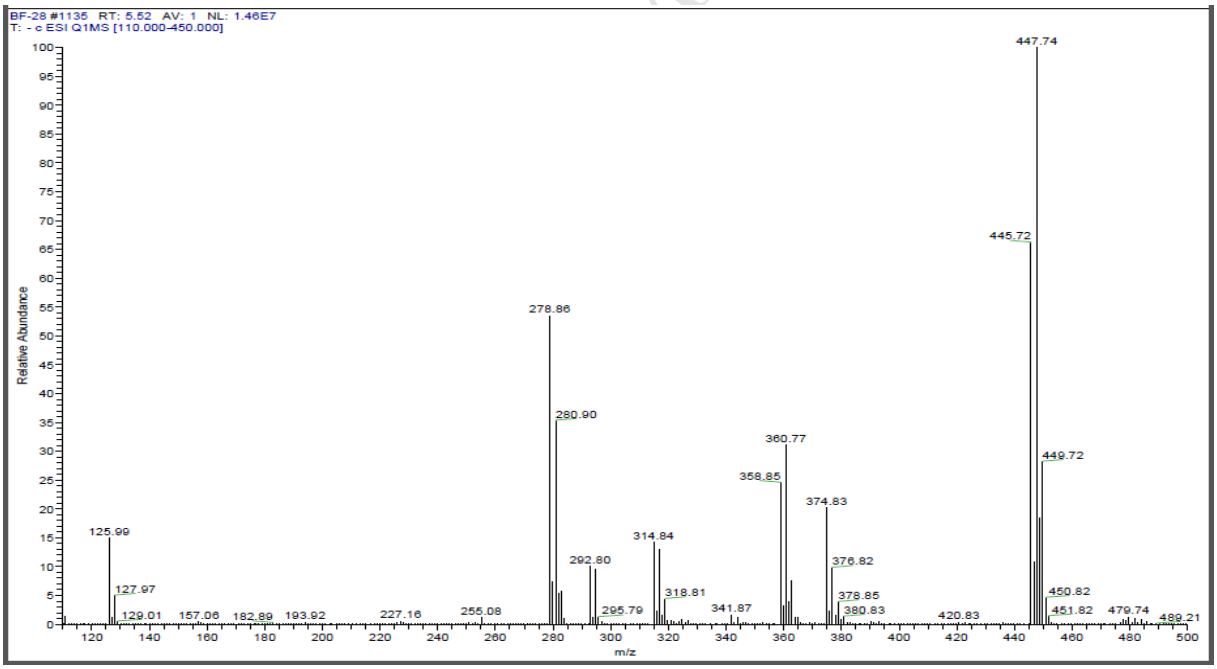
BF-28 #1135 RT: 5.52 AV: 1 NL: 1.46E7
T: - c ESI Q1MS [110.000-450.000]
Relative Abundance
m/z
447.74
445.72
278.86
280.90
360.77
358.85
374.83
449.72
376.82
314.84
292.80
318.81
125.99
127.97
129.01
157.06
182.89
193.92
227.16
255.08
295.79
341.87
378.85
380.83
420.83
450.82
451.82
479.74
489.21

SM 29. ^{1}H and ^{13}C NMR and MS spectra of e29

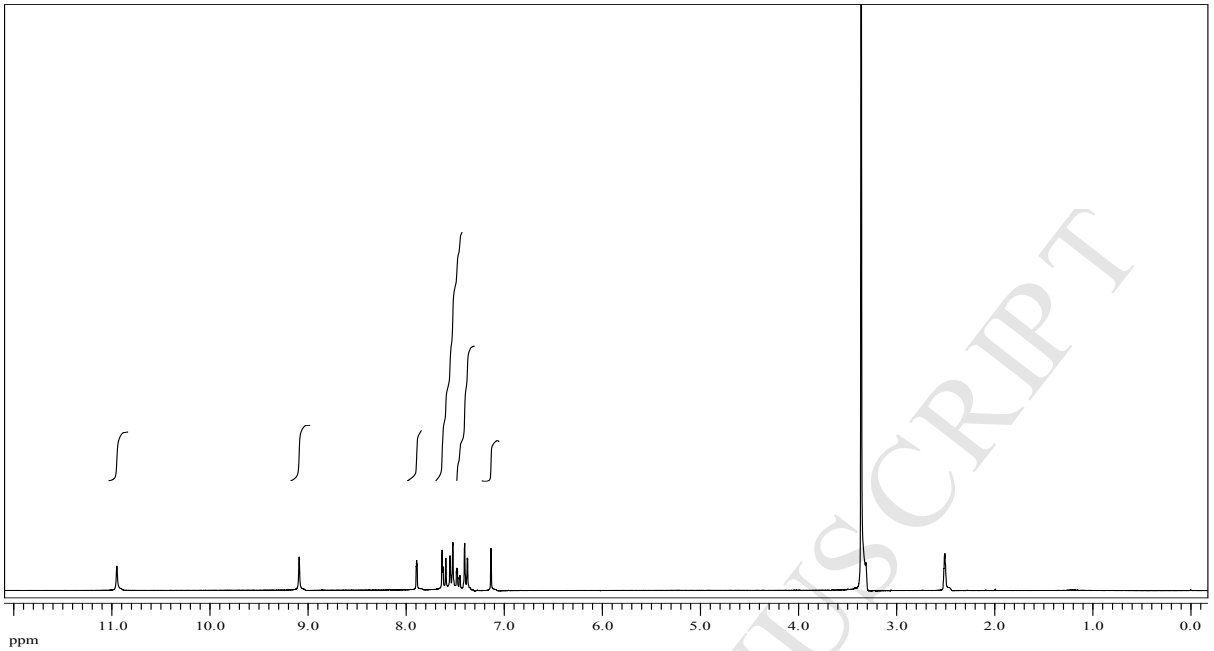

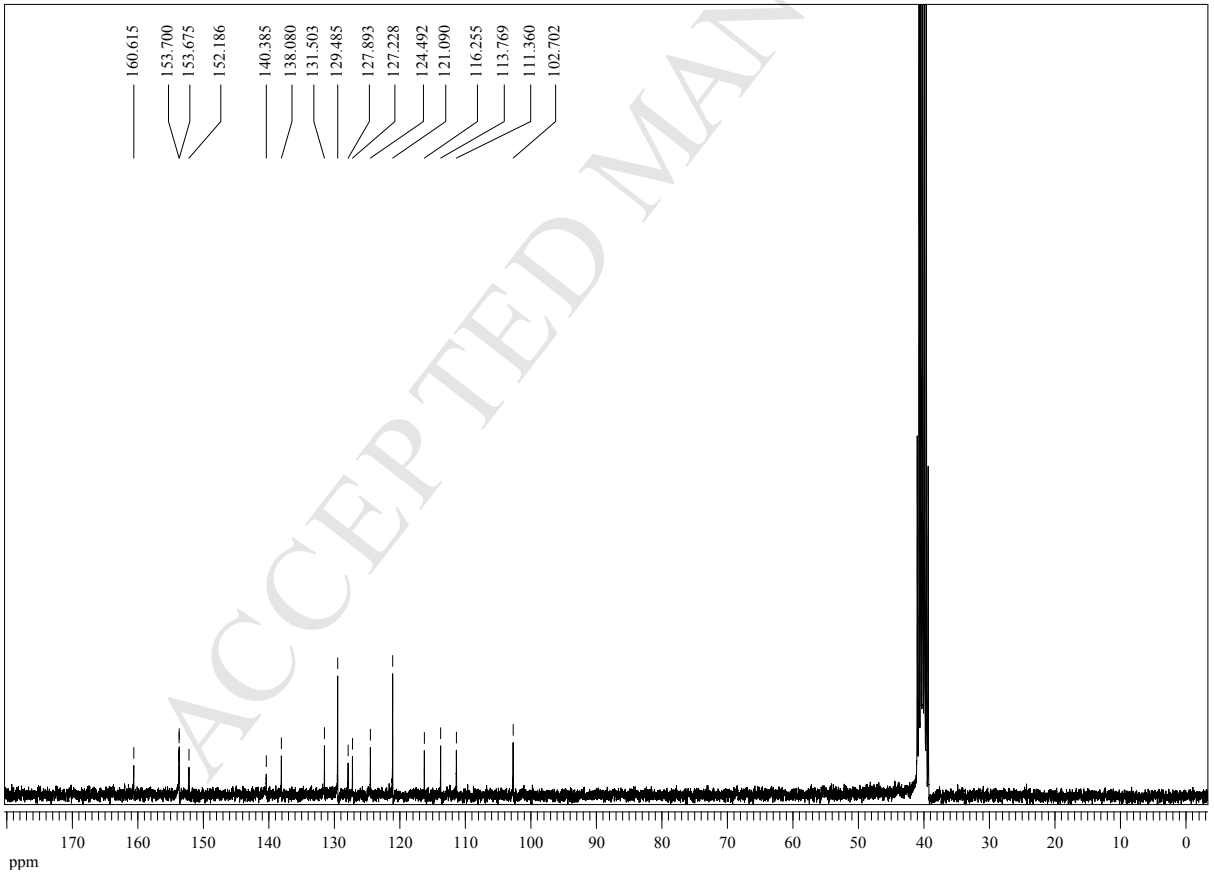

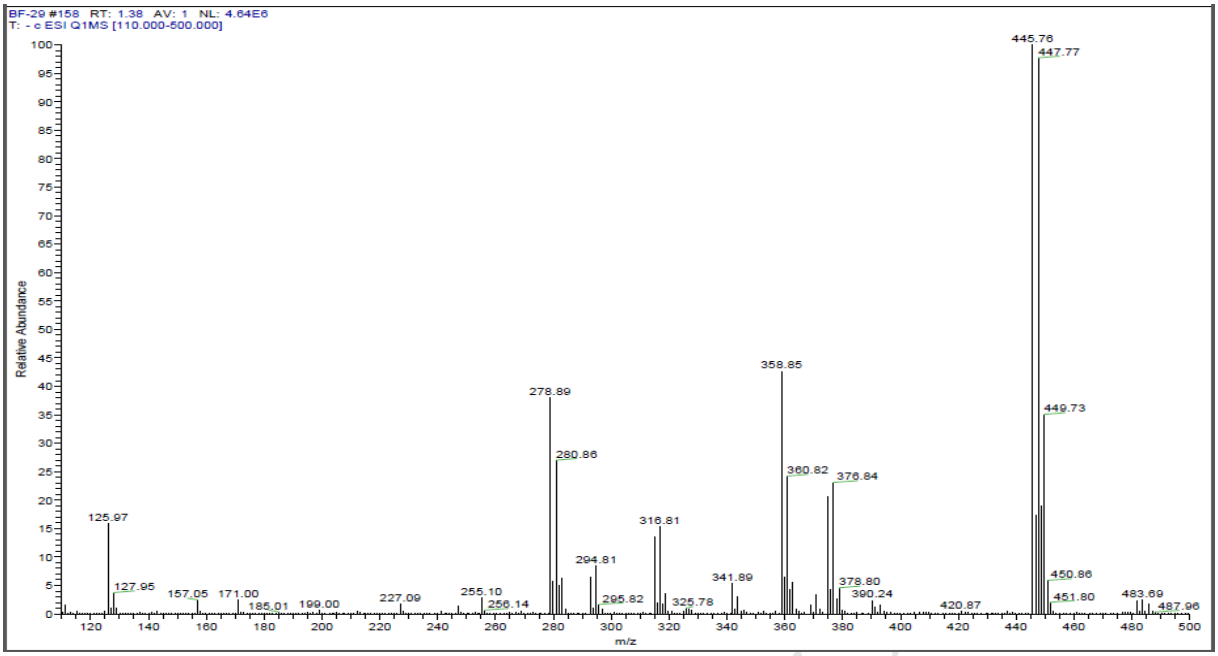

SM 30. ^{1}H and ^{13}C NMR and MS spectra of e30

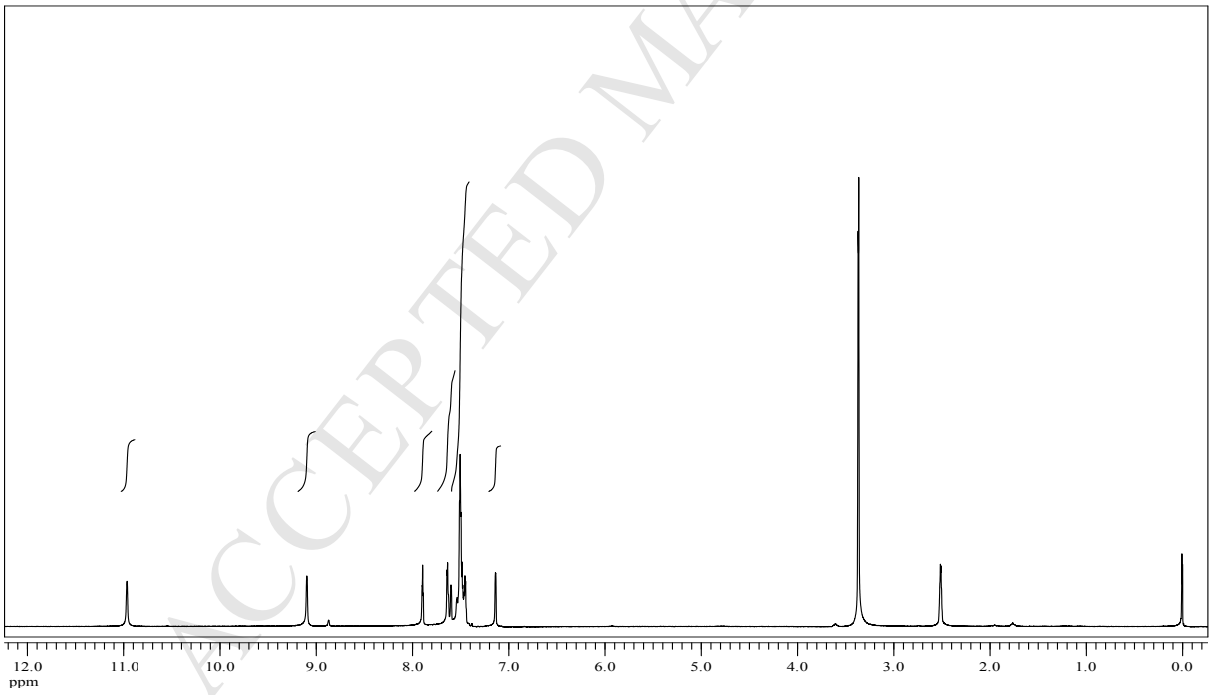

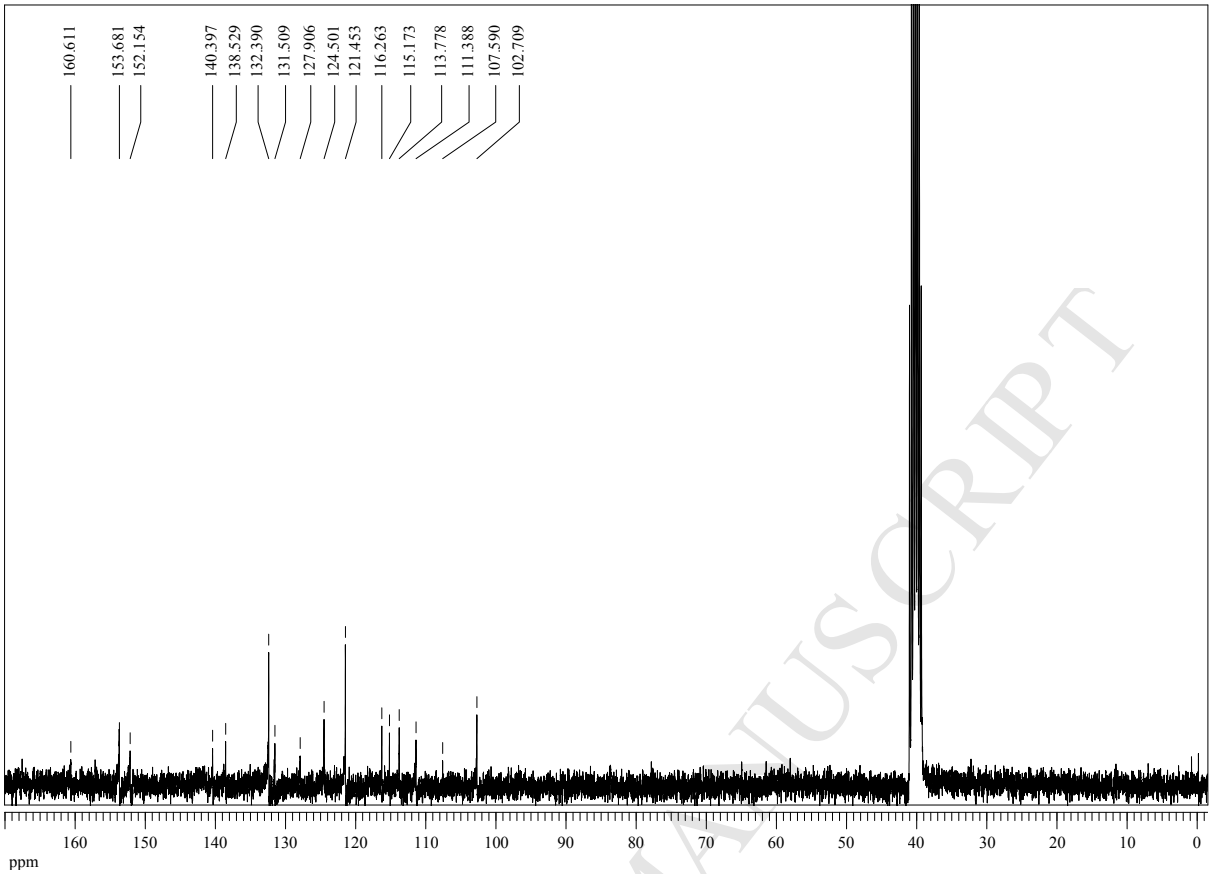
160.611
153.681
152.154
140.397
138.529
132.390
131.509
127.906
124.501
121.453
116.263
115.173
113.778
111.388
107.590
102.709
160
150
140
130
120
110
100
90
80
70
60
50
40
30
20
10
0
ppm

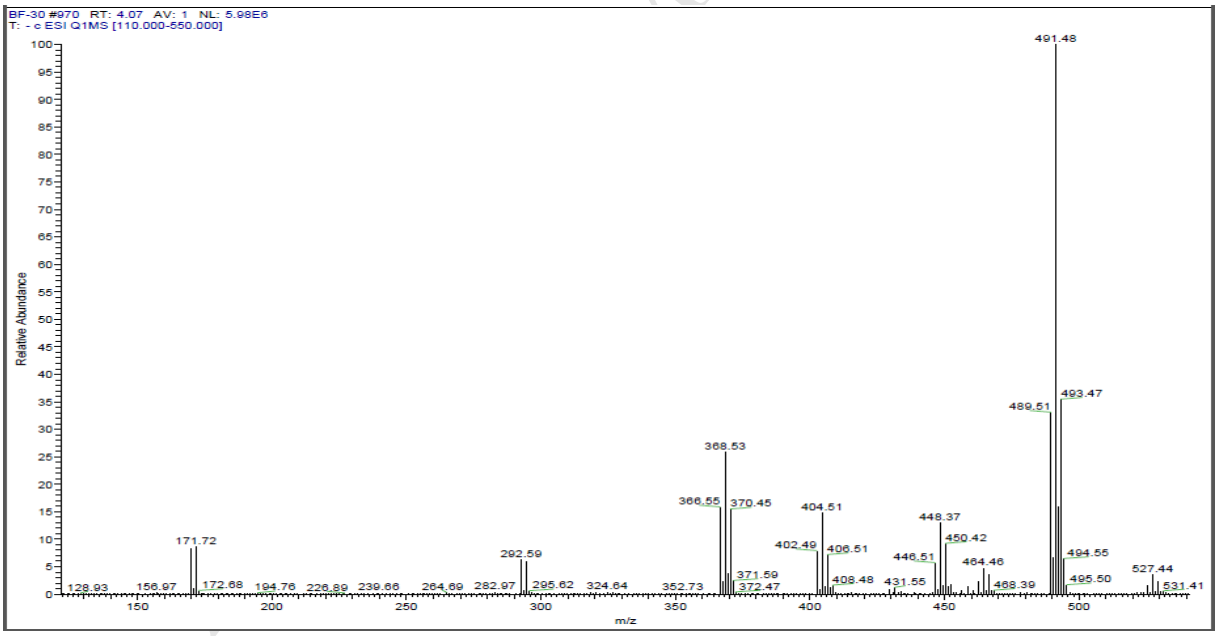
BF-30 #970 RT: 4.07 AV: 1 NL: 5.98E6
T: - c ESI Q1MS [110.000-550.000]
Relative Abundance
m/z
491.48
493.47
489.51
368.53
366.55
370.45
404.51
448.37
450.42
402.49
406.51
446.51
464.46
494.55
527.44
171.72
292.59
371.59
372.47
408.48
431.55
468.39
495.50
531.41
128.93
156.97
172.68
194.76
226.89
239.86
264.69
282.97
295.62
324.64
352.73

SM 31. ^{1}H and ^{13}C NMR and MS spectra of e31

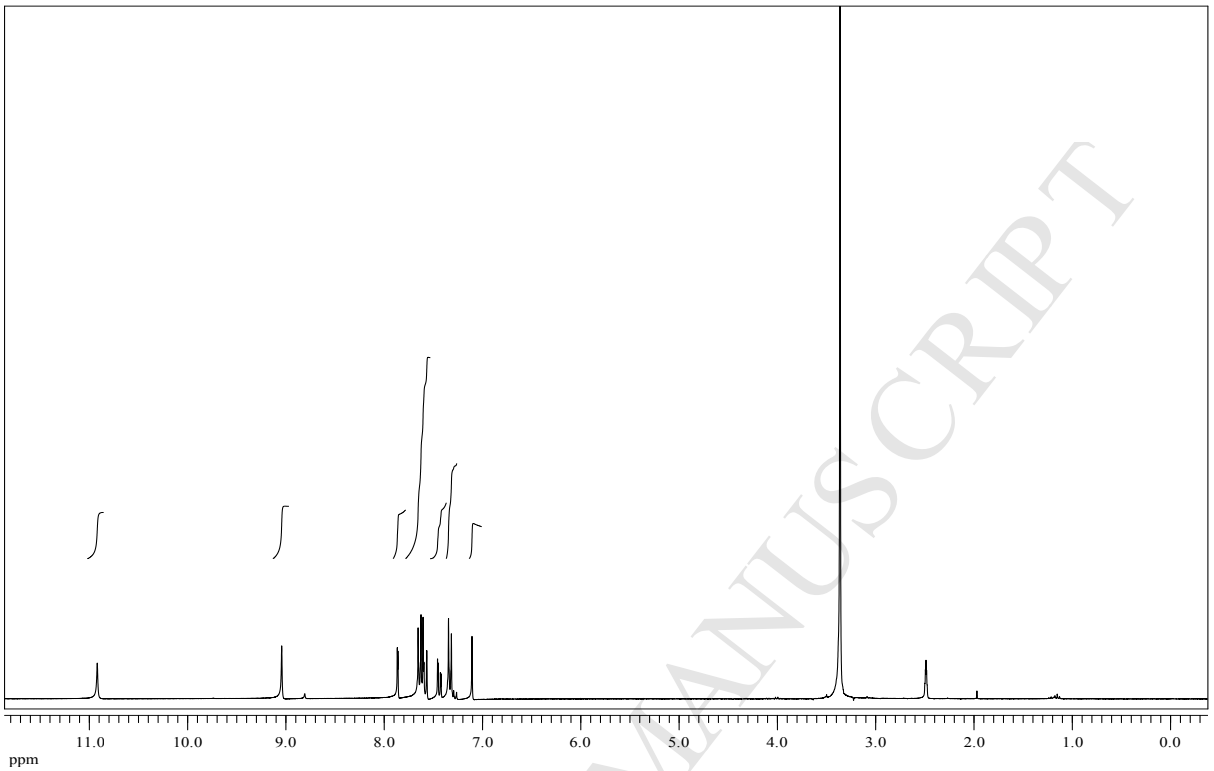

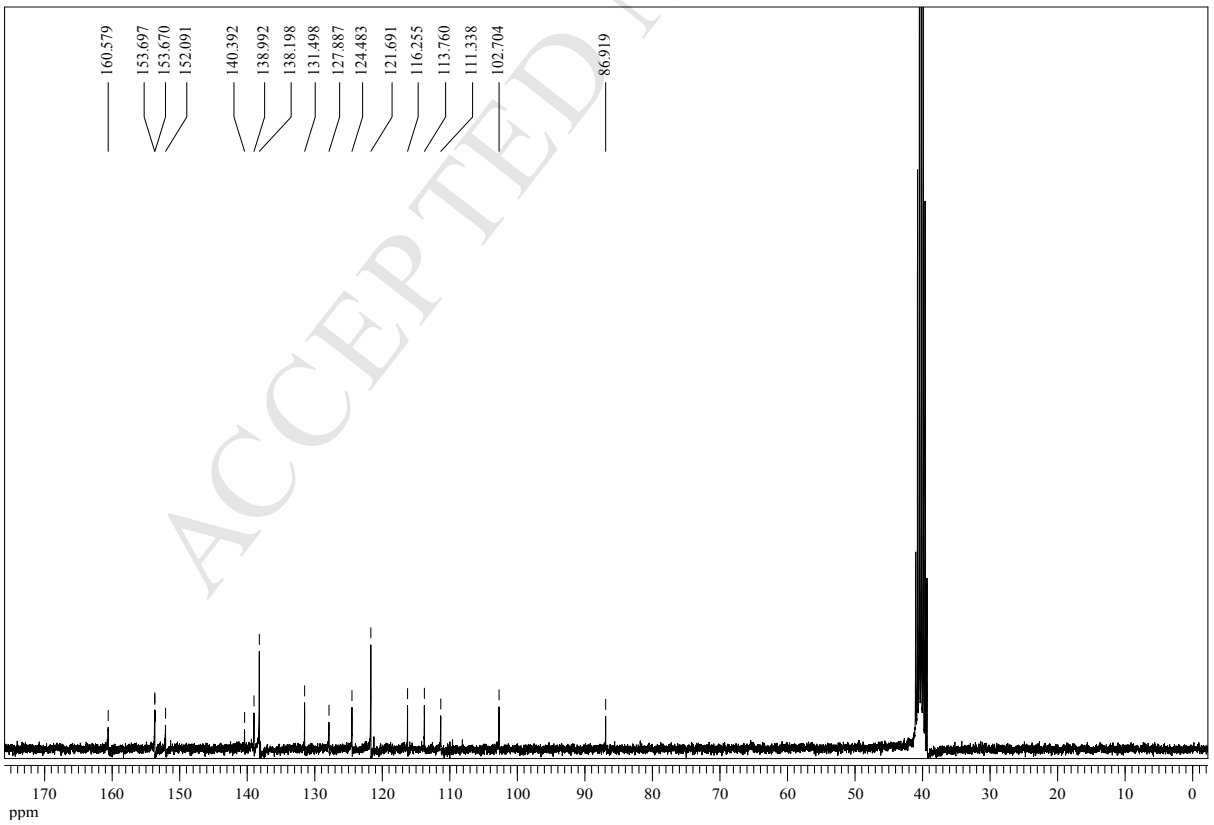

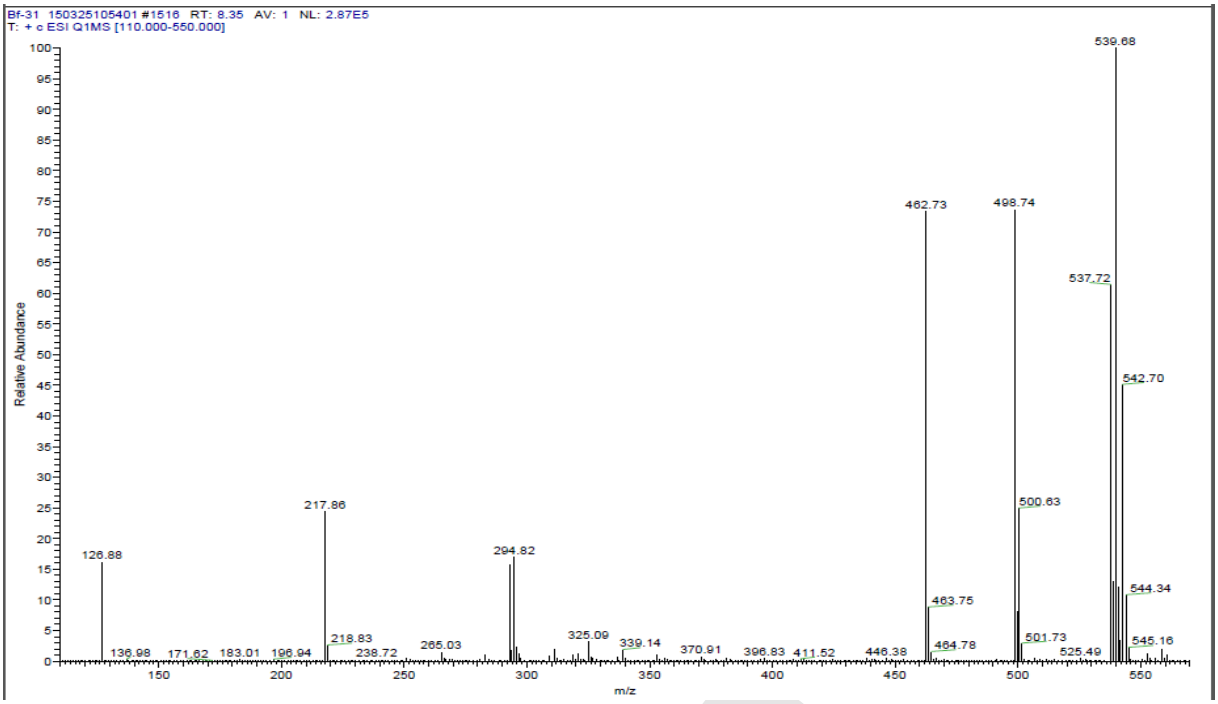

SM 32. ^{1}H and ^{13}C NMR and MS spectra of e32

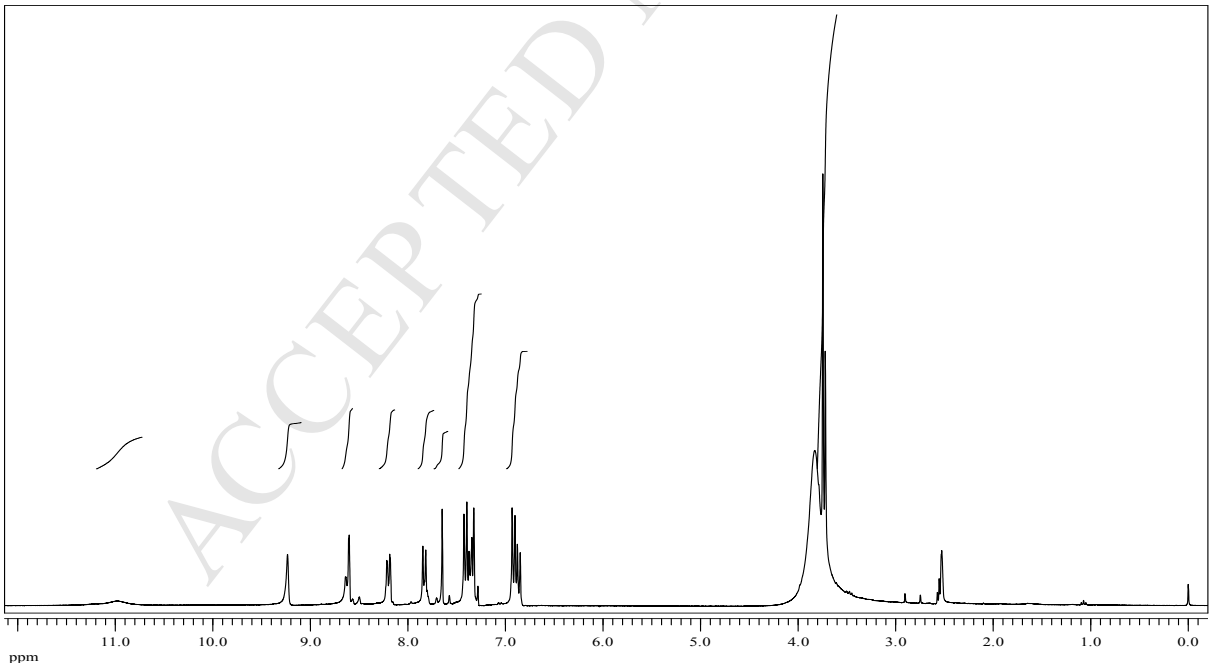

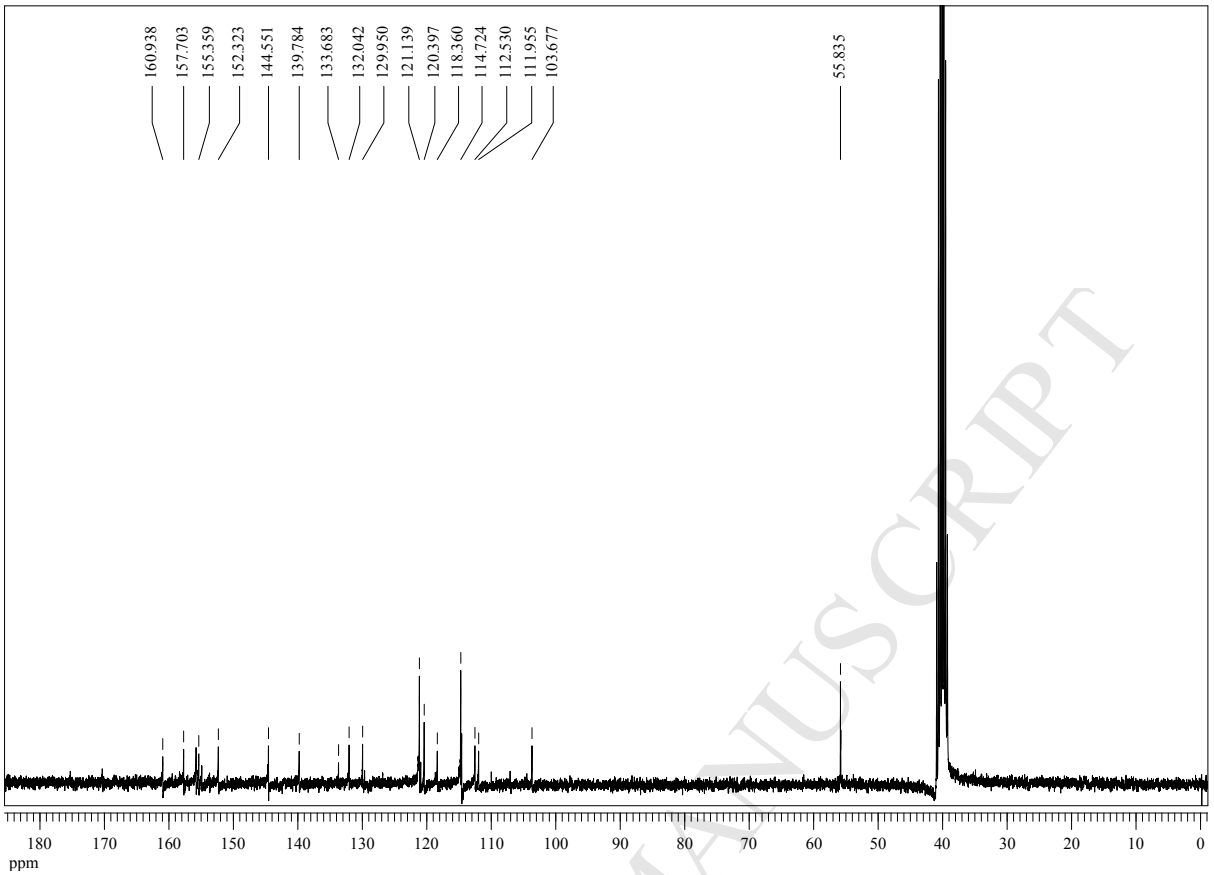
160.938
157.703
155.359
152.323
144.551
139.784
133.683
132.042
129.950
121.139
120.397
118.360
114.724
112.530
111.955
103.677
55.835
180
170
160
150
140
130
120
110
100
90
80
70
60
50
40
30
20
10
0
ppm

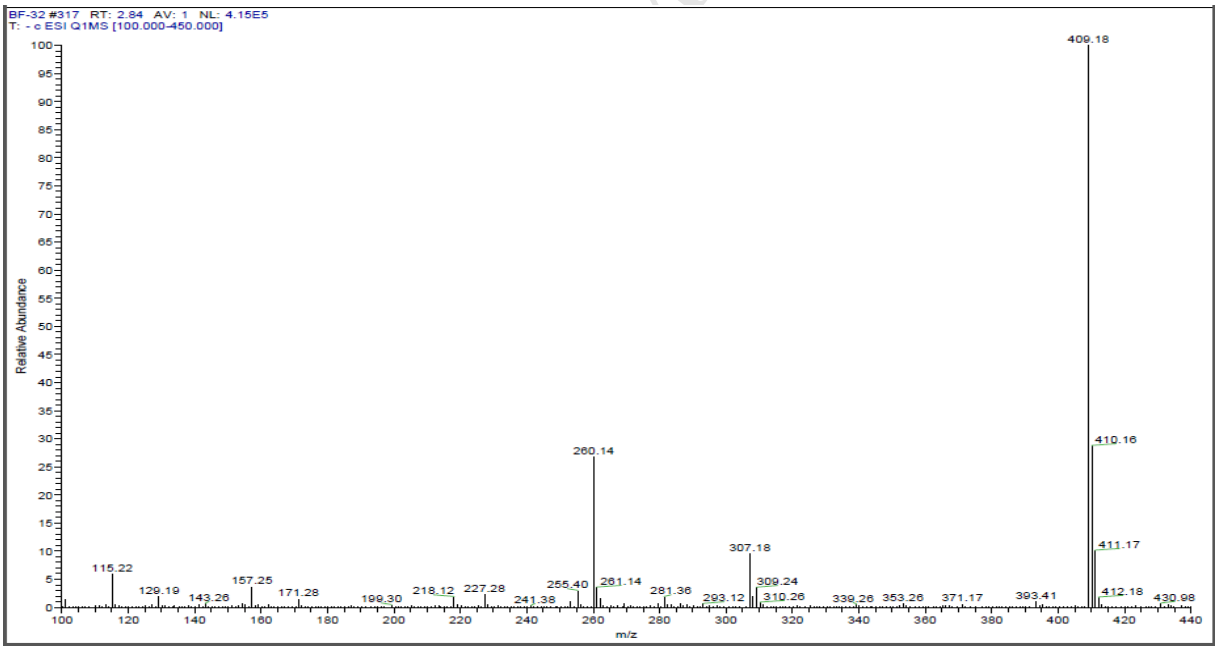
BF-32 #317 RT: 2.84 AV: 1 NL: 4.15E5
T: - c ESI Q1MS [100.000-450.000]
Relative Abundance
m/z
409.18
410.16
411.17
412.18
430.98
260.14
307.18
309.24
310.26
115.22
129.19
143.26
157.25
171.28
199.30
218.12
227.28
241.38
255.40
261.14
281.36
293.12
339.26
353.26
371.17
393.41

SM 33. ^{1}H and ^{13}C NMR and MS spectra of e33

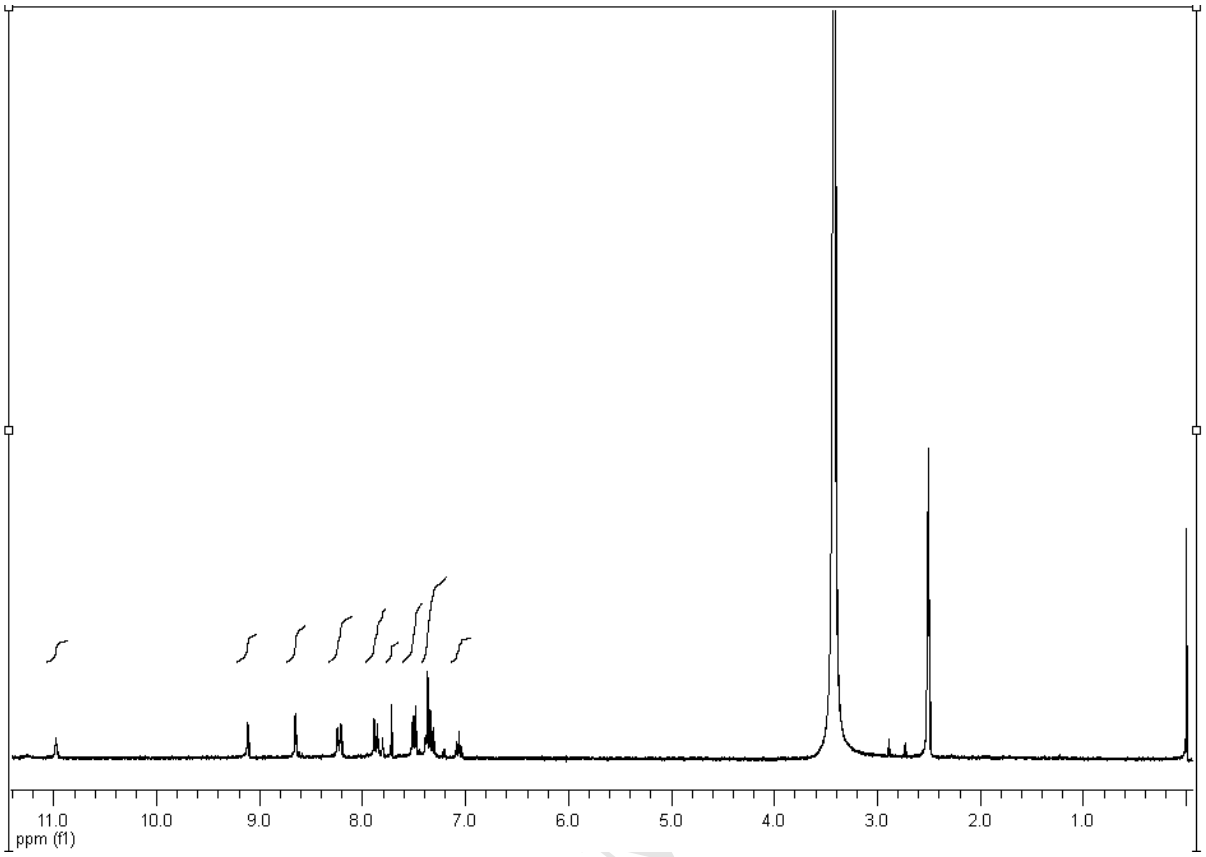

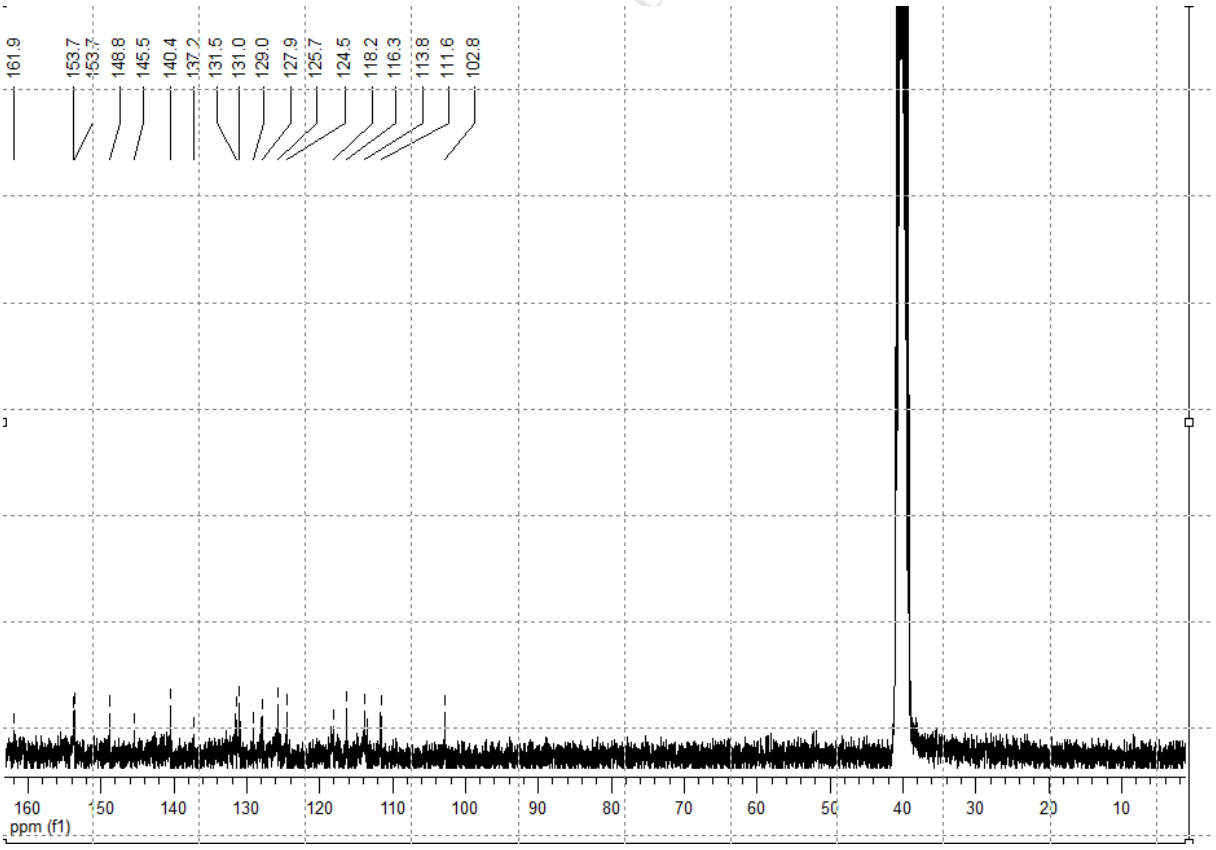

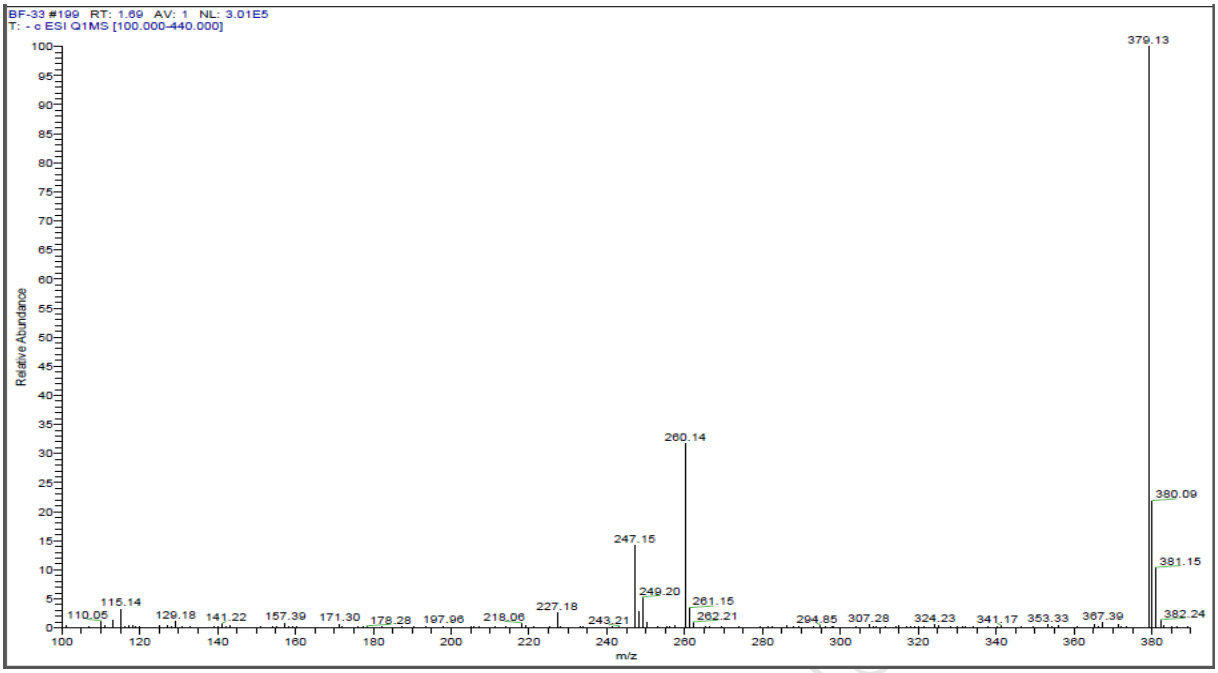

SM 34. ^{1}H and ^{13}C NMR and MS spectra of e34

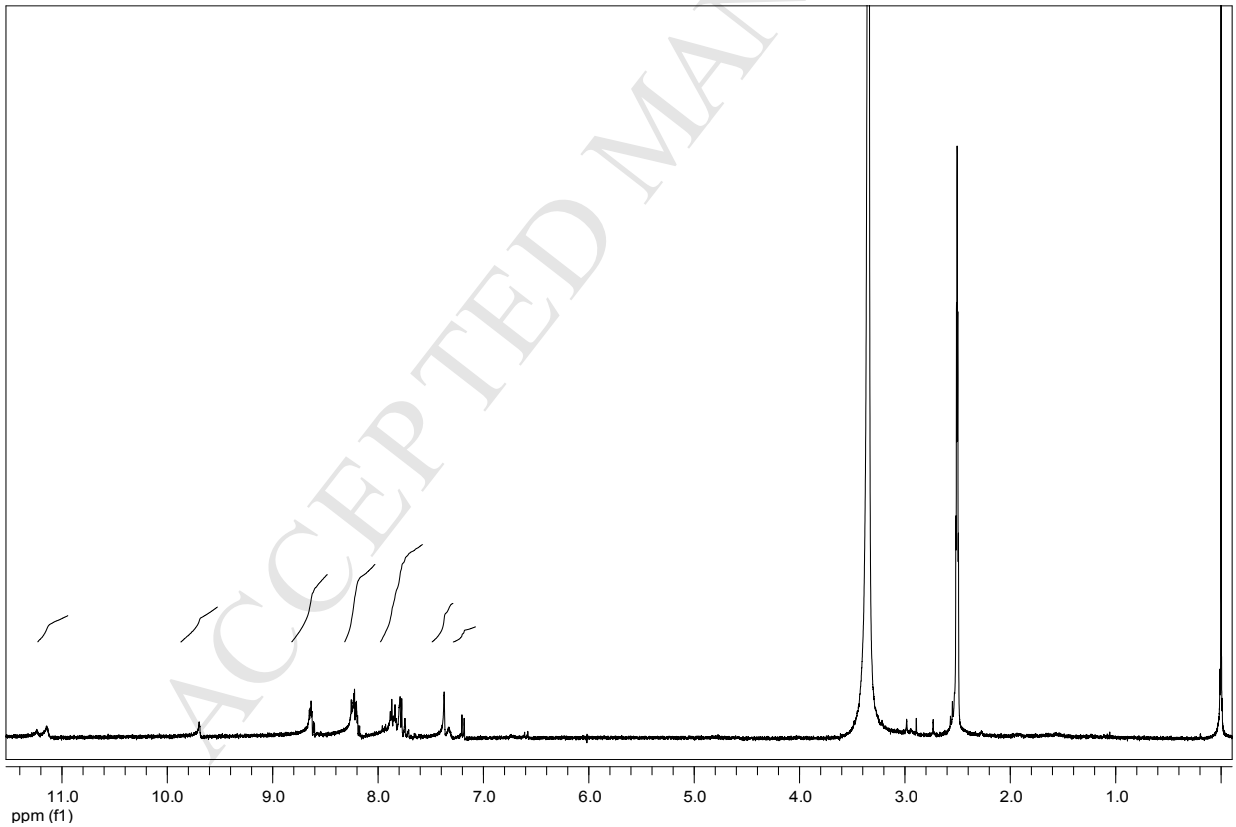

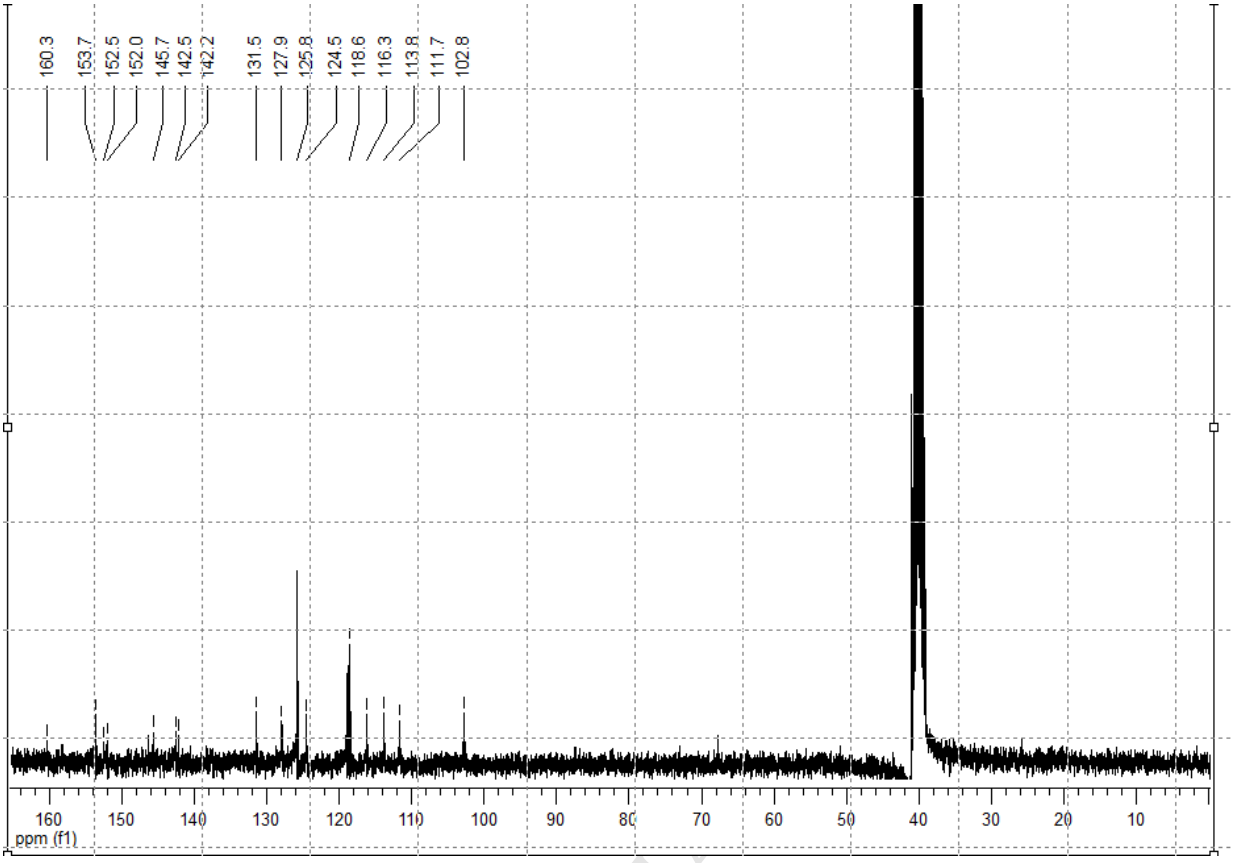
160.3
153.7
152.5
152.0
145.7
142.5
142.2
131.5
127.9
125.8
124.5
118.6
116.3
113.8
111.7
102.8
160
150
140
130
120
110
100
90
80
70
60
50
40
30
20
10
ppm (f1)

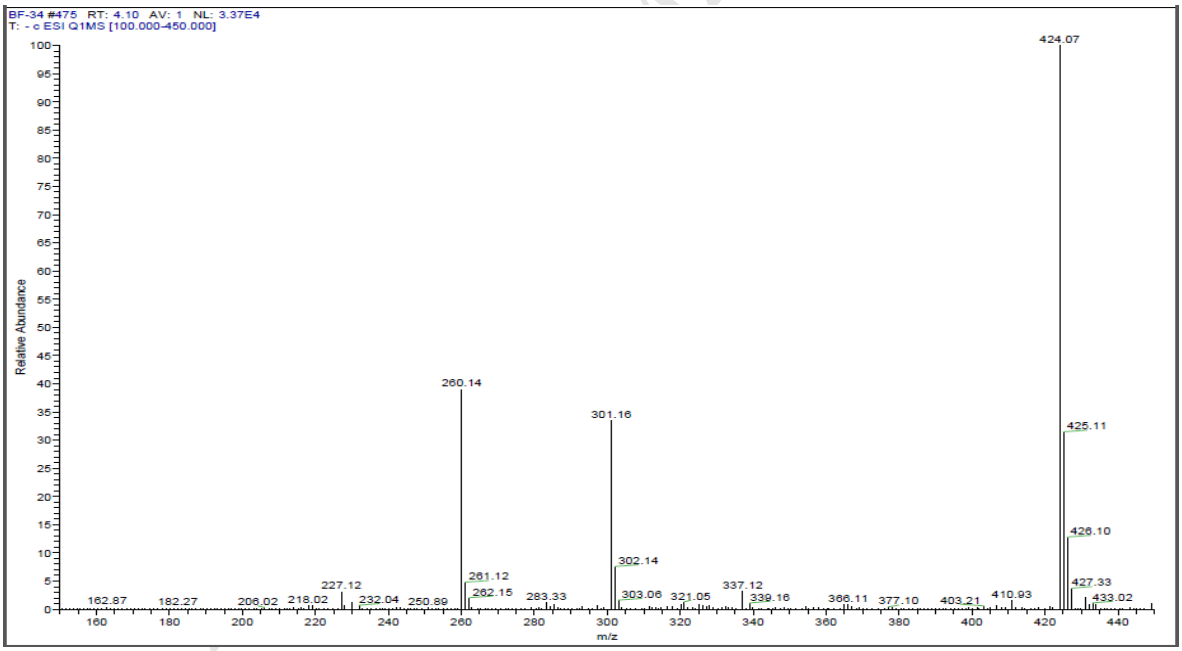
BF-34 #475 RT: 4.10 AV: 1 NL: 3.37E4
T: - c ESI Q1MS [100.000-450.000]
Relative Abundance
m/z
424.07
425.11
426.10
427.33
433.02
260.14
261.12
262.15
301.16
302.14
303.06
337.12
339.16
227.12
162.87
182.27
206.02
218.02
232.04
250.89
283.33
321.05
366.11
377.10
403.21
410.93

SM 35. ^{1}H and ^{13}C NMR and MS spectra of e35

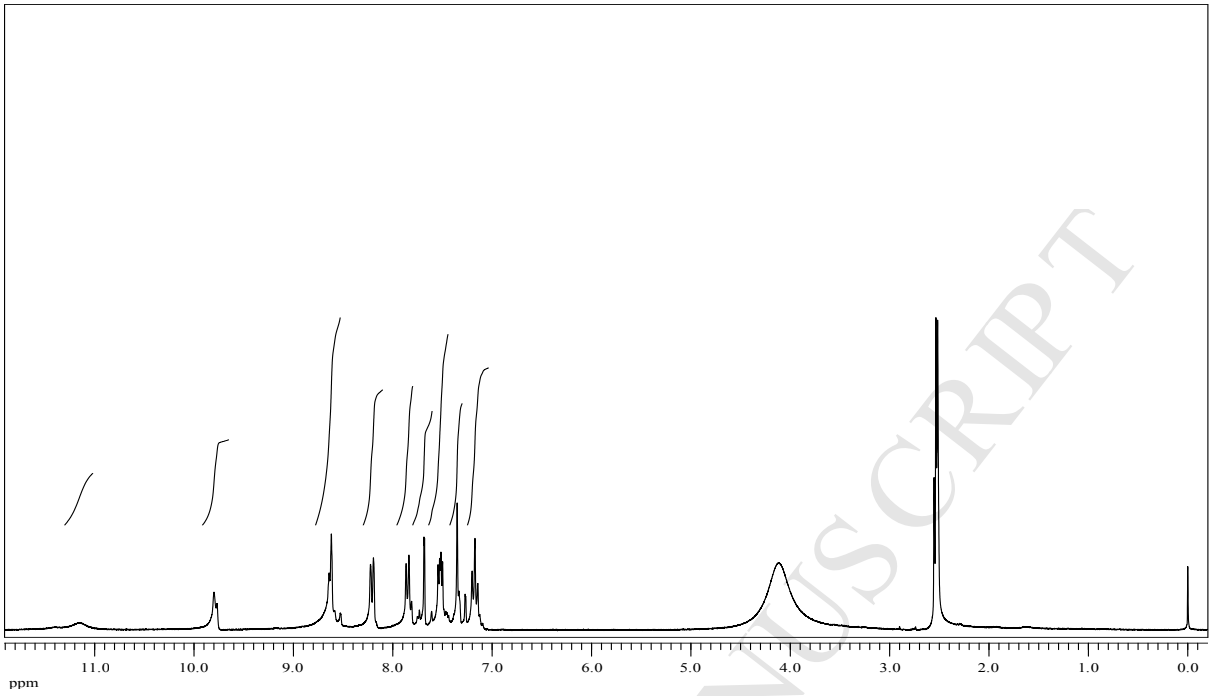

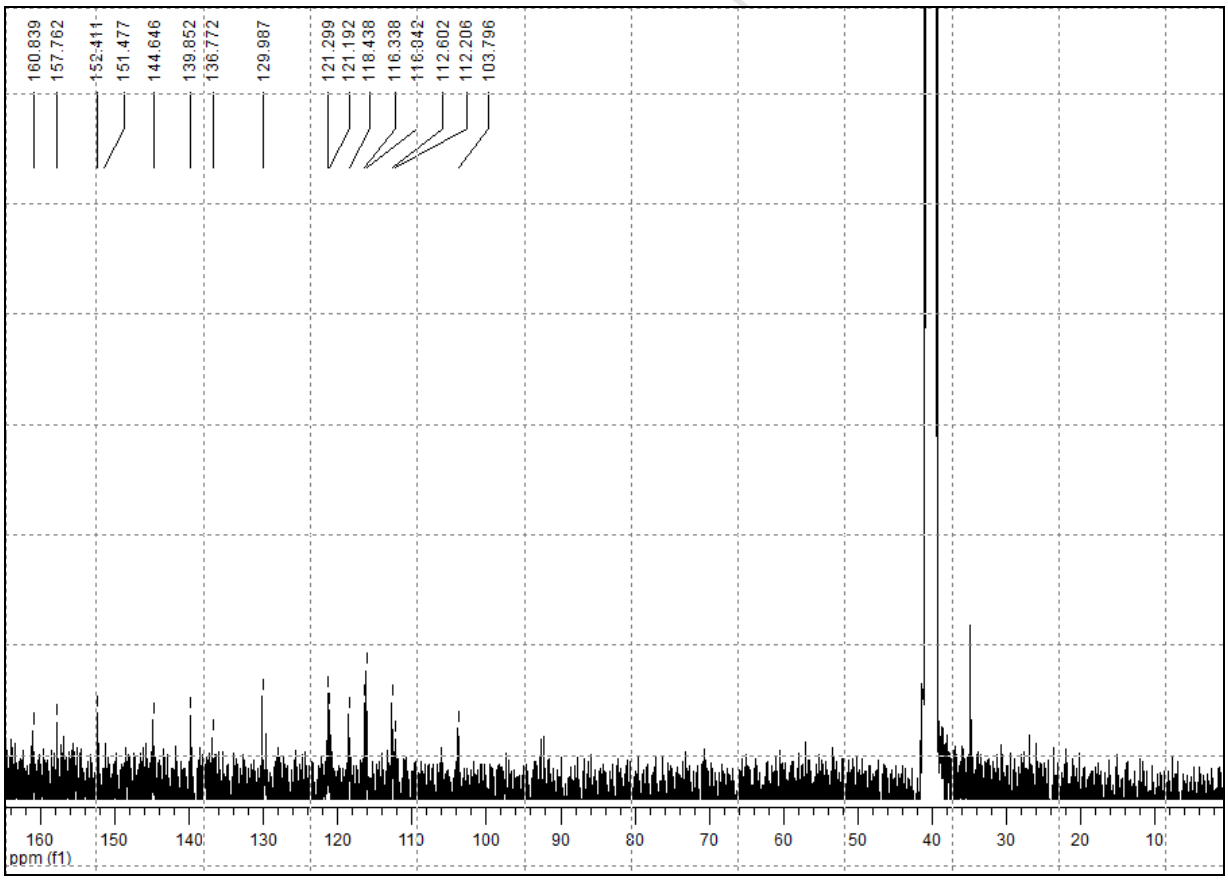

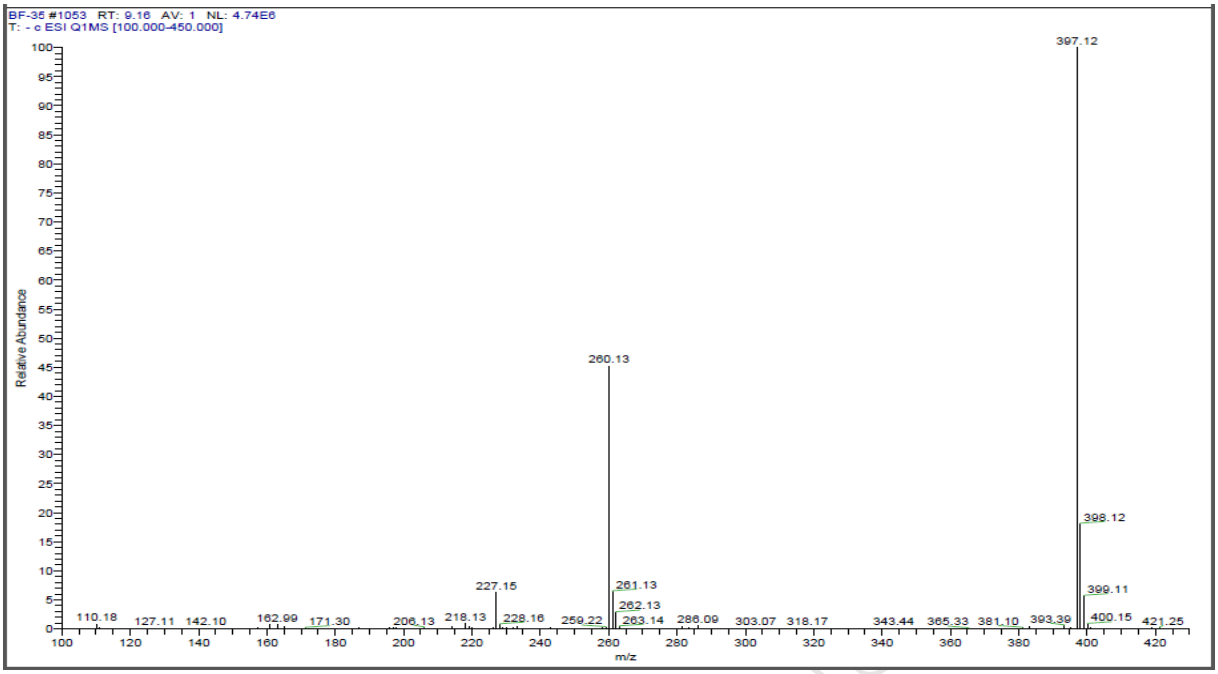

SM 36. ^{1}H and ^{13}C NMR and MS spectra of e36

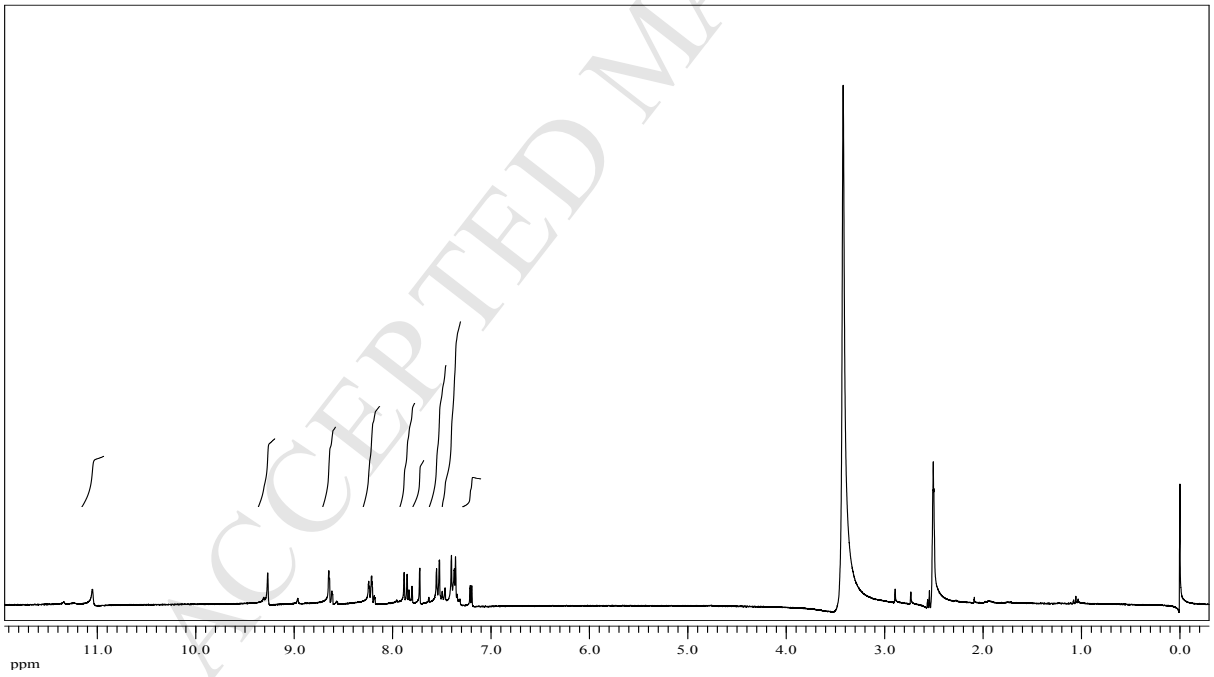

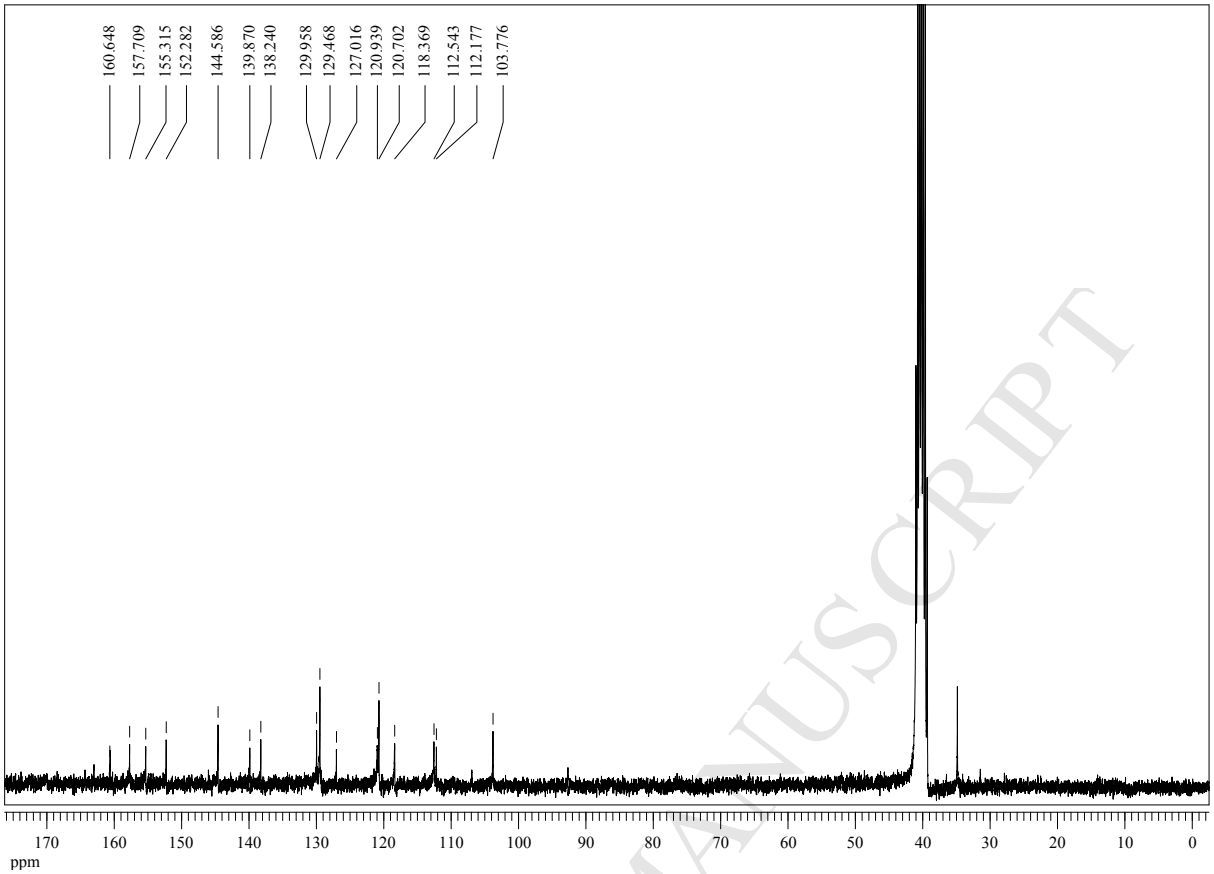
160.648
157.709
155.315
152.282
144.586
139.870
138.240
129.958
129.468
127.016
120.939
120.702
118.369
112.543
112.177
103.776
170 160 150 140 130 120 110 100 90 80 70 60 50 40 30 20 10 0
ppm

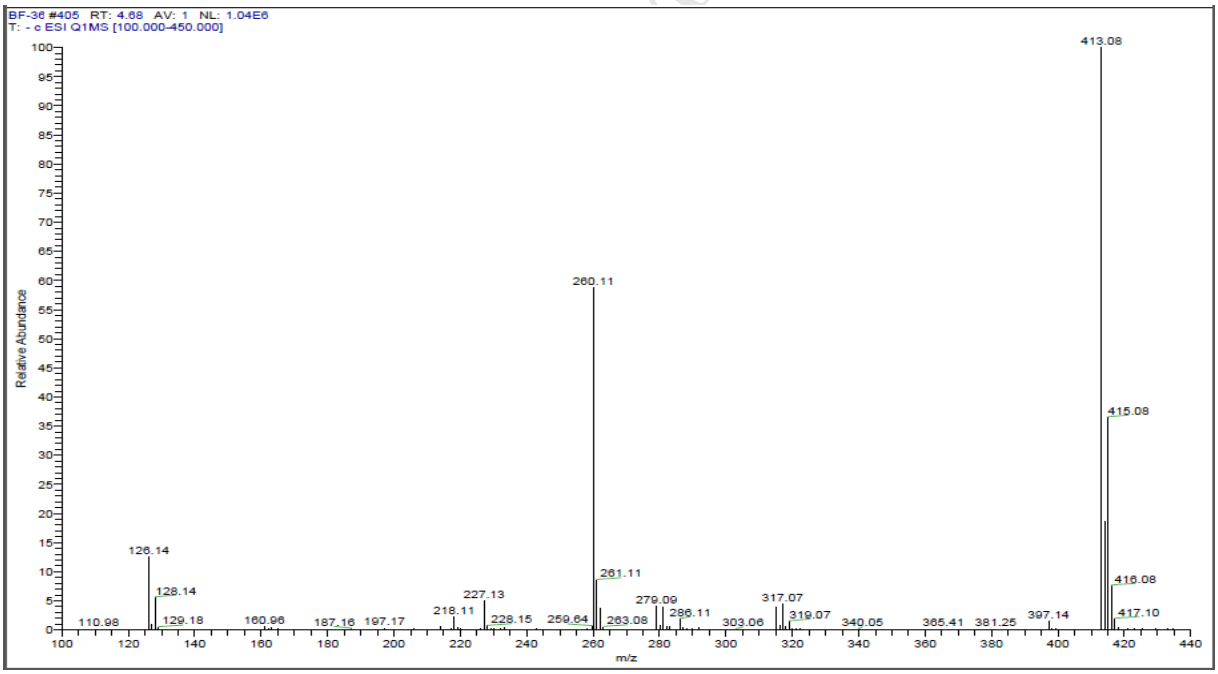
BF-36 #405 RT: 4.68 AV: 1 NL: 1.04E6
T: - c ESI Q1MS [100.000-450.000]
Relative Abundance
m/z
413.08
260.11
415.08
126.14
261.11
128.14
227.13
279.09
317.07
416.08
417.10
110.98
129.18
160.96
187.16
197.17
218.11
228.15
259.64
263.08
286.11
303.06
319.07
340.05
365.41
381.25
397.14

SM 37. ^{1}H and ^{13}C NMR and MS spectra of e37

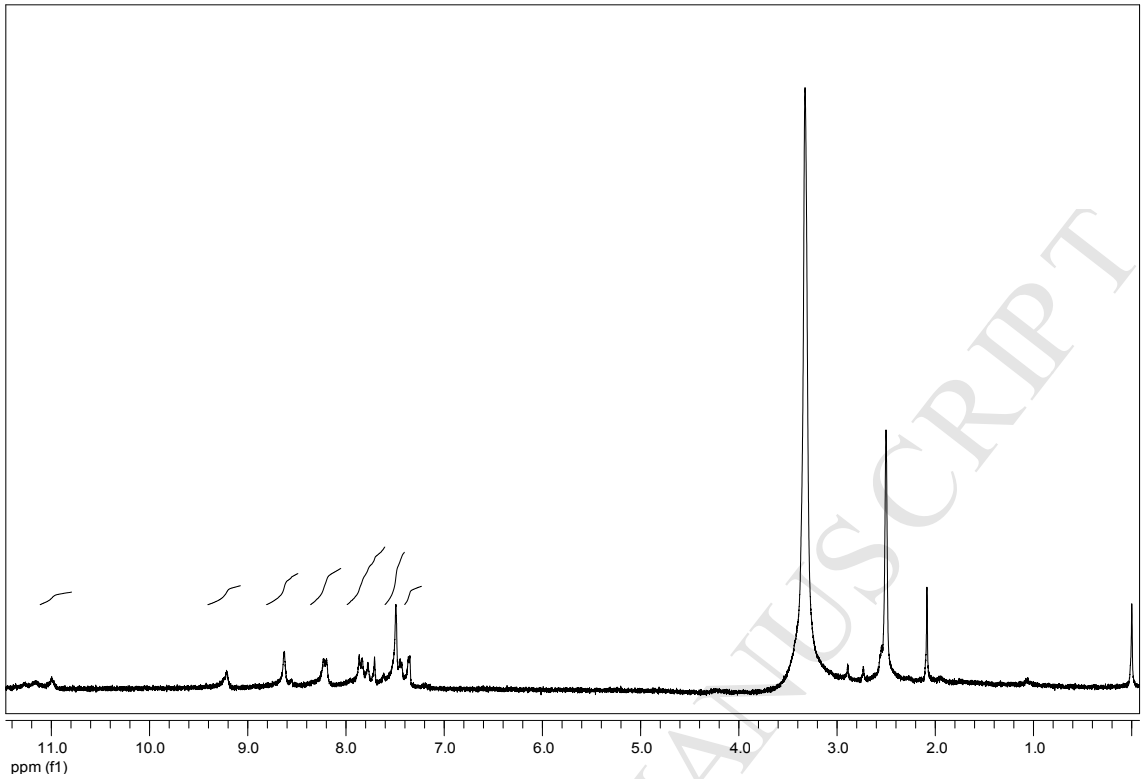

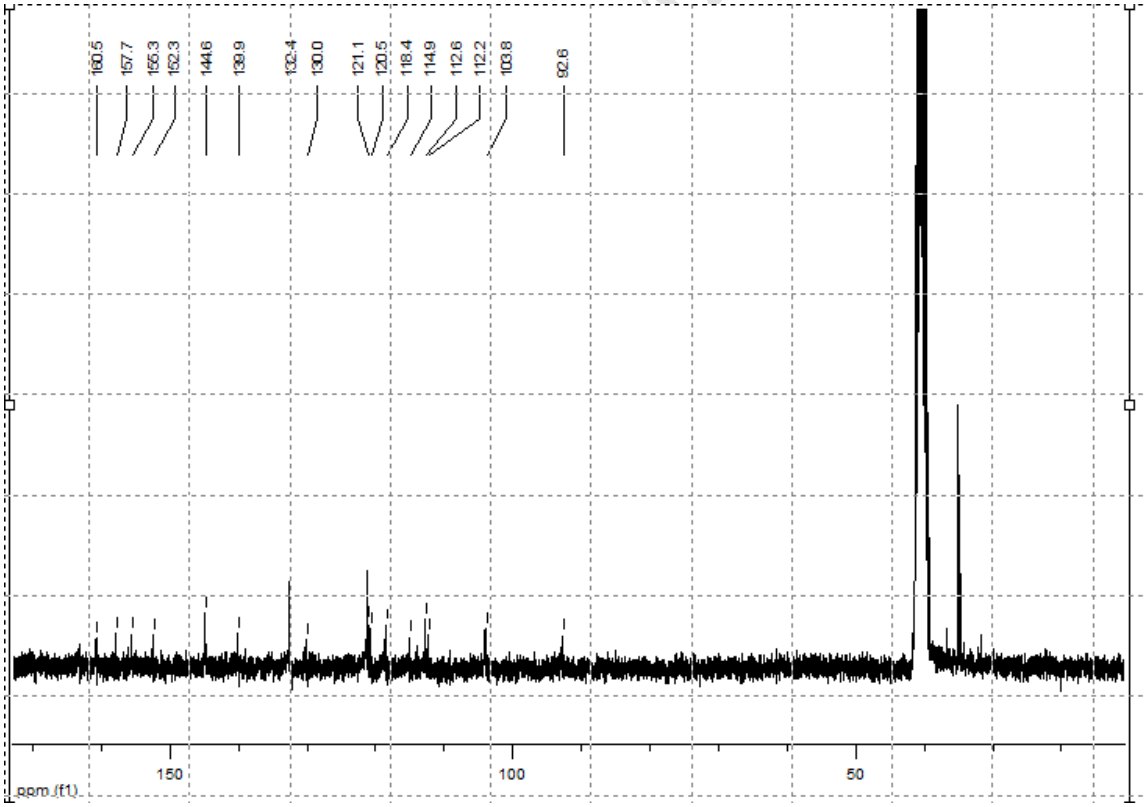

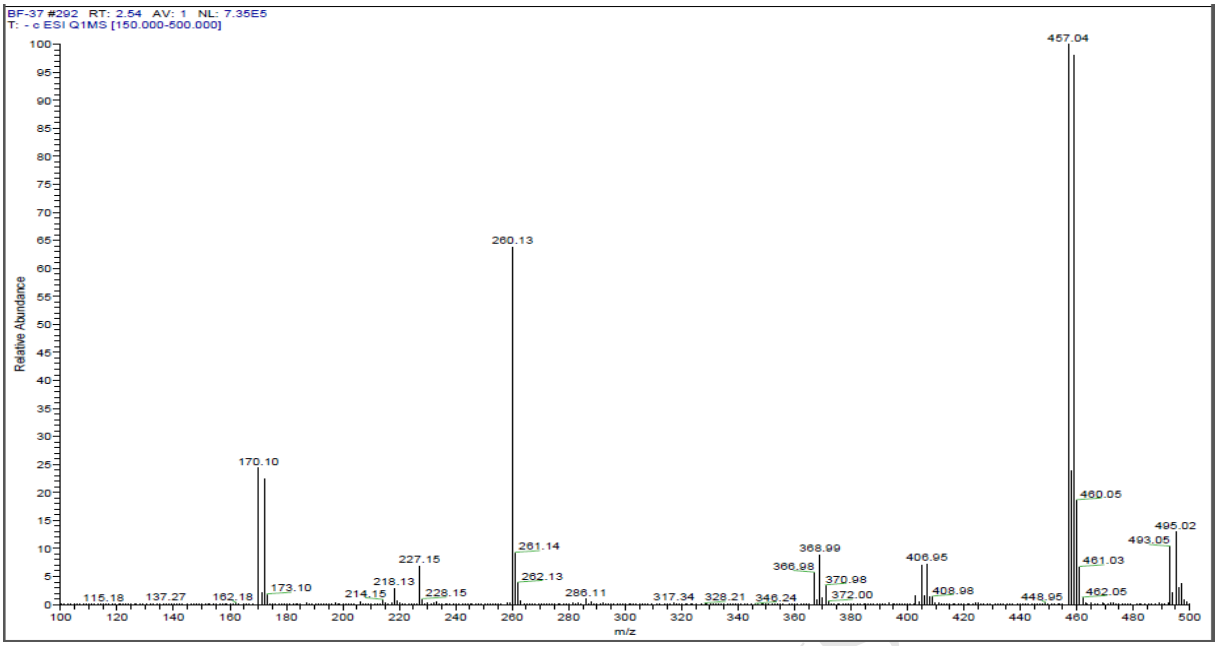

SM 38. ^{1}H and ^{13}C NMR and MS spectra of e38

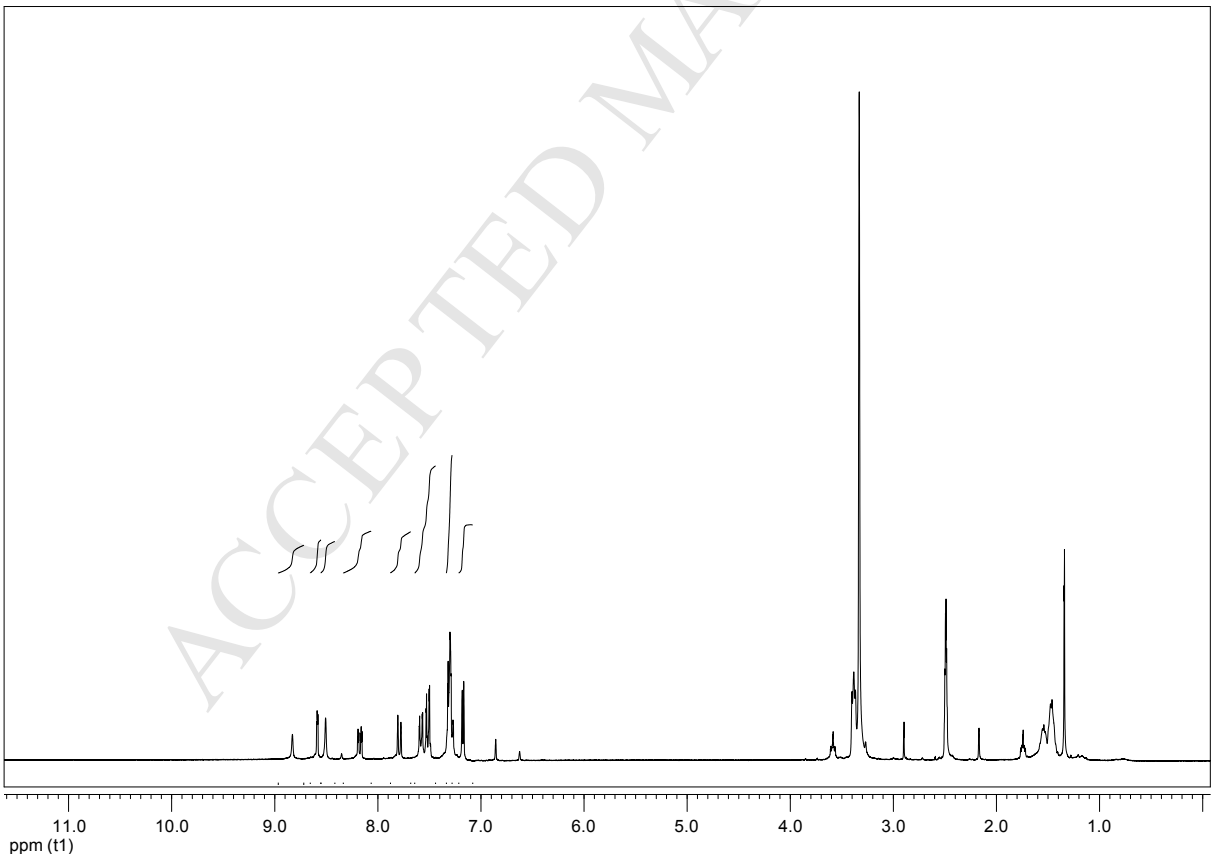

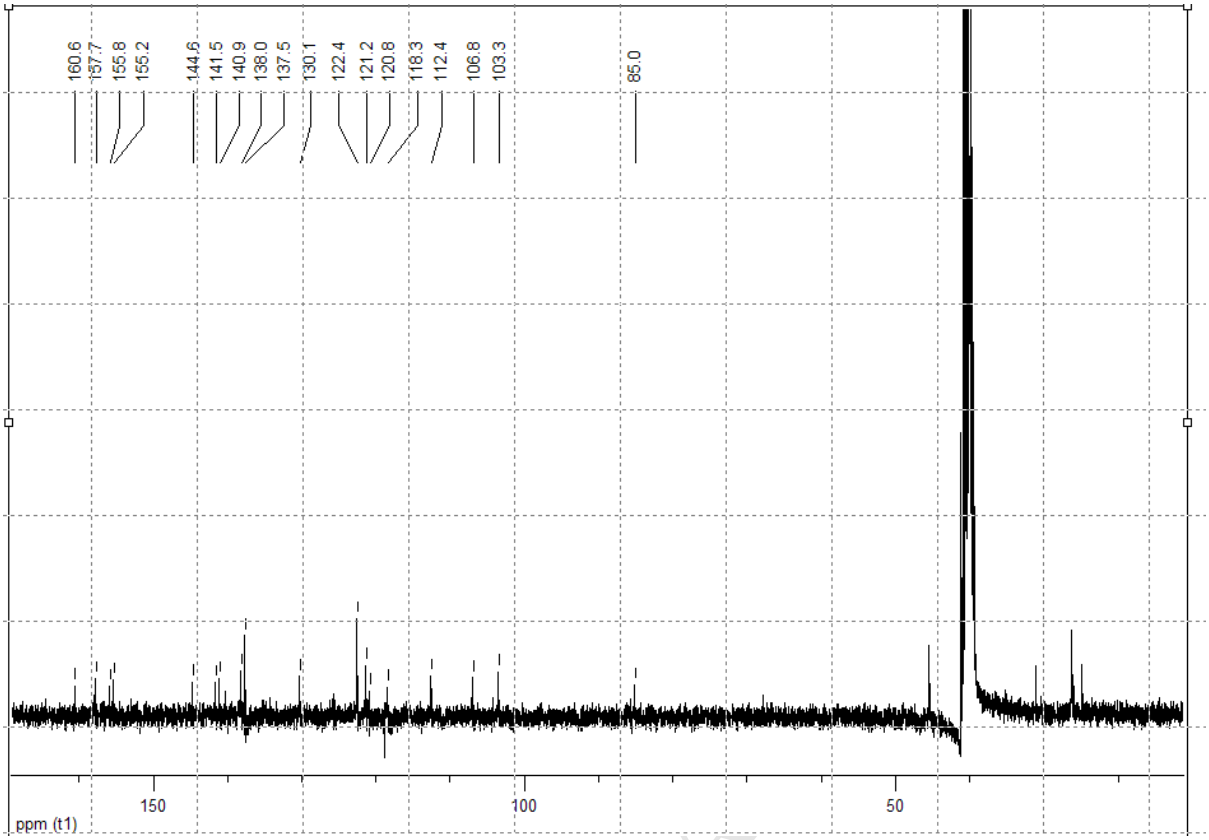
160.6
157.7
155.8
155.2
144.6
141.5
140.9
138.0
137.5
130.1
122.4
121.2
120.8
118.3
112.4
106.8
103.3
85.0
150
100
50
ppm (t1)

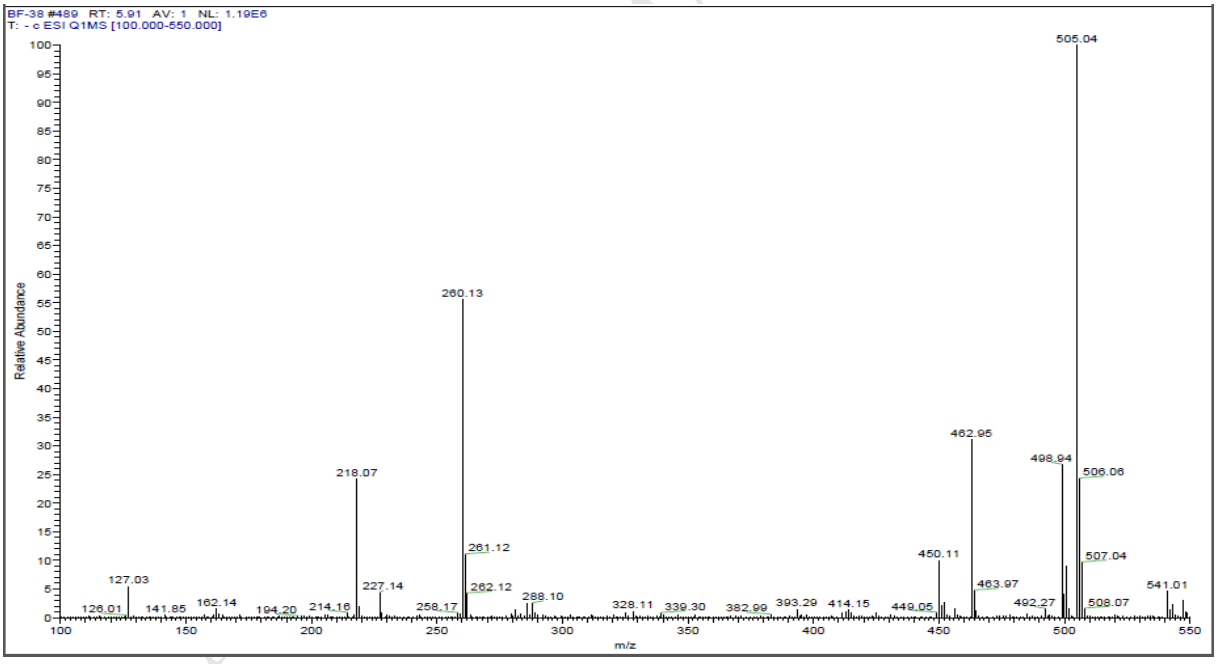
BF-38 #489 RT: 5.91 AV: 1 NL: 1.19E6
T: - c ESI Q1MS [100.000-550.000]
Relative Abundance
m/z
505.04
260.13
462.95
498.94
506.06
218.07
261.12
450.11
507.04
463.97
541.01
127.03
227.14
262.12
288.10
492.27
508.07
126.01
141.85
162.14
194.20
214.16
258.17
328.11
339.30
382.99
393.29
414.15
449.05